POLITECNICO DI MILANO

IV Faculty of Engineering

Mechanical Department

Ph.D. in Manufacturing and Production Systems

XXIII Cycle

Study of the Back Tempering Phenomenon in Laser Hardening of Large Surfaces

Supervisor: Ch.mo Prof. Barbara PREVITALI

Coordinator: Ch.mo Prof. Bianca Maria COLOSIMO

Ph.D. Candidate:
Anmin LIU
Matr. N. 724323

To my parents for their endless love and continued support

To my husband Chonghao for his profound love and understanding

ACKNOWLEDGEMENTS

I would like to express my sincere gratitude and appreciation to my supervisor Prof. **Barbara PREVITALI** for her generous encouragement, support and guidance throughout my studies as a Ph.D. student. Without her advice, it is improbable that this work would have been completed.

I would like to thank everyone in SITEC group for all of their invaluable help and suggestions during these three years.

I would also like to sincerely thank the Department of Manufacturing and Production Systems and the Laboratory stuff for their time and assistance.

My very special thanks to **Marcella NETTI** for her patient help throughout my studies.

Content

1 Preface

Laser beam is a low divergence, parallel beam which can be focused on a small spot, on which the full beam power concentrated. These features of the laser beam make it unique in modern industry. In the mean time, the power enhanced laser makes it possible to apply the high power beam to various production processes. Compared to the conventional methods, high power laser creates a new process method which is faster, more flexible, net shape and cleaner.

Today's highly competitive markets require the industries to look for new technologies to improve the product performance and productivity. For industrial equipments, most engineering components not only rely on their bulk material properties but also on the design and characteristics of their surface. Surfaces are the bounding faces of the solid components; they always interact with the working environment, and under severe conditions their performance and reliability can be limited due to the wear and corrosion. The solution of the problem is surface treatment. Surface engineering involves different special treatments to alter the properties of the surface phase in order to reduce the degradation over time; this makes the surface robust to the environment in which it will be used and prolongs the component life.

The most common processes of the surface treatment include flame and induction hardening, carburizing, nitriding. As a result, the chemistry and mechanical performance of the surface is modified and improved. Nowadays, high power laser has become a new heat source for the same job. Laser surface treatment can be applied in both coating and hardening in the surface treatment fields; it has many

advantages compared with the traditional ways, such as smaller distortions and less post-process time.

Laser surface treatment is a very flexible process, because of the self-quench and easily controlled laser power; it has been wildly used in automobile sectors and other industrial areas. One important application is the laser hardening, which involves only a thermal effect on the surface where a new structure with high hardness is obtained on the top surface. In most of these applications, laser does not treat the complete surface of the components but rather small local tracks. With a designed and delicate movement control system, laser hardening is suitable for some components with complex geometry, *i.e.* edges, corners and holes.

Because of the small spot dimension of laser beam, limitations and drawbacks are induced when the surface to be treated is larger than the laser beam. To gain a large treated surface by laser hardening, multi-pass technique is required where the hardened tracks slightly overlap each other. . But this technique is far from perfect due to a main drawback called “back tempering”, which means every hardened track is partly reheated and tempered by the consequential ones. The structure of the reheated part transforms from martensite into tempered martensite, resulting in low hardness, and end up with a non-uniform hardened zone. The back tempering happens on planar and cylindrical surfaces. In order to overcome this drawback, different techniques are proposed, e.g. laser melting, scanning laser head, to obtain a desired laser beam.

This thesis studies the characterizations of the back tempering phenomenon in the overlapped zone, and reduces effects of this drawback by different techniques to get a large treated surface on planar and cylindrical surfaces.

In chapter 2, an overview of laser hardening is given, first, the principle of laser hardening, development of this technique and the industrial applications are discussed. And then the works on back tempering drawback and some solutions will be focused.

In chapter 3, the objectives of this thesis will be summarized.

Chapter 4 gives the details of the experimental setup, including the laser with a control system, the metallurgic analyzing method for the hardened samples.

In chapter 5, the effects of different parameters on the hardened zone and hardness decrease in the overlapping are the main topic of chapter, where the planar surface laser hardening study are carried out, both single track and multi-pass are investigated.

In chapter 6 and chapter 7, some solutions for the back tempering phenomenon on the planar surface are given. Laser melting technique is studied; overlapping process is carried out by melting the surface. The other solution is scanning laser head hardening, different scanning conditions are applied.

Chapter 8 gives a solution to eliminate the back tempering on the cylindrical surface. Experimental results in this chapter show that apparent Spot (AS) is an effective solution to get a uniform hardened zone.

In the end, chapter 9 summarizes the results of this thesis work and the future works are suggested.

2 State of the art

Laser hardening is an important surface modification technique in today's industry, in this chapter, a review of the bibliography is given.

A general introduction of the laser surface engineering, especially laser hardening process is presented, including the process principle, development and industrial applications. Following the bibliography research is focused on the laser hardening technique on large surfaces. The back tempering is the main drawback when multi-pass is applied to treat a large surface and different solutions are proposed.

2.1 Introduction

Since the first laser was built 50 years ago, laser has evolved from a source of high-intensity monochromatic radiation into a powerful tool in engineering and manufacturing. In industrial applications, a focused laser beam is one of the highest power-density sources for materials processing today, because of its highly concentrated energy.

Since the first functional laser was generated, this innovative technology has developed fast for most important types of lasers. With the increase of laser power, in the 1970s, CO_2 lasers were firstly applied in materials processing such as cutting and joining, the power of the CO_2 laser up to 10 kW entered the market in 1990 [1]. In the meantime, the first lamp pumped Nd:YAG lasers in the kilowatt range were

invented at the beginning of the nineties, and then semiconductor lasers were available a few years later [2], until today diode lasers with power up to 10 kW are commercially available. Solid state lasers became the new development trend since it is possible to couple the solid state laser light in flexible guiding fibers. Its advantages enable solid state lasers widely applied in industrial field, where the most important applications were in automotive industry and new applications for surface engineering [3]. In the beginning of the twenty-first century, new promising technologies in solid laser - fiber laser and dick laser had been developed. These two kinds of laser are described as high brightness laser family, which are featured as high laser beam quality, unlimited laser powers. Welding and cutting are the most interesting applications of high brightness lasers [4].

Compared to the conventional processing, laser in material processing has several unique advantages e.g. non-contact processing, controlled and automated processing, net-shaped operation, high productivity, economic manufacturing, improved product quality, greater material utilization and minimum heat affected zone. With the development of its high power and high quality, laser processing has become a useful technology in the growing number of processes and wider bandwidth of applications. Figure 2-1 shows some main laser material processing in today's industrial applications.

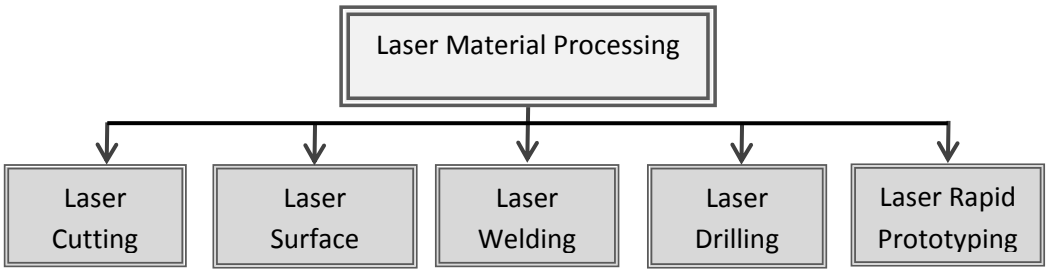

Figure 2-1 Laser materials processing technologies.

From the true application point of view, that laser power is not the only parameter to make a successful process; interaction time with the materials and power density are also important. Figure 2-2 illustrates the possible operating regimes for various types of laser processing [5].

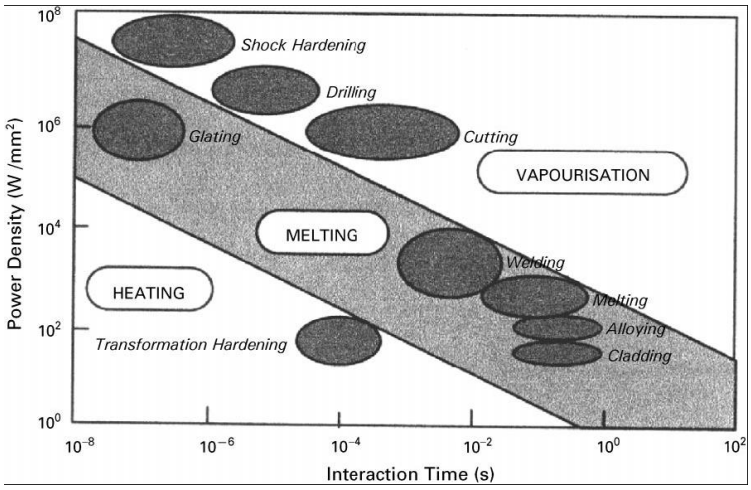

Figure 2-2 Effects and possible applications of lasers under various operating conditions.

The processes are divided into three major domains in the processes, involving solid to solid (only heating, without melting/vaporizing), solid to liquid (melting) and solid to liquid (vaporizing). Usually the power density is the most often considered factor when determining possible type of laser processing or choosing laser sources for different process. Generally speaking, surface heating without melting requires low power density and other processes with phase transform needs higher power density.

There are some other parameters which influence the results of laser materials processing, including wavelength of the laser, the wavelength absorptivity of different materials, and laser beam quality [6]. For examples, carrying out material processing by CO_2 laser, a pre-coating process is necessary to increase the absorptivity of the wavelength of CO_2 laser; fiber laser is the best choice for a keyhole welding because of the high beam quality and diode laser is suitable for surface treatment because of the high metallurgical absorptivity and uniform energy distribution.

2.2 Laser surface engineering techniques

2.2.1 Principle and classification

The surface of the materials acts as an interface to the surrounding environment. The contact with the surroundings results in degradation due to wear, erosion and corrosion [7].The industrial solution to minimize or eliminate such surface initiated

failure is based on changing the surface microstructure and/or composition of the workpiece but without affecting the substrate [8][9].

The basic physics of laser surface treatment is using laser as energy source to interact with the surface of an absorbing material and subsequently cooled by heat conduction into the bulk material. In industry there are two kinds of surface treatment applications (see Figure 2-3). One involves thermal transformation process with the base materials, such as laser hardening and laser melting, which is related the modification of surface properties by changing the microstructure of the surface layer. The other application involves both thermal and chemical process, such as laser cladding and alloying, where new materials are applied on the surface of substrate during the laser irradiation. The new materials are melted, then coats and joins in the substrate, a modification is also involved in the surface of the substrate.

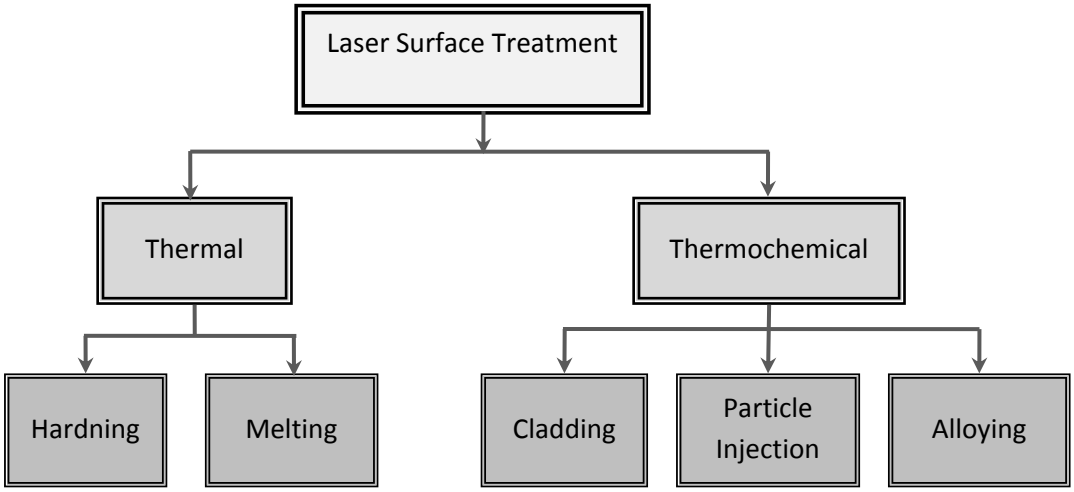

Figure 2-3 Classification of laser surface treatment.

The modification of the surface zones leads to an improved durability of the component that allows cost reduction and therefore an enhanced profitability.

2.2.2 Laser sources for laser surface engineering

At the beginning of laser hardening application, the most traditional high power CO_2 lasers have been widely used, since only CO_2 lasers were able to deliver the high power which was needed for hardening. The absorption of metal decreases as the wavelength lengthens, and CO_2 laser-beam light has a comparatively long wave-length, 10.6 μm, the absorption of steel and iron at CO_2 laser beam is very small, some experiments have shown that an absorptivity between 2-3% and 3% for a CO_2

laser beam incident on polished iron [10] [11]. 9-10% absorptivity values have been obtained for AISI 304 austenitic stainless steel [12]. To decrease the energy loss, pre-coating is needed for CO_2 laser.

With the development of Nd:YAG laser, it replaced the CO_2 lasers in laser surface applications. Nd:YAG laser operates at a shorter wavelength 1.06 μm. The shorter wave length significantly improves the absorption characteristics of the metal, e.g. the between 28.6% and 30% for low alloy steels [13]. But the electrical to optical efficiency for Nd:YAG laser is definitely low, which makes the equipment bulky and costly to run [14].

Recently high power diode laser (HPDL) has become industry available and overcome some barriers referred to CO_2 and Nd:YAG lasers [15]. The lower wavelength, typically 0.8 and 0.94 μm, improves the absorption characteristics for the laser beam. And due to the very high absorptivity of metal for this wave length which can reach 35-40% for a polished, non-oxidized steel surface by theoretical calculations [16]. HPDL hardening leads to the unnecessary of coating, which means saving time and cost, also the environment is improved. Other than the absorptivity advantage, the hat top power distribution and rectangular shape spot of the laser beam are also two important benefits for laser hardening application [17] [18]. These two characteristics make HPDL hardening has wider and more uniform hardened zone in width and depth respectively. The electrical to optical efficiency is relative high compared with other kinds of laser, HPDL equipments are also remarkably smaller in size than CO_2 and Nd:YAG lasers of the same power, which make it possible of integration in the production line.

2.3 Laser surface hardening

Laser surface hardening is also called laser transformation hardening or laser hardening. It is a technique to obtain hard and wear resistant surface layer with a typical thickness of 0.5 to 1.5 mm [19]. A laser is as a heat source, scans and heats the surface, the rest of the component acts as a heat sink resulting in a high cooling rate. Laser hardening is a promising process for ferrous family to produce a hardened layer on the surface as shown in Figure 2-4.

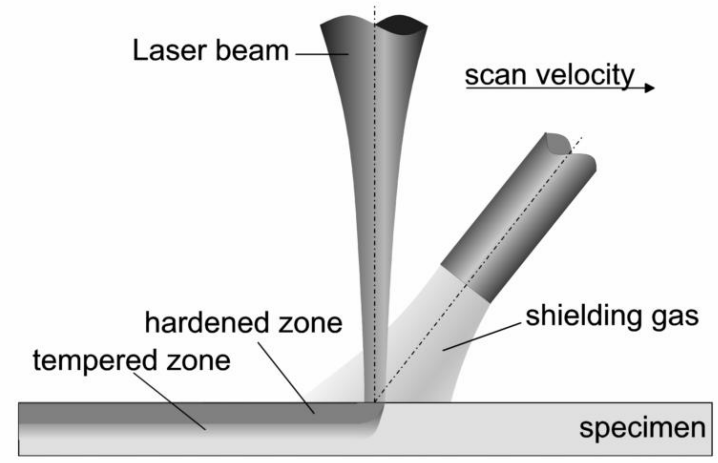

Figure 2-4 Principle of laser hardening Process [8].

2.3.1 Process description

The surface of the material is heated rapidly above the Ac_3 temperature, then the structure is transformed from the initial ferritic / pearlitic structure (α + Fe3C) to an austenitic where the carbon is dissolved. Hardening takes place when the material is subsequently cooled down at a high cooling rate that there is not enough time available for the reverse transformation and the carbon does not excrete but remains in the crystal structure. Instead of the ferritic or pearlite, very hard and compact martensite structure is obtained [20][21][22].

The formation of martensite is a multiply factors process, Figure 2-5 shows the detail phase transitions during the laser surface hardening.

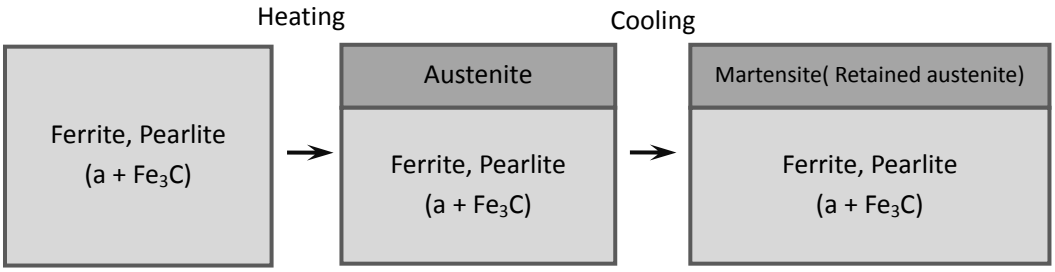

Figure 2-5 Process and material component during laser hardening process.

There are some important criteria which affect the process strongly [23] [24][25]:

1. Surface temperature of the hardened zone should reach austenization temperature. Only if the surface temperature reaches the austenization temperature level Ac_3, both the pearlite and ferrite will transform to austenite.
2. Between the heating and cooling cycle, surface of the substrate should be maintained above the austenization temperature long enough for carbon diffusion to form homogeneous austenite and get a uniform hardness in hardened zone.
3. The heated surface of the workpiece should not reach the melting temperature.
4. The heating and cooling rate should be high enough. At the heating phase, a high temperature gradient is required to heat a sufficient thick surface layer in a short time and to prevent heating the bulk material. For cooling phase, martensite is a non equilibrium phase; the cooling rate should be fast enough to avoid the formation of pearlite and ferrite.
5. The transformation temperatures and the process are affected by the microstructure, *e.g.* the presence and the distribution of alloying elements in the material.

In conventional hardening the product is heated by flame, in a furnace or electron beam. Compared with these ways, the advantages of laser heat treatment can be categorized as following [26][27]:

1. Due to limited energy input, only the surface is heated, the bulk is still cool; self-quenching is established during the process.
   - Laser heat treatment is a saving energy process and the heat affected region of the component is limited.
   - Minimal thermal distortion of the work piece after the treatment.
   - No milling, grinding or cleaning is needed for the final workpiece.
2. Without the need of quenching, laser hardening could be the last process in a production line and the hardening process is clean for environment [28].
3. Laser hardening is a flexible process.
   - The energy of the laser can be well controlled by software or hardware.
   - With different optical system, *e.g.* focusing lenses, different degrees of defocus and scanning system, the dimension and shape of the laser beam can be easily changed.
   - With the assist of smart movement system, laser hardening can be adapted to complex shape workpiece.
4. Laser hardening is also a high productivity process.
   - Laser hardening is a rapid process, because of the fast heating and cooling phase.
   - It is suitable to incorporate a laser source in an automation production line.

Figure 2-6 shows the comparison in the process chain between internal laser hardening and external induction hardening in the production of a metal forming tool [29], the left column shows the time consuming and costly in conventional way, the right column demonstrates the target laser process.

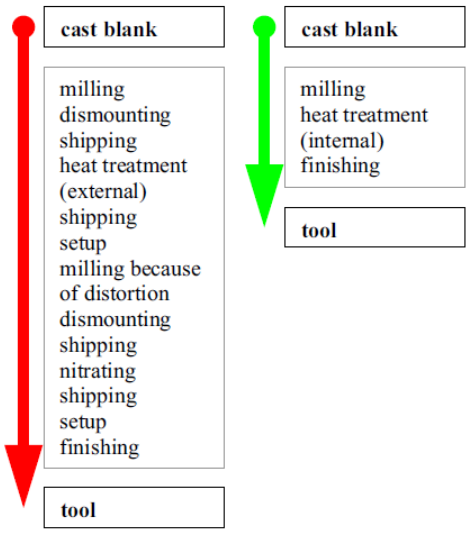

Figure 2-6 Comparison of the process chain when laser hardening and induction hardening are used.

2.3.2 Process development

In early work laser hardening process is related with CO_2 and Nd:YAG lasers. C.H.Chen applied a continuous 10 kW CO_2 laser to harden nodular and gray cast iron for enhanced hardness and erosion resistance [30]. Henrikki Pantsar studied the oxide layer during the process; it makes the oxide film increases the absorptivity especially distinct in CO_2 laser [31].

Study has shown a possibility of applying low power CW CO_2 laser (100W) laser to improve the microhardness of the steel surface [32]. With the development of diode laser, more and more laser hardening is carried out with a diode laser source. At 1997 Chen W, Roychoudhuri CS and Banas CM got a 0.1 mm thickness hardened zone using a 15 W fiber delivered HPDL on 400 series stainless-steel surface [2]. Klocke et al successfully hardened 42CrMo4 steel to hardness over 700HV with a depth of approximately 0.5mm using a 650W HPDL [3]. Until now, up to 10kW diode laser has been applied in industrial surface treatment.

2.3.2.1 Parameters and microstructure analysis

As the temperature range for laser hardening is very narrow (should be above the Ac_3 temperature and below the melting point), and the process is very fast, laser hardening is an unstable process, it is quite difficult to get a high quality and repeatable hardened zone. Laser hardening process involves different parameters, such as the initial condition and thermo-physical properties of the base material, the laser beam properties i.e. power, shape and energy distribution, scanning speed. All these parameters highly influenced the performance of the treatment. At the early stage of the laser hardening development, the parameters investigations were studied by most researches to obtain a hardened zone.

Pashby studied the depth of laser hardened zone under different power and scan speed combinations [33], the result shows that both 080M40 and 817M40 (British standard) can be surface hardened using a high power diode laser. The affected depths (up to 0.5 mm) and maximum hardness achieved varied with power and speed, as well as with steel type. I.RF. Lusquinos used a pyrometer and closed loop control for AISI 1045 flat sheets HPDL hardening [34], confirmed the hardened depth is proportional to the power divided by the inverse square root of the laser spot size times speed, as shown in Figure 2-7.

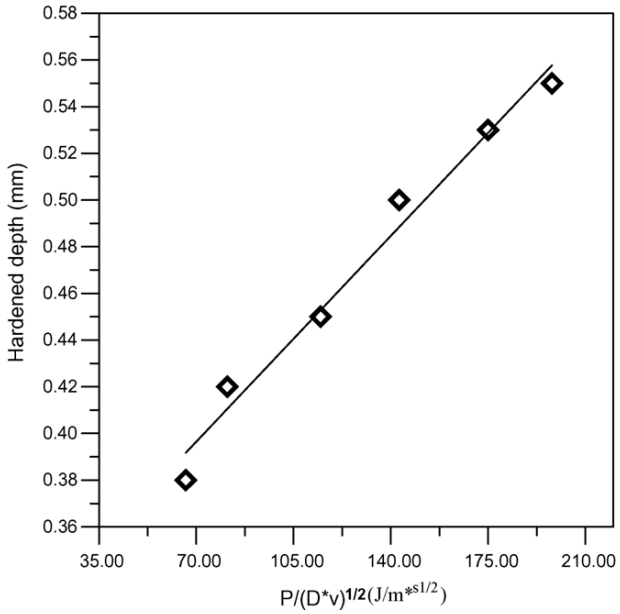

Figure 2-7 Evolution of the hardened dept with the parameter $P/(V*D)^{1/2}$ [34].

Different kinds of laser beam shapes are also investigated. Shakeel Safdar investigated the influence of circular, rectangular and triangular beam geometries for laser hardening [35]. Relationships between temperature and time, hardness and depth, microstructures of hardened zones were given for different laser shapes. Figure

2-8 gives an example of difference of the obtained hardened zones, (a) obtained by circular laser beam and (b) obtained by rectangular laser beam.

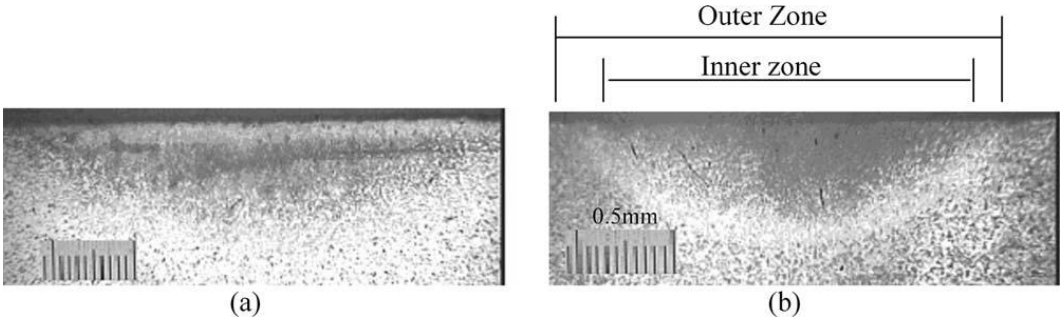

Figure 2-8 hardened zones obtained by different laser beam shapes [35].

Based on the results, the beam geometry strongly influences the temperature distribution during the process; a relative low heating rate is beneficial for the laser transformation hardening process, if the cooling rate is fast enough. This result agrees well with the basic transformation hardening theory established in the [36]. An experimental and numerical study [37]of non-uniform energy distribution during the hardening process strongly recommended a uniform power distribution for the laser spot, whereas the shape of the beam plays less important role in the same process. The relationships between geometry of the hardened track/hardened depth and laser beam distributions were investigated [38] as shown in Figure 2-9.

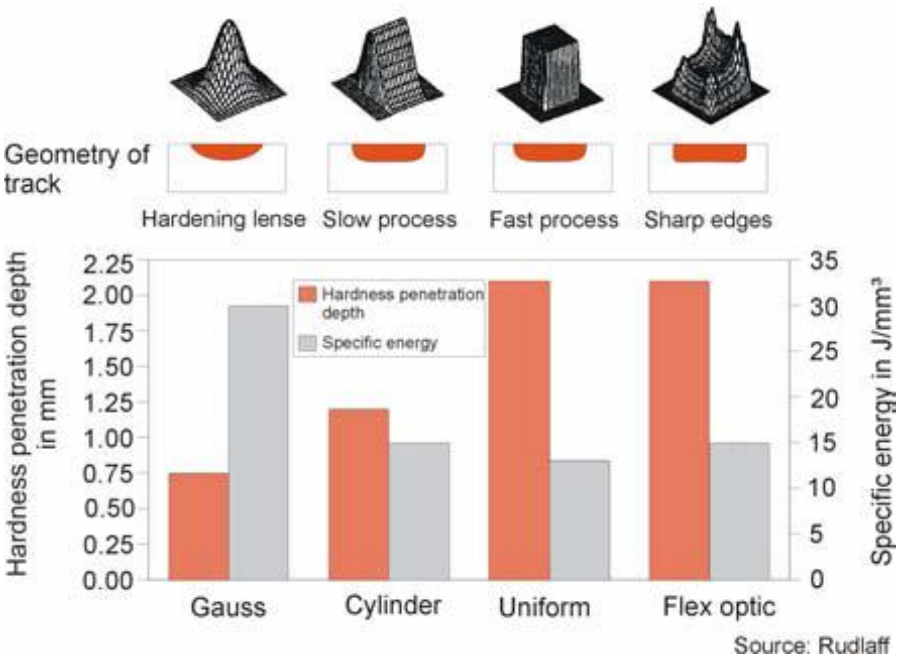

Figure 2-9 Hardened shape and depth obtained by different laser beam distributions.

In metallurgical point of view, the correlation between the surface temperature and cooling rate on the resulting hardness was explained by K. Subramanian [39], which confirmed a cooling rate were about 5000℃ /s, and a 2-fold increase in wear resistance for the laser-hardened AISI 5135steel. The retained austenite was studied in [40] for carbon and low-alloyed steels, indicating the cooling rate is high only at high temperatures. But when the temperature decreases, the cooling phase could be even lower than typical rates for conventional quenching. This leads to bainite transformation and, as result, increased retained austenite content. Hardened zones also were analyzed in terms of microhardness, dislocation density, and grain size by K. Obergfell [41], different pro-processes of the base materials affect the microhardness distribution. When the base material was tempered at 300℃ before hardening, the constant microhardness was observed near the top surface. On the contrary, microhardness started to decrease from the top surface if tempered by 600℃, but both tempering conditions shown a transition zone where the values decrease. Other than different kinds of steels, cast irons are the other group materials which are suitable for laser hardening process. The surface layer hardening to martensite takes place mainly by transformation of the perlitic region of the gray iron, the ferrite zones become totally or partially martensite due to the graphite solution [42]. Martensite or/and ledeburite eutectic, including certain retained austenite were also observed in the hardened zone of the gray cast iron [43].

2.3.2.2 Modeling and simulation

Finite Element Methods (FEM) is applied to study the influence of the process parameters on the thermal cycles and hardening results. Some researchers involve modeling the temperature distribution during the process in order to predict the microstructure, hardening depth, hardness and the residual stresses of the hardened zone. Rahul Patwa and Shin successfully set a 3D kinetic temperature distributions model in the cylindrical workpiece to predict the near surface structure and hardness [44]. In order to verify the simulation results, an experiment was carried out; it achieved a case depth of 0.54mm with uniform hardness of 63 RC in the AISI 5150 steels with 500W diode laser power. Skvarenina et al also successfully predicted and experimentally achieved 2.5 mm hardening depth with a uniform hardness of 57 HRC on a 1536 steel cylinder of 60 mm diameter with 2.9 mm/s scanning speed and 1220W diode laser power [45]. It indicated that with complex geometric feature, both of the hardness and depth decrease, in case of 2 mm radius, a depth of 1.5 mm and hardness of 55 HRC hardened zone is achieved. A transient 3D thermal and kinetic model is gotten by Neil S. Bailey et al [46]. Tobar established a combined methodology for building a laser transformation hardening with good predicting capabilities, the model allows detailed study and optimization on the selected parameters range [47].

2.3.2.3 Sensor and process control

With the increased requirement of industrial applications, control and optimizing laser hardening process are widely studied. The main reasons of control can be summarized as

- Heat accumulates during the hardening process; in this case, the initial condition is changing.
- Absorptivity of the surface for laser beam energy increases as the temperature increases [48], also the dust or oil which is on the surface influences the absorptivity.
- The geometry of the component is a most common disturbance of the laser hardening process.

In these cases using a constant laser beam power and constant scanning speed will lead to a non-uniform hardened surface. From the efficiency point of view, industry production should be high efficiency and minimize the time and money cost. Offline measurement and control result a lot of time and money loss, because correcting errors or doing the whole process again with a new workpiece would be required. Other than that, a control system should be inexpensive and less complicated. Therefore real time online measurement and control was developed for by many researchers [49][50][51]. The temperature at the spot could be used as control signal during the process; the temperature signal could be obtain by measuring the emitted inferred energy from the high temperature surface with a pyrometer or sensor. Based on the real time temperature obtained, the laser power and /or scanning speed can be controlled as expected, and then the surface temperature could be maintained on the required level.

A pyrometer controlled laser hardening system for 4140 steel and class 40 gray cast iron was investigated in [52], the surface temperature of the spot was monitored and the output power was controlled to maintain a constant temperature on the surface. The hardness and depth could be controlled in some degree by the input power and scanning speed. By the pyrometer temperature measurement, the hardness in the range of 50-65 RC and depth between 0.7 to 1.5 mm could be produced. It also indicates that laser surface transformation hardening not only increases the wear resistance, but under certain conditions the fatigue strength is also increased due to the compressive tresses induced on the surface of the component. A low cost CCD camera based sensor system was used by Steffen Bonss et al. [53], the camera had a larger field of view than the laser spot size, contains over 400.000 single infrared sensitive measuring points, but the price was only about 20% of the standard infrared camera system. Zhiyue Xu used an infrared sensing system to monitoring Nd:YAG laser hardening [54], the infrared monitor was integrated into the Nd:YAG laser beam delivery optics and off-axis to get the infrared emission signal. The system collected

the infrared emission signal associated with laser hardening process to monitor the hardness and depth of the hardened zone. The results show a linear relationship between the monitor output DC level voltage and hardness up to the maximum hardness possible and also between the monitor output DC level voltage and depth as shown in Figure 2-10.

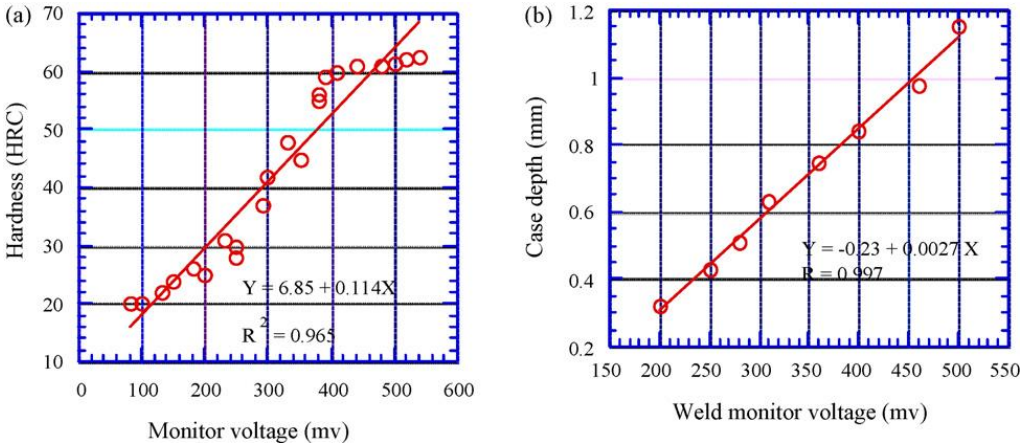

Figure 2-10 Plots of (a) hardness and (b) depth vs. monitor DC voltage level for gray cast iron [54].

Dietmar Hömberg and Wolf Weiss have developed PID control strategies for laser hardening the non uniform geometrical workpiece [55], it induced an idea that the best solution is not controlling the temperature on the top surface, but controlling the temperature close to the lower boundary of the hardened zone on a constant temperature (Ac_3), and then computing the optimal temperature in the laser spot. The computed temperature is the control signal for the real process to obtain a uniform hardened layer. Figure 2-11 gives an example of the control strategies for a variable thickness workpiece.

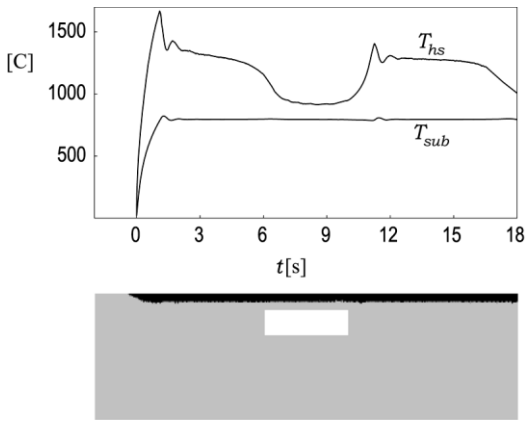

Figure 2-11 A hardened zone obtained by PID controlling of subsurface temperature.

2.3.3 Industry applications

Because of the low distortion, localized hardening position and other advantages in the laser hardening process compared with the conventional ways, laser hardening process has been widely used in industry. The automotive industry is one of those industries which benefit a lot from laser hardening for mass and precise production, exhaust valves, valve guides and gears could be laser hardening to enhance ware resistance [56]. One example for complex shape and local hardening application is shown in Figure 2-12. Torsion springs could be hardened over 170 °and depth 0.2-0.4 mm by two diode lasers, the rest of the component was not affected by the process as shown in the cross section [17]. A cast iron of grade SCh25 or VCh40 made valve is hardened by a continuous CO_2 laser with a power up to1.2 KW. The mean hardening depth is 0.2 mm, whereas the micro hardness in the hardened zone was 600 – 800 HV, as showed in figure 2-13 [57].

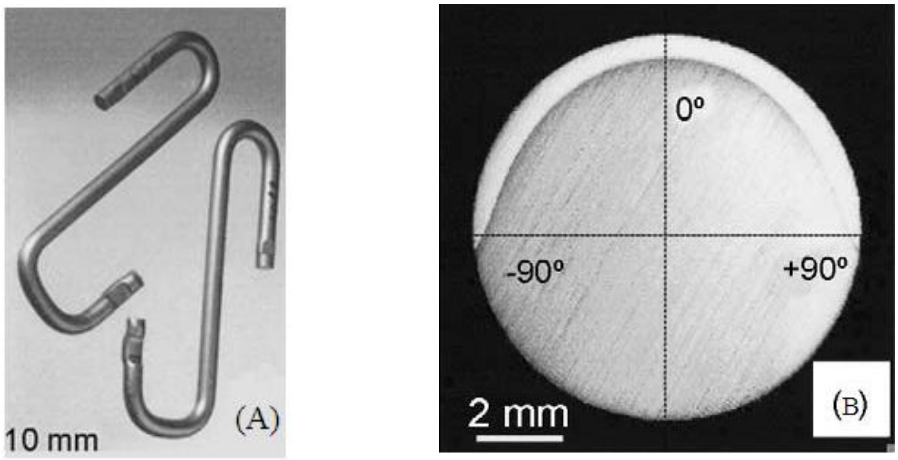

Figure 2-12 Hardening of torsion springs and the hardened zone.

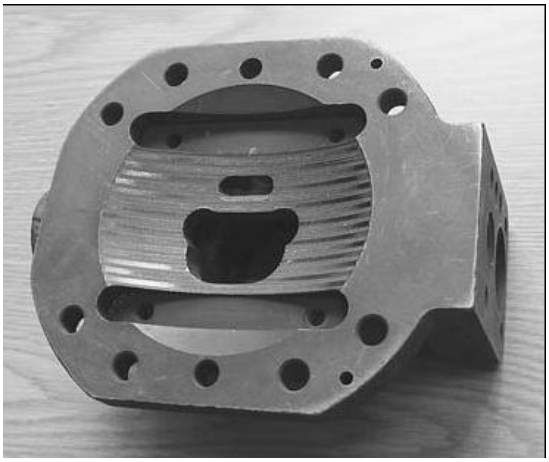

Figure 2-13 A hardened surface of regulating valve body.

2.4 Existing drawback and solutions for laser hardening

The localized laser hardening has been widely applied in nowadays industry; one limitation for the laser hardening application is the large surface hardening.

2.4.1 Main drawback of laser hardening – Back tempering

As the laser beam has a limited spot dimension, when the area to be hardened is larger than the laser spot, multiple passes have to be applied, the later track reheats the previous track slightly, due to the less severe thermal cycles undergone by the overlapped area, the existing martensite is transformed into tempered martensite, which characters as lower hardness, this is the well known back tempering problem as shown in Figure 2-14 [58].

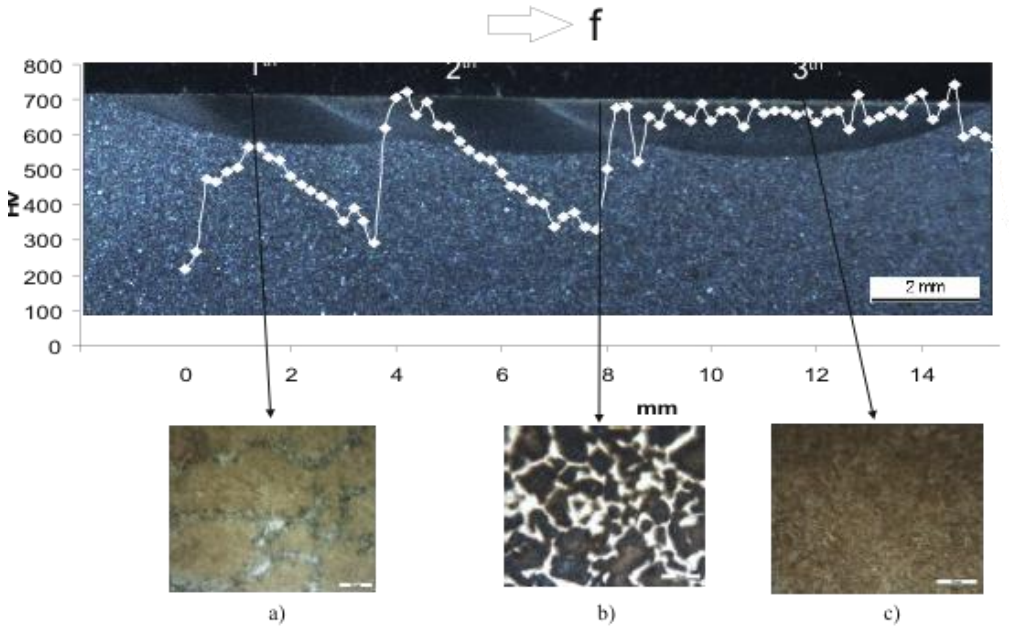

Figure2-14 Microstructure changes in laser hardened steel.

As a consequence a local reduction in hardness is observed [59]. Overlapping process was also applied to cast iron used for marine diesel piston ring [60], it confirmed a hardness drop from 800-950 to 470 $HV_{0.1}$ in the overlapped zone. The result of overlapping is non-uniform on hardness and depth, as illustrated in Figure 2-15 [61]. Many works have been performed in order to understand the influence of the overlapping and the effects of different overlapping conditions.

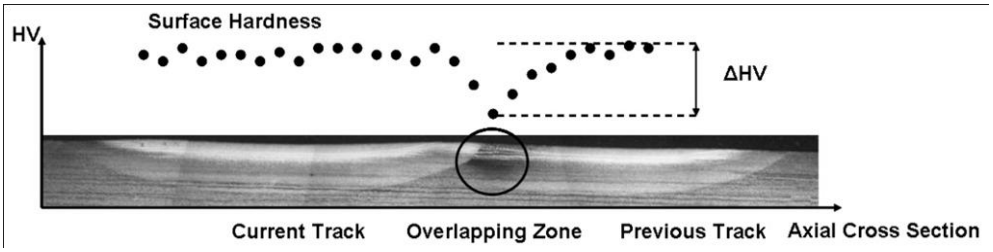

Figure 2-15 Back tempering effect in the overlapping technique.

The overlapping process happens not only in the large planar surface, but also in the cylindrical surface, such as steel shafts, camshafts, cylinder liners, pistons, piston rings. When a large scale surface is hardened, the cylindrical workpiece will be rotated by a lathe; in the meantime, a laser beam scans the surface parallel to the rotation axis. In this way, a continues helicoidal track is obtained [62], and the

overlapping still exists between the adjacent tracks. The overlapping happens also when a narrow annular surface is hardened, in this kind of application, the initial part and the finishing part are overlapped, and back tempering occurs in this zone.

A. Fortunato presents a polynomial expression tempering model to predict the hardness reduction in multiple laser paths for hypo eutectoid steel and the software is able to simulate other laser hardening processes [63]. Ritesh S. Lakhkar, Yung C. Shin developed a three-dimensional transient temperature model and a kinetic hardening–tempering mode to predict the case depth [64], hardness for AISI 4140 steel and determine the optimum operating conditions in which the hardenen depth gets maximize (at least obtain 2 mm) and reduces back tempering. The optimized process was carried out by changing the extent of overlapping of the tracks, the major portion of the back tempered track was in the range of 480–571HV. The difference in the case depths of the two adjacent tracks was approximately 0.2 mm. Based on the single track hardening, the overlapping was studied on grey cast iron surface by a temperature measuring and control system [65], decreased hardness 400HV was observed in the overlapped zone for grey cast iron. The soften behaviors of different materials (C45, 9Cr2Mo and W18Cr4V steel) were also investigated by authors [66], the softening width of C45 steel was the broadest and that of W18Cr4V steel was the narrowest as shown in Figure 2-16. The authors also pointed out, by tempering the laser hardened samples, a uniform hardness distribution will be obtained in the cross section (see Figure 2-17).

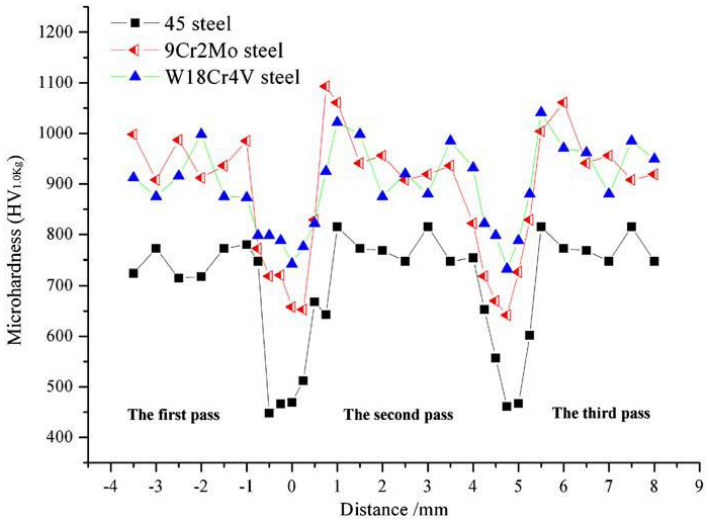

Figure 2-16 Hardness distributions of different materials by laser-overlapping hardening.

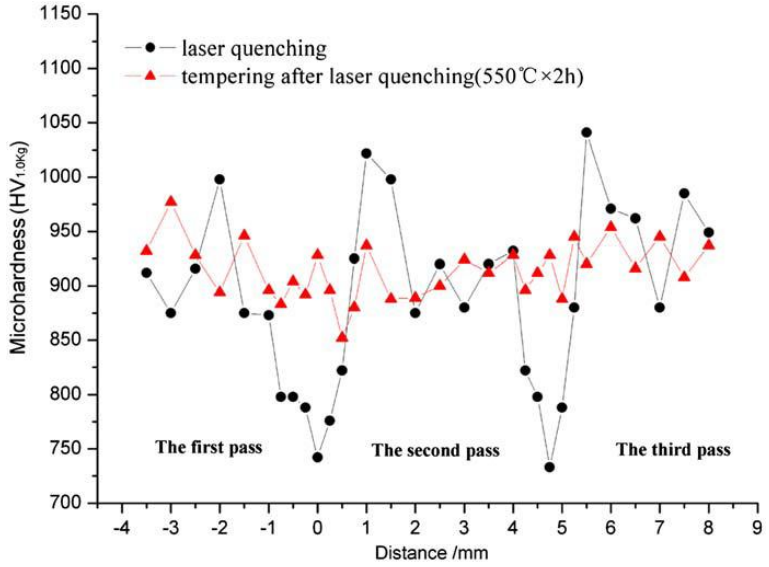

Figure 2-17 Hardness distributions after laser-overlapping hardening and tempering.

Guy Claus focused on the hardening of large areas on flat surfaces and other geometrical workpiece [67], by testing different degrees of the overlapping, a high overlapping degree gave the best results in terms of hardness variations as shown in Figure 2-18, but hardness in the non overlapped zones also decreased compared with the 0% overlapping process.

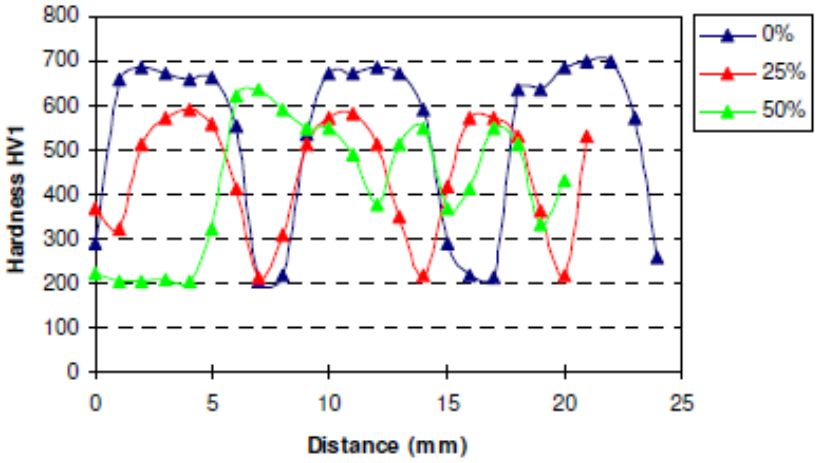

Figure 2-18 Hardness distributions with different overlapping degrees.

Overlapping quote, focus height and beam velocity were studied to optimize the hardening process for cylindrical surface [68], the works indicated the hardness decrease in overlapped zone was mainly related to the thermal cycle, it should not depend on the overlapping. It is more likely to accumulate heat inside the specimen

when a cylindrical workpiece was rotated by a lathe and irradiated by laser [69], Figure 2-19 shows that the hardening depth, width and overlap length gradually increase as the number of hardening tracks increases.

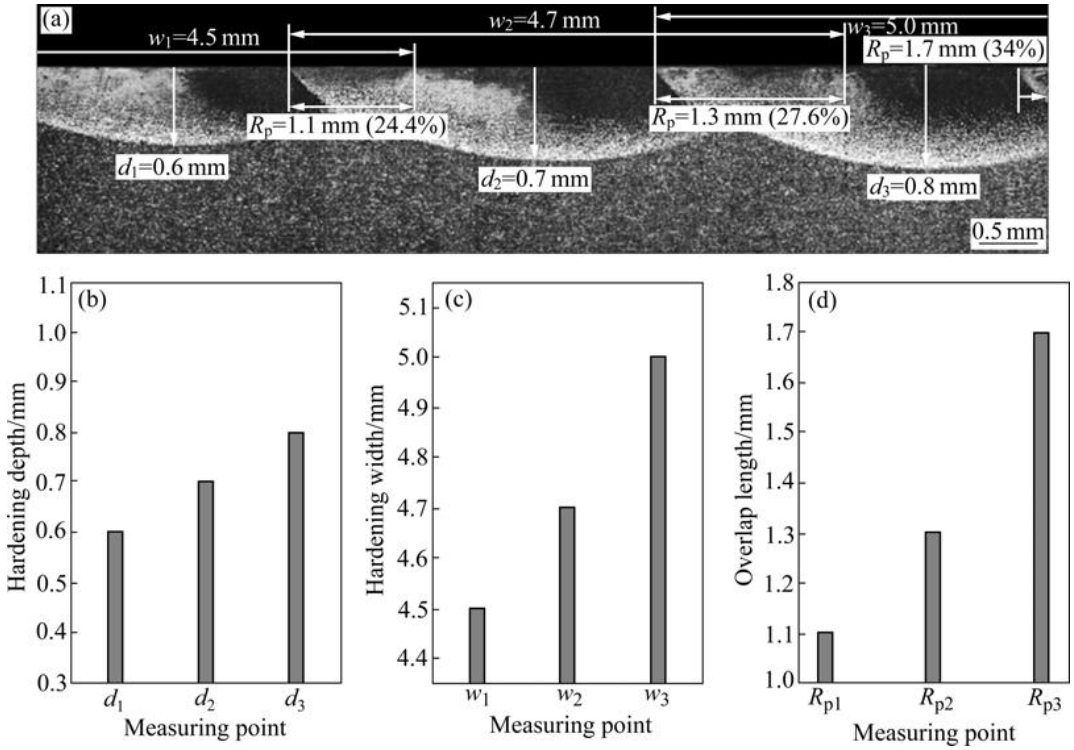

(a) Cross section image; (b-d) Measured values of each hardened track

Figure 2-19 Effect of heat deposition on hardening depth, width and overlap length.

2.4.2 Solutions to overlapping on planar surface

Literally the solution to the back-tempering consists substantially in avoiding the overlapping making use of very large spots. The spot can be enlarged with a traditional solution by a scanner head, which allows large, shaped spot to be obtained moving the laser beam with high frequency and programmed paths in x and y directions. Laser hardening making use of scanner head permits to cover larger area, even though the industrial experience limits the spot no larger than 100 mm, since the laser power has to be correspondently increased. Thanks to the recent events of high power fiber laser, this limit can be exceeded, and it is time to apply the laser hardening to the large surface in industry. Once the process operability range was investigated and auxiliary equipments, such as pyrometer or thermocameras to keep

the control of the surface temperature, have been optimised for the active fiber laser sources. Figure 1.5 gives an example of the scanner head hardening.

M. Seifert, S. Bonß, B. Brenner, E. Beyer [70] used a 4 kW HPDL with scanning optics to investigate the influence of different scanning functions on the hardening results. Different laser power density distributions were obtained by different scanning functions, and the structures in the cross sections shows that the geometrical features of the hardened zone are influenced by the scanning function (see Figure 2-20 (a) (b), (a) sine function, (b) triangle function).

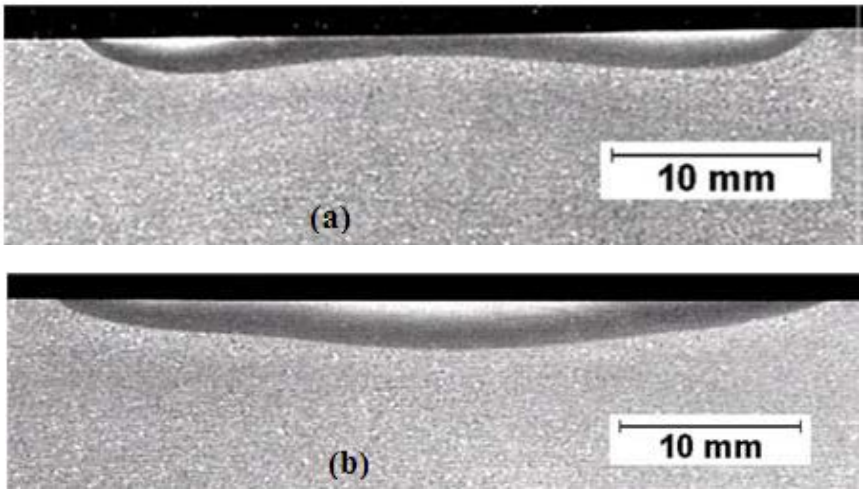

Figure 2-20 hardened zones with scanning laser head technique.

In Figure 2-21, a 27 mm wide hardened track was obtained with homogenous hardness distribution across the hardening zone.

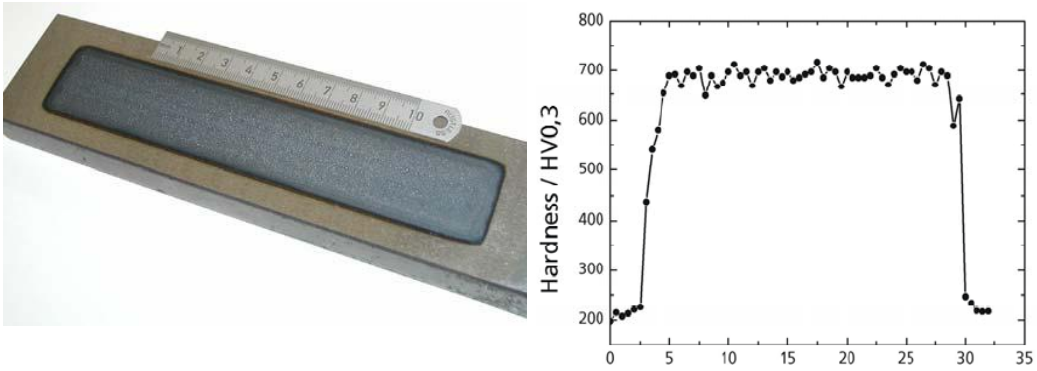

(a) Top surface (b) hardness distribution

Figure 2-21 Top surface microview and hardness distribution in carbon steel treated with a diode laser source and scanning optics.

S. Bonss [71] applied two separate 6 kW high power diode lasers for simultaneous laser hardening, and use beam splitter optics. Under these conditions on high alloyed steel a 100 mm wide track is possible to generate. Figure 2-22 also shows a designed laser beam for the hardening process, the hardened width is 10 – 42 mm.

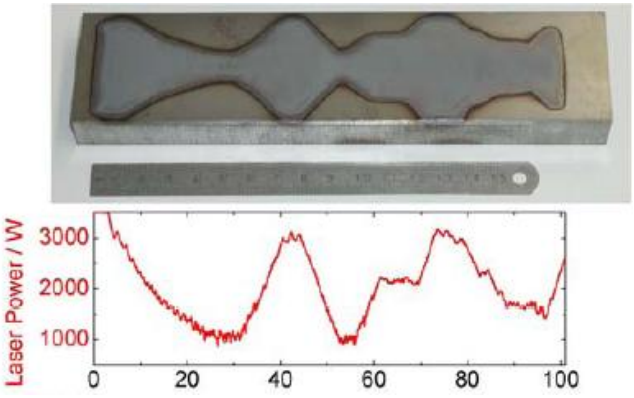

Figure 2-22 Heat treatment of tool steel with scanning optics and variable track width.

The scanning head technique is supported by the high laser power; for HPDL a main problem to scan the laser beam is to find a suitable scanning mirror with high reflectivity for the combination of two different wavelengths (808 and 940 nm) [66].

The other solution for the overlapping phenomenon is laser melting. With this technique the melting temperature is reached, so a part of the material adjacent to the surface melts, through the rapid solidification, very fine microstructures with improved hardness and wear resistance are yielded [72].

On grey and nodular irons surfaces, fine grained and very hard ledeburite microstructures were created in the melted surface layer and greater depth of the austenite transformation in the material was achieved [73][74]. Tulloch melted the gray cast camshafts for combustion engines applications [75], V. Lopez investigated the laser melting process with different ductile cast irons [76]. The melting process eliminated the porosity on the surface, but transverse cracks appeared on the surface with this treatment, the research also pointed out that the treatment process was strongly affected by the attributes of the materials, only the ductile iron with a perlitic matrix produced a layer of uniform hardness. H13 steel, which usually has bad thermal conductivity and diffusivity, was also investigated [77]. C. Li et al [78] developed an FEM based mathematical model to predicted that an ideal hardness and residual stress distribution can be obtained by choosing 30% overlapping ratio by melting process, but hardness still dropped in the overlapped zone. Experiments [79] also showed that the greatest residual stress at the surface is obtained when there is no overlap of the melted tracks.

2.4.3 Solutions to overlapping on cylindrical surface

Another solution to back tempering, in the case of cylindrical workpiece proposed by the authors, is to rotate the workpiece at high speed instead of low speed in traditional, and then increase the dimensions of the laser spot in a fictitious way. E. Capello and L. Giorleo [60] got an apparent spot (AS) by rotating a cylinder of 15mm diameter at 2100 rpm; a 1200 W diode laser was used to harden the surface of the cylinder. Uniform hardened zones without overlapping were achieved in AISI 1040 steel under different explosion time; the hardness is stable around 600HV and without drop. The effects of the process parameters (rotation speed, laser power and diameter of the workpiece) on the dimensions and hardness values of the hardened zones were pointed out [80]. Guy Claus and M. Seifert use two 6 kW high power diode laser [81], four different diameters 30, 40, 50, 60 mm. cylinders made of 42CrMo4V. Internal holes with diameters 10 mm and 20mm in 20 mm are hardened at 6000 rpm and different scan speeds. Hardness around 65HRC was achieved and its hardening depth between 0.3-0.8 mm depends on the different processes. Their research also indicates that the holes are more sensitive to the process. G.Tani used Finite Difference Method to develop a laser hardening simulator [82] [83], the simulator could choose the correct process parameters for operating time to treat the cylindrical workpiece by high rotation speed. The result of the simulator matches the real experiment results, that a hollow martensitic stainless steel AISI 420 cylinder of 72 mm diameter, a thickness of 2 mm could be hardened at 2 kW laser and 900 rpm.

Steffen Bonss [84] integrated the laser hardening system for cylindrical workpiece into production line to meet the industrial requirements. The valve cones were hardened within the turning machines, only 1.5 s was needed for the process.

However this technique still has to be addressed while lack of existing knowledge and deeper investigation is needed.

2.5 Conclusions

The review of the state of the art showed that laser hardening is a promising process for heat treatment, especially suitable for the workpieces need local hardening and/or with complex geometry. Nowadays, High Power Diode Laser (HPDL) is considered as a suitable laser source for laser heat treatment due to its beam properties.

But when large areas have to be treated by slightly overlapped multi-pass, one well-known drawback is the back tempering in the overlapped zone which induces a hardness decrease. Some studies worked on reducing or eliminating this problem, the

main solutions include scanning the laser beam into a desired shape and laser melting process for the planar surface; for the cylindrical surface, Apparent Spot technique was proposed to cover this drawback.

3 Objectives

This chapter is dedicated to the definition of the main objectives of the thesis work.

Chapter 2 has indicated that the laser hardening is a promising technology in nowadays industry, but the drawback of back tempering limits the laser hardening applications in some industrial areas. With the increase of the industrial requirement, the features and solutions to this drawback are investigated to extend the field of laser hardening applications.

According to this consideration, the main aim of the thesis work is to study the performance of the back tempering phenomenon in large laser hardened surfaces. The back tempering phenomenon on two kinds of surface, *i.e.* planar surfaces and cylindrical surfaces are investigated. Based on the investigation of this drawback, some techniques are proposed to reduce the overlapping and back tempering phenomenon on different surfaces.

With the purpose above, the objectives of this thesis are as follows:

1 Study of the features of the hardened zone obtained by laser hardening process without overlapping.

As the basis of this thesis work, the aims of this objective will be:

- Study the laser hardening performance by single track hardening, establish a relationship between the features of hardened zones, *i.e.* hardness,

geometrical features, and the investigated hardening parameters, *i.e.* scanning speed and hardening temperature.

- Optimize the process parameters to obtain a maximum productivity of the large surfaces hardening process.

2 Study and characterize the back tempering phenomenon in the overlapped zone.

After the investigation of the features of the hardened zone, attention will be focused on the overlapping process and back tempering phenomenon.

- On a planar surface
  (a) Investigate the effects of the overlapping length on planar surfaces to obtain uniform hardened depth.
  (b) Characterize the hardness decrease due to the back tempering phenomenon in the overlapped zones.
- On a cylindrical surface
  (a) Study the laser hardened overlapped zone on annular surfaces, without the laser feed rate.
  (b) Study the overlapped zones on wider cylindrical hardened surfaces.

3 Investigate different techniques to reduce or solve the back tempering phenomenon on large surfaces.

The solutions for the back tempering phenomenon will be proposed based on different kinds of surface.

- Execute laser melting technique on planar surfaces. Hardness features of the new microstructure and the hardness distribution in the overlapped zones during the laser melting process will be studied.
- Apply remote laser hardening process. Analyze the parameters used in the remote scanner head laser hardening process to obtain a large laser spot for large surfaces hardening.
- Investigate Apparent Spot (AS) technique to treat annular and cylindrical workpiece.

4 Base material, experimental setup, measurement procedure

In this chapter the experimental setup of the laser hardening process is introduced, including the analysis of the investigated base material, the setup of the laser system, and the short description of the measuring equipments and the definition of the measurement procedures.

4.1 Base material analysis

Two types of materials were analyzed in the laser hardening process. For the planar surface, the investigated material wasgrey cast iron, expressly used in mechanical components where the bulk material has to have high toughness and vibration damping properties, while the surface has to have high wear resistance. For the cylindrical workpiece, carbon steel was chosen, as it is one of the most widely used materials for crankshafts, valve cores, couplings and cold headed parts and so on.

4.1.1 Gray cast iron

Gray cast iron castings are readily available in nearly all industrial areas and are used in lots of components such as pistons, guides, and tool beds. Gray cast iron has excellent machining qualities, producing easily disposed of chips and yielding a surface with excellent wear characteristics. The investigated cast iron has a typical microstructure with pearlite matrix and the graphite flakes shown in Figure 4-1. The nominal chemical compositions of the grey cast iron used in the experimentation are listed in Table 4-1.

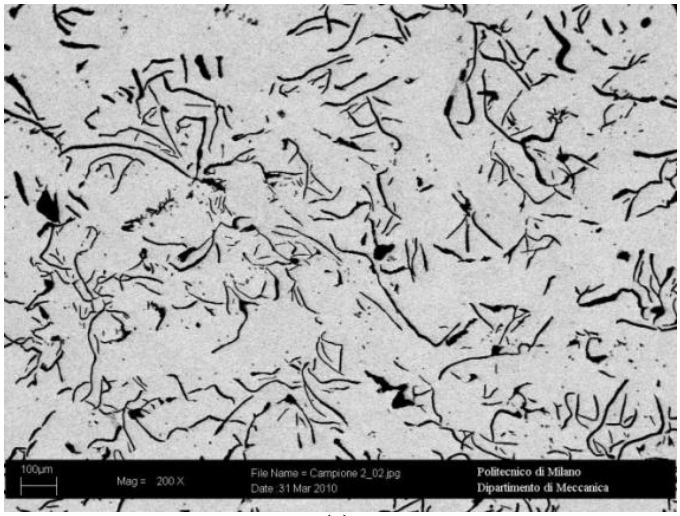

(a)

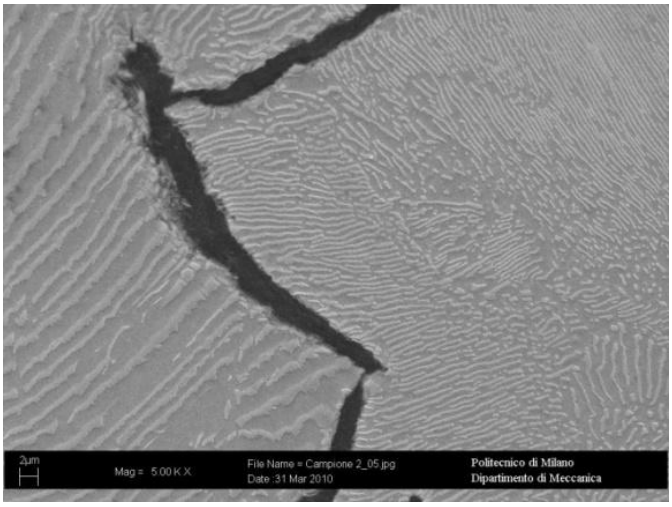

(b)

Figure 4-1 SEM images of microstructure of the cast iron (a) with low and (b) and high magnification.

Table 4-1 Nominal chemical composition (weight %) of the cast iron.

C	Si	Mn	P	S
3 – 3.2	1.5 – 1.8	0.7 – 0.9	< 0.15	< 0.12

In addition to the microstructure and the nominal composition, Vickers hardness tests were taken random positions on the surface to evaluate the original hardness of the basic material. The measured Vickers microhardness values are shown in Table 4-2

Table 4-2 Initial microhardness of the gray cast iron used.

	Microhardness (HV 0.3)								
No.	1	2	3	4	5	6	7	Average	Standard Deviation
HV	244-9	269.4	257.6	239.3	238.5	262.3	237	250	13

Based on the standard Fe-C diagram, the melting temperature of the base material was predicted using the carbon content, determined in the chemical composition analysis, as shown in Figure 4-2. This temperature was then confirmed to be around 1150-1200 ℃ by temperature measurements made with a pyrometer (details of the experiment will be explained in chapter 5).

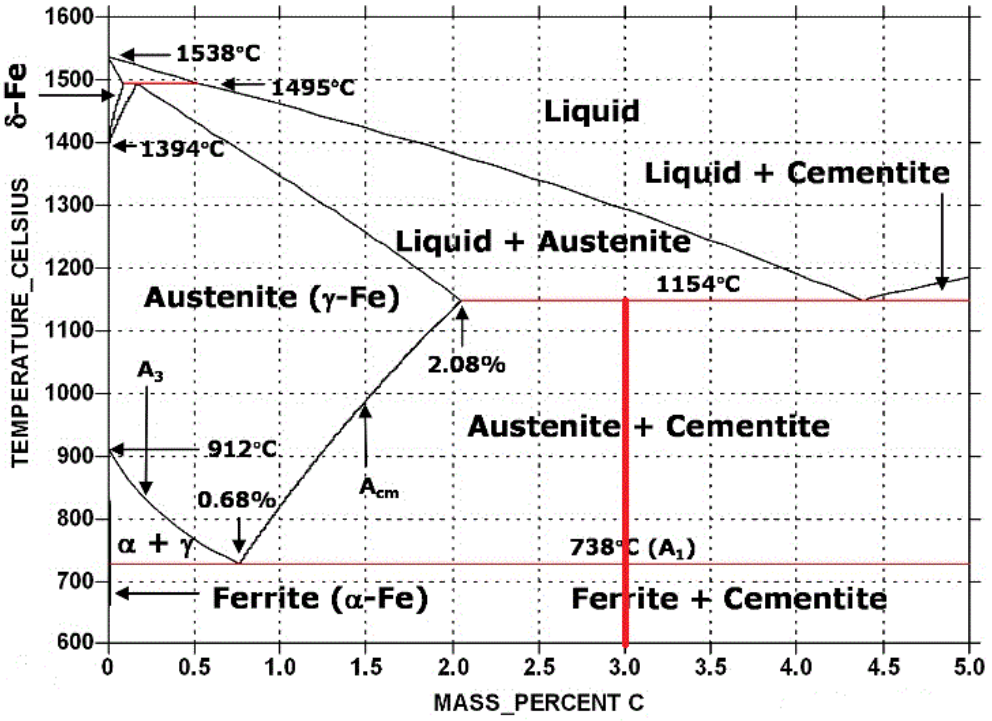

Figure 4-2 Fe-C% diagram.

The melting temperature of the base material was predicted by evaluating the chemical composition, and then was confirmed to be around 1150-1200 ℃ by temperature measurements made with a pyrometer (details of the experiment will be explained in chapter 5).

4.1.2 Carbon steel

Medium carbon steel, AISI 1040, was selected as working material for the cylindrical workpiece, with the microstructure shown in Figure 4-3, and the nominal chemical composition and microhardness of the used steel are reported in Table 4-3. The melting point was predicted and measured in the same way as cast iron, which was then found to be in the range of 1500-1550 ℃.

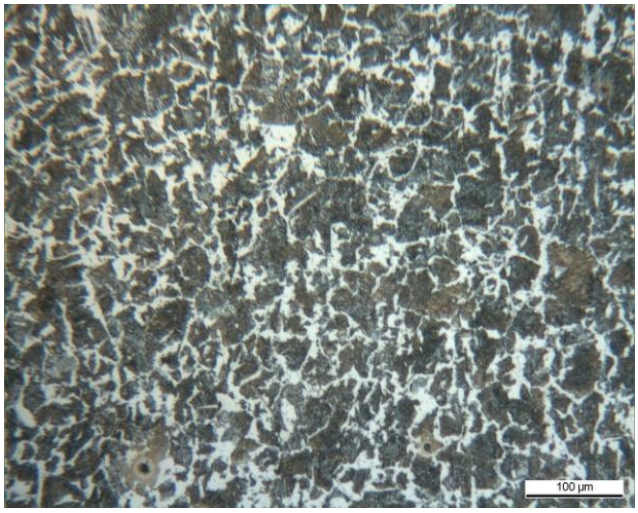

Figure 4-3 Microstructure of AISI 1040 the carbon steel.

Table 4-3 Nominal chemical composition (weight %) of the carbon steel.

C	Fe	Mn	P	S
0.37-0.44	Bal.	0.6-0.9	< 0.04	< 0.05

Table 4-4 Initial microhardness of the AISI 1040 carbon steel.

Microhardness (HV 0.5)												
No.	1	2	3	4	5	6	7	8	9	10	Average	Standard Deviation
HV	221	234	246	257	209	226	238	243	258	235	237	15

4.2 Laser hardening systems

Two different strategies, involving two different types of laser equipment, are investigated. Firstly, the heat treatment of large areas was obtained by slightly overlapping several single passes that are laser hardened by a proximity head focusing a direct diode laser beam (Figure 4-4(a)). This configuration is named in the following "proximity laser hardening". Successively, a short experimentation is also performed making use of a scanning laser head, operating with an active fiber laser, which allows obtaining large spot area by the fast oscillation of the laser beam in two directions. This configuration, named in the following "remote laser hardening", is depicted in Figure 4-4(b).

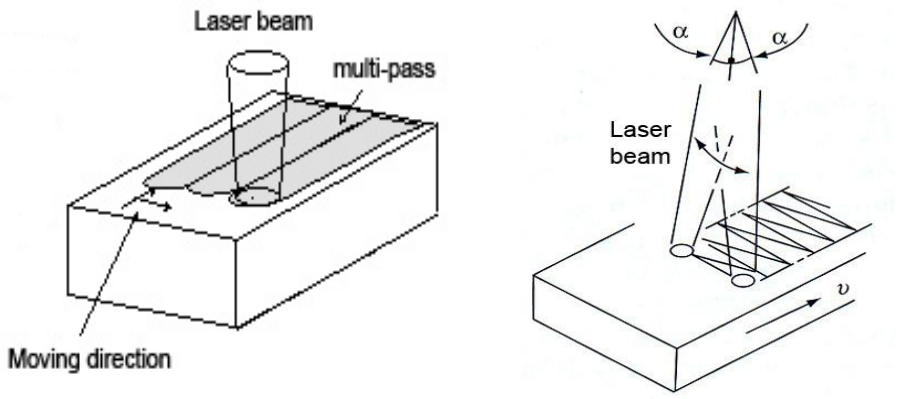

(a) Proximity laser hardening (b) Remote laser hardening

Figure 4-4 Scheme of laser hardening systems.

4.2.1 Proximity laser hardening equipment

The proximity laser hardening system is composed by a diode laser, an anthropomorphic ABB robot, a pyrometer and a control system. The scheme and practical setup of the hardening system is shown in Figure 4-5. Tset is the reference temperature value, T(t) is the real time measured temperature, based on these two values, P(t) – the laser power is controlled in real time.

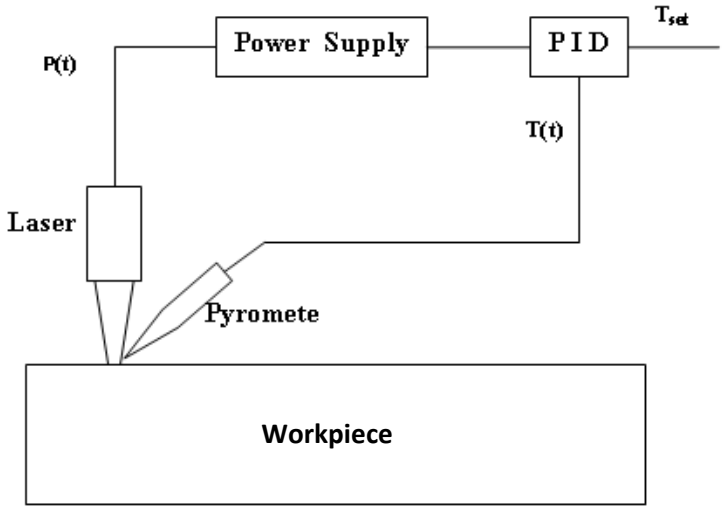

(a) Scheme of the proximity laser system.

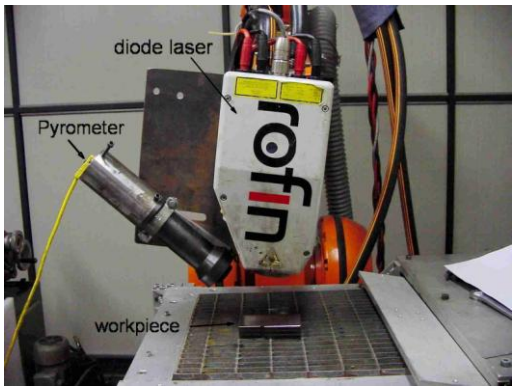

(b) Practical setup for planar surface.

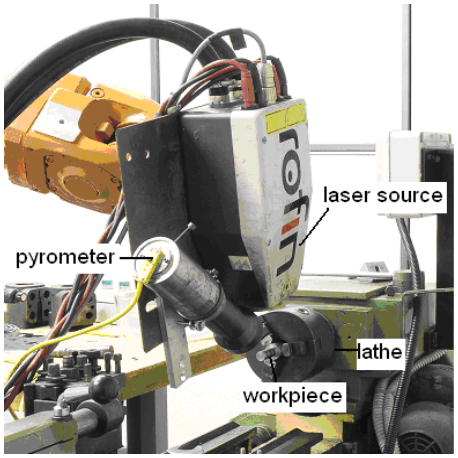

(c) Practical setup for cylindrical surface.

Figure 4-5 Scheme and practical setup of the hardening system.

Diode lasers have many inherent properties which make them particularly suitable for heat treatment applications. Some of their main characteristics are as follows:

– Wavelength

The wavelength of the radiation emitted from most practical diode is between 800 and 940 nm. Due to its shorter wavelength, diode laser radiation has a considerably higher degree of absorption into metallic surfaces compared with CO_2 or Nd:YAG laser. This means coating is not necessary for the hardening process.

– Beam profile

The beam profile of diode laser is generally top-hat in the slow axis direction and Gaussian in the fast axis direction with a rectangular shaped spot due to the nature of the beam formation process. Figure 4-6 shows the laser beam profile of the diode laser used in the experimentation.

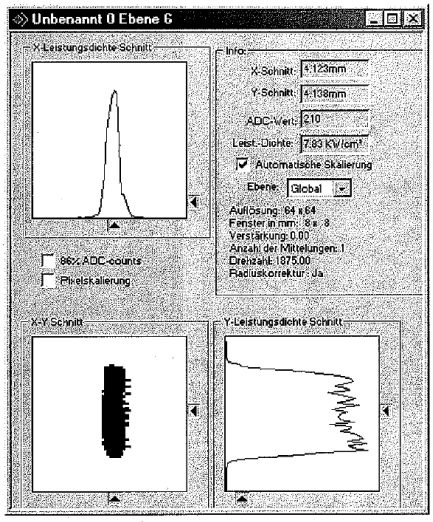

Figure 4-6 Diode laser beam profile of SITEC.

In addition, diode laser is also known for the high wall plug efficiency, compact size, and high temporal stability.

At SITEC, a 1250 W continuous wave Rofin DL022 diode laser (λ=808 nm and 940 nm) is used for laser hardening. The laser is fixed on a 6- axis ABB robot. The laser spot has a rectangular form with dimensions of 2 mm x 6 mm. In order to achieve the maximum power density on the hardening area, the laser was focused on the material surface. During the process, the laser scanning direction is parallel to the slow axis of the spot as shown in Figure 4-7 (a). For the cylindrical surface, the 2 mm axis of the laser beam was parallel to axis of the workpiece. The directions of the laser beam are shown in Figure 4-7(b). No shield gas was applied.

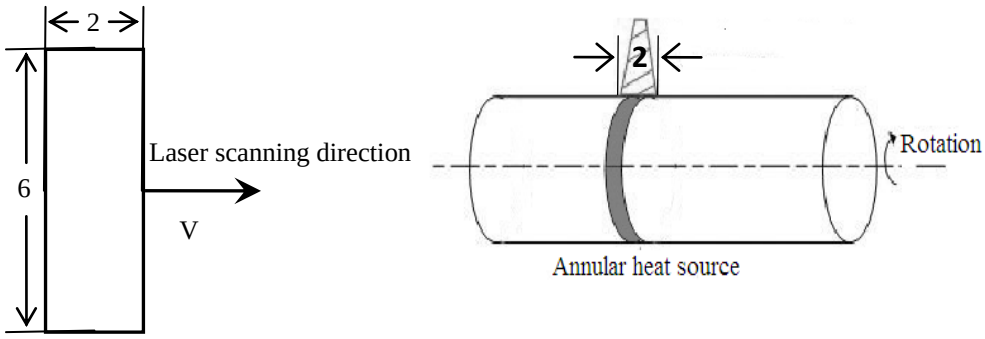

(a) on planar surface (b) on cylindrical surface

Figure 4-7 Geometry features of the laser beam on the workpieces.

Some typical features of the laser hardening process that require further attention can be listed as such:

- Laser hardening is a very fast process, the heating and cooling rates in the order of 1000 K/s are common;
- The operating window is quite narrow from austenite temperature AC_3 to melting point;
- The coefficient of absorption of a metallic surface has a stepwise increase when the temperature reaches the melting point and can vary significantly in presence of superficial discontinuities, such as roughness difference, dirt and oil traces, different colour and optical properties.

Therefore to monitor and control the hardening temperature is essential to keep the depth of the treated area constant. For this purpose, In SITEC the power supply of the laser is connected to a measurement and close-loop control system composed of a pyrometer and a PID regulator.

- Pyrometer

The SITEC handmade pyrometer is composed by a germanium sensor, several filters and a focus lens. The germanium sensor has a very large pass band from 800 to1800 nm, and is sensible in the near infrared zone, where the optical power of the surface at high temperature is at maximum. A set of filters are used for cutting off the reflection of the diode laser beam and avoiding the attenuation of the air. The focus lens is used to focus the emitted optical energy on the germanium sensor. The scheme and practical parts of the pyrometer are reported in Figure 4-8

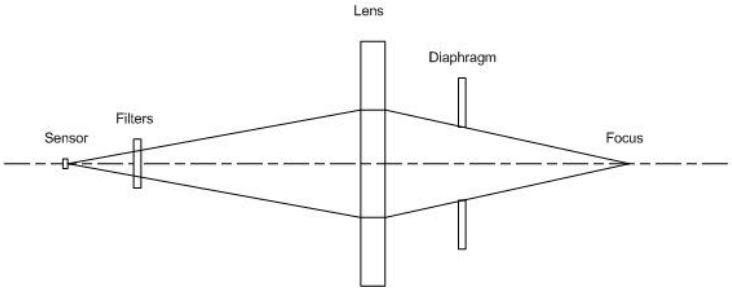

(a) Scheme of the pyrometer

(b) Practical pyrometer

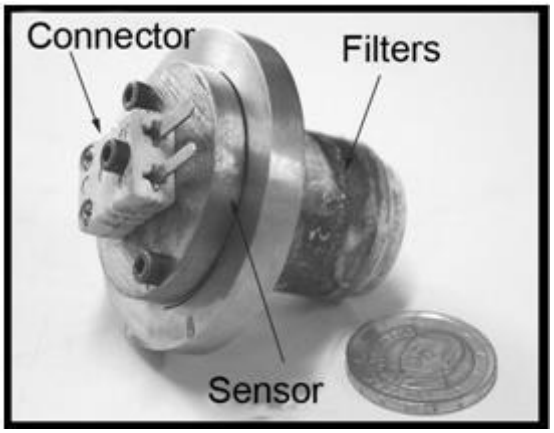

(c) Practical parts of the pyrometer

Figure 4-8 scheme and practical parts of the pyrometer.

- Control system

The control system is composed by LabView software and a data acquisition board provided by National Instruments (NI-DAQ) for signal acquisition. An amplification circuit is adopted to amplify the electrical signal generated by the pyrometer to several voltages which can be measured by the DAQ. During the process, the pyrometer measures the thermal radiation from the workpiece surface and then transforms the measured emission to temperature values. This temperature values is then compared to a reference value. Then the PID regulator produces a signal used by

the laser source to control the power. The surface temperature is kept at the reference temperature by varying the laser power.

The most important features of the pyrometer are reported in Table 4-5, where t_r is the rise time of the pyrometer considering the delay of both the amplifying and the measuring circuit.

Table 4-5 Important features of the pyrometer.

t_r [ms]	Measurement spot Diameter [mm]	Accuracy [℃]	Measuring range [℃]
0.3	2	± 20	700 - 1500

With this measuring and control system, it is possible to control and get a stable temperature on the workpiece surface, as shown in the example of Figure 4-9.

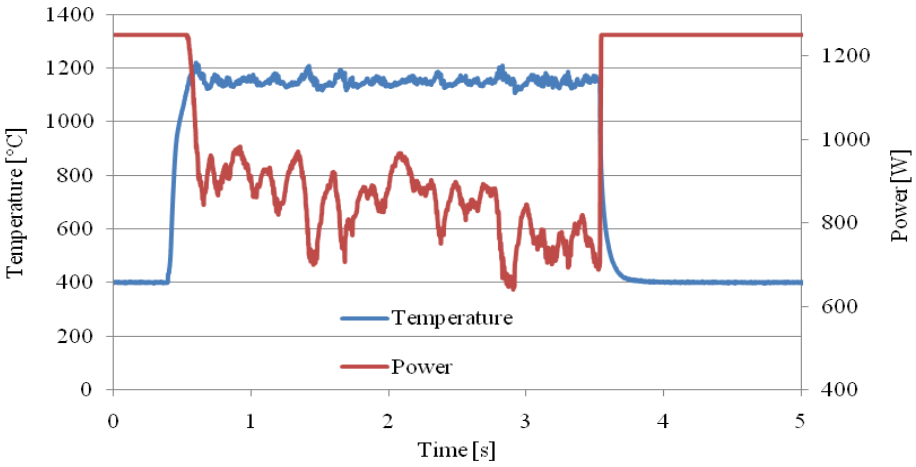

Figure 4-9 Real time measurements of temperature and controlled laser power.

With the measurement and control system, different combinations of temperature on the surface and laser scanning speed were tested to optimize the hardening process.

4.2.2 Remote laser hardening equipments

As discussed above, the remote laser hardening is based on high power laser; the scanning laser head system is composed by an IPG 5kW fiber laser and a galvanometric scanner heard produced by Gruppo El.En. The scanner and the laser system are shown in Figure 4-10.

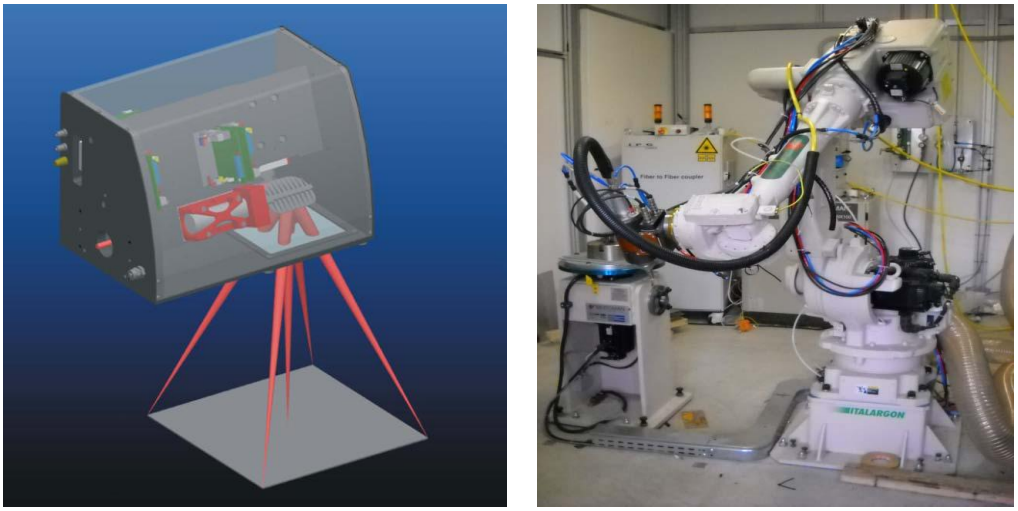

(a) Galvanometric scanner (b) Laser system

Figure 4-10 Remote laser hardening system.

The scanner head is composed by a collimating lens, focus lenses, two galvanometers and digital control system. The parameters of the scanner head are listed in Table 4-5. Table 4-6 gives the characteristics of the fiber laser.

Table 4-5 Parameters of the scanner head.

Collimating length	Focusing length to gavanometers	Focusing length of the system	Working distance
60 [mm]	135 [mm]	300 [mm]	214.2 [mm]

Table 4-6 Characteristics of the fiber laser.

1. Optical characteristics							
N	Characteristics	Test conditions	Symbol	Min.	Typ.	Max.	Unit
1	Operation Mode			CW / Modulated			
2	Polarization			Random			
3	Nominal Output Power		P_{nom}	5000			W
4	Output Power Tuning Range			10		105	%
5	Emission Wavelength	Output power: 5000 W	λ	1070		1080	nm
6	Emission Linewidth	Output power: 5000 W	Δλ		3	6	nm
7	Switching ON/OFF Time	Output power: 5000 W			50	100	μs
8	Output Power Modulation Rate	Output power: 5000 W				5	kHz
9	Output Power Instability	Output power: 5000 W Time interval: 8 hrs (T=Constant)			±1	±2	%
10	Red Guide Laser Power				0.5	1	mW

2. Optical output							
N	Characteristics	Test conditions	Symbol	Min.	Typ.	Max.	Unit
1	Feeding Fiber connector			HLC-8, QBH-compatible			
2	Beam Parameter Product (1/e2)	Feeding Fiber core diameter 50 μm length 15 m	BPP		2	2.5	mm* mrad
3	Feeding Fiber Core Diameter			50			μm
4	Feeding Fiber Length		L	15			m
5	Feeding Fiber Bending Radius		R	100			mm

4.3 Measurement and analysis procedure

After the experiments the treated samples were analyzed for geometric features, hardness values and wear behavior of the hardened zone. Sections of the heat treated tracks were prepared under some common metallographic procedures. The samples were cut along the cross sections using an abrasive disc while water cooling was used to avoid microstructure damage. Abrasive papers with different grit meshes were used in the initial fine grinding; the finest abrasive paper is 2500. Water cooling and lubricate were used throughout the grinding process. Three kinds of nylon cloth

wheel, 6μm, 3μm and 1μm were used in sequence for final polishing, ethanol was applied for lubricant. 2% Nital reagent (2% nitric acid and 98% ethanol) was applied for 5-10 seconds to etch the samples.

4.3.1 Geometrical features of the treated samples

In single pass laser hardening the cross section of the hardened zone was observed with the optical microscope and the SEM. The geometric features of the treated area, width (W_H) and depth (D_H) were measured by means of standard image analysis with the standard image analysis software.

In laser hardening process the measured geometric features of the hardened zone are shown in Figure 4-11.

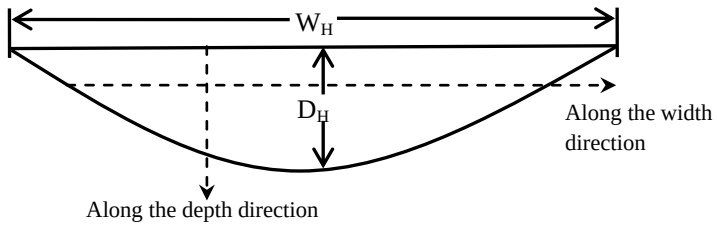

Figure 4-11 Geometrical features of the laser hardened zone.

In laser melting process two kinds of treated zones are observed, i.e. the melted zone in the upper part of the surface and the heat treated zone in the lower part. The two kinds of the treated zones are shown in Figure 4-12. The geometrical features of the treated zone are the same as the hardening process; the dimension of the melted zone is measured in terms of width (W_M) and depth (D_M).

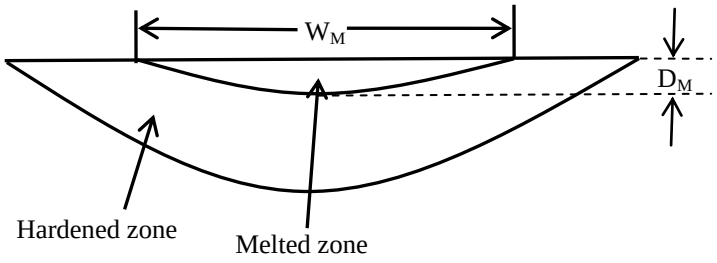

Figure 4-12 Geometrical features of the laser melted zone.

In multi-pass laser hardening two geometrical attributes, overlapping length (OL) and overlapping depth (OD), allows the overlapping zone to be characterized, as shown in Figure 4-13. In preliminary design of the experimentation, the approximate OL was

calculated considering the width of the hardened zone equals to the width of laser spot.

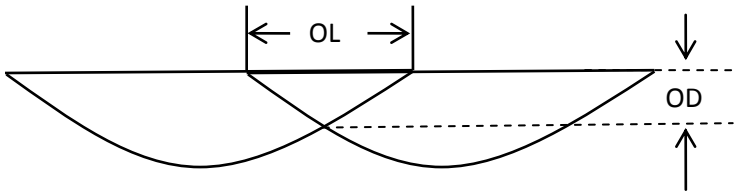

Figure 4-13 Overlapping length (OL) and overlapping depth (OD) in the multi-pass process.

4.3.2 Hardness measurements

Hardness measurements are used to obtain information on the mechanical properties of the hardened layers and base material, Vickers hardness tests were applied. The measurements were performed with a load of 300 g applied for 15 seconds. Micro hardness tests in the hardened zone were executed in longitudinal direction at certain distance, *e.g.* 0.15 mm, from the top surface and along the depth direction at a centre of the treated area as shown in Figure 4-14 (a). In the overlapping process, the hardness tests were executed also in the overlapped zone (see Figure 4-14 (b)).

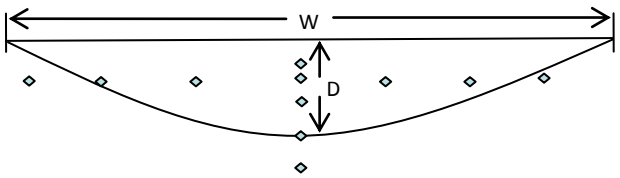

(a) Hardness measurement in the hardened zone

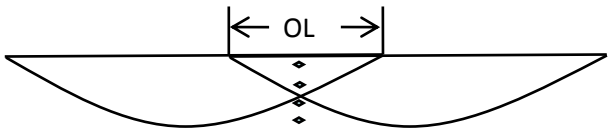

(b) Hardness measurement in the overlapping area

Figure 4-14 Vickers hardness test procedure.

5 Proximity laser hardening on planar workpiece

With the measurement and control diode laser system, both single track hardening and multi-pass hardening were carried out on the cast iron surface. In the single track process, different combinations of scanning speed and constant temperature on the surface were investigated; geometrical features and microhardness of the hardened zone were analyzed. Based on the single track hardening, multi-pass hardening was executed with different overlapping length.

5.1 Base material melting point analysis

The hardening temperature and the scanning speed are parameters that influence the process mostly. Higher temperature on the surface induces deeper hardened zone, and when the temperature is set, the limitation of the scanning speed is determined by the laser power.

To ensure the transformation of pearlite to austenite is completed, high temperature above Ac_3 and below the melting point on the surface should be achieved, and the melting point of cast iron is lower, so the operating window of the hardening process,

so the melting point has to be ascertained for the maximum hardening temperature level. By the Fe-C% diagram, the melting point of cast iron is between 1100-1200 ℃; three levels of temperature in this range and two levels of scanning speed were chosen to investigate the melting point of the basic material. The parameters of experimental setting up are in Table 5-1.

Table 5-1 Experimental parameters for melting point test.

No.	temperature (℃)	Scanning speed (mm/s)
1	1200	10
2	1100	10
3	1100	4
4	1150	4

The experimental results showed that from 1150 ℃ with the lower scanning speed 4mm/s, the surface starts to melt as shown in Figure 5-1, there was a distortion on the top surface because of the melting (a) and the structure on the top surface is shown in (b), in the centre of the top surface, compared with the hardened zone, the graphite flakes were not present, but dissolved in the melted surface. The experimental tests confirmed the melting point of the basic material from the Fe-C% diagram; the melting point of the base material is 1150 ℃ – 1200 ℃. With the measurement and control system, it is possible to control the temperature on surface below the melting point. 1100 ℃ was chosen as the maximum temperature for the subsequent experiments.

(a) Deformed top surface by melt

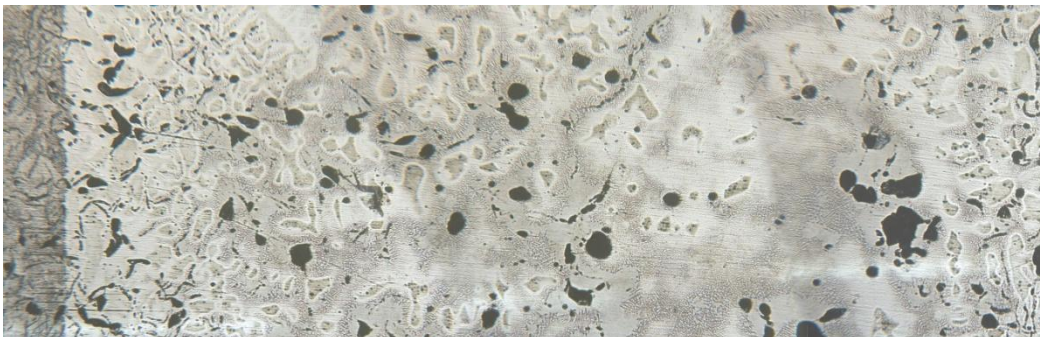

(b) Melted top surface

Figure 5-1 Cross section and top surface of the melted sample (1150 ℃-4 mm/s).

5.2 Proximity single track laser hardening

5.2.1 Experimental parameters for proximity single track laser hardening

Two experimental campaigns of single track laser hardening were designed to investigate the parameters of the process. Independent single passes were executed to understand the effects of different levels of scanning speed and temperature on the hardened zone. The temperature and scanning speed levels are listed in Table 5-2.

Table 5-2 Process parameters used in single pass hardening campaign.

Temperature on the surface [℃]	1100, 1000
Scanning speed [mm/s]	10, 7, 4

For each process condition the temperature values and the controlled laser power were recorded in real time as shown in Figure 5-2.

Speed [mm/s]	Temperature [℃] 1100	1000
4	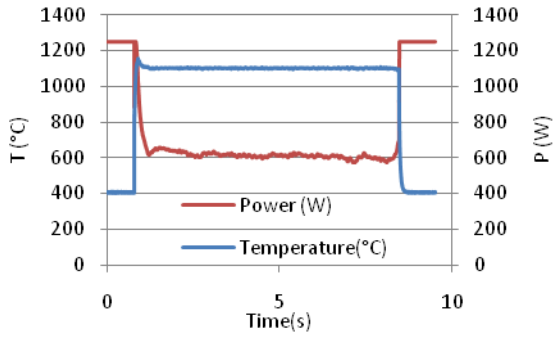	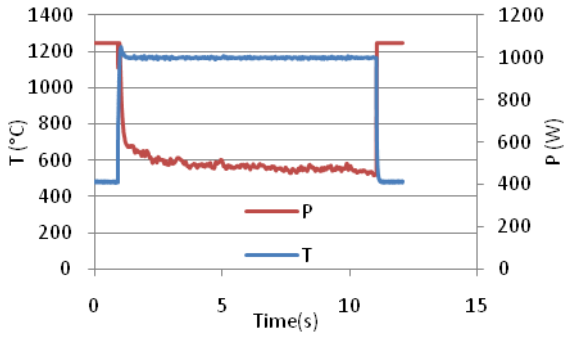
7	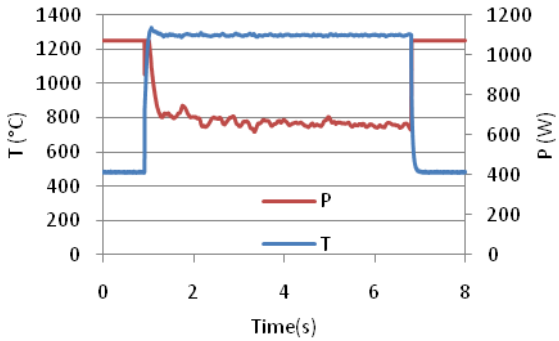	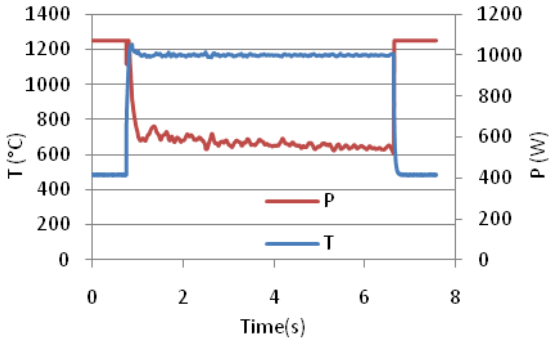

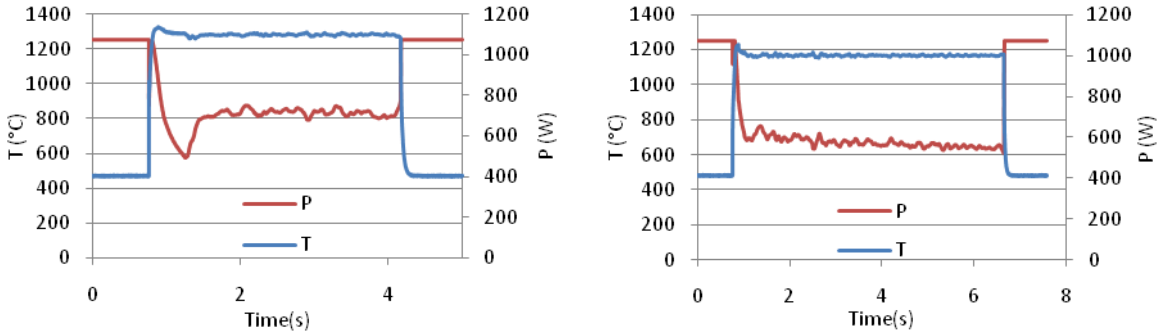

Figure 5-2 Real time measured temperature and controlled laser power for single track.

Five intervals were taken to evaluate the average power for every process. During every interval, one average power was calculated by averaging the power measurements in the stable phase. The five average powers for every process are shown in Figure 5-3.

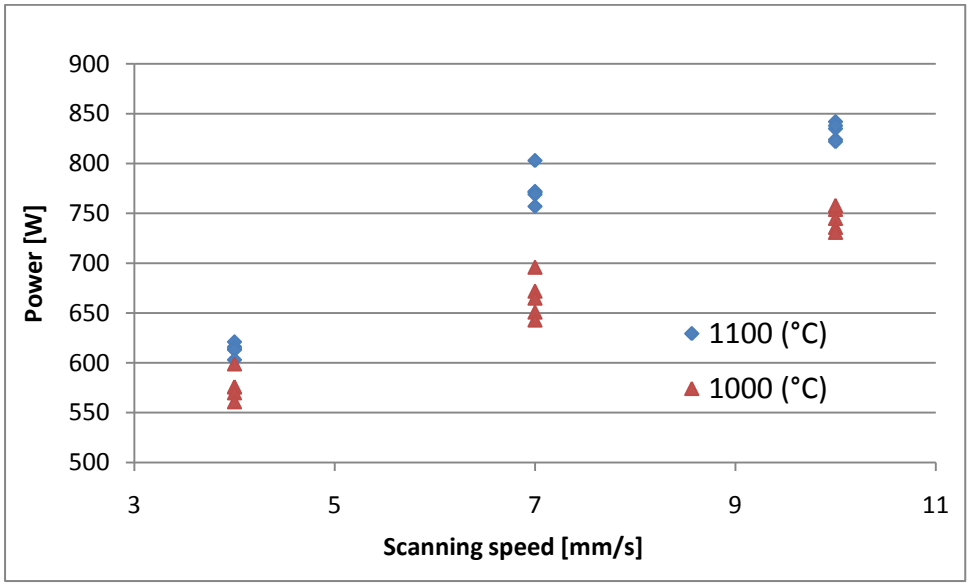

Figure 5-3 Laser power related with scanning speed and temperature.

5.2.2 *Microhardness feature for proximity single track hardening*

Figure 5-4 (a)-(d) shows the microstructure and microhardness analysis along the depth of the hardened zone. The analysis of results shows that during the laser hardening process, a homogeneous microstructure is obtained in the hardened zone regardless of the depth.

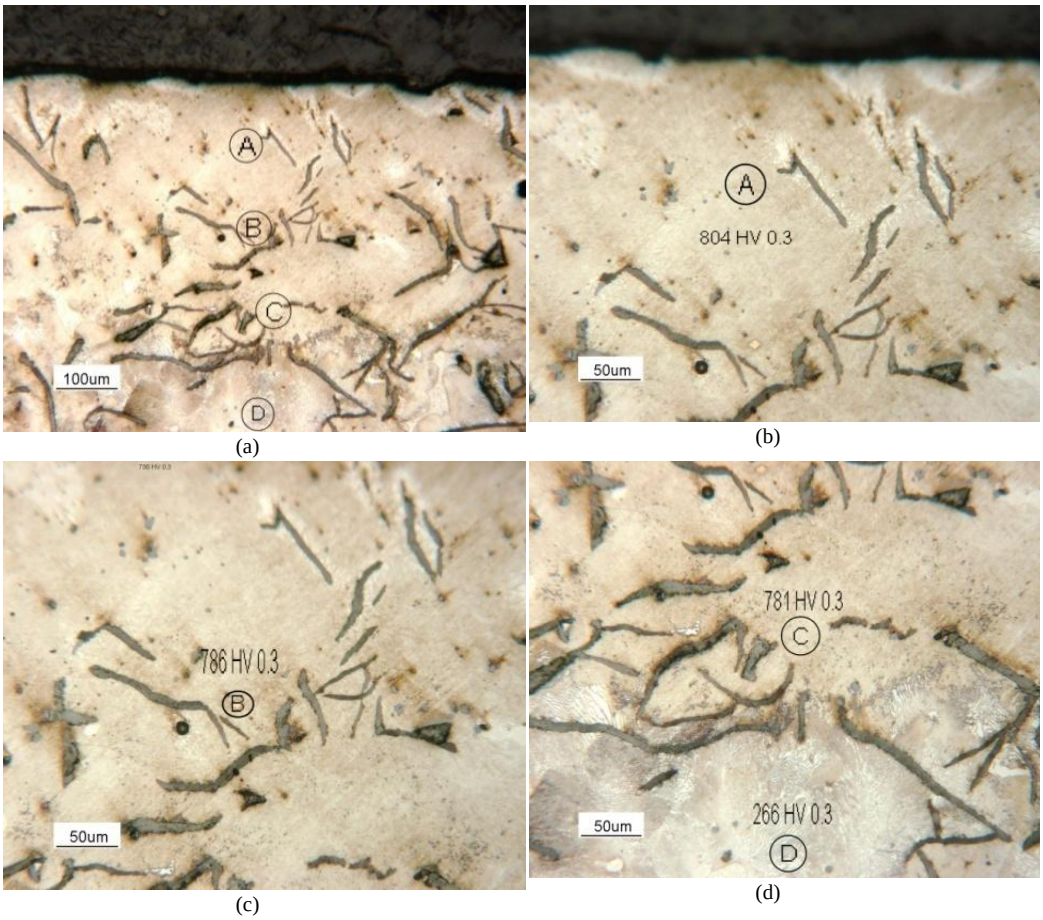

Figure 5-4 Microstructures of the hardened zone by single track hardening.

For every hardened sample, the hardness tests were carried out along the width and depth direction of the hardened zone, the hardness profiles are reported in Figure 5-5 and 5-6. Hardness profiles indicate that the hardness is related neither to the temperature nor to the scanning speed. A uniform hardness distribution is obtained in each hardened zone. The hardness range was 700-800$HV_{0.3}$.

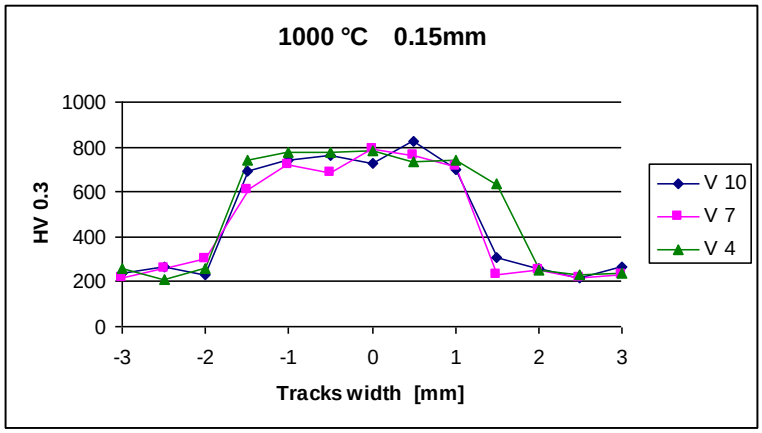

(a)

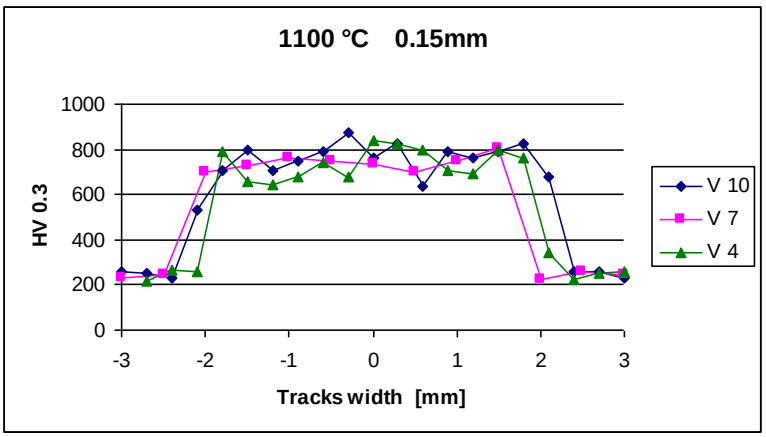

(b)

Figure 5-5 Hardness profile along the track width of the single track hardening.

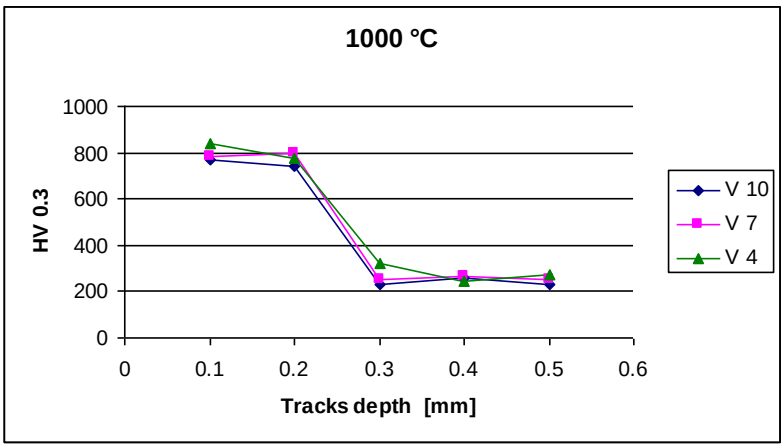

(a)

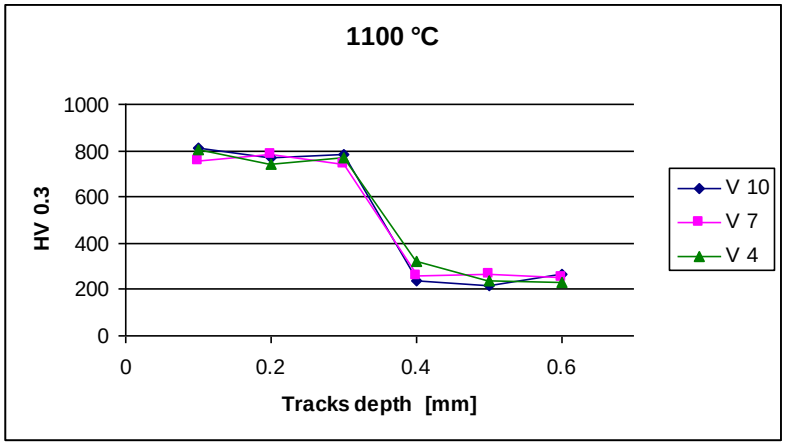

(b)

Figure 5-6 Hardness profile along the track depth of the single track hardening.

The results of the single track hardening show that by the measurement and control system, when the temperature reaches Ac_3, each combination of different levels of temperature and scanning speed produces a homogeneous hardened zone and uniform hardness distribution. This is also confirmed by the SEM as shown in Figure 5-7. Microstructures were analyzed along the depth of the hardened zone, the pearlite on the top and in the middle of the hardened zone have been completely transformed; on the other hand, some pearlite and partially transformed materials were observed at the boundary of hardened zone and base material. The depth of the hardened zone is strongly influenced by the investigated parameters. Considering the high productivity, high temperature and high scanning speed were chosen as the parameters for multi-pass investigation.

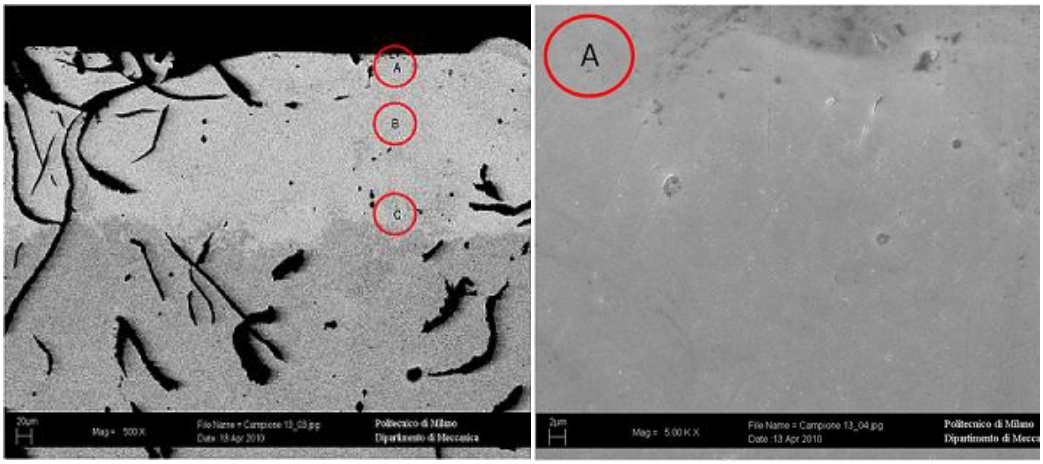

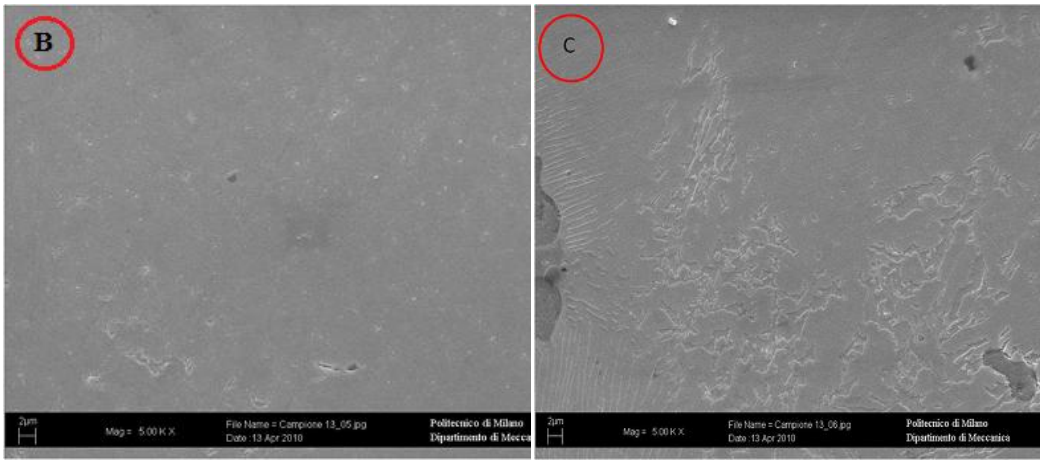

Figure 5-7 SEM analysis of the hardened zone.

5.2.3 Selection of the best condition

The microhardness tests confirmed the high hardness was obtained in the hardened zone; the geometrical features were investigated to obtain an optimized process and ensure a required hardened depth.

Figure 5-8 shows the typical geometric dimensions of the laser hardened zones. In Figure 5-9, the experimental results are reported in terms of width and depth as a function of scanning speed and surface temperature.

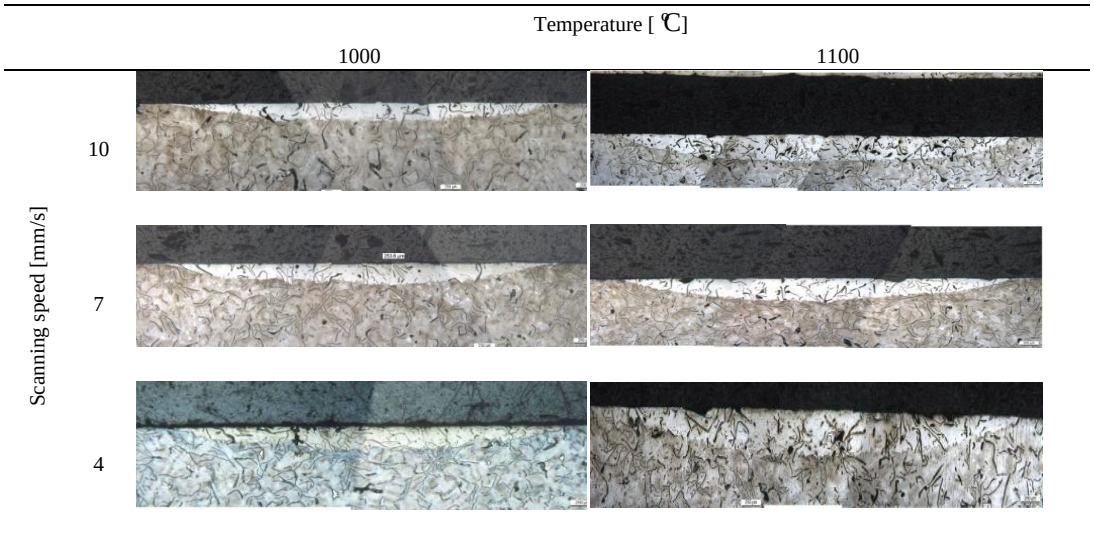

Figure 5-8 Hardened zone obtained by different parameters.

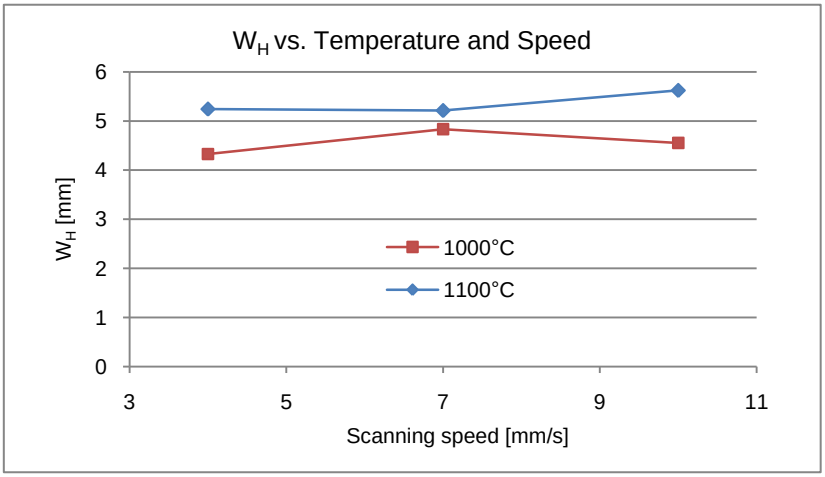

(a) Hardened width vs. temperature and scanning speed

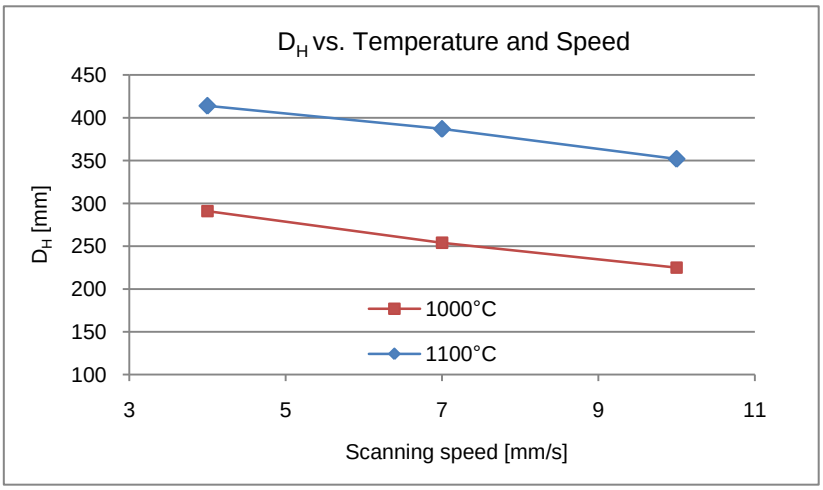

(b) Hardening depth vs. temperature and scanning speed

Figure 5-9 Geometric dimensions of laser hardened zone.

The width of the hardened zone is mainly determined by the dimension of the laser spot, on the contrary the treated area depth is affected by both parameters: temperature and speed.

In terms of the temperature values, it can be interpreted that higher temperature on the surface means more energy input, which induces a deeper hardened zone. When the temperature on the surface is constant, faster scanning speed needs higher laser power and induces a faster thermal cycle that produces a thinner hardened zone. The maximum hardening depth can reach 0.41 mm by keeping the temperature at 1100 ℃, and scanning the workpiece at the lowest speed 4 mm/s.

With higher temperature on the top surface, deeper hardened zone was obtained, considering the productivity, higher temperature 1100 ℃ and higher scanning speed 15 mm/s were chosen as the parameters for the multi-pass laser hardening.

5.3 Proximity multi-pass laser hardening

To treat a large area, multi-pass technique is adopted. Since the overlapping process induces two main drawbacks: non uniform surface hardness and non uniform hardening depth, the parameters should be adopted carefully to minimize these drawbacks.

5.3.1 Experimental parameters for proximity multi-pass laser hardening

Based on the results of single pass hardening, process parameters for overlapping process were set and overlapping experiments were carried out. From the results of the previous experiment, temperature and scanning speed parameters were set as 1100 ℃ and 15 mm/s to get a productive system. Four levels of overlapping lengths were adopted: 0.75 mm, 1 mm, 1.25 mm, 1.5 mm.

5.3.2 Microhardness and geometrical features for proximity multi-pass hardening

A large surface was treated by the overlapping process with different overlapping length, as shown in Figure 5-10. The top surface was covered by the hardened zones; and the overlapped zones exist between the two adjacent hardened zones. The microstructure shows the reheated material in the previous track, it is tempered martensite with lower hardness.

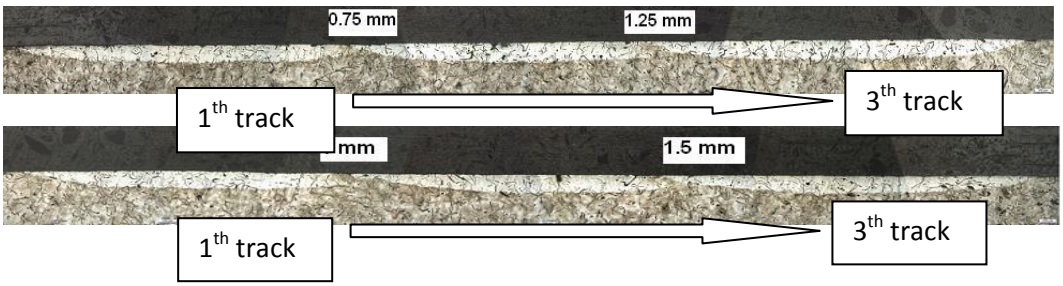

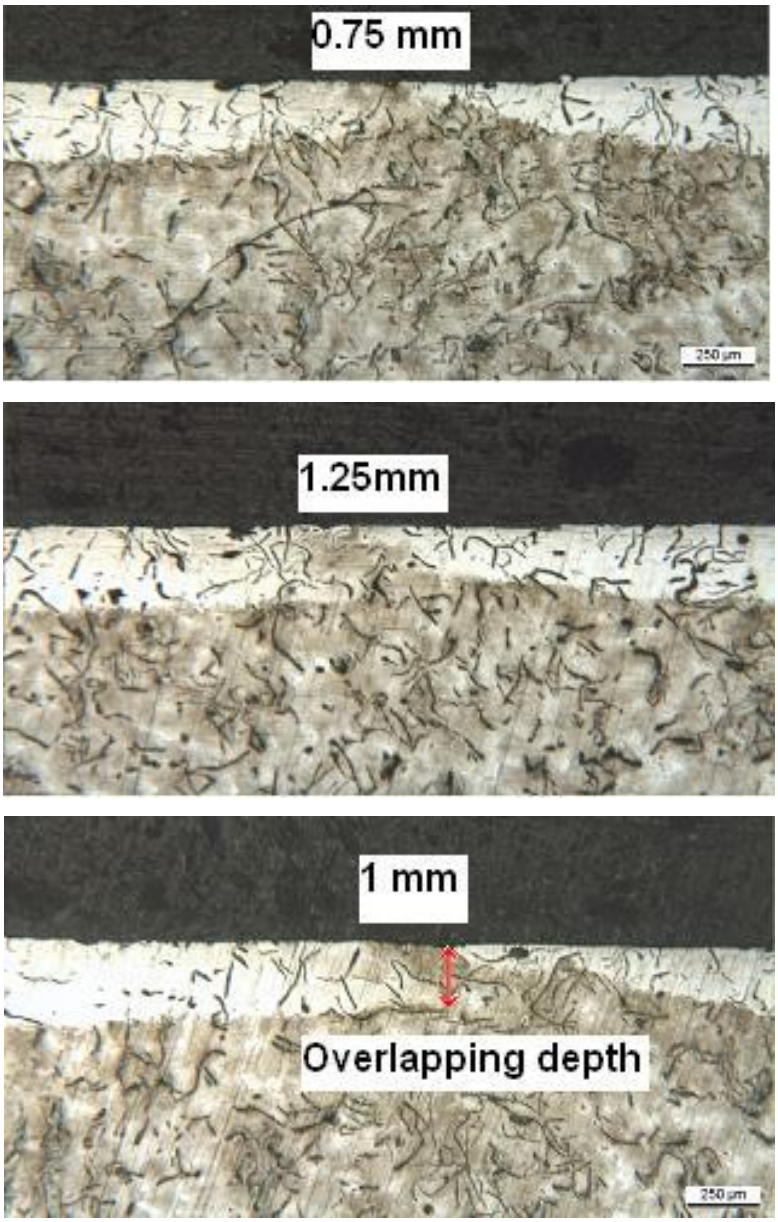
0.75 mm
1.25mm
1 mm
Overlapping depth

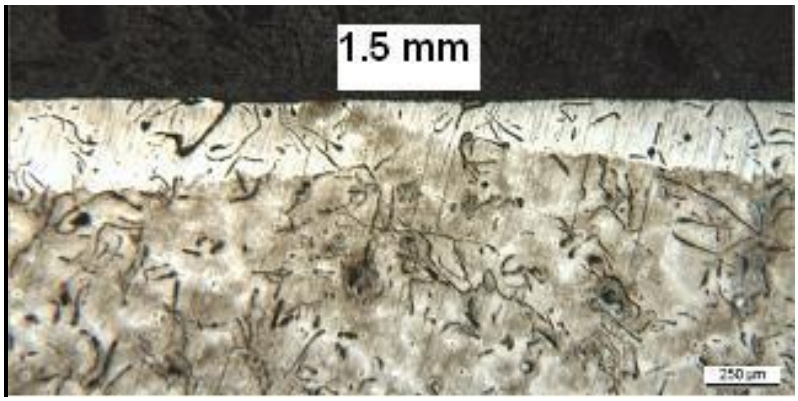

Figure 5-10 Microstructures of hardened zone with different overlapping lengths.

The measured temperature and controlled laser power were recorded in real time and listed in Figure 5-11, the measurements show that by means of the control system, the power of the laser decreased because of the accumulated heat in the bulk, constant temperature was obtained for each track, in the meantime.

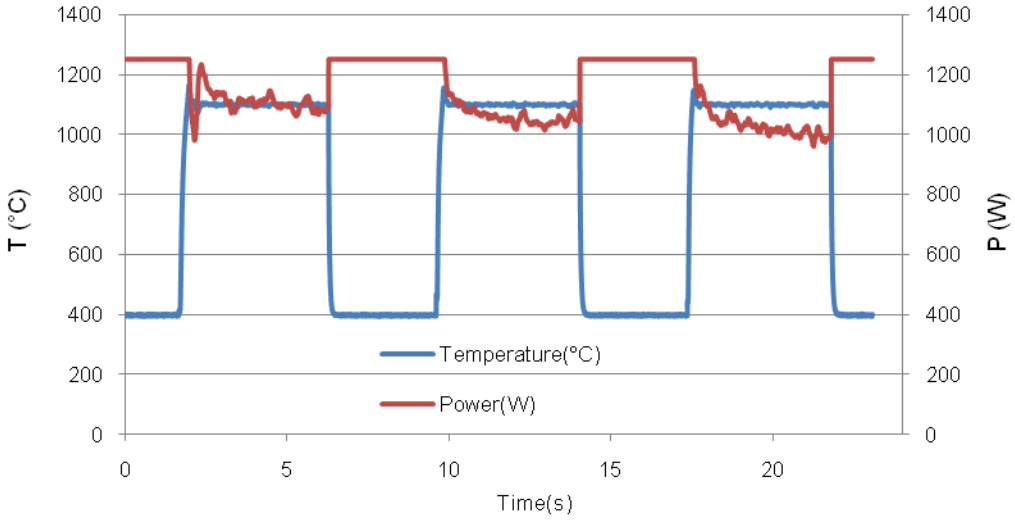

Figure 5-11 Real time temperature and laser power for multi-pass hardening.

One disadvantage exists in the overlapping process is the non uniform depth of the hardened zone; it is influenced by the overlapping depth. With different overlapping lengths, different overlapping depths were achieved. For every overlapping depth, five measurements were carried out; the results are reported in Figure 5-12. Only a thin layer is obtained with a small overlapping length equal to 0.75mm. An increased depth was obtained by adopting larger overlapping length.

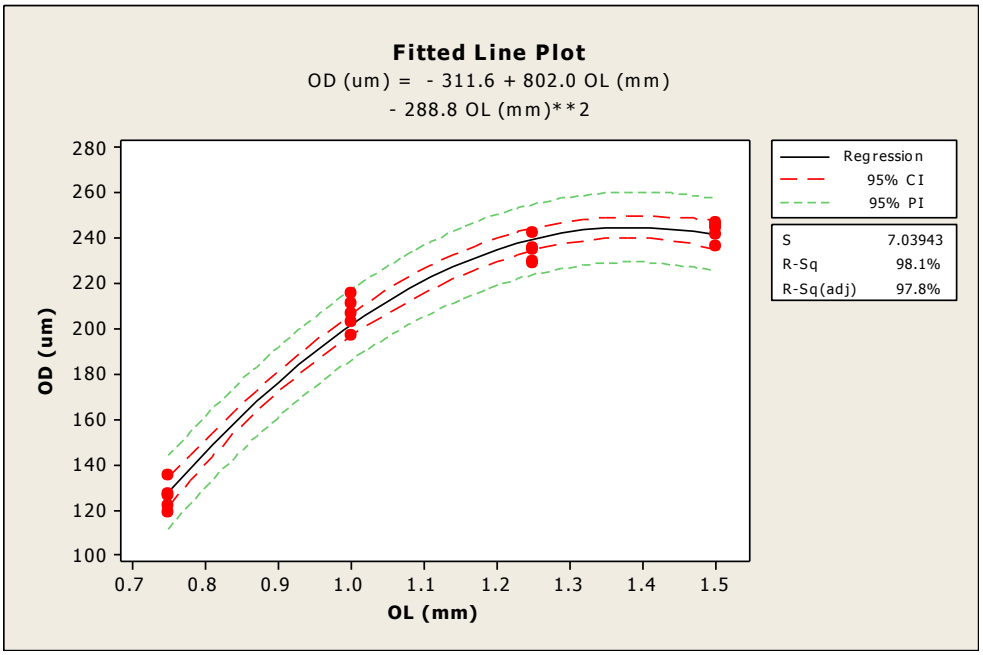

Figure 5-12 Overlapping depths (OD) in different overlapped zones.

Figure 5-13 shows the hardened top surface by overlapping process, overlapped zones could be recognized on the top surface. Microhardness was tested on the top surface and in the cross section along the width direction, based on the red coordinate axis; in the cross section, the test distance is 0.15 mm from the surface. The distance between each test is 0.3 mm. The microhardness profiles across the transverse direction are reported in Figure 5-14.

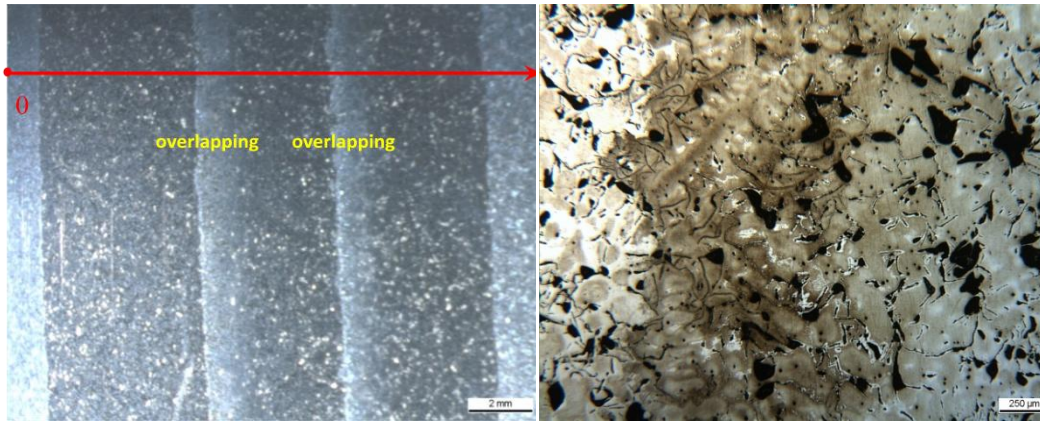

(a) Top surface of the hardened sample by overlapping process

(b) Microstructure of the overlapped zone on the top surface

Figure 5-13 Treated top surface by overlapping process.

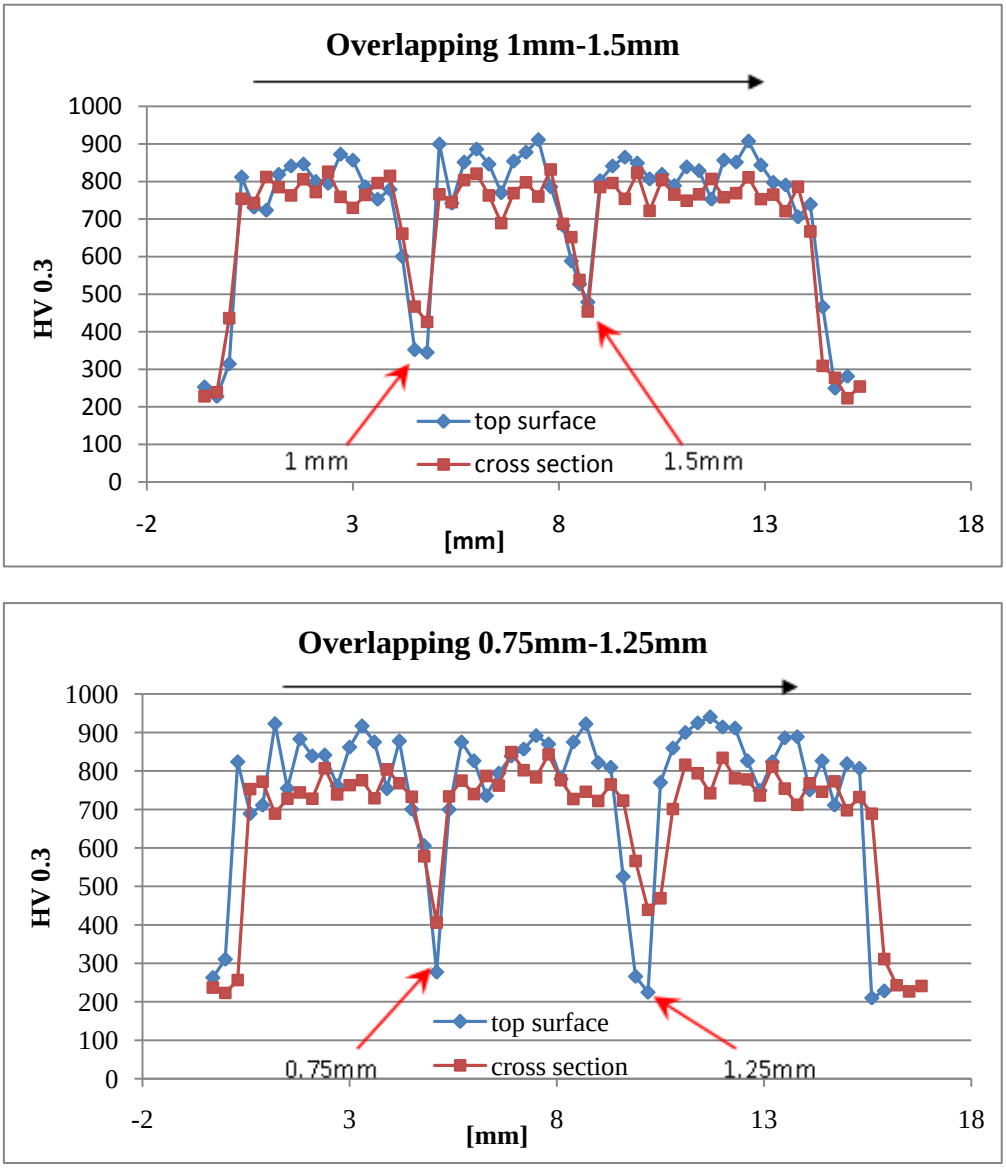

Figure.5-14 Hardness profiles on the surface of overlapped zones.

By comparing the measured hardness on the top surface and in the cross section, the results indicate that, for the hardened zone, the hardness on the surface is higher (in the range of 800HV to 900HV) than it in the cross section (in the range of 700HV to 800HV). On the contrary, the hardness reduction in the overlapped zone was observed both on the top surface and in the cross section, but the hardness decreased severely on the top surface, could be lower than 300HV. To investigate the hardness

distribution in the overlapped zone, the hardness was tested along the depth of the cross section and the hardness profiles are shown in Figure 5-15-

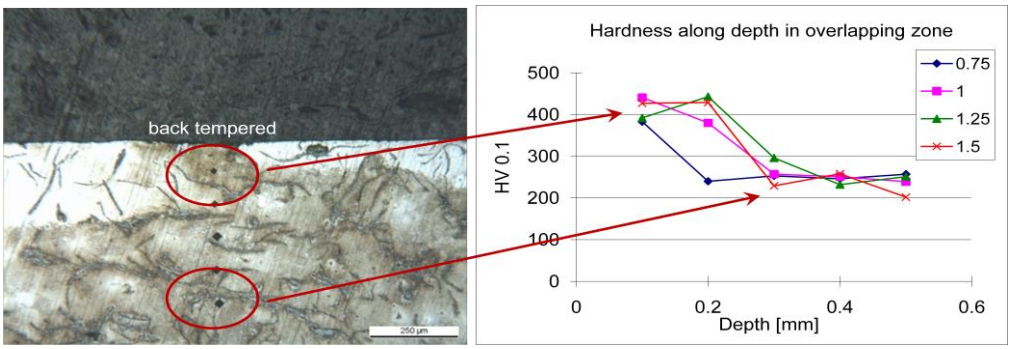

Figure 5-15 Hardness test in the cross section of the overlapped zones.

In the back tempered area the reduction of microhardness values is uniform, the hardness in the overlapped zone is around 400 HV, when the tests were carried out in deeper zone, the hardness decreased to the value of basic material. The hardness tests in the overlapping also indicate the overlapping depths in different overlapping width process, for small overlapping length process, *i.e.* 0.75 mm, only 0.1 mm overlapped zone with 400HV was obtained, and then the hardness drops to the base material value. With wider overlapping length (1 mm-1.5mm), overlapping depth more than 0.2 mm was ensured.

High temperature on the top surface ensures a high productivity, under the requirement of certain hardened depth. The hardened tracks obtained by 1100 ℃ were investigated in terms of laser power and geometrical features. The first hardened track during the multi-pass hardening could be considered as a hardened zone treated by single track. Combined with the single track hardening results, the relationship between controlled laser power and scanning speed is shown in Figure 5-16. The other important factor that influences the industrial applications is the depth of the hardened zone, for every hardened zone, five measurements were carried out, and the depth of the hardened zones obtained by different scanning speeds are shown in Figure 5-17. The adjusted coefficient of determination R^2_{adj} is 98.5%. The normal probability plot of the residuals shown in Figure 5-18 also indicates that data are distributed normally.

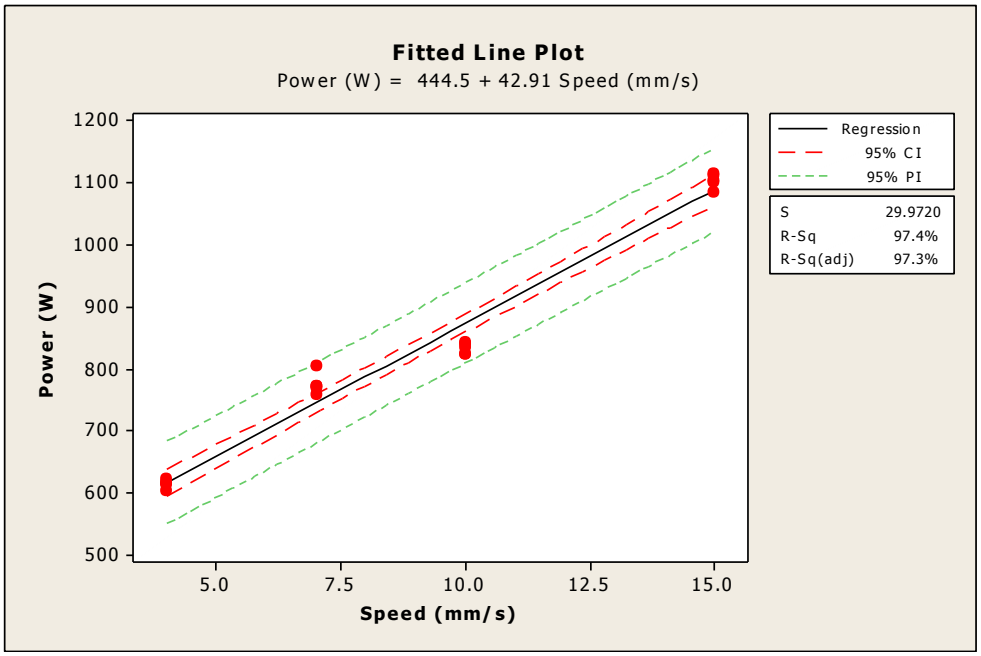

Figure 5-16 Relationship between controlled laser power and scanning speed.

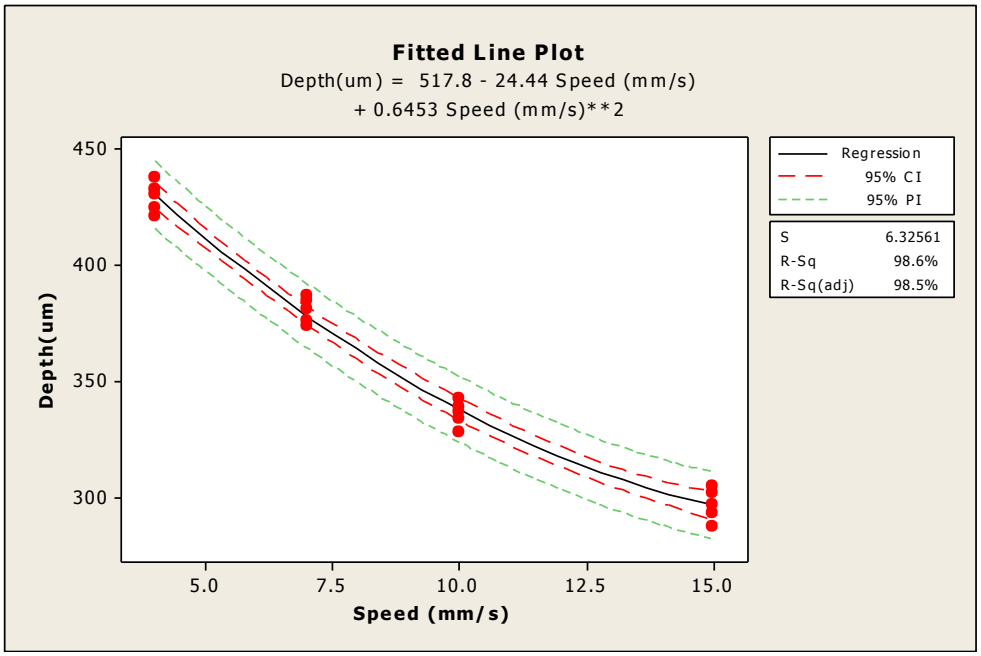

Figure 5-17. Relationship between depth of the hardened zone and scanning speed.

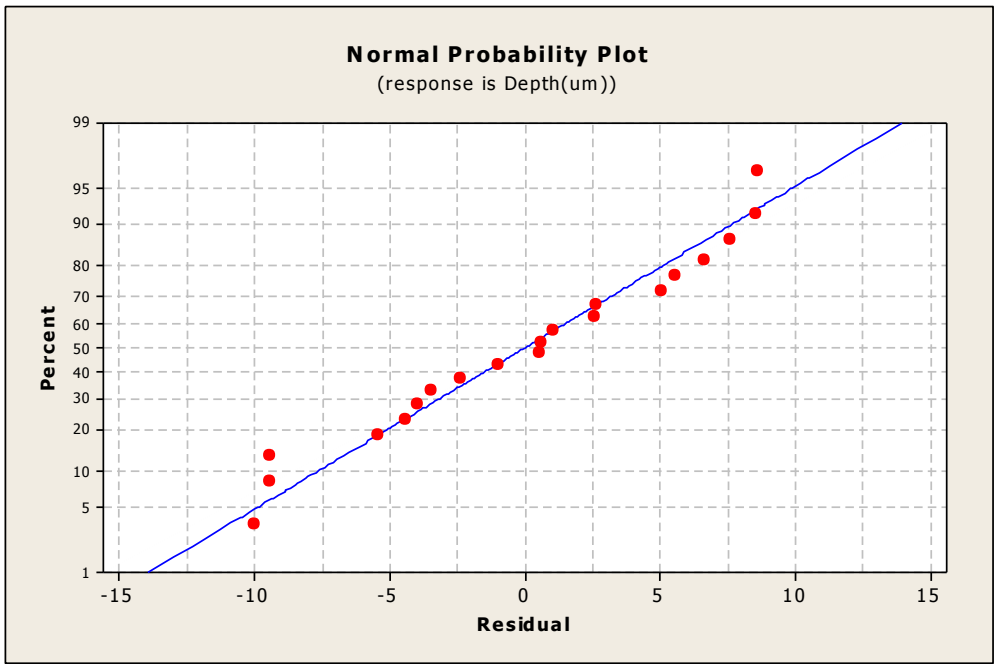

Figure 5-18 Normal probability plot of the residuals for hardened depth.

Considering the combination of uniformity of hardening depth and uniformity of hardness, the parameters for overlapping process can be optimized. Larger overlapping length ensures a uniform hardening depth, but for a given surface, it also means more hardening tracks, and induces more overlapped zones with hardness reduction. In case of diode laser hardening with a rectangular laser spot and uniform energy distribution, the depth of the hardened zone is more uniform than that obtained by other kinds of laser with a Gaussian distribution. In diode laser hardening, when overlapping length reaches a certain point, the depth in overlapped zone does not increase significantly, and a uniform hardened zone in depth can be obtained. When the overlapping length exceeds this point, it induces more overlapped zones and hardness reduction. For this experimental campaign, the critical point is 1.25mm. A valid range for overlapping length is from 1 mm to 1.25 mm, which corresponds to the 16.7-20.8% of the nominal hardening track width. The following experiments for wear test selected the overlapping length within this window.

5.4 Conclusions

A uniform hardened zone can be obtained in single pass laser hardening of gray cast iron with a high power diode laser. Within the operable window, two levels of high temperature (1000 ℃ and 1100 ℃) were chosen and different scanning speeds were carried out to study the effects of the parameters on the hardened zone, in terms of geometrical features and hardness distribution. Considering of the high productivity,

a higher speed 15mm/s was used to investigate the back-tempering phenomenon in the overlapping area.

The main conclusions of this experimental study are:

1. Uniform hardness was obtained in the laser hardened zone, whose hardness values range from 700 to 800 $HV_{0.3}$ in the cross section, regardless to the temperature and scan speed. The hardness on the top surface was higher than it in the cross section (800 – 900 $HV_{0.3}$).
2. Geometrical features of the hardened zone were determined by both temperature and scanning speed.
   - The width of the hardened zone was mainly determined by the dimension of the laser spot.
   - The depth of the hardened zone is affected by both parameters. High temperature and low scanning speed induce more heat input, which results deeper hardened depth.
   - In the industrial applications, the hardening temperature on the surface is set before the hardening process; in this case, considering the temperature as a constant, under a certain requirement of hardened depth, the scanning speed and minimum laser power are decided.
3. In the overlapping area the micro-hardness values show an abrupt decrease, due to the re-heating of the previous obtained martensite which is temped. The loss of hardness value is uniform in depth; the hardness in the overlapped zone is 400HV. Different overlapping lengths do not affect the range of hardness decrease.
4. Large overlapping length ensures a uniform overlapped depth. In this experimental study, the overlapping length from 1 mm to 1.5 mm ensures 0.2 mm overlapping depth.

6 Laser surface melting

As discussed in the previous chapters, back tempering phenomenon is the main drawback of the laser hardening applications on large surfaces. In this chapter, one solution to the back tempering problem – laser surface melting technique is proposed for planar surfaces. When the surface of the base material is heated above the melting point, a fine grained microstructure with high hardness is obtained in the melted zone, with appropriate melting process, a uniform thickness of the melted surface could be ensured in spite of the overlapping process. Other than the uniform thickness, greater depth of hardened zone is achieved. Experimental campaigns for laser melting process were designed with a standard diode laser for single track and multi-pass. Different melting conditions were studied and a large surface was treated by laser melting, no hardness decrease was observed in the overlapped zones

6.1 Single track laser melting process

The single track laser melting experiments were carried out to understand the effects of the melting process on the cast iron surface. The features of the melted zone were investigated to look for an optimized condition for the overlapping process.

For single track laser melting process, three levels of temperature above the melting point and two levels of scanning speed were chosen. The investigated parameters are

listed in Table 6-1, the real time measurements and the microstructures of the melted zones are shown in Table 6-2 and 6-3.

Table 6-1 Process parameters used in single pass melting campaign.

Temperature on the surface (T) [℃]	1300, 1400, 1500
Scanning speed (V) [mm/s]	3, 5

Table 6-2 Real time measurement for laser melting process.

T [℃]	Speed [mm/s]	
	3	5
1300	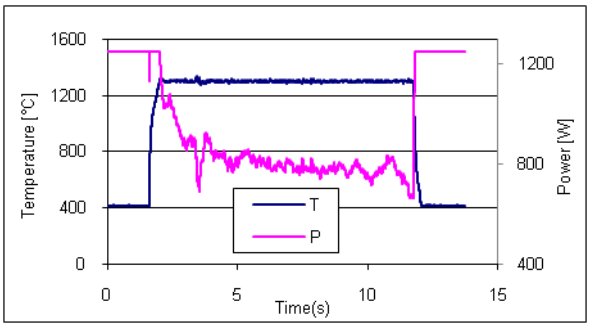	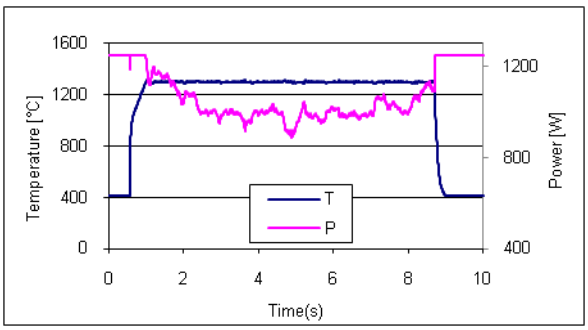
1400	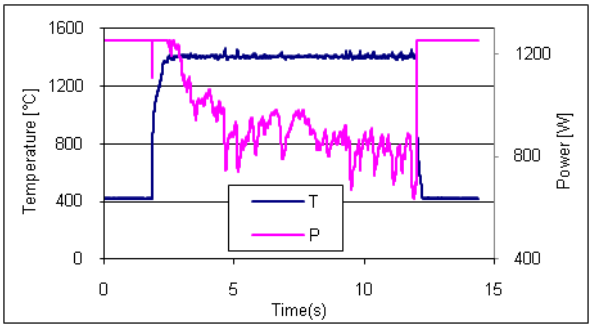	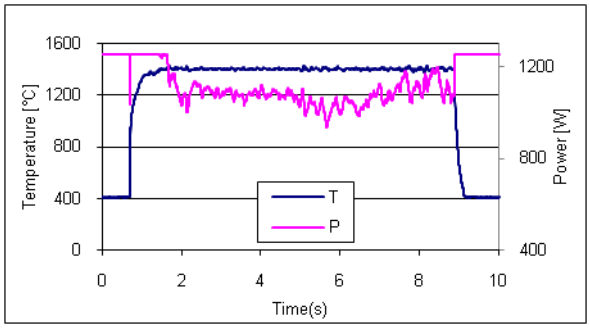
1500	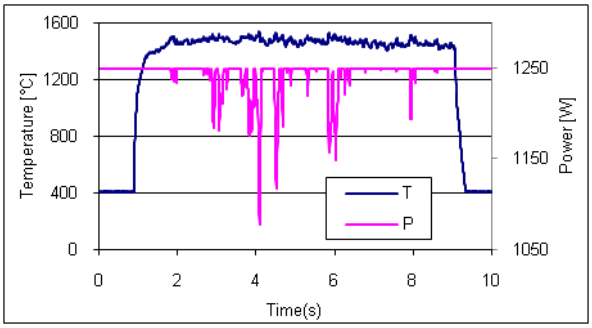	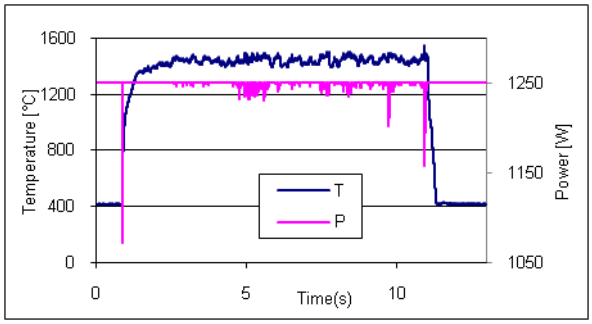

Table 6-3 Melted-hardened zones obtained in the melting process.

V[mm/s]	T[℃]	Melted-hardened zones obtained in the melting process
3	1300	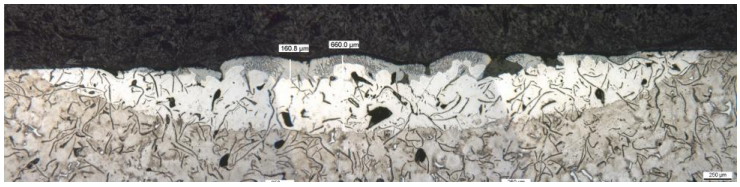
	1400	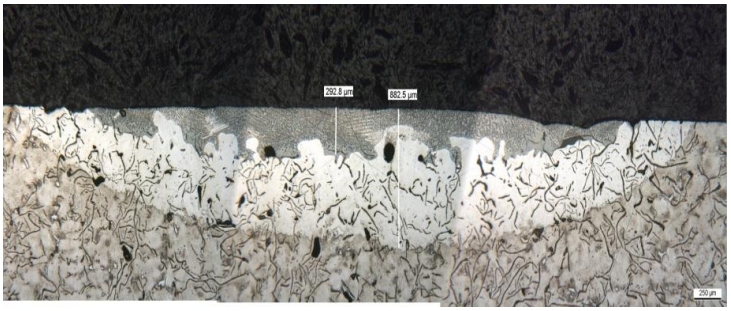
	1500	
5	1300	
	1400	

	1500	

In the single track laser melting process, when the controlled temperature on the top surface is above the melting point, melted layers were obtained in all the experimental conditions regardless to the scanning speed. The modified surface consisted of two different microstructure zones, i.e. a melted zone in the upper part of the surface layer and a hardened zone in lower part. In Figure 6-1(a) and (b) microstructures in the melted zones are shown with different magnification. Compared to the hardening process, the graphite flakes in the base material dissolved in the melted zone, hardened zone was obtained as shown in Figure 6-2.

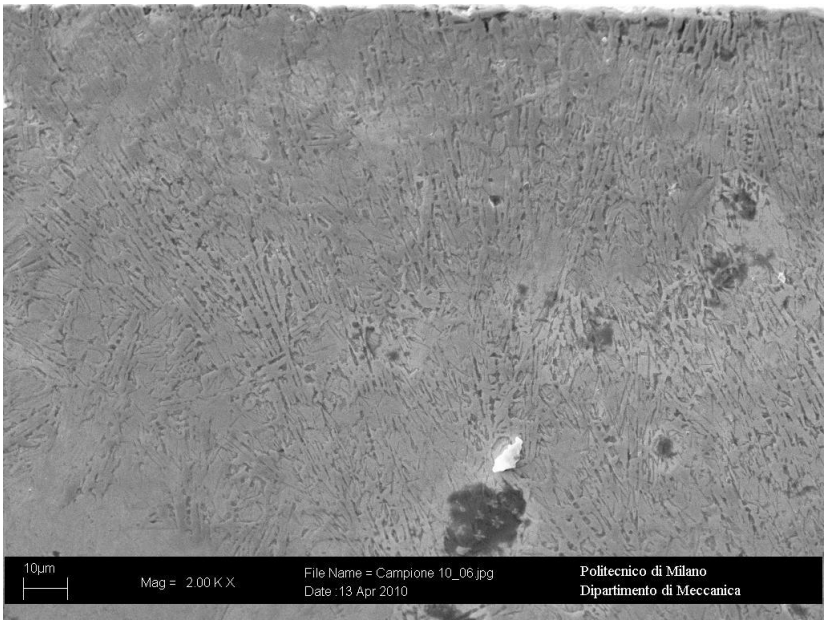

(a) Small magnification

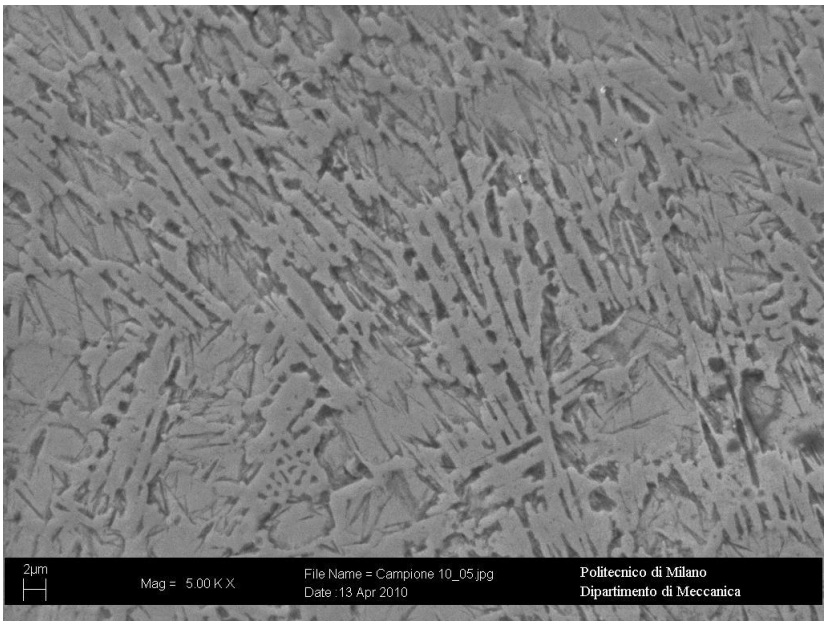

(b) large magnification

Figure 6-1 Microstructures in the melted zone.

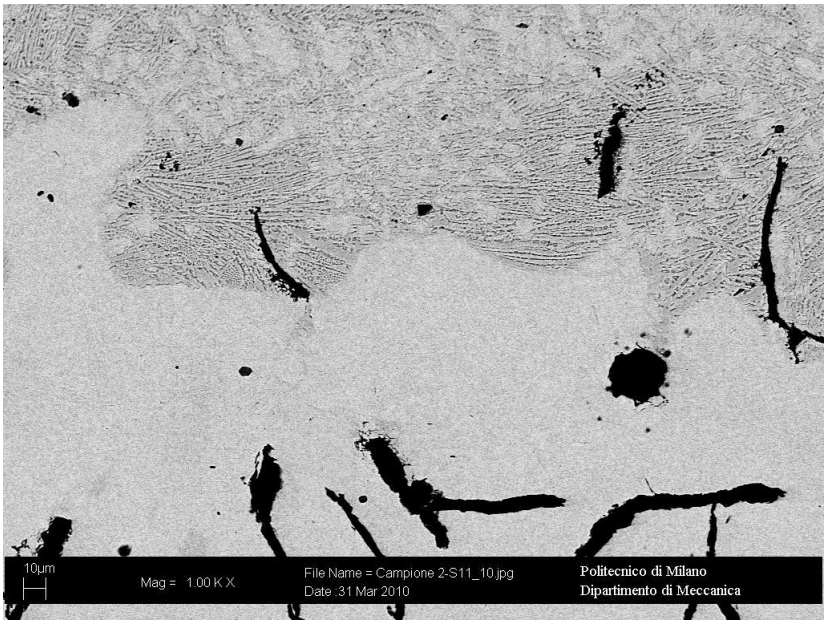

Figure 6-2 The boundary of melted zone and hardened zone.

Although melted zones were obtained in all the process when the temperature is above the melting point, the melted surface is non uniform in the case of low

temperature and high scanning speed. The depth of the melted zone and hardened zone are illustrated in Figure 6-3 (a) and (b).

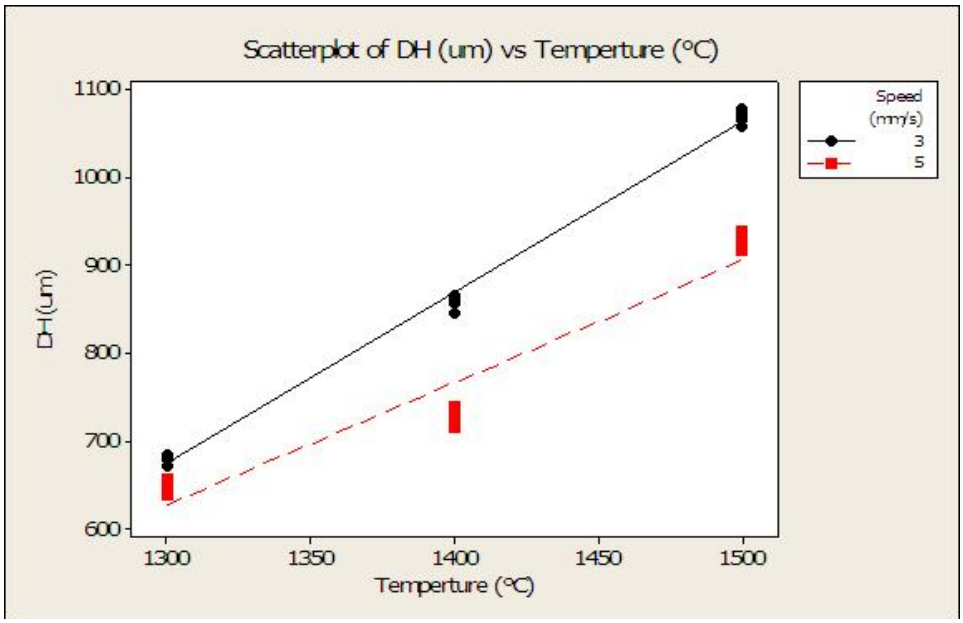

(a) Hardened zone

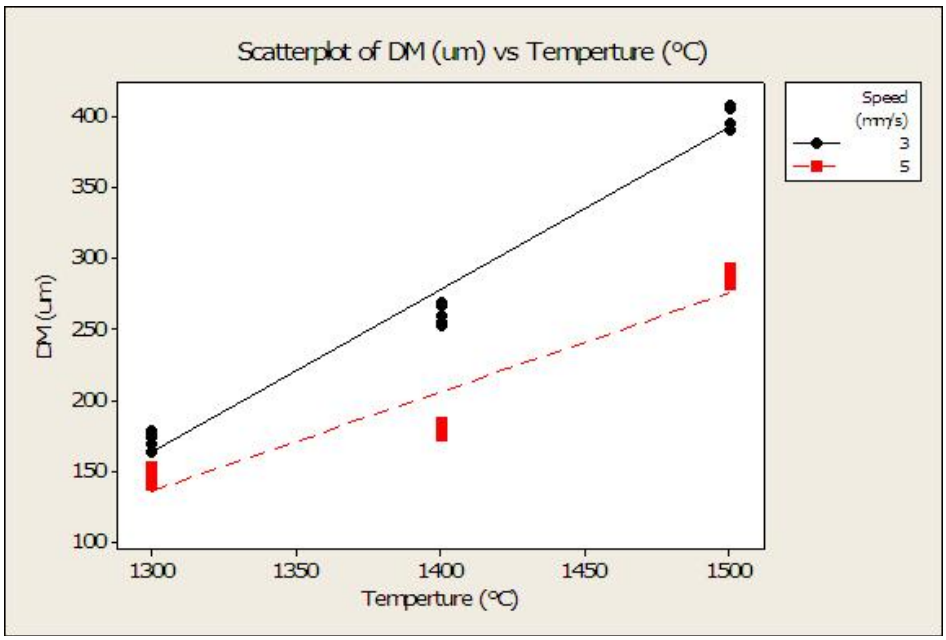

(b) Melted zone

Figure 6-3 Depth of the hardened and melted zone in laser melting process.

Bothe of the structures and the depths of the melted-hardened zones indicate that only a slight melted layer is on the top surface, when the temperature is a hundred above the melting temperature or the specimen was scanned with a high speed. In order to get a large and uniform melted zone which is not affected by the overlapping process, a combination of high temperature and low scanning speed makes the most sense.

The microhardness was tested in the cross section of the sample (1500 ℃ – 3 mm/s), the hardness profiles along the width and depth are given in Figure 6-4(a) and (b). The hardness tests along the width were carried out under the top surface 0.15 mm. The hardness profiles indicate that in the high temperature and low scanning speed process, a uniform hardness distribution is achieved in the melted zone. The microhardness in the melted zone is higher than that of hardened zone, 800-900 HV 0.3.

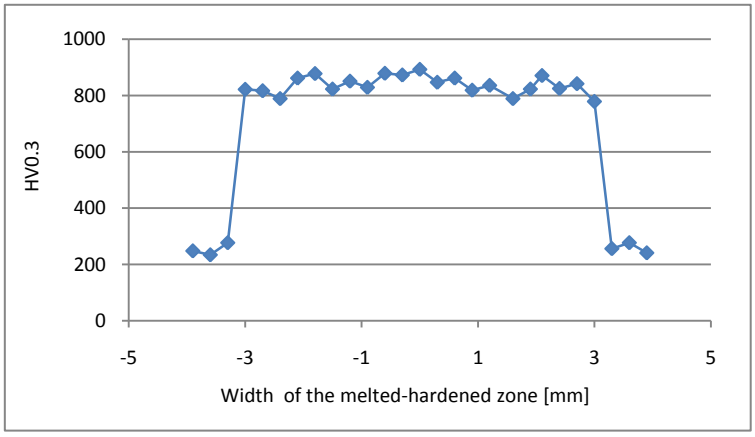

(a) Hardness distribution along the width

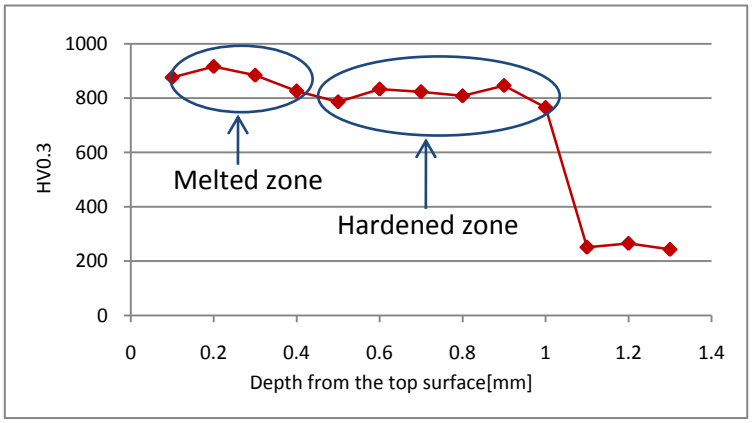

(b) Hardness distribution along the depth

Figure 6-4 Hardness profiles in the cross section of melted-hardened zone.

6.2 Multi-pass laser melting process

As discussed in chapter 6-2, a new microstructure with high hardness was observed in the melted zone, the results of single track hardening show that high temperature and low scanning speed ensure a deeper and uniform melted layer on the top surface. To obtain a uniform melted zone on a wide surface, low scanning speed (3mm/s) and temperature range from 1300 ℃ to 1500 ℃ were adopted during the multi-pass process. Lower temperatures were also adopted in the overlapping process to study the trend of the reduction of the back tempering effect due to the melted layer. Compared with hardening process, the width of the hardened zone is larger, more than 6 mm, thus smaller overlapping length was chosen in the overlapping length window. The parameters used in the overlapping laser melting process are listed in Table 6-4.

Table 6-4 Experimental parameters for overlapping laser melting process.

Temperature (℃)	Scanning speed (mm/s)	overlapping length (mm)
1300		
1400	3	1
1500		

After the experiments, the results were evaluated in terms of the uniformity of the melted surface depth, as the microhardness distribution along the width of the treated surface.

6.2.1 Multi-pass laser melting process by 1300℃ and 1400℃

When low temperature controlled at 1300 ℃ was on the top surface, the melted surfaces were obtained only in the center of every treated track; no melted layer was obtained in the overlapped zones. In the hardened zone, the martensite was reheated and back tempering occured as in the multi-pass hardening process, the structures of the melted and hardened zones are shown in Figure 6-5. Under the top surface 0.15 mm the hardness tests were carried out, the hardness profile (see Figure 6-6) in the cross section confirmed the hardness decreased in the overlapped zone.

(a) Cross section

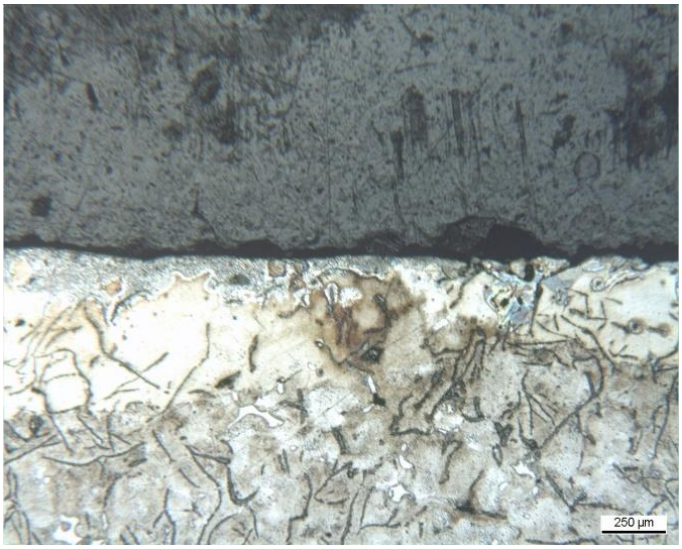

(b) Overlapped zone between 1st and 2nd tracks.

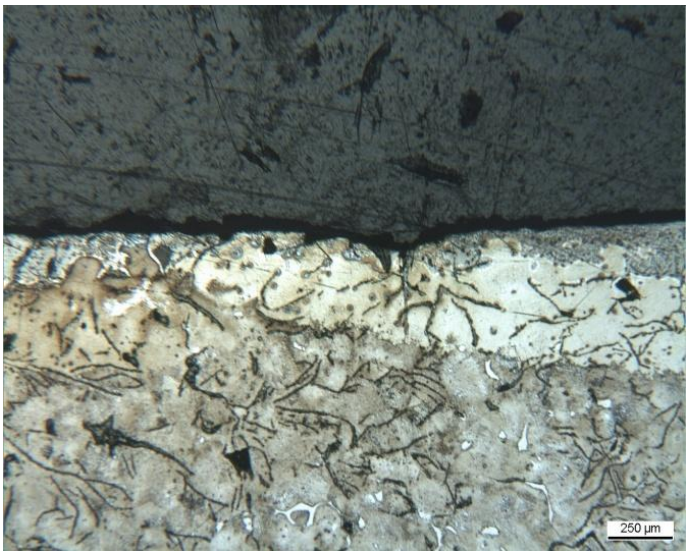

(c) Overlapped zone between 2th and 3th track

Figure 6-5 Structures of the overlapping melted zone – 1300 ℃, 3mm/s.

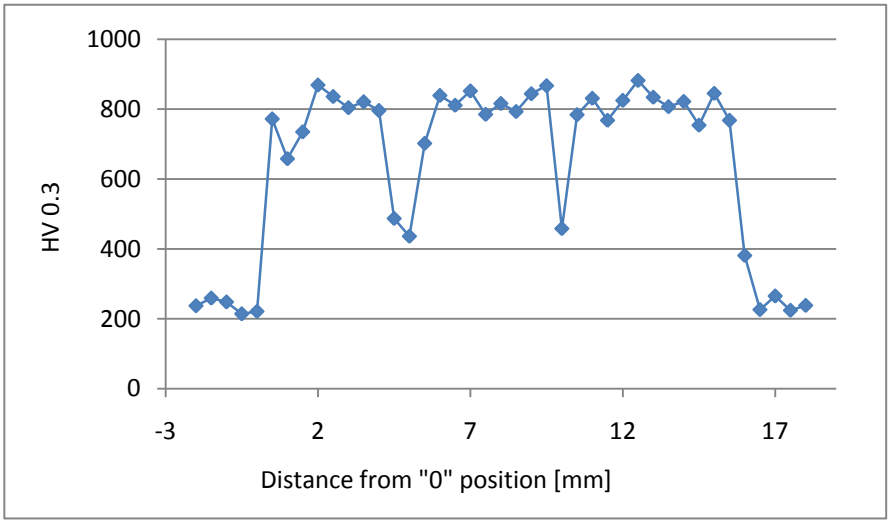

Figure 6-6 Hardness profile in the cross section of the overlapping melted zone – 1300 ℃.

The microstructures and hardness tests confirm that with lower temperature, only slight melted layers were obtained in the center of the treated tracks, these melted layers could not cover the overlapped zones when multi-track was applied.

Higher temperature 1400 ℃ was induced to enlarge the melted zone; the results are shown in Figure 6-7.

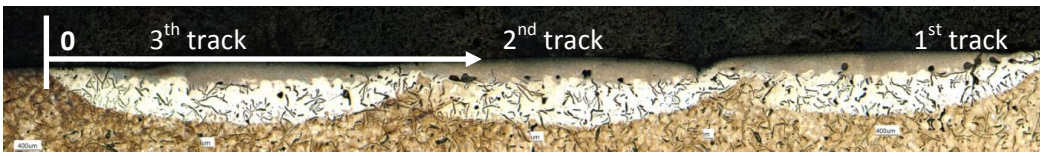

(a) Cross section

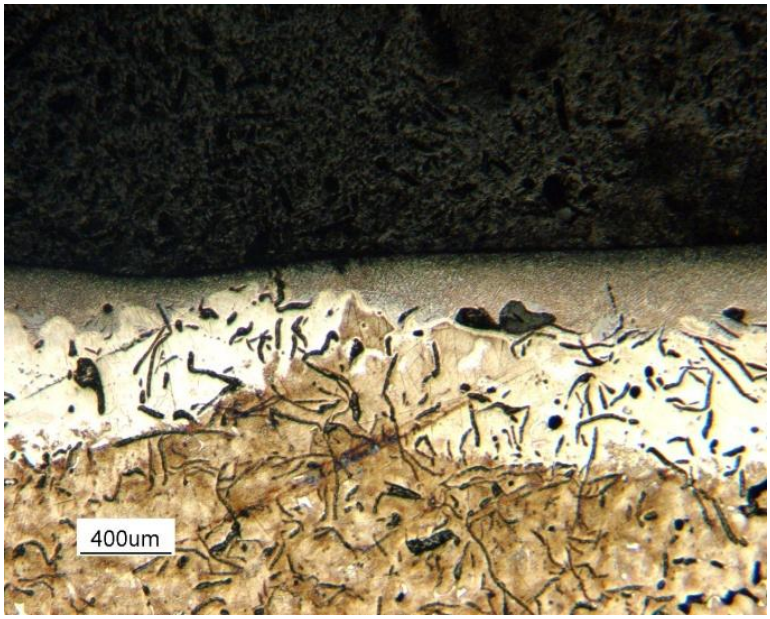

(b) Overlapped zone between the 2nd track and 3th track

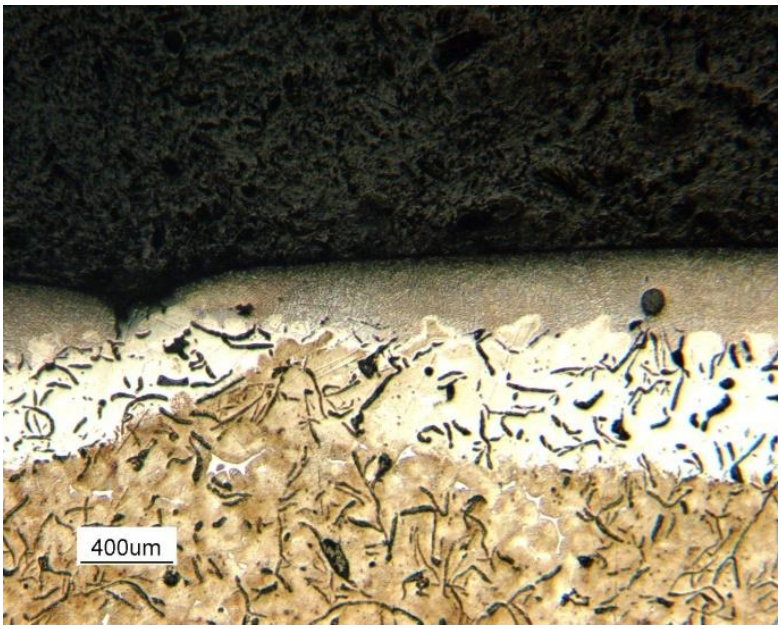

(c) Overlapped zone between the 1st track and 2nd track

Figure 6-7 Structures of the overlapping melted zone – 1400 ℃, 3mm/s.

With a higher temperature, a melted layer was obtained on the top surface; the shape of the melted zone is similar to the hardened zone, which has a maximum depth in the center, and decreases gradually to the edge of the melted zone. According to the

microstructures of the cross section, above the overlapped zones, melted surfaces were observed. Although melted surfaces up to 300 μm were achieved in the center of the melted zone, the melted layer is still superficial in the overlapped zones, as shown in Figure 6-7 (b) and (c), the minimum depth of the melted layer above the overlapping is less than 100 μm. The hardness test (Figure 6-8) along the width direction also indentified the hardness decrease in the overlapped zone which is covered by a superficial melted layer (Figure 6-7(b)). The hardness tests were carried out under the top surface 0.15 mm.

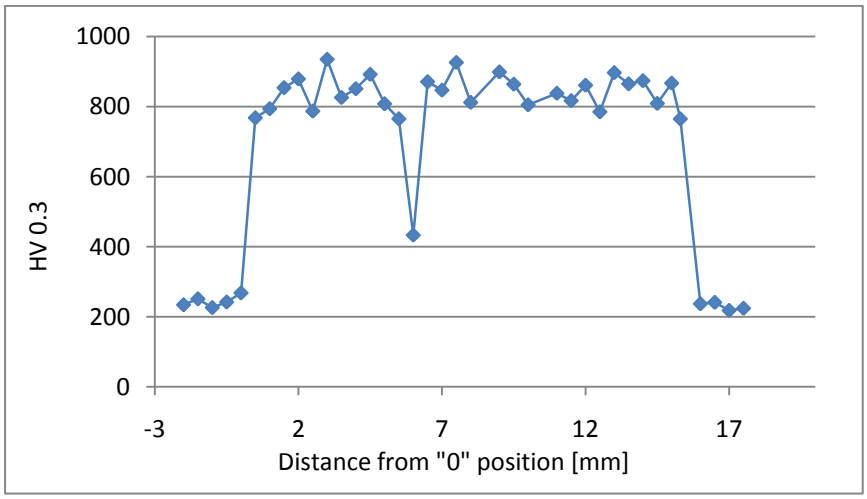

Figure 6-8 Hardness profile in the cross section of the overlapping melted zone – 1400 ℃.

Although hardness still decrease in the overlapped zone due to the superficial melted layer, the hardness tests show an improved behavior over its obtained by 1300 ℃, the areas with hardness decreased due to the fact that back tempering was reduced.

6.2.2 Multi-pass laser melting process by 1500 ℃

The overlapping melting processes with 1300 ℃ and 1400 ℃ have proved the melted layer could improve the hardness behavior in the overlapped zone by increasing the temperature. With higher temperature (1500 ℃ was adopted to treat a large surface); a uniform melted layer was obtained on the larger surface, as shown in Figure 6-9.

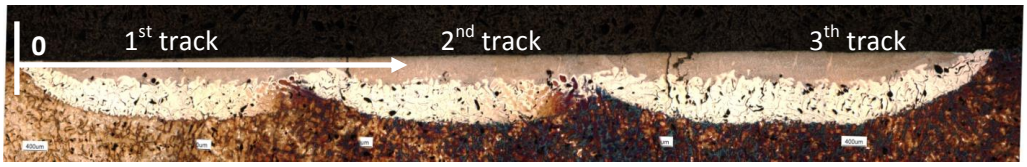

(a) Cross section

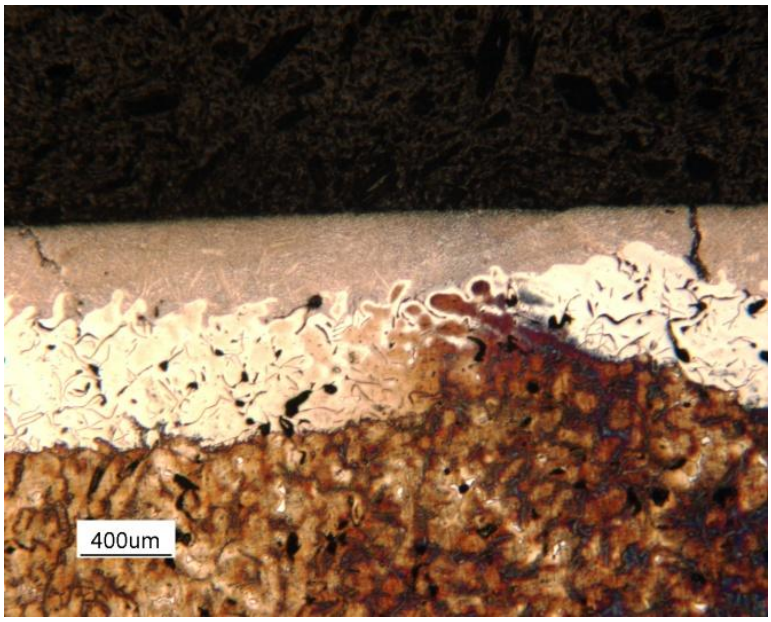

(b) Overlapped zone between the 1st track and 2nd track

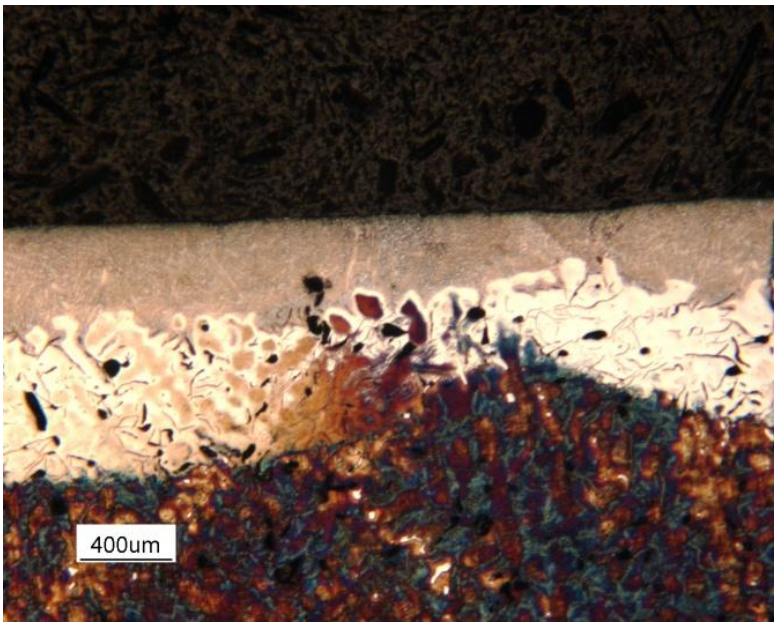

(c) Overlapped zone between the 2nd track and 3th track

Figure 6-9 Structures of the overlapping melted zones – 1500 ℃, 3mm/s.

Figure 6-9 shows that even if the back tempering phenomenon still esists in the hardened material inside overlapped zones, a uniform melted layer was obtained for all the treated surface, including the overlapped zone. The minimum scale of melted

surface in the overlapped zone can achieve 200 μm. Microhardness measurements were carried out along the width direction as the arrow shown in Figure 6-9 (a) at different distances (0.1 mm, 0.2 mm and 0.4 mm) from the top surface and also along the depth direction at different distances (3 mm, 5 mm, 8 mm, 10 mm and 13 mm) from the "0" position.

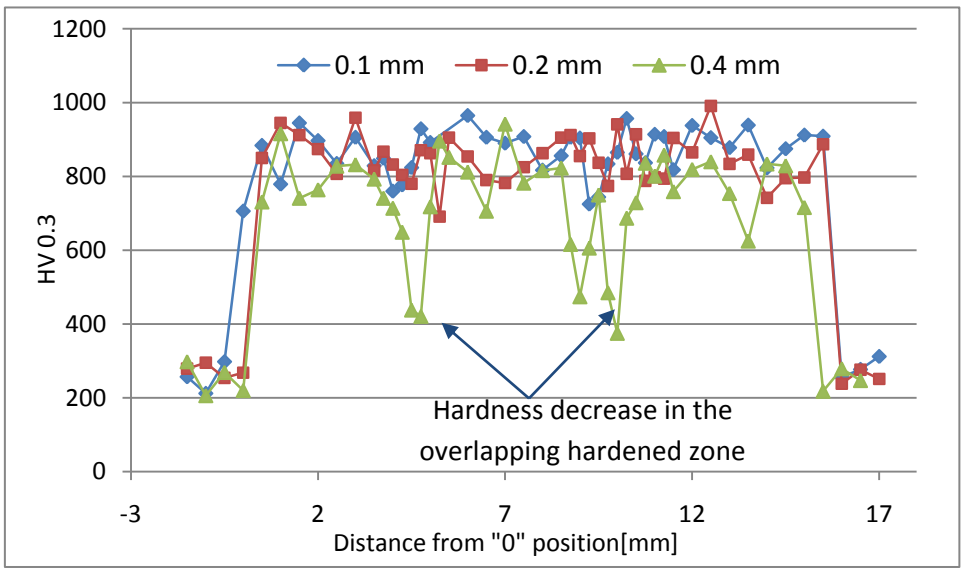

(a) Hardness profiles along the width direction

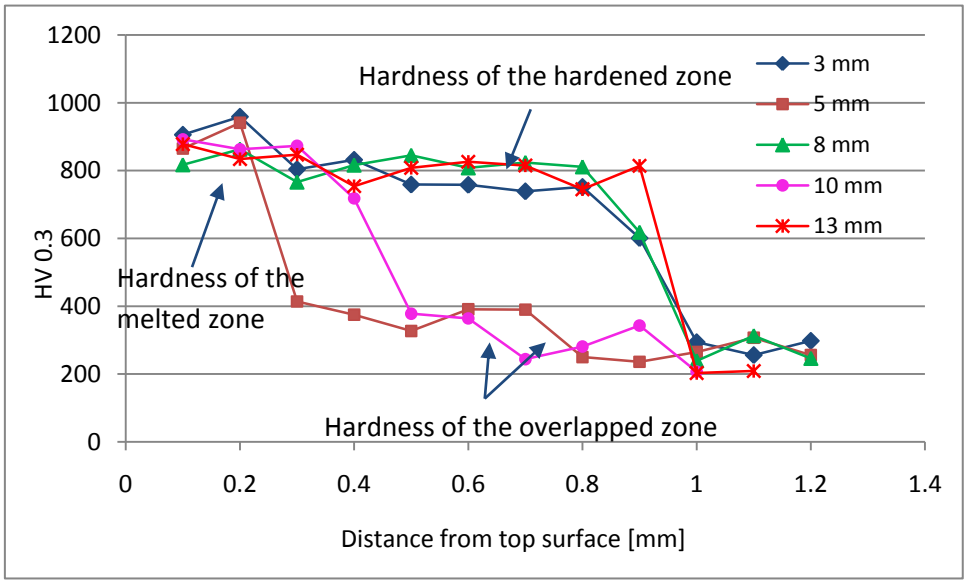

(b) Hardness profiles along the depth direction

Figure 6-10 Hardness distribution in the treated zones obtained by multi-pass laser melting.

The hardness tests in the cross section show that a treated surface with a uniform hardness distribution was obtained in the cross section by laser melting process, the depth of the treated surface reached 0.2 mm, and the microhardness was between 800 – 900$HV_{0.3}$. As the depth increased, hardened zones were obtained, the martensite in the hardened zones were affected by the back tempering decrease of hardness in overlapping zones was found under the surface 0.4 mm in the microhardness. The hardness profiles along the depth also confirm the back tempering phenomenon in the overlapped zone for the hardened materials.

A single specimen was executed with the high temperature and low scanning speed, a melt layer was covered on the surface of the specimen as shown in Figure 6-11.

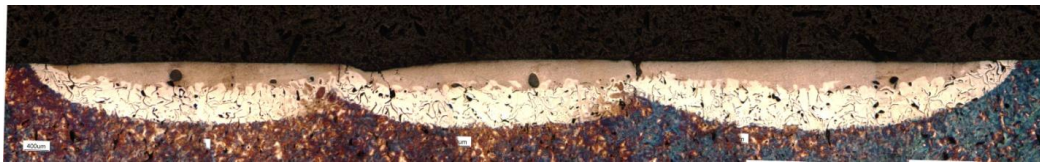

Figure 6-11 Single specimen performed with the optimized multi-pass laser melting process.

The multi-pass experimental campaigns have proved that, a large melted surface which can cover the overlapped zone could be obtained by increasing the temperature on the surface, and the uniform melted layer could improve the hardness behavior in the overlapped zones.

6.3 Conclusions

The laser melting process is a very promising surface treatment method for larger workpieces which cannot get a homogeneous hardened zone by traditional laser hardening. A fine grained microstructure with uniform microhardness and depth is obtained in the melted zone.

1. In single track laser melting process of gray cast iron, when the temperature on the surface is above the melting point, melted zones can be obtained by different combination of temperature on the surface and scanning speed.
    - When the temperature is above the melting point, the base melts and the graphite flakes dissolve into the melted material, due to the fast cooling, new microstructure with high hardness presents on the top surface.
    - The dimension of the melted zone is strongly affected by the process parameters, high temperature and low scanning speed should be adopted to obtain a uniform melted layer. In other words, high energy input is required during the melting process.

- The hardness of the melted zone was 800 – 900$HV_{0.3}$, which is higher than the hardened zone (700 – 800$HV_{0.3}$).

2. The microstructures and hardness profiles in the cross section of the multi-pass laser melted zones confirm that high energy should be used to get a large uniform melted surface.
   - Under low temperature condition, only the center of the treated zone was melted, the melted layer cannot cover the overlapping zone, hardness decrease still occurs at 0.15 mm under the top surface.
   - By high temperature on the surface, a melted layer was achieved on the whole surface of the treated zone, a surface without hardness drop was ensured; the depth of the uniform surface is 0.2 mm.
3. Although laser surface melting is one solution for back tempering problem, there are several drawbacks of the melting process.
   - The pores in the melted zone. They are induced mainly by the graphite dissolution and volume increase.
   - The thermal crack. It is a common drawback when a rapid solidification is achieved.
   - Post machining is necessary for applications.

7 Remote laser hardening

As the development of laser power, new techniques are proposed to overcome the back tempering phenomenon in the large surface treatment. With a high power laser, it becomes possible to defocus the laser beam to obtain a large laser beam, whose energy is still high enough for the laser hardening process.

Except defocusing the laser beam to enlarge the laser beam, shaping laser beam into a desired and large treated area becomes a new trend for the laser hardening process. With some high frequency scanning optics, the laser beam could be scanned into different shapes to meet the requirement for large surface; it is named remote laser hardening.

7.1 Experimental parameters for remote laser hardening

Along with the laser power and scanning speed, some new parameters were considered and under investigation (shown in Figure 7-1).

1. Laser spot Diameter (LD): Fiber laser is featured high beam quality, bringing new future of laser cutting and welding. But in the application of laser hardening, the laser usually works out of the focus to get a big laser spot with lower power

density. For a given laser power output, different laser spots determine the power density, and eventually, the scanning speed.

2. Scanning shape: other than shaping the laser beam straight into a line, other shapes were tested in the end of the experiment, *e.g.* round, ellipse.
3. Scanning Stroke (SS): It is the distance between the starting and finishing point of the laser beam during scanning the laser head. For the ellipse scanning shape, the scanning stroke includes scanning width (SW) and scanning length (SL).
4. Scanner head Frequency: It affects the time cost for shaping the laser spot into a line. In case of round and ellipse scanning locus, it is calculated from scanner head speed (m/min).

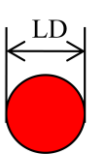

(a) Laser spot diameter

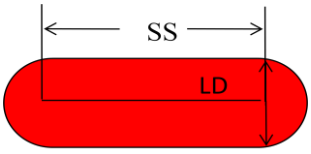

(b) Line shaped laser beam

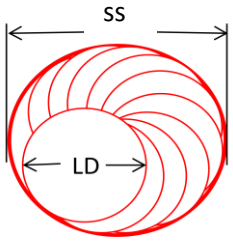

(c) Round shaped laser beam

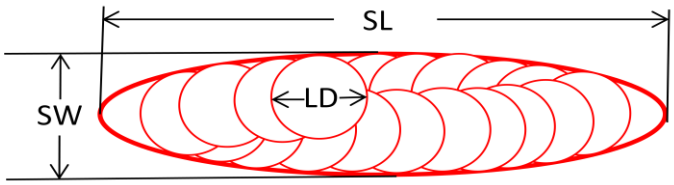

(d) Ellipse shaped laser beam

Figure 7-1 Sketch of fiber laser spot diameter and scan stroke.

No power measurement equipment was applied in the process. The initial condition of the remote laser hardening was chosen on the basis of the proximity laser hardening which was executed by diode laser. In the case of the laser spot size at 2 mm, and the scanner stroke at 6 mm, the shaped laser beam has the same dimension as the diode laser spot. 1250 W and 15 mm/s were chosen to simulate the proximity laser hardening. The initial parameters of the remote laser hardening are listed in Table 7-1; the power density is the same as the proximity laser hardening.

Table 7-1 Initial parameters of the remote laser hardening.

Hardening type	Laser	Power	Scanning speed	Power density
Proximity laser hardening	Diode laser	1250 W	15 mm/s	104 W/mm^2
Remote laser hardening	Fiber laser	1250 W	15 mm/s	104 W/mm^2

The surface was melted under the same condition as the diode laser hardening, and the surface is shown in Figure 7-2. Parameters were regulated based on this initial condition; Table 7-2 lists all the combinations of experimental parameters in the following experiments.

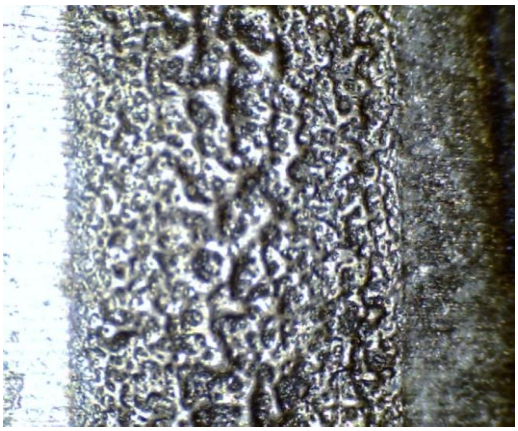

Figure 7-2 Treated surface of the remote laser hardening- initial parameters.

Table 7-2 Different experimental condition for fiber laser hardening.

Sample No.	Power	Speed	Spot size	Scanner stroke	Frequency	Scanning shape	Result
	(W)	(mm/min)	(mm)	(mm)	(Hz)		
1	1250	900	2	6	400	Line	Melt
2	1000	900	2	6	400	Line	Melt
3	3000	3000	2	6	400	Line	Melt
4	1000	1000	2	6	400	Line	Melt slightly
5	3000	5000	2	6	400	Line	Melt
6	1500	2500	2	6	400	Line	Hardening only in the center
7	1500	2000	2	6	400	Line	Hardening only in the center
8	2500	2000	2	11	400	Line	Melt
9	2500	3000	2	11	400	Line	Melt
10	1000	1000	5	-	400	-	Good
11	1200	1000	5	2	400	Line	Good
12	1200	1000	5	8	400	Line	No hardening
13	3600	1000	5	8	400	Line	Good
14	1200	330	5	8	400	Line	OK
15	5000	1000	5	32	400	Line	Not uniform
16	3000	1000	5	8	400	Line	OK

17	3000	1000	5	8	400	Line	Good
18	2000	1000	5	6	400	Line	No hardening
19	2000	1000	5	6	400	Line	No hardening
20	2000	1000	3	8	50	Line	Melt
21	2000	2000	3	8	50	Line	Melt
22	1000	2000	2	8	50	Line	Melt
23	2000	1000	5	8	50	Line	Melt in center
24	2000	1000	5	8	50	Line	Melt in center
25	2000	1000	5	8	200	Line	No hardening
26	2000	1000	5	8	400	Line	No hardening
27	2000	600	5	8	200	Line	OK
28	2000	500	5	8	200	Line	OK
29	2000	400	5	8	200	Line	Good
30	2000	1000	5	2	200	Line	No hardening
31	2000	1000	5	-	200	Line	Melt slightly
32	2000	1200	5	-	200	Line	Melt
33	2000	1000	5	2	200 m/min	Round	Melt
34	2000	1000	5	3	200 m/min	Round	Good
35	2000	1000	5	3	200m/min	Round	Good
36	2000	1000	5	6	200m/min	Round	No hardening
37	2000	1000	5	6x2	200m/min	Ellipse	No hardening
38	2000	1000	5	12x2	200m/min	Ellipse	No hardening
39	2000	1000	5	9x2	200m/min	Ellipse	No hardening

The remote scanner head laser hardening was carried out for every condition. The results show that the hardening with a scanner head is a complex process, which is affected by all the parameters. Different defects on the treated surface, *i.e.* all the treat surface is melt, the surface is melt in the center, rather hardened, were observed during the processes.

7.1.1 Influence of the laser spot diameter (LD)

With a small LD (2 mm and 3 mm), the power density of the laser beam is high; this could induce the surface melting. Under a small LD (2 mm), Figure 7-3 shows the melted surfaces of samples. Sample 1 was obtained by the same power and scanning speed as the diode laser (1250W, 900mm/min). This melted surface can be explained by Gaussian power distribution of fiber laser. When the laser beam was less

defocused; a small laser spot was formed, so the power density is quite high in the laser spot, it induces a melt surface

To reduce the melting phenomenon, sample 4 was treated with a decreased power (1000 W) and increased scanning speed (1000 mm/s), no hardened layer was obtained at the edges of the track, but the center of the surface was still melted. This means the temperature distribution in non homogenous in the shaped laser beam.

	Power	Scanning speed	LD	SS	Frequency
Sample 1	1250W	900 mm/min	2 mm	6 mm	400
Sample 4	1000W	1000 mm/min	2 mm	6 mm	400

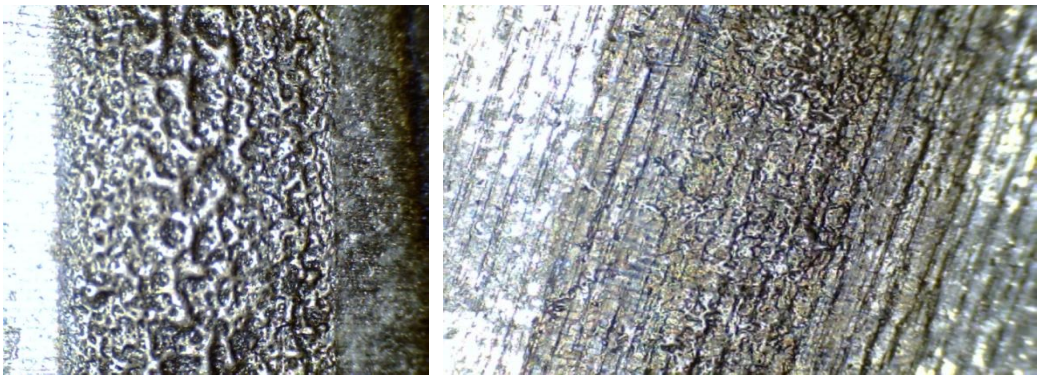

(a) Sample 1 (b) Sample 4

Figure 7-3 Melted surface obtained by the small LD.

7.1.2 Influence of the scanner head frequency

Three kinds of frequency 400 Hz, 200 Hz and 50 Hz were applied in the experiments. Figure 7-4 shows three samples which are hardened under same conditions except the frequency. (a) sample 24: 50 Hz, melting happened in the center of the surface; (b) sample 25: 200 Hz, no hardened zone; (c) sample 26: 400 Hz no hardened zone even worse than sample 25. The common treated condition is as following:

Power	Scanning speed	LD	SS	Frequency
1000W	2000 mm/min	5 mm	8 mm	50

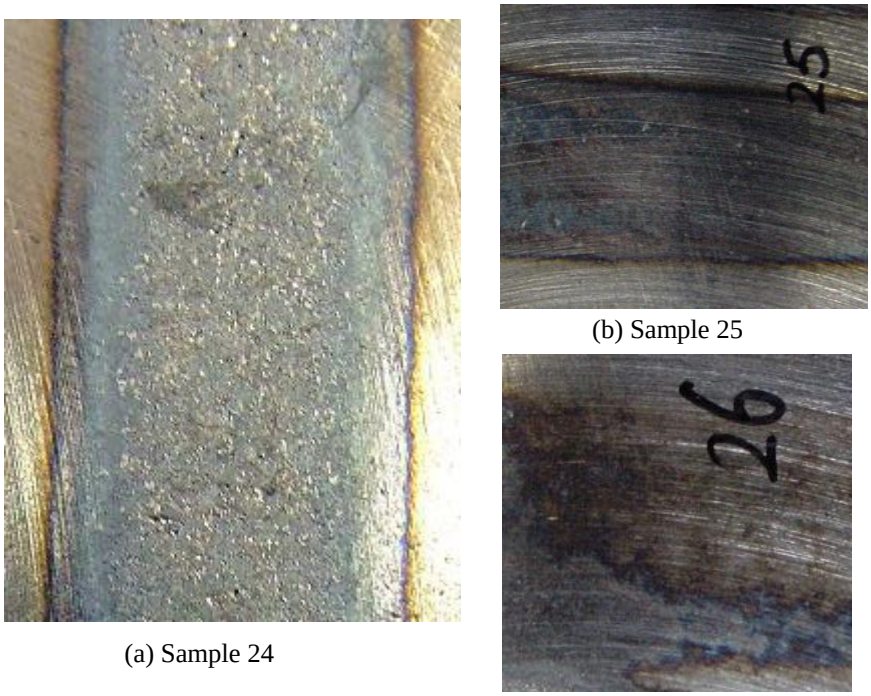

(a) Sample 24

(b) Sample 25

(c) Sample 26

Figure 7-4 Comparison of treated surfaces by different frequency.

Low scanning frequency is the other reason for the melted surface lower speed of the laser beam along the cross section induces longer heating time. Figure 7-5 (sample 22) shows a treated surface by the combination of small LD and low scanner head frequency, the treated condition is as following:

	Power	Scanning speed	LD	SS	Frequency
Sample 22	1000W	2000 mm/min	2 mm	8 mm	50

Compared with sample 4 and sample 24, sample 22 has the most serious melting phenomenon. On the contrary, under a high scanner head frequency, a hardened zone was achieved by increasing the power and decreasing the scanning speed, as shown in Figure 7-6 (sample 27).

	Power	Scanning speed	LD	SS	Frequency
Sample 27	2000W	600 mm/min	5 mm	8 mm	200

Figure 7-5 Melted surface obtained by small LD and low scanner head frequency.

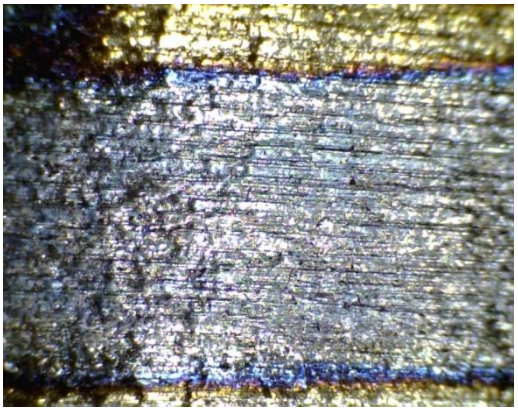

Figure 7-6 Hardened surface obtained by large LD and high scanner head frequency.

Insufficient energy input resulted in the non-hardened surface (Figure 7-7); it could be caused by low laser power, high scanning speed, large scanning stroke and high scanner head frequency.

Sample 18	Power	Scanning speed	LD	SS	Frequency
	2000W	1000 mm/min	5 mm	6 mm	400

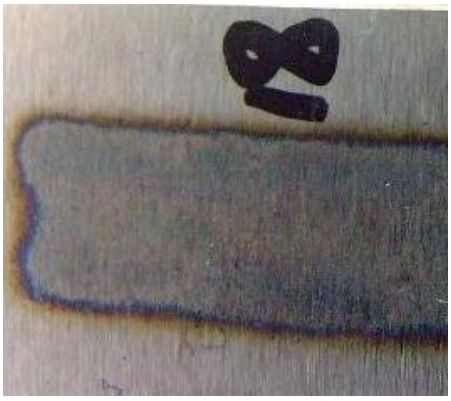

Figure 7-7 Non-hardened surface by the scanner head laser.

7.2 Hardness analysis for remote laser hardening

After the results evaluated by eyes at the first sight, hardness tests were executed on the surface of selected samples. The selected samples for hardness test are highlighted

in Table 7-1. The microstructure in cross section was investigated in Sample 13 to understand the depth of the hardening zone.

The microhardness tests were carried out for the samples which were highlighted in Table 7-1. The tests were carried out on the top surface, the tested positions are shown in every picture of the treated sample with a red line.

1. Sample 10

Sample No.	Power (W)	Speed (mm/min)	Spot diameter (mm)	Scanner stroke (mm)
10	1000	1000	5	-

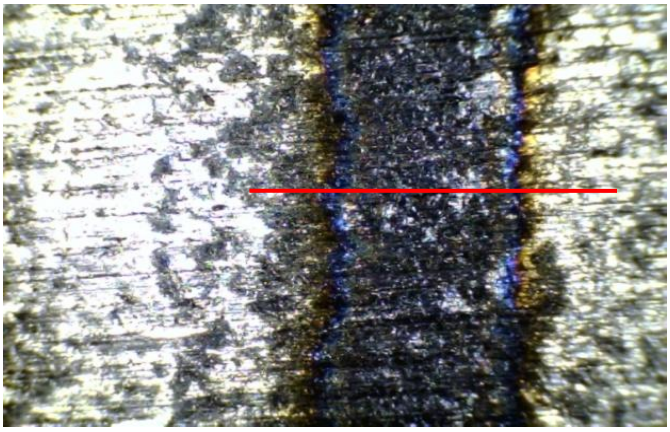

(a)

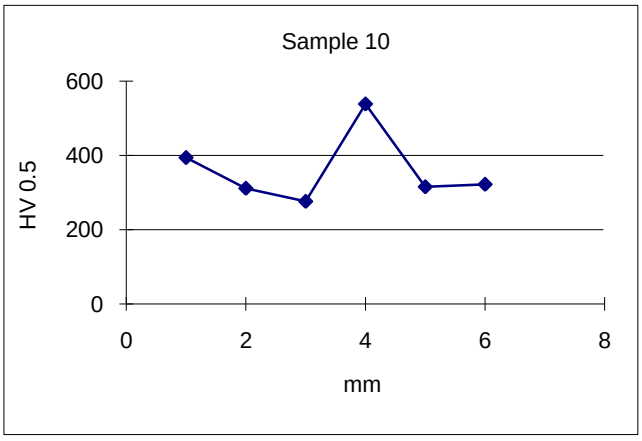

(b)

Figure 7-8 Structure and hardness test on the surface of fiber laser hardening sample 10.

2. Sample 11

Sample No.	Power (W)	Speed (mm/min)	Spot diameter (mm)	Scanner stroke (mm)
11	1200	1000	5	2

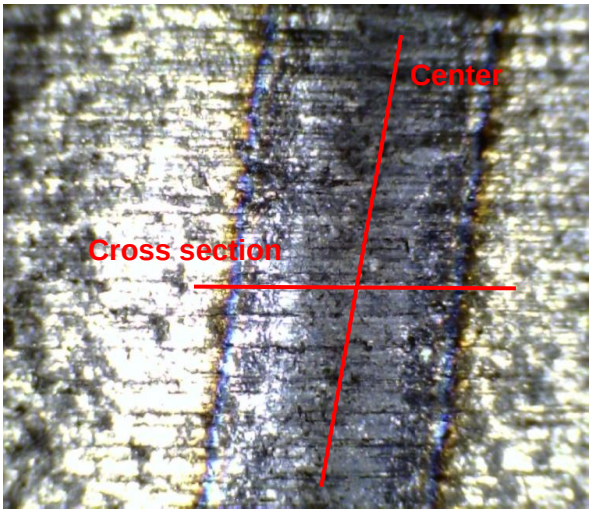

(a)

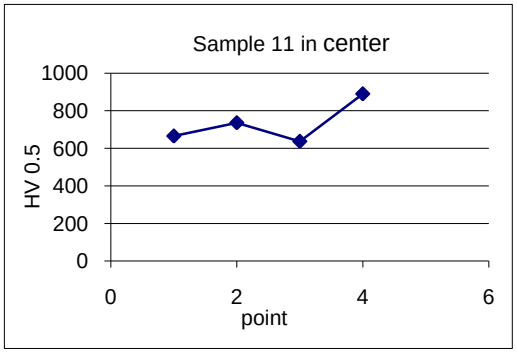

(b)

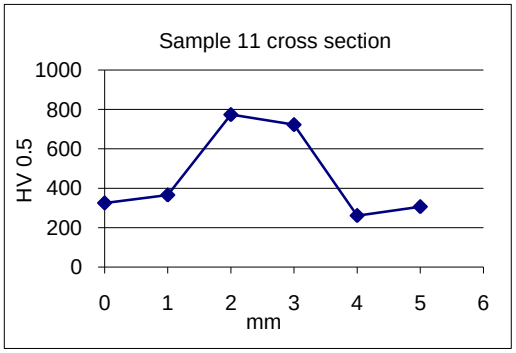

(c)

Figure 7-9 Structure and hardness test on the surface of fiber laser hardening sample 11.

3. Sample 13

Sample No.	Power (W)	Speed (mm/min)	Spot diameter (mm)	Scanner stroke (mm)
13	3600	1000	5	8

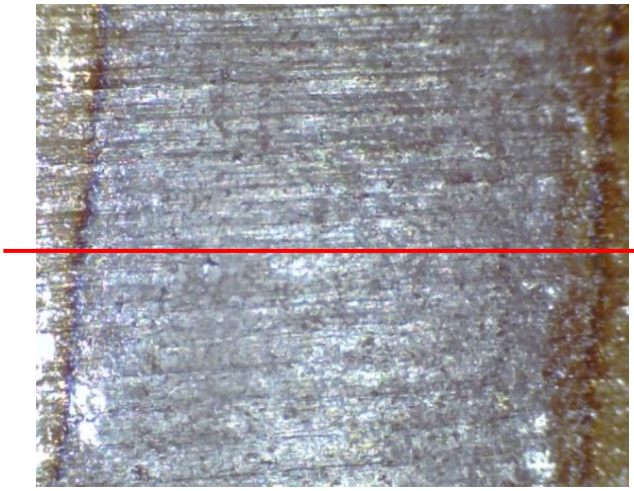

(a)

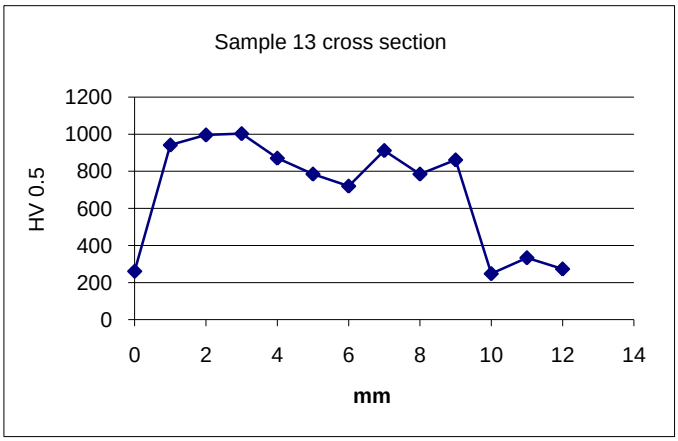

(b)

Figure 7-10 Structure and hardness test on the surface of fiber laser hardening sample 13.

The hardness test along the cross section shows that a hardened layer with hardness higher than 800 HV and width 8 mm was obtained. In order to get more detail about the hardened zone, the microstructure of the cross section was investigated (Figure 7-12).

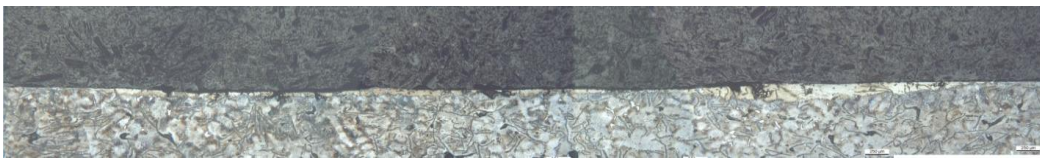

(a)

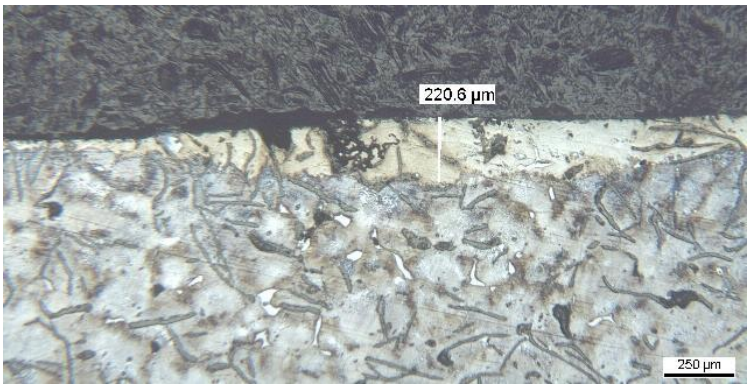

(b)

Figure 7-11 Microstructure in the cross section of fiber laser hardening sample 13.

In the cross section, a hardened layer was obtained by the remote scanner head laser hardening, as confirmed in the hardness test on the top surface, the microstructures of the cross section show that the depth of the hardened layer is quite shallow and non-uniform. The maximum depth of the hardening zone is 220.6 µm, the depth of other position is 10 -20 µm.

4. Sample 14

Sample No.	Power (W)	Speed (mm/min)	Spot diameter (mm)	Scanner stroke (mm)
14	1200	330	5	8

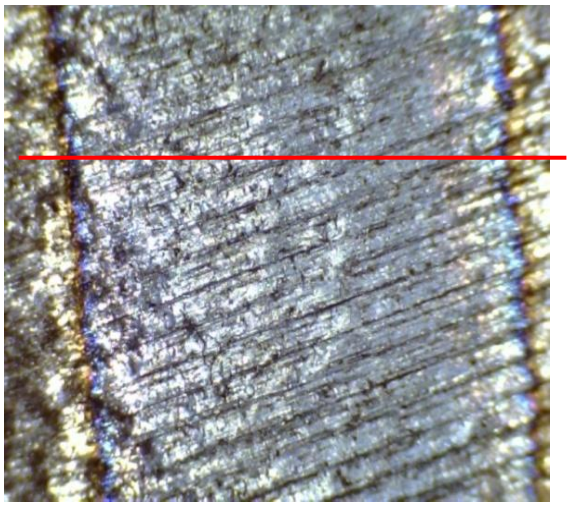

(a)

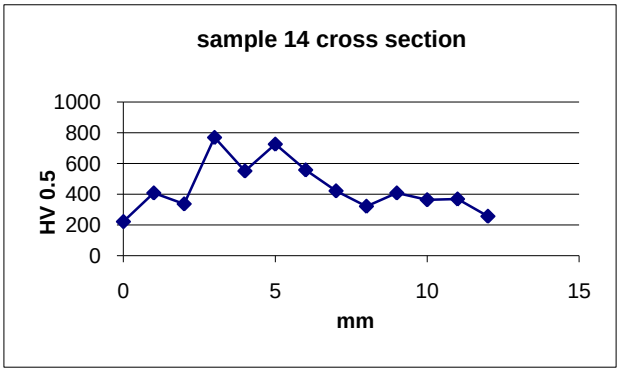

(b)

Figure 7-12 Structure and hardness test on the surface of fiber laser hardening sample 14.

5. Sample 15

Sample No.	Power (W)	Speed (mm/min)	Spot diameter (mm)	Scanner stroke (mm)
15	5000	1000	5	32

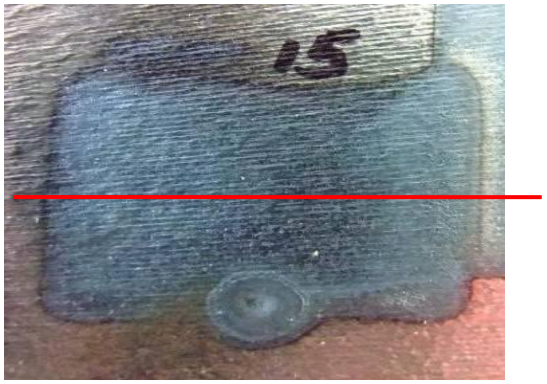

(a)

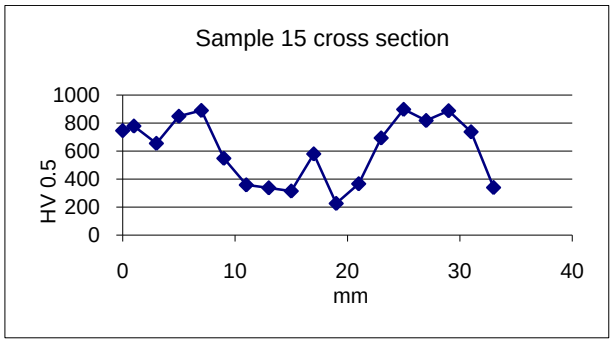

(b)

Figure 7-13 Structure and hardness test on the surface of fiber laser hardening sample 15.

6. Sample 18

Sample No.	Power (W)	Speed (mm/min)	Spot diameter (mm)	Scanner stroke (mm)
18	2000	1000	5	6

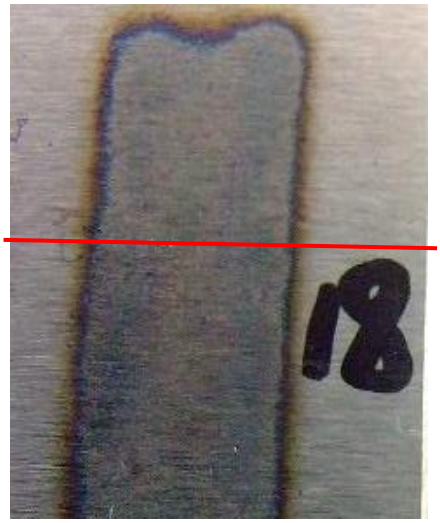

(a)

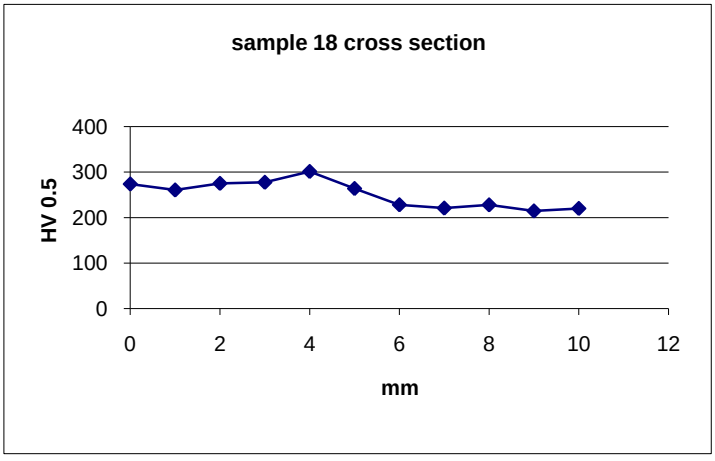

(b)

Figure 7-14 Structure and hardness test on the surface of fiber laser hardening sample 18.

7. Sample 34

Sample No.	Power (W)	Speed (mm/min)	Spot diameter (mm)	Scanner stroke (mm)
34	2000	1000	5	3

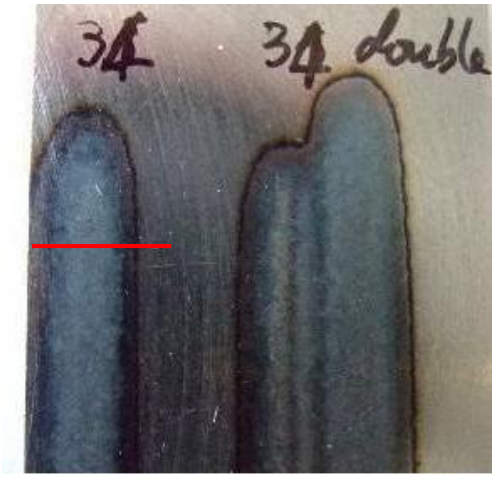

(a)

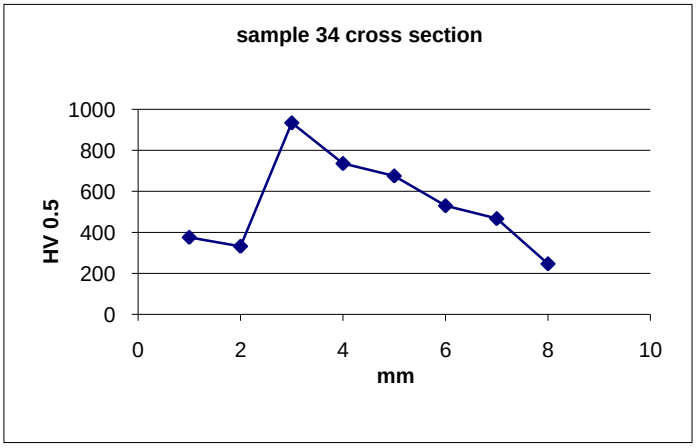

(b)

Figure 7-15 Structure and hardness test on the surface of fiber laser hardening sample 34.

The hardness tests for the hardened samples uncovered a common problem that most samples were hardened only in the center of the tracks. This is because of the Gaussian power distribution and heat accumulation in the hardened track. With a Gaussian power distribution, the power is centralized, if the laser beam gets defocused, the power in the periphery of the laser beam decreases, so that no hardened zone was obtained in the edge of the treat track.

7.3 Conclusions

With the high power fiber laser and a scanner head, it is possible to shape the laser beam into large dimension to treat a large surface. Except of the laser power and

scanning speed, some new parameters, *i.e.* laser spot diameter (LD), scanning stroke (SS) and scanner head frequency, were investigated. Through the experimental campaigns, the following results and conclusions were given:

1. The hardening process is strongly influenced by the energy distribution in the laser beam. The energy in the fiber laser has a Gaussian distribution, a small defocus length which means high power density could induce melted surface. Large laser beam with lower power density is necessary for a good hardening process.
2. The scanner head frequency is another essential factor for a successful hardening. Ceteris paribus, the lower scanner head frequency induces longer heating time for every treated point where melt surface is obtained, whereas higher frequency means repeated fast heating and cooling phases for a certain cross section, induces slow temperature increase.
3. An 8 mm width of hardened layer was obtained on the top surface. But the microstructure in the cross section indicated that the minimum depth of the hardened zone is only 10-20 μm, which is the result of the low absobtivity of metal for the fiber laser beam.
4. The hardness in the cross section shows a non-uniform distribution, the center of the hardened track obtained high hardness, and then the hardness decreased in the radius till the edges. This could be explained by the Gaussian energy distribution, when a large defocus length is applied, the power density decreases fast on the periphery of the laser beam, and therefore no hardened zone is obtained on the edge of hardened track.

According to the above results, it can be concluded that to obtain a hardened surface with a scanner head, lower power density in the laser spot (compared to laser welding or cutting process) and high scanner head frequency are required. Then based on the required hardened width, scanning stroke is determined with appropriate laser power and scanning speed.

8 Apparent Spot technique

As discussed in the previous chapters, back tempering happens not only on planar surfaces, but also on cylindrical surfaces. In this chapter, the back tempering phenomenon will be studied on cylindrical surfaces, and a new technique – Apparent Spot (AS) will be proposed to eliminate this drawback for cylindrical workpiece.

8.1 Back tempering on the cylindrical surface

Circular laser hardening is a particular treatment used in case of cylindrical workpieces. During the circular laser hardening, the workpiece is rotated by a lathe, in the mean time, laser beam treats the surface, and an annular hardening zone is obtained during the rotation.

There are two kinds of applications of this circular hardening technique: single annular track hardening and cylindrical surface hardening. The single annular track is used when the treatment of a narrow surface is required, *e.g.* for the treatment of bearing housing of a shaft, valve cone. In this case, only one revolution of the workpiece is executed and one annular hardened track is obtained. The cylindrical surface hardening is applied when a wider surface of the cylindrical workpiece is to be treated. In this application, a feed rate parallel to the rotation axis of the workpiece is given to the laser; this eventually results in a continuous helicoidal hardened track,

as shown in Figure 8-1. For the hardened cylindrical workpiece, the drawback of back tempering happens on both single annular workpiece and wider cylindrical surface.

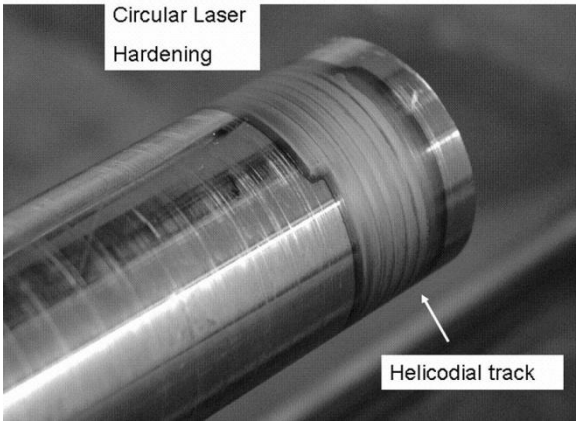

Figure 8-1 wider hardened surface obtained by helicodial track.

8.1.1 Overlapping phenomenon on single annular surface

When only one revolution is executed to the cylindrical workpiece, the laser beam does not move, during the laser hardening, the initial and final points of the workpiece are overlapped and treated twice as shown in Figure 8.2, and the back tempering happens in the initial/finishing part.

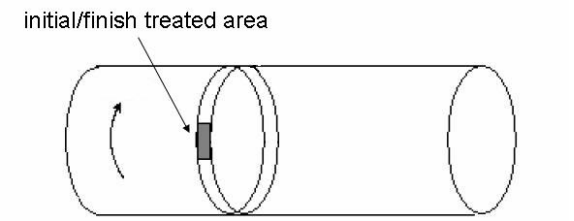

Figure 8-2 Scheme of single annular track laser hardening.

A shaft (Ø 15mm) was used to investigate the single annular hardening, the shaft was rotated at 45 rpm, and 1200 ℃ was chosen as the temperature on the top surface. Figure 8-3 gives the microstructure and microhardness of hardened surface.

(a) Microstructure of the single annular hardened surface

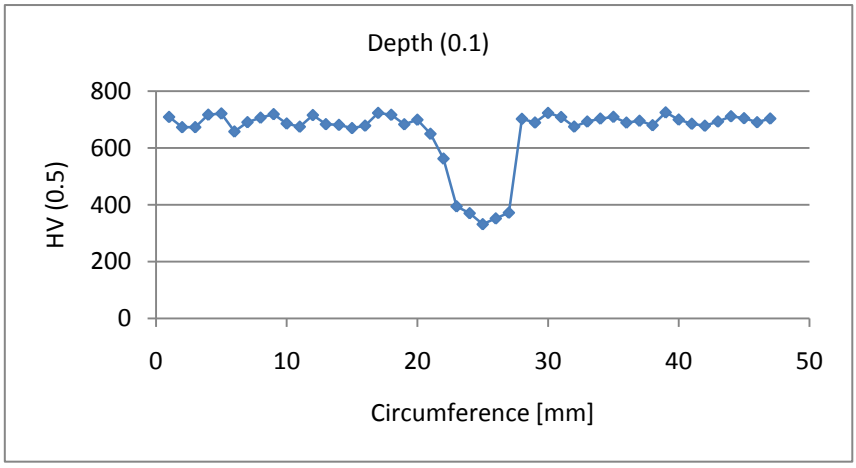

(b) Microhardness of the single annular hardened surface

Figure 8-3 Single annular hardened surface for cylindrical workpiece.

By single annular hardening process, the treated surface got a uniform hardness 700 $HV_{0.5}$, except of the initial and finishing parts. The hardness decreased less than 400 $HV_{0.5}$ in the overlapped zone.

8.1.2 Overlapping phenomenon on wider cylindrical surface

As discussed above, if a wider cylindrical surface to be treated, the laser scans the workpiece along the rotation axis. In this case, the overlapping phenomenon happen between the helicodial tracks, as shown in Figure 8-4.

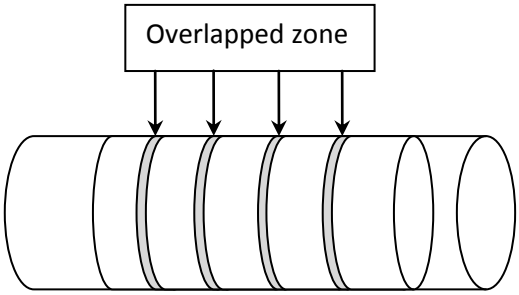

Figure 8-4 Scheme of wider cylindrical surface laser hardening.

The back tempering drawback of overlapping tracks process has the same theory as it happens on a planar surface – the current track reheats the previous one. When the back tempering happens in the overlapped zone, the microstructure and the hardness distribution in the overlapped zone of a cylindrical workpiece are shown in Figure 8-5. A shaft with 15 mm diameter was used, and the temperature on the surface was kept at 1200 ℃.

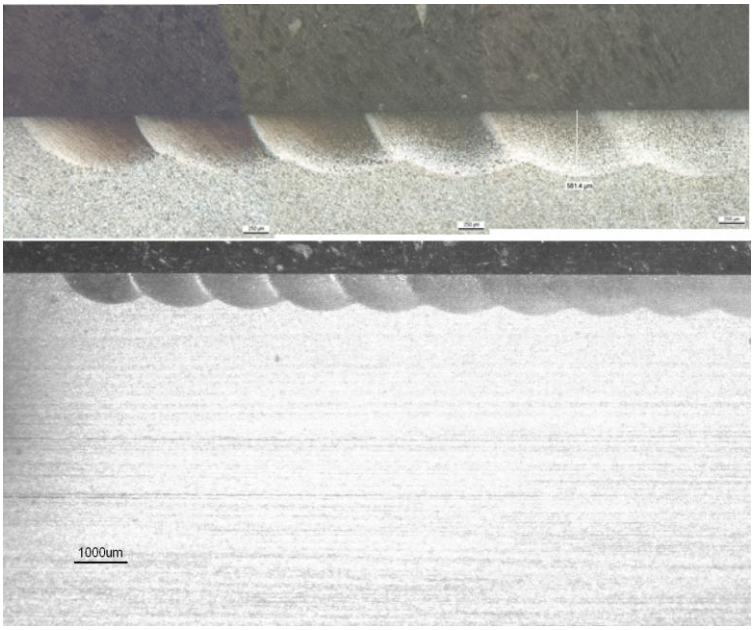

(a) Structures in the overlapped tracks with different magnifications

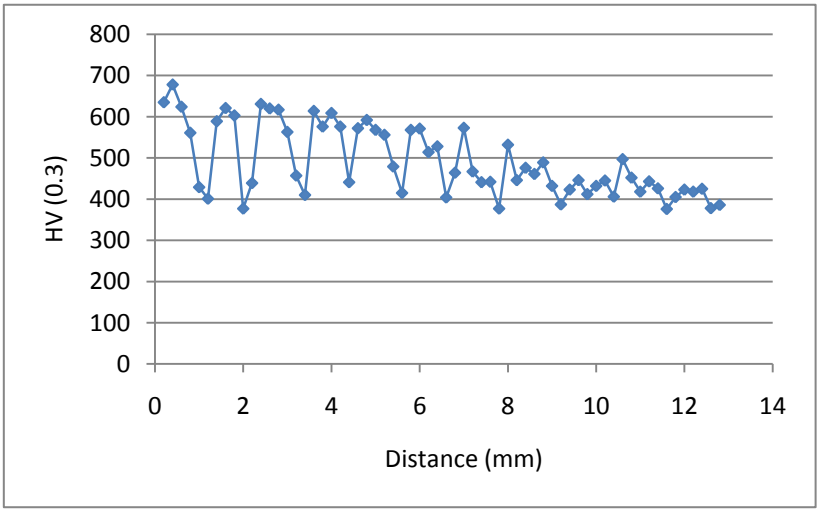

(b) Hardness distribution in the overlapped zones

Figure 8-5 Overlapping track applied in cylindrical workpiece.

The hardness tests in the cross section shows that, back tempering happened in the overlapped zone between two hardened tracks, the hardness dropped from 600 $HV_{0.3}$ to 400 $HV_{0.3}$, the hardened depth was 0.5 mm. As the hardened tracks increased, no obvious overlapped zone was observed, and the hardness decreased to 400 $HV_{0.3}$ in the hardened zones. The microstructures of the 1st, 6th, 11th and 16th overlapped zones are shown in Figure 8-6 (a) – (d) respectively.

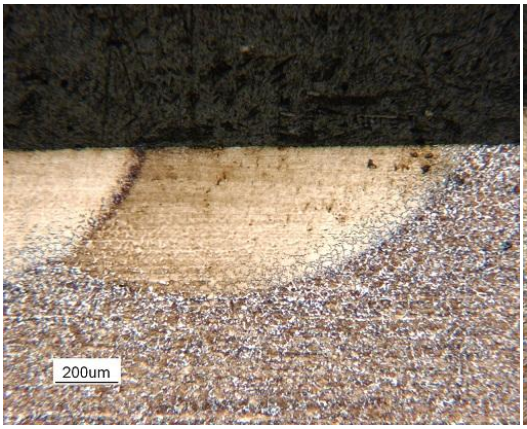

(a) the 1st overlapped zone

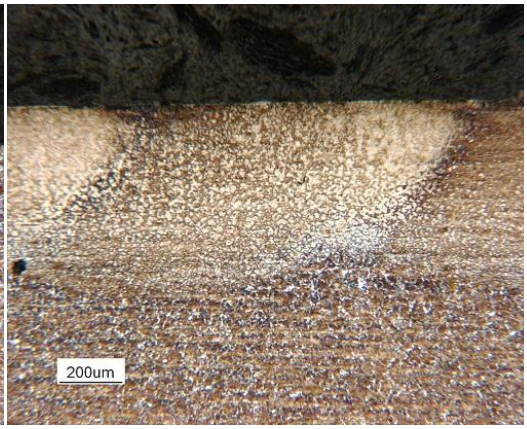

(b) the 6th overlapped zone

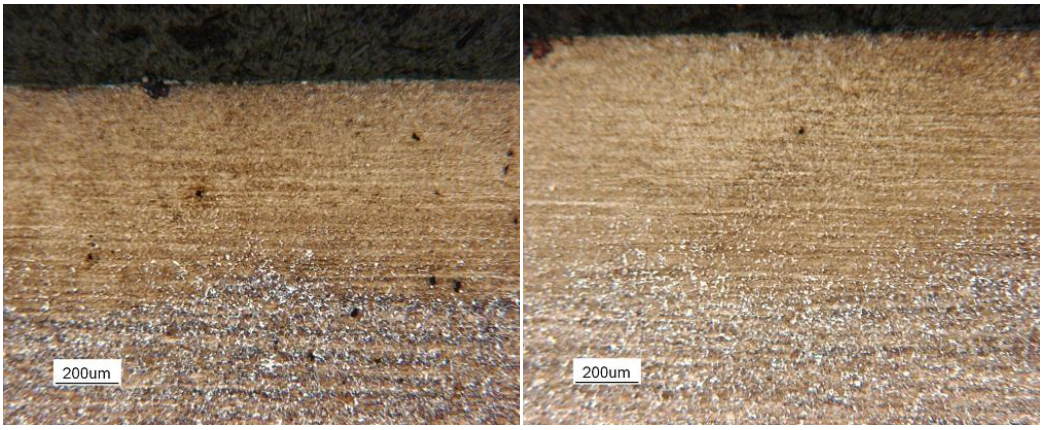

(c) the 11th overlapped zone (d) the 16th overlapped zone

Figure 8-6 Overlapped zones in the cylindrical workpiece.

The microstructures of different overlapped zones explained the hardness decrease along the axis direction in the cross section of the hardened sample. While the treatment was carried out, continuous laser beam radiated the workpiece, so the heat has been accumulated in the workpiece. Only the first several tracks were hardened when the bulk material was still cold. With the heat accumulation, the cooling phase was not enough for the last tracks, the austenite transformed or partly transformed into pearlite and ferrite, no hardened material was obtained.

The structures of the overlapped zone also show a non-uniform depth of the hardened surface, which is the same drawback on the planar surfaces.

8.2 Parameters investigation of Apparent Spot technique

In order to solve the back tempering phenomenon, a new technique was proposed for the surface hardening of cylindrical workpieces. This technique uses a high speed rotation instead of a low speed rotation during the circular hardening process. Due to this high speed rotation an apparent circular spot can be obtained as Figure 8-7, so this new technique is also called Apparent Spot (AS) technique. It increases the dimensions of the laser spot in a fictitious way, and the laser power distributes uniformly along this virtual circular laser spot. This circular spot has the same circumference as the workpiece, in this case, the laser beam treats the annular circumference at the same time, and a uniform hardening zone without overlapping and back tempering is obtained. If a wider surface has to be treated, a feed along the longitudinal direction can be imparted to the laser beam. Thanks to the AS technique, both the back tempering effect and the non-uniform hardness depth are solved.

Figure 8-7 Apparent Spot technique applied in cylindrical surface.

Due to the complexity of the AS technique the proper selection of processing parameters has to be carefully. Parameters involved in AS are the laser spot dimension, laser power, rotating speed, heating time and diameter of the workpiece. The parameters' choosing is based on some important considerations:

1. Power density. It is a combination of the laser spot dimension and laser power. High power density assures a fast heating phase, which avoids heating the bulk materials as in the self-quenching process. In order to achieve the maximum power density, the working distance is set equal to the focus one.
2. Heating time (t_H). With the control system, the heating time is controlled by the pre-set temperature on the surface. Once the measured temperature reaches the setting point, the laser power will be shut off automatically while the real time temperature is recorded by the system (see Figure 8-8).

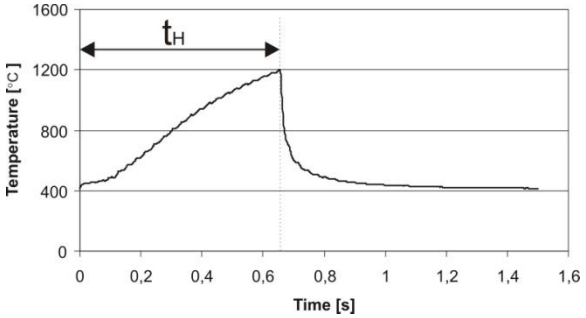

Figure 8-8 real time temperature and heating time during AS hardening.

3. Rotation speed. The thermal condition of every point on the circular surface consists in a heating phase and a cooling phase when one revolution is executed. With a high rotation speed, heating phases and cooling phases are repeated; whereas the heat accumulates and the temperature on the top

surface is reaching the setting point. The rotation speed affects the treatment mode and temperature increasing rate of the workpiece. Figure 8-9 show two simulated temperatures during the hardening process under different rotation speeds. Since the heating time is controlled against temperature, the rotation speed affects the heating time. A high revolution speed allows that the small spot becomes a ring-shaped heat source and induce a uniform temperature filed to the workpiece.

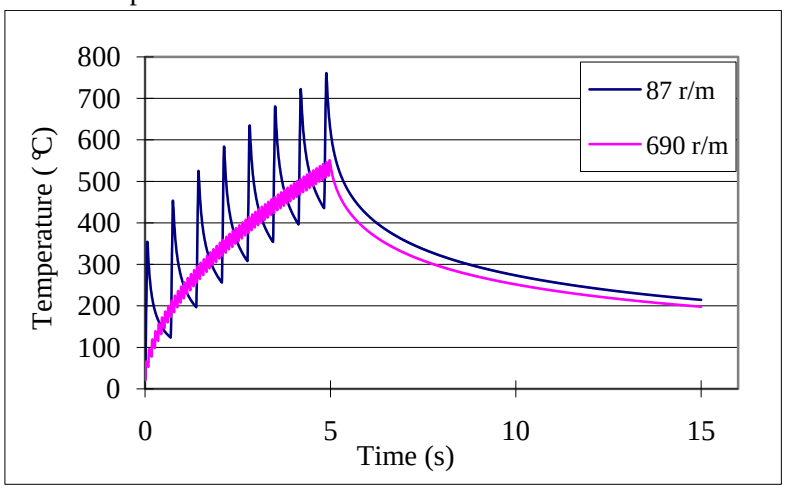

Figure 8-9 Influence of different rotation speed.

4. Diameter of the workpiece. It affects the dimension of the Apparent Spot, under a fixed laser power; it means that the power density of the Apparent Spot is affected by the diameter of the workpiece.

8.3 Experimental campaigns for annular surface by AS technique

As mentioned above, annular hardened surface is required by industrial applications, *e.g.* bearing housing of a shaft, and Apparent Spot technique is s solution of the overlapping phenomenon when a low rotation speed is applied during the hardening process. A set of experimental campaigns were investigated the effects of different parameters.

8.3.1 Experimental parameters for annular track hardening

Experimental campaigns are designed in order to understand the effects of different process parameters on single annular track laser hardening executed by the AS technique. The parameters are listed in Table 8-1.

Table 8-1 Process parameters used in the annular surface AS experimental campaign.

Process parameters	Levels
Power *P*	1250, 1000 [W]
Rotational speed *n*	2100, 1150 [rpm]
Temperature	1200 [℃]
Input energy *E*	28.6, 35.7, 52.2, 65.2 [J]
Workpiece diameters *Φ*	5,10,15,20,25 [mm]

The input energy E is the energy for every revolution, and is calculated by:

$$E = \frac{P}{n/60}$$

For each condition, four replicas were executed.

8.3.2 Experimental results of annular track AS hardening

Both the geometrical features and the hardness were investigated for the treated samples. Figure 8-10 gives some samples of the hardened zones, (a)-(f) are treated under same condition: 1250 W, 2100 rpm, but with different diameters of the workpiece, (f) shows a non treated surface.

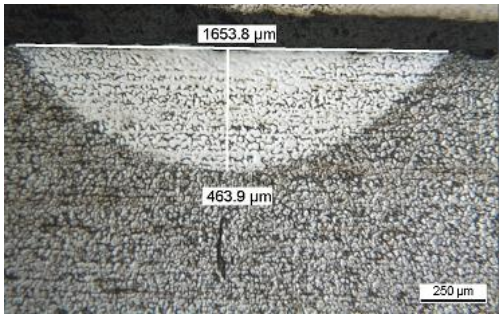

(a) 5 mm

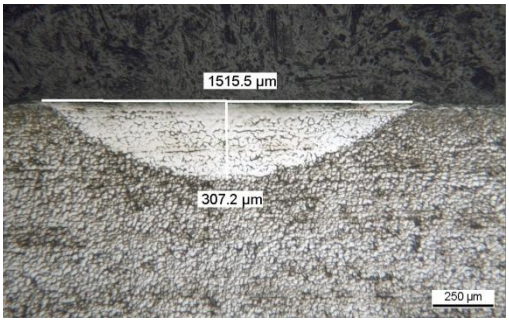

(b) 10 mm

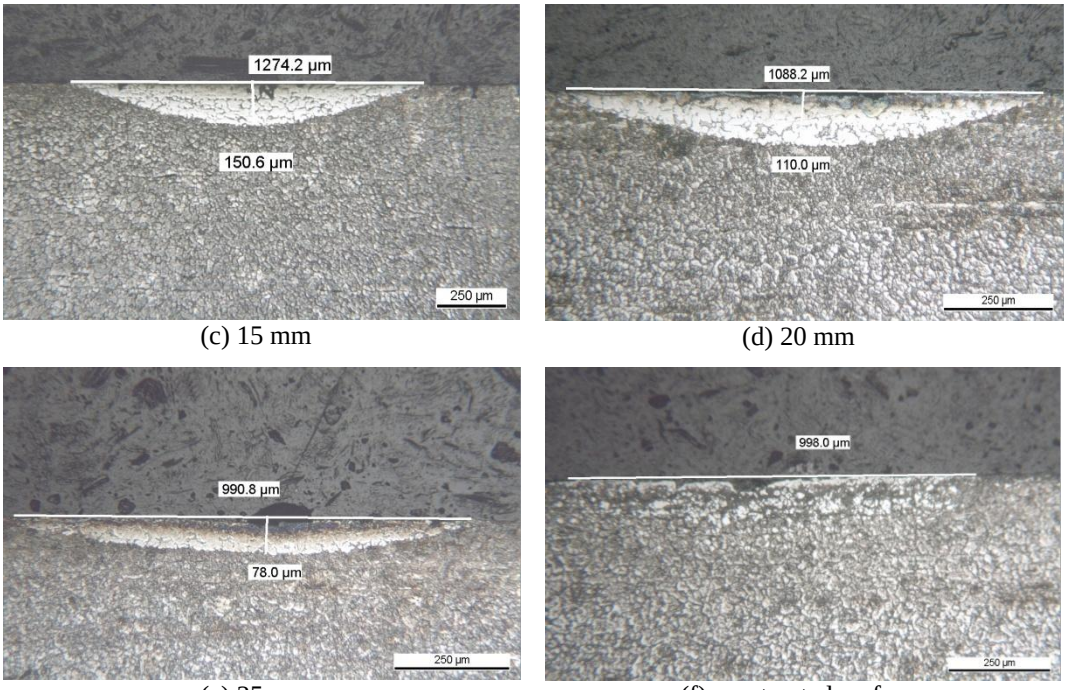

(c) 15 mm (d) 20 mm

(e) 25 mm (f) non treated surface

Figure 8-10 hardened zone obtained by single track AS technique.

Based on the measurements of the width and depth of hardened zones, Figures 8-11 and 8-12 report the geometrical features of the hardened zones, in terms of height and width as a function of the workpiece diameters.

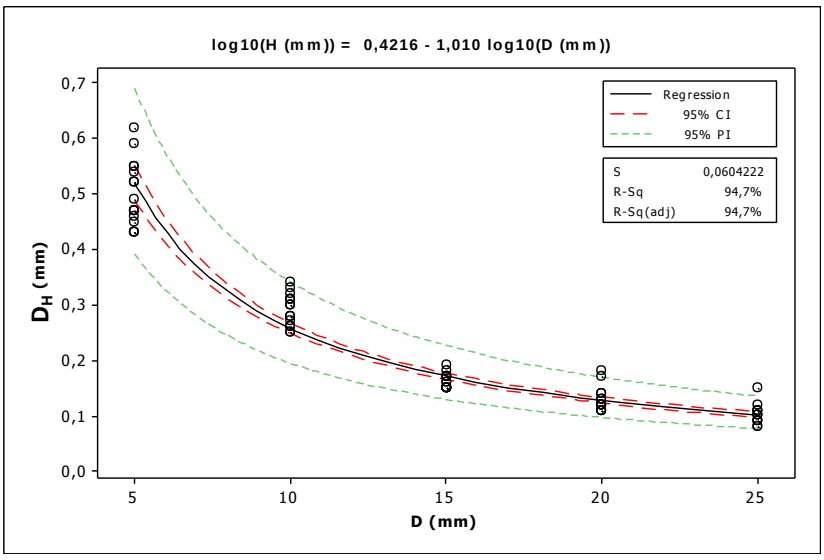

Figure 8-11 Height of the hardened zone vs. workpiece diameter (AS).

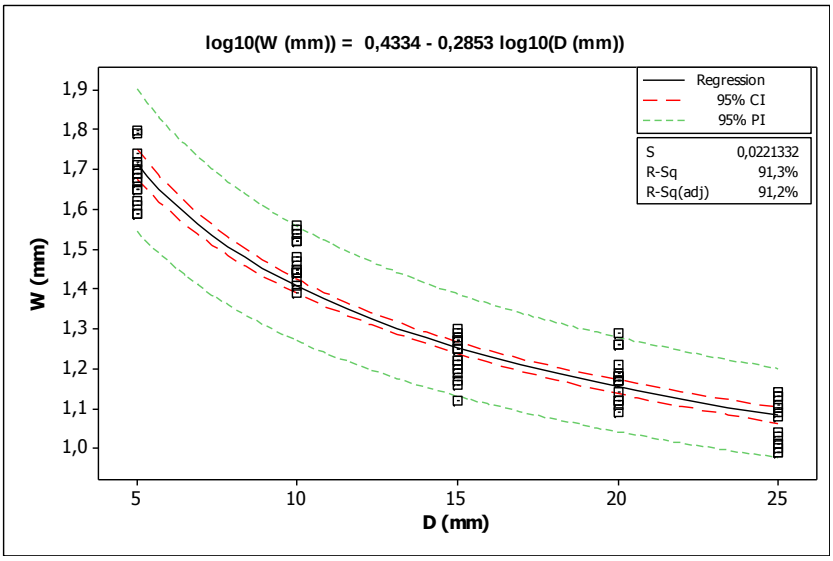

Figure 8-12 Width of the hardened zone vs. workpiece diameter (AS).

The regression analysis confirms that the geometrical attributes, *i.e.* W and H, are not affected by the energy input, but by the workpiece diameter. Both of them indeed decrease when the workpiece diameter increases.

The microhardness tests were carried out in the cross section of the samples. The tests show two different behaviors depending on the workpiece diameters (see Figure 8-13).

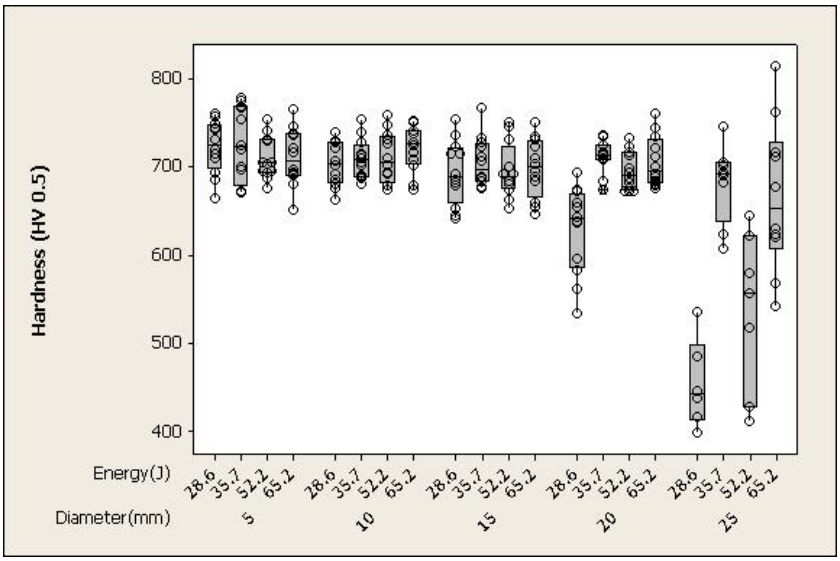

Figure 8-13 Microhardness vs. input energy and workpiece diameter (AS).

For the workpieces whose diameter is smaller than 15 mm, hardened layers were obtained. In this diameter range, neither the input energy nor the diameter affect the microhardness values (average value: 709±22 HV), as the ANOVA analysis confirms. On the contrary in the case of larger workpiece diameters, *i.e.* 20 and 25 mm, the input energy affects the laser hardening results. Particular in the case of 20 mm diameter, the single track hardened zones are obtained only by higher energy inputs. When it comes to the largest diameter, *i.e.* 25 mm, surface is not completely laser hardened even in the case of the highest input energy. This is probably due to the long heating time that characterizes the largest diameter, especially in the case of the lowest energy input. As shown in figure 8-14, when the workpiece diameter increases, the time that is needed to reach the fully austenization strongly increases, that the bulk material is not able to rapidly cool down the treated surface layer.

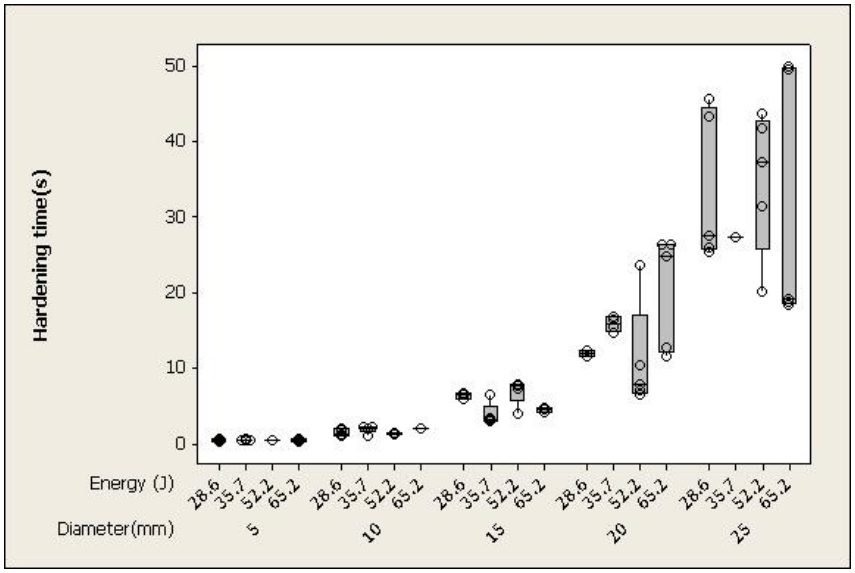

Figure 8-14 Heating time vs. input energy and workpiece diameter (AS).

The experiments pointed out the effects of the process parameters on the dimensions and hardness values of the single track in case of a circular laser hardening executed by AS technique. The results show that workpiece diameter is the major factor of the hardened surface, while the input energy is less effective. In particular, with a fixed laser power the AS technique has a limitation of the workpiece diameters, which makes it inapplicable to the large workpiece diameters. This can be explained by considering that when the diameter increases the heating time increases to the point that the consequent rapid self-quenching is not further guaranteed.

8.4 Preliminary experiments of overlapping AS hardening

To obtain a wider hardened surface two steps are included in the AS technique. For the first step, the workpiece was treated by an annular track AS hardening, considered as preheat step, during this step, the maximum power was applied without regulation. When the temperature on the surface reaches the setting point as the trigger of the second step, then the laser begins to move along the direction of the rotation axis. During the second step, the power of the laser is regulated to keep the temperature at a constant level.

Based on the annular surface AS hardening, to reduce the heat accumulation in the substrate material, high power density was applied. A shaft with 20 mm diameter was chosen, as the maximum diameter that could be treated by AS technique with a 1250 W diode laser. Other than the parameters investigated in the single track annular AS hardening experiments, the feed rate of the laser beam is also in consider. Two feed rates (1 mm/s and 2 mm/s) were executed to hardening the shaft. The details of the hardening condition are listed in Table 8-2. The treated surface is shown in Figure 8-15.

Table 8-2 Process parameters used in the cylindrical surface AS experimental campaign.

Process parameters	Levels
Power *P*	1250 [W], automatic controlled
Rotational speed *n*	1150 [rpm]
Temperature	1200 [℃]
Rotation speed	1150 [rpm]
Input energy *E*	65.2 [J]
Workpiece diameters *Φ*	20 [mm]
Feed rate	1,2 [mm/s]

Figure 8-15 A wider cylindrical hardened surface obtained by AS technique.

By different feed rates of the laser beam, laser power was regulated and the real time laser power and temperature are reported in Figure 8-16. In the first phase, because of the power in maximum the temperature increased fast until the temperature reached the setting point (1200 ℃) and then the laser beam started to move. For the first seconds of the second step, the temperature on the surface drops due to the cold bulk material, so maximum power was applied automatically. Because of the heat accumulation in the cylindrical workpiece, the temperature reached the setting point and power started to decrease to keep a constant temperature (see Figure 8-15 (a)). On the contrary, when a fast feed rate is given, the maximum power will not be enough to keep the temperature on the set valve as shown in Figure 8-15 (b).

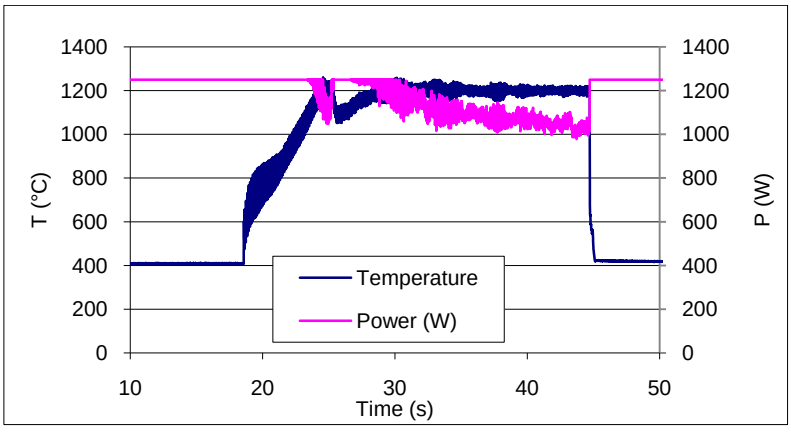

(a) feed rate – 1 mm/s

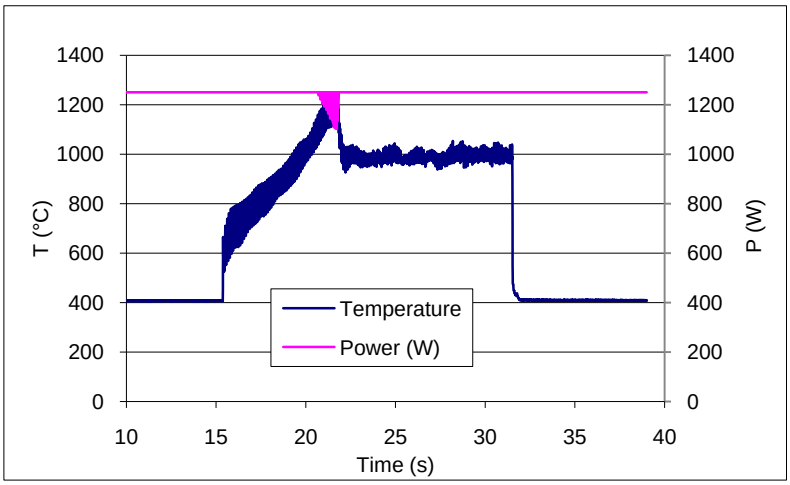

(b) feed rate – 2 mm/s

Figure 8-16 Real time and power record in overlapping AS hardening.

The hardness tests in the cross section were carried out under the surface 75 μm, the profiles are given in Figure 8-17.

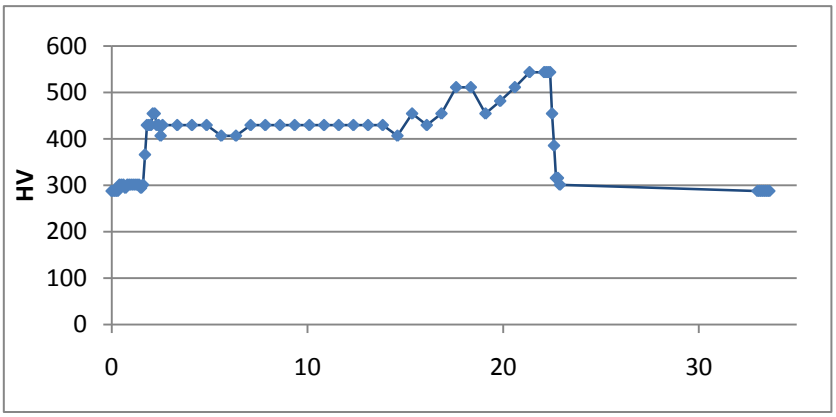

(a) feed rate – 1 mm/s

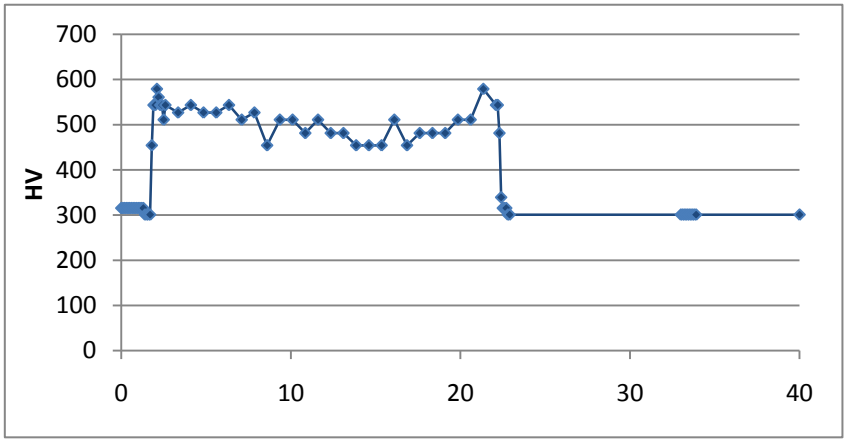

(b) feed rate – 2 mm/s

Figure 8-17 Hardness profiles of the hardened samples by overlapping AS technique.

The records of the real time power and temperature of the heated shaft reveal that by automatic controlling the laser power, the cylindrical surface AS hardening takes place. It can be noted from the hardness profiles that, the hardness of the treated layer is not uniform and lower than the single annular track hardening. This can be ascribed mainly to the temperature increase in the bulk of the shaft as discussed above. To avoid or reduce the heat accumulation, high feed rate should be carried out, and as a result, high laser power should be guaranteed.

8.5 Conclusions

In this chapter, the laser hardening process was applied to cylindrical workpiece. Different hardening methods were discussed, due to back tempering drawback happened in the cylindrical workpiece, a new technique – AS hardening was proposed.

The main results are listed as following:

1. During the laser hardening process for a cylindrical workpiece, if a low rotation speed is imparted to the workpiece, overlapping has to be applied for both single annular treated surface and wider treat surface.
   - A single annular hardened surface could be obtained by rotating the workpiece only one revolution. The overlapping happens in the initial and finishing parts of the hardened surface, other positions of the hardened zone have a uniform hardness.
   - In the overlapping process of the low rotation speed hardening, the overlapping was applied for every rotation; in this case, the back tempering happens in the

entire hardened surface. As the overlapping tracks increases, the hardness decreases along the axis direction; this is due to the heat accumulation in the workpiece.

2. The Apparent Spot technique is proposed to solve the overlapping and back tempering phenomenon in the cylindrical workpiece. This technique is the combination of high rotation speed and high laser power.
   - For the single track AS hardening, annular hardened zones are obtained in the case of the small diameter workpiece.
   - The geometrical features of the hardened zone were related only to the diameter of the workpiece, the power density and rotation speed have no effect on the geometrical features. Both the width and height of the hardened zone decrease as the diameter of the workpiece enlarged.
   - The hardness tests of the AS hardened zone are decided by the diameter and input energy. For small diameter (less than 15 mm), the hardness is effected neither by diameter nor input energy, a uniform hardness 709 ± 22 HV is obtained. For bigger diameter (20 mm) the hardened layer is obtained only by the high input energy. For the shaft with 25 mm diameter, no uniform hardness was obtained even by the high input energy.
3. With the automatic power control, AS technique is applied to treat the wider surface. The hardness of the treated surface is lower than it in the single track AS hardening process. This is mainly due to the discussed heat accumulation in the shaft.

Finally, this AS technique has still to be addressed since a lack of knowledge exists and deeper investigation is needed.

9 Conclusions

In this chapter the main conclusions of the thesis work are reported and discussed.

Laser hardening has been developing fast and widely applied in industrial fields due to its unique advantages such as self-quenching, small deformation and flexible controlled. The limited dimension of the laser beam makes the laser hardening be suitable for the complex geometrical workpiece and localized hardening; on the other hand, treatment on a large surface becomes its limitation currently.

The purpose of this research work was to study and reduce the overlapping and back tempering phenomenon in the case of a large surface treated by laser. In this thesis work both planar surface and cylindrical surface are investigated under the overlapping condition, and then some solutions are proposed to reduce or eliminate this back tempering drawback.

Different results are obtained by this thesis work.

For planar surface:

1. The effects of laser hardening parameters on the hardened surface were studied. Thanks to the control system, where the temperature was controlled in the feasibility window, hardened surface can be obtained by different combinations of laser power and scanning speed. The hardness drops in the overlapped zone when a large surface is treated.

2. One solution to the back tempering phenomenon is laser melting. When the surface of the workpiece is melted and solidified rapidly, a new refined structure with high hardness is formed on the top surface, this new structure is not affected by the back tempering in the overlapped zone, and a uniform treated surface could be obtained by overlapping laser melting process. To get a uniform melted surface on the top surface, high temperature must be guaranteed.
3. Scanning laser head to shape the laser spot into a large dimension is a way to avoid the overlapping process. Under the investigation of scanning a fiber laser beam, the most important two facts are the dimension of the laser beam and scanning frequency. An 8 mm width of hardened layer was obtained on the top surface. But due to the low absobtivity of metal for the fiber laser beam, the minimum depth of the hardened zone is only 10-20 μm.

For the cylindrical surface:

1. The back tempering phenomenon happens in both single annular track hardening and wider surface hardening, if the cylindrical workpiece is under a low speed rotation during the hardening process. When a single annular track is required, the overlapping exists in the initial and finishing parts. For a large cylindrical surface, the overlapping happens between the nerghbor tracks as it in the planar surface.
2. Apparent Spot hardening is a new technique to solve the overlapping phenomenon for the cylindrical workpiece. The mechanism of this technique is to rotate the workpiece at a high speed, and a virtual circular laser spot is obtained around the circumference of the workpiece.
3. When the AS technique is applied to treat a single annular track, the hardened results are depend on the diameter and input energy. When the diameter of the workpiece is too large, the input energy cannot get a fast heating phase. Consequently, the rapid self-quenching is no longer ensured and lower hardness is obtained in the hardened zone.
4. The heat accumulation in the cylindrical workpiece is an important factor which has to be considered during the hardening process for a cylindrical workpiece. To treat a lager surface by AS technique, high power and high feed rate must be applied to reduce the heat accumulation in the bulk material.

List of Figures

List of Tables

References

1 John C. Ion, (2005), Laser processing of engineering materials pp.15-16

2 C. Emmelmann, C. Tuchel (2001), Latest production innovations in of laser technologies-shown with diode pumped solid state lasers. High productive joining processes, Proc. 7th International Aachen Welding Conference (ASTK 01)

3 L. Migliore, Laser material processing. Laser Kinetics, Inc., Mountain View, California. Theory of laser operation, pp.1-30.

4 Beyer, (2006), Fiber laser welding. Industrial laser solution 21 (7).

5 L. Li, R. Dewhurst (1999), Chewing gum removal by lasers. UK Patent Application, GB9926638.9, Tidy Britain Group.

6 L. Li, (2000), The advances and characteristics of high power diode laser materials processing, Opt. Lasers Eng. 34, pp.231-253.

7 P. Molian, (1989) Surface modification technologies-An engineers guide TS Sudarshan (NewYork: Marcel Dekker), pp.421

8 J.M.F. Vollertsen, K. Partes., (2005), State of the art of laser hardening and cladding, Proceeding of The Third International WLT Conference.

9 J.C. Ion, (2002), Laser transformation hardening, Surface Engineering 18, pp.14-31,

10 R.A. Seban, (1965), J. Heat Transfer, pp.173

11 W.W. Duley, (1986) Laser material interactions of relevance to metal surface treatment, Proceedings of NATO Advanced Study Institute on Laser Surface Treatment of Metals, Martinus Nijhoff Publishers, Dordrecht, pp. 3.

12 T.J. Wieting, J.T. Schriempf, J. Appl. (1976) Phys. 47 4009

13 G. Stern, (1990) Proceedings of the Third European Conference on Laser Treatment of Materials, pp. 25

14 J. Grum, T. Kek, (2004), The influence of different conditions of laser-beam interaction in laser surface hardening of steels, Thin Solid Films 453 -454, pp. 94-99

15 Wolfgang Schulz, Reinhart Poprawe, (2000) Manufacturing with Novel High-Power Diode Lasers, IEEE Journal of Selected Topics In Quantum Electronics 6

16 F. Dausinger, J. Shen, (1993), ISIJ Int. 33, pp.925.

17 Friedrich Bachmann, (2003), Industrial applications of high power diode lasers in materials processing, Applied Surface Science 208-209, pp.125-136

18 Henrikki Pantsar, Veli Kujanpaa, (2004), Diode laser beam absorption in laser transformation hardening, Journal of Laser Applications 16, pp.147-153

19 E. Kennedy, G. Byrne, D.N. Collins, (2004), A review of the use of high power diode lasers in surface hardening, Journal of Materials Processing Technology 155–156, pp.1855–1860

20 R. Komanduri, Z.B. Hou, (2001), Thermal analysis of the laser surface transformation hardening process, International Journal of Heat and Mass Transfer 44, pp.2845-2862

21 R. Komanduri, Z.B. Hou, (2004), Thermal analysis of laser surface transformation hardening – optimization of process parameters, International Journal of Machine Tools & Manufacture 44, pp.991–1008

22 Stephen Skvarenina, Yung C. Shin, (2006), Predictive modeling and experimental results for laser hardening of AISI 1536 steel with complex geometric features by a high power diode laser, Surface & Coatings Technology 201, pp.2256–2269

23 A. Weisheital, B.L. Mordike, (1991) Laser surface modification of materials, Processing IMT Conf., Birmingham,

24 F. Lusquinos, J.C. Conde, S. Bonss, A. Riveiro, F. Quintero, R. Comesana, J.Pou, (2007), Theoretical and experimental analysis of high power diode laser (HPDL) hardening of AISI 1045 steel, Applied Surface Science 254, pp.948–954

25 L.J.YANG, S.JANA, S.C.TAM, (1990) Laser Transformation Hardening of Tool-Steel Specimens, Journal of Materials Processing Technology 21, pp.119-130

26 J. Grum, (2007), Comparison of different techniques of laser surface hardening, Journal of Achievements in Materials and Manufacturing Engineering 24, pp.17-25

27 S.A.Fedosov, (1999), Laser Beam Hardening of Carbon and Low Alloyed Steels: Discussion Of Increased Quantity Of Retained Austenite, Journal of materials Science 34, pp.4259-4264

28 Jae-Ho LEE, Jeong-Hwan JANG, Byeong-Don JOO, Young-Myung SON, Young-Hoon MOON, (2009), Laser surface hardening of AISI H13 tool steel, Trans. Nonferrous Met. Soc. China 19, pp.917-920

29 J. Hannweber, S. Bonss, B. Brenner, E. Beyer, (2004) Integrated laser system for heat treatment with high power diode laser. ICALEO 2004 congress proceedings

30 C.H.Chen, C.J.altstetter, J.M. Rigsbee, (1984) Laser Processing of Cast Iron for Enhanced Erosion Resistancee, Metallurgical Transactions A, volume 15A

31 Henrikki Pantsar, Veli Kujanp, (2006), Effect of oxide layer growth on diode laser beam transformation hardening of steels, Surface & Coatings Technology 200, pp.2627– 2633

32 R.A.Ganeev, (2002), Low Power Hardening of Steel, Journal of Materials Processing Technology 121, pp.414-419

33 I.R. Pashby, S. Barnes, B.G. Bryden, (2003), Surface hardening of steel using a high power diode laser, Journal of Materials Processing Technology 139, pp.585–588

34 F. Lusquinos , J.C. Conde, S. Bonss, A. Riveiro, F. Quintero, R. Comesana, J. Pou, (2007), Theoretical and experimental analysis of high power diode laser (HPDL) hardening of AISI 1045 steel, Applied Surface Science 254, pp.948–954

35 Shakeel Safdar, Lin Li, M. A. Sheikh, Zhu Liu, (2006) An Analysis of the Effect of Laser Beam Geometry on Laser Transformation Hardening, Journal of Manufacturing Science and Engineering 128, pp.659-667

36 H. J. Hegge, J. T. M. De Hosson, (1987), The Relationship between Hardness and Laser Treatment of Hpyo-Eutectoid Steels, Scr. Metall, 21, pp.1737–1742.

37 L. M. Galantucci, L. Tricario, (1999), An Experimental and Numerical Study on the Influence of Not Uniform Beam Energy Distribution in Laser Steel Hardening, Annals of the CIRP Vol. 48/1/1999, pp.155-158

38 P. Hoffmann, R. Dierken, (2003) Temperature Controlled Hardening of Single Part Tools for Automotive Industry With High Power Diode Laser Systems, Proceedings of the Second International WLT-Conference on Lasers in Manufacturing

39 J. Senthil Selvan, K. Subramanian, A.K. Nath, (1999), Effect of laser surface hardening on En18 (AISI 5135) steel, Journal of Materials Processing Technology 91, pp.29-36

40 S. A. FEDOSOV, (1999), Laser Beam Hardening of Carbon and Low Alloyed Steels: Discussion of Increased Quantity of Retained Austenite, Journal of Materials Science 34 pp.4259 - 4264

41 K. Obergfell, V. Schulze ,O.Vohringer, (2003), Classification of microstructural changes in laser hardened steel, Materials Science and Engineering A355, pp.348-356

42 J.Ruiz, V.Lòpez, B.J.Fernandez, (1996), Effect of surface laser treatment on the microstructure and wear hehaviour of grey iron, Material & Design 17, pp.267-273

43 X. Liu, G. Yu, J.Guo, Q.Shang, Z.Zhang, Y. Gu, (2007), Analysis of Laser Surface Hardened Layers of Automobile Engine Cylinder Liner, Journal of iron and steel research, international 14(1), pp.42-46

44 Rahul Patwa, Yung C. Shin, (2007), Predictive modeling of laser hardening of AISI5150H steels, International Journal of Machine Tools & Manufacture 47, pp.307–320

45 Stephen Skvarenina, Yung C. Shin, (2006), Predictive modeling and experimental results for laser hardening of AISI 1536 steel with complex geometric features by a high power diode laser, Surface & Coatings Technology 201, pp.2256–2269

46 Neil S. Bailey, Wenda Tan, Yung C. Shin, (2009), Predictive modeling and experimental results for residual stresses in laser hardening of AISI 4140 steel by a high power diode laser, Surface & Coatings Technology 203, pp.2003–2012

47 M.J.Tobar, C. Álvarez, J.M. Amado, A. Ramil, E. Saavedra, A. Yáñez. (2006), Laser Transformation Hardening of a Tool Steel: Simulation-based parameter optimization and experimental results, surface & coatings technology 200, pp.6362-6367

48 H.Pantsar and V.Kujanpaa, (2004), Diode laser beam absorption in laser transformation hardening of low alloy steel, Journal of Laser Applications 16, pp.147-153.

49 E.Hensel, (2003) Close-loop Hardening of Automotive Components, Proceeding of Advanced automotive laser applications (ALAC2003)

50 E.Capello, M.Castelnuovo, B.Previatli, (2006), Optimization of production rate in diode laser hardening, ICALEO 2006 Congress Proceedings.

51 E.Capello, M.Castelnuovo, (2005), Real time control of diode laser hardening in view of near net-shape manufacturing, Proceeding of the 58th annual assembly and international conference of international institute of welding.

52 C.M.Cook, J.M.Haake, (2000), Monitoring and controlling the temperature in a high power direct diode laser surface hardening application, 20th ASM Heat Treating Society Conference Proceedings, pp.183-191

53 Steffen Bonss, Marko Seifert, Jan Hannweber, Udo Karsunke, Eckhardt Beyer, (2005), Low Cost Camera Based Sensor System for Advanced Laser Heat Treatment Processes, ICALEO 2005 Congress Proceedings, pp.851-855

54 Zhiyue Xu, Keng H. Leong, Claude B. Reed, (2008), Nondestructive evaluation and real-time monitoring of laser surface hardening, Journal of Materials Processing Technology 206, pp.120–125

55 Dietmar Hömberg, Wolf Weiss, (2006), PID Control of Laser Surface Hardening of Steel, IEEE Transactions on Control Systems Technology 14, pp.896-904

56 K. Bewilogua, G. Brauer, A. Dietz,J.Gabler, G. Goch, B. Karpuschewski, B.Szyszka, (2009), Surface Technology for Automotive Engineering, CIRP Annals - Manufacturing Technology, CIRP-436,

57 V. S. Maiorov, S. V. Maiorov, (2009), Solid laser hardening of iron parts, Metal Science and Heat Treatment Vol. 51, pp.106-108

58 Edoardo Capello, Barbara Previtali, (2008), Optimization of production rate in diode laser hardening, Journal of Laser Applications 20

59 Ritesh L.J.Yang, S.Jana and S.C.Tam, (1990), The Effects of Overlapping Runs in The Laser Transformation Hardening of Tool-Steel Specimens, Journal of Materials Processing Technology 23, pp.133-147

60 J.H Hwang, Y.S Lee, D.Y Kim, J.G Youn, (2002), Laser Surface Hardening of Gray Cast Iron Used for Piston Ring, Journal of Materials Engineering and Performance, Volume 11(3) June, pp.294-300

61 E. Capello, L. Giorleo, (2008), Apparent Spot in Circular Laser Hardening, conference proceeding AMST 2008, pp 405-416

62 A.N. Savonof, (1997), Basic directions of effective use of laser equipment for heat treatment of alloys, Metal Science and Heat Treatment 39, pp. 275

63 G. Tani, L. Orazi, A. Fortunato, (2008), Prediction of hypo eutectoid steel softening due to tempering phenomena in laser surface hardening, CIRP Annals - Manufacturing Technology 57, pp.209–212

64 Ritesh S. Lakhkar, Yung C. Shin, (2008), Matthew John M. Krane, Predictive modeling of multi-track laser hardening of AISI 4140 steel, Materials Science and Engineering A 480, pp.209–217

65 A. Liu, B. Previtalia, (2010), Laser surface treatment of grey cast iron by high power diode laser, conference proceeding LANE 2010, pp.439-488

66 C. Yao, B.Xu, J.Huang, P.Zhang, Y.Wu, (2010), Study on the softening in overlapping zone by laser-overlapping scanning surface hardening for carbon and alloyed steel, Optics and Lasers in Engineering 48, pp.20–26

67 Guy Claus, Transformation hardening with high power diode laser systems using single and multiple tracks, ICALEO 2004 Conference Proceedings

68 E. Capello, B. Previtali, (2005), Effect of overlapping quote, focus height and beam velocity in the optimization of line laser hardening, 7th AITEM Conference

69 J.D. Kim, M.H.n Lee, S.J. Lee, W.J. Kang, (2000), Laser transformation hardening on rod-shaped carbon steel by Gaussian beam, Transactions of Nonferrous Metals Society of China 19, pp.941-945

70 M. Seifert, S. Bonß, B. Brenner, E. Beyer, (2004), High power laser beam scanning in multi-kilowatt range, ICALEO 2004 Conference Proceedings

71 S. Bonss, J. Hannweber, M. Seifert, F. Tietz, S. Kühn, U. Karsunke, B. Brenner, E. Beyer, (2007), Novel machine system for simultaneous heat treatment with dynamic beam shaping, ICALEO 2007 Congress Proceedings, pp.1081-1086

72 B.L. Mordike, (1995), Surface treatment with high power lasers, Laser in Engineering 4, pp. 187-200

73 Janez Grum, Roman Sturm, (1997), Laser surface melt-hardening of gray and nodular irons, Applied Surface Science 109/110, pp. 128-132

74 Janez Grum, Roman Sturm, (1998), Influence of laser surface melt-hardening conditions on residual stresses in thin plates, Surface and Coatings Technology 100-101, pp. 455-458

75 M.H.Tulloch, (1992), Laser melting of camshafts saves wear, Photonics Spectra, pp.20

76 V. Lopez, J. M. Bello, J. Ruiz and B. J. Fernandez, (1994), Surface laser treatment of ductile irons, Journal of Materials Science 29, pp. 4216-4224

77 K.A Chiang, Y.C. Chen, (2005), Laser surface hardening of H13 steel in the melt case, Materials Letters 59, pp. 1919– 1923

78 C. Li, Y. Wang, Z. Zhang, B. Han, T. Han, (2010), Influence of overlapping ratio on hardness and residual stress distributions in multi-track laser surface melting roller steel, Optics and Lasers in Engineering 48, pp. 1224–1230

79 J. Grum, R. Sturm, (2005), Influence of laser beam guiding and overlapping on residual stress in melting process, Surface Engineering 2, pp.27-34

80 L.Giorleo, A.Liu, B.Previtali, (2010), Apparent spot in circular laser hardening: effect of process parameters, conference ESAFORM 2010, pp. 1119 – 1122

81 Guy Claus, M. Seifert, (2007), High speed rotation hardening of steel shafts and holes with high power diode laser, ICALEO 2007 Congress Proceedings, pp.266-270

82 A.Fortunato, L.Orazi, G.Campana, A.Ascari, G.Cuccolini, G.Tani, (2009), Laser hardening of large cylindrical martensitic stainless steel surface, Proceedings of the Fifth International WLT-Conference LIM 2009

83 G. Tani, A. Fortunato, A. Ascari, G. Campana, (2010), Laser surface hardening of martensitic stainless steel hollow parts, CIRP Annals-Manufacturing Technology 59, pp.207–210

84 S.Bonss, J.Hannweber, U.Karsunke, S.Kuehn, M.Seifert, E.Beyer, G.N.Drollinger, (2008), Integrated laser beam hardening in turing machines for process chain reduction, ICALEO 2008 Congress Proceedings, Poster Presentation Gallery, pp.94-99

Content

1 Preface

Laser beam is a low divergence, parallel beam which can be focused on a small spot, on which the full beam power concentrated. These features of the laser beam make it unique in modern industry. In the mean time, the power enhanced laser makes it possible to apply the high power beam to various production processes. Compared to the conventional methods, high power laser creates a new process method which is faster, more flexible, net shape and cleaner.

Today's highly competitive markets require the industries to look for new technologies to improve the product performance and productivity. For industrial equipments, most engineering components not only rely on their bulk material properties but also on the design and characteristics of their surface. Surfaces are the bounding faces of the solid components; they always interact with the working environment, and under severe conditions their performance and reliability can be limited due to the wear and corrosion. The solution of the problem is surface treatment. Surface engineering involves different special treatments to alter the properties of the surface phase in order to reduce the degradation over time; this makes the surface robust to the environment in which it will be used and prolongs the component life.

The most common processes of the surface treatment include flame and induction hardening, carburizing, nitriding. As a result, the chemistry and mechanical performance of the surface is modified and improved. Nowadays, high power laser has become a new heat source for the same job. Laser surface treatment can be applied in both coating and hardening in the surface treatment fields; it has many

advantages compared with the traditional ways, such as smaller distortions and less post-process time.

Laser surface treatment is a very flexible process, because of the self-quench and easily controlled laser power; it has been wildly used in automobile sectors and other industrial areas. One important application is the laser hardening, which involves only a thermal effect on the surface where a new structure with high hardness is obtained on the top surface. In most of these applications, laser does not treat the complete surface of the components but rather small local tracks. With a designed and delicate movement control system, laser hardening is suitable for some components with complex geometry, *i.e.* edges, corners and holes.

Because of the small spot dimension of laser beam, limitations and drawbacks are induced when the surface to be treated is larger than the laser beam. To gain a large treated surface by laser hardening, multi-pass technique is required where the hardened tracks slightly overlap each other. . But this technique is far from perfect due to a main drawback called “back tempering”, which means every hardened track is partly reheated and tempered by the consequential ones. The structure of the reheated part transforms from martensite into tempered martensite, resulting in low hardness, and end up with a non-uniform hardened zone. The back tempering happens on planar and cylindrical surfaces. In order to overcome this drawback, different techniques are proposed, e.g. laser melting, scanning laser head, to obtain a desired laser beam.

This thesis studies the characterizations of the back tempering phenomenon in the overlapped zone, and reduces effects of this drawback by different techniques to get a large treated surface on planar and cylindrical surfaces.

In chapter 2, an overview of laser hardening is given, first, the principle of laser hardening, development of this technique and the industrial applications are discussed. And then the works on back tempering drawback and some solutions will be focused.

In chapter 3, the objectives of this thesis will be summarized.

Chapter 4 gives the details of the experimental setup, including the laser with a control system, the metallurgic analyzing method for the hardened samples.

In chapter 5, the effects of different parameters on the hardened zone and hardness decrease in the overlapping are the main topic of chapter, where the planar surface laser hardening study are carried out, both single track and multi-pass are investigated.

In chapter 6 and chapter 7, some solutions for the back tempering phenomenon on the planar surface are given. Laser melting technique is studied; overlapping process is carried out by melting the surface. The other solution is scanning laser head hardening, different scanning conditions are applied.

Chapter 8 gives a solution to eliminate the back tempering on the cylindrical surface. Experimental results in this chapter show that apparent Spot (AS) is an effective solution to get a uniform hardened zone.

In the end, chapter 9 summarizes the results of this thesis work and the future works are suggested.

2 State of the art

Laser hardening is an important surface modification technique in today's industry, in this chapter, a review of the bibliography is given.

A general introduction of the laser surface engineering, especially laser hardening process is presented, including the process principle, development and industrial applications. Following the bibliography research is focused on the laser hardening technique on large surfaces. The back tempering is the main drawback when multi-pass is applied to treat a large surface and different solutions are proposed.

2.1 Introduction

Since the first laser was built 50 years ago, laser has evolved from a source of high-intensity monochromatic radiation into a powerful tool in engineering and manufacturing. In industrial applications, a focused laser beam is one of the highest power-density sources for materials processing today, because of its highly concentrated energy.

Since the first functional laser was generated, this innovative technology has developed fast for most important types of lasers. With the increase of laser power, in the 1970s, CO_2 lasers were firstly applied in materials processing such as cutting and joining, the power of the CO_2 laser up to 10 kW entered the market in 1990 [1]. In the meantime, the first lamp pumped Nd:YAG lasers in the kilowatt range were

invented at the beginning of the nineties, and then semiconductor lasers were available a few years later [2], until today diode lasers with power up to 10 kW are commercially available. Solid state lasers became the new development trend since it is possible to couple the solid state laser light in flexible guiding fibers. Its advantages enable solid state lasers widely applied in industrial field, where the most important applications were in automotive industry and new applications for surface engineering [3]. In the beginning of the twenty-first century, new promising technologies in solid laser - fiber laser and dick laser had been developed. These two kinds of laser are described as high brightness laser family, which are featured as high laser beam quality, unlimited laser powers. Welding and cutting are the most interesting applications of high brightness lasers [4].

Compared to the conventional processing, laser in material processing has several unique advantages e.g. non-contact processing, controlled and automated processing, net-shaped operation, high productivity, economic manufacturing, improved product quality, greater material utilization and minimum heat affected zone. With the development of its high power and high quality, laser processing has become a useful technology in the growing number of processes and wider bandwidth of applications. Figure 2-1 shows some main laser material processing in today's industrial applications.

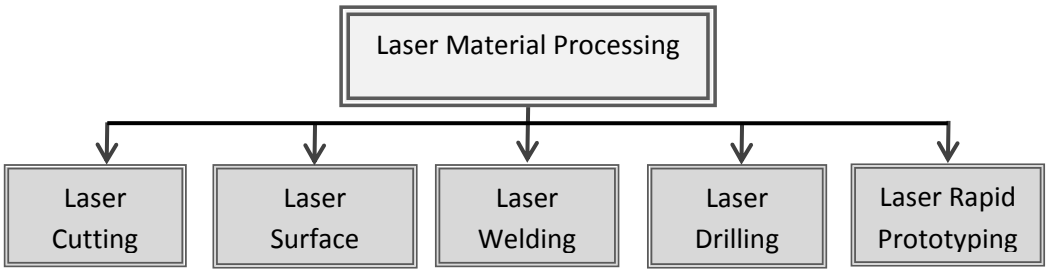

Figure 2-1 Laser materials processing technologies.

From the true application point of view, that laser power is not the only parameter to make a successful process; interaction time with the materials and power density are also important. Figure 2-2 illustrates the possible operating regimes for various types of laser processing [5].

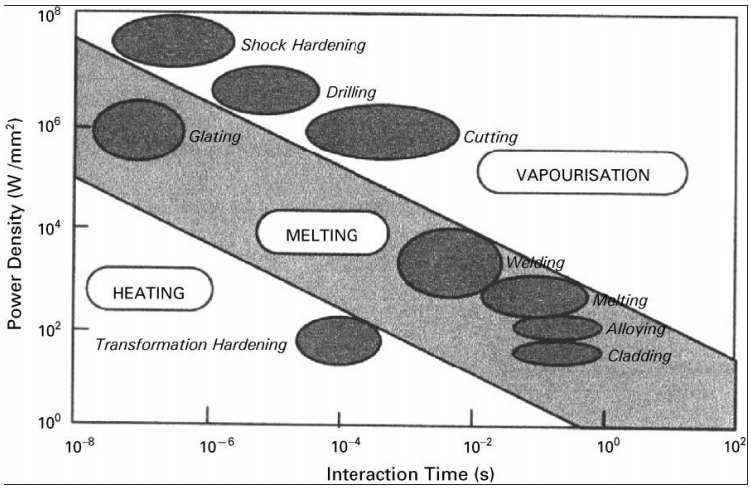

Figure 2-2 Effects and possible applications of lasers under various operating conditions.

The processes are divided into three major domains in the processes, involving solid to solid (only heating, without melting/vaporizing), solid to liquid (melting) and solid to liquid (vaporizing). Usually the power density is the most often considered factor when determining possible type of laser processing or choosing laser sources for different process. Generally speaking, surface heating without melting requires low power density and other processes with phase transform needs higher power density.

There are some other parameters which influence the results of laser materials processing, including wavelength of the laser, the wavelength absorptivity of different materials, and laser beam quality [6]. For examples, carrying out material processing by CO_2 laser, a pre-coating process is necessary to increase the absorptivity of the wavelength of CO_2 laser; fiber laser is the best choice for a keyhole welding because of the high beam quality and diode laser is suitable for surface treatment because of the high metallurgical absorptivity and uniform energy distribution.

2.2 Laser surface engineering techniques

2.2.1 Principle and classification

The surface of the materials acts as an interface to the surrounding environment. The contact with the surroundings results in degradation due to wear, erosion and corrosion [7].The industrial solution to minimize or eliminate such surface initiated

failure is based on changing the surface microstructure and/or composition of the workpiece but without affecting the substrate [8][9].

The basic physics of laser surface treatment is using laser as energy source to interact with the surface of an absorbing material and subsequently cooled by heat conduction into the bulk material. In industry there are two kinds of surface treatment applications (see Figure 2-3). One involves thermal transformation process with the base materials, such as laser hardening and laser melting, which is related the modification of surface properties by changing the microstructure of the surface layer. The other application involves both thermal and chemical process, such as laser cladding and alloying, where new materials are applied on the surface of substrate during the laser irradiation. The new materials are melted, then coats and joins in the substrate, a modification is also involved in the surface of the substrate.

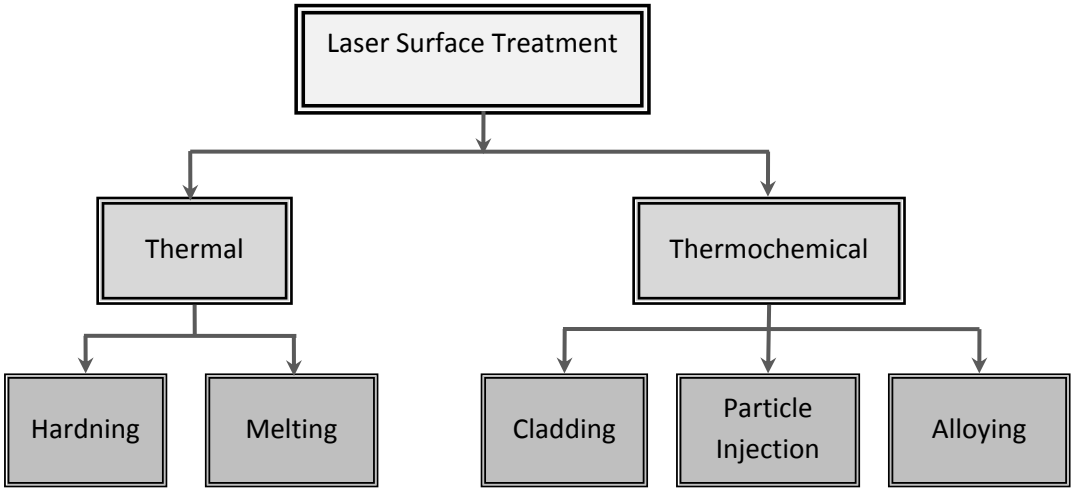

Figure 2-3 Classification of laser surface treatment.

The modification of the surface zones leads to an improved durability of the component that allows cost reduction and therefore an enhanced profitability.

2.2.2 Laser sources for laser surface engineering

At the beginning of laser hardening application, the most traditional high power CO_2 lasers have been widely used, since only CO_2 lasers were able to deliver the high power which was needed for hardening. The absorption of metal decreases as the wavelength lengthens, and CO_2 laser-beam light has a comparatively long wave-length, 10.6 μm, the absorption of steel and iron at CO_2 laser beam is very small, some experiments have shown that an absorptivity between 2-3% and 3% for a CO_2

laser beam incident on polished iron [10] [11]. 9-10% absorptivity values have been obtained for AISI 304 austenitic stainless steel [12]. To decrease the energy loss, pre-coating is needed for CO_2 laser.

With the development of Nd:YAG laser, it replaced the CO_2 lasers in laser surface applications. Nd:YAG laser operates at a shorter wavelength 1.06 μm. The shorter wave length significantly improves the absorption characteristics of the metal, e.g. the between 28.6% and 30% for low alloy steels [13]. But the electrical to optical efficiency for Nd:YAG laser is definitely low, which makes the equipment bulky and costly to run [14].

Recently high power diode laser (HPDL) has become industry available and overcome some barriers referred to CO_2 and Nd:YAG lasers [15]. The lower wavelength, typically 0.8 and 0.94 μm, improves the absorption characteristics for the laser beam. And due to the very high absorptivity of metal for this wave length which can reach 35-40% for a polished, non-oxidized steel surface by theoretical calculations [16]. HPDL hardening leads to the unnecessary of coating, which means saving time and cost, also the environment is improved. Other than the absorptivity advantage, the hat top power distribution and rectangular shape spot of the laser beam are also two important benefits for laser hardening application [17] [18]. These two characteristics make HPDL hardening has wider and more uniform hardened zone in width and depth respectively. The electrical to optical efficiency is relative high compared with other kinds of laser, HPDL equipments are also remarkably smaller in size than CO_2 and Nd:YAG lasers of the same power, which make it possible of integration in the production line.

2.3 Laser surface hardening

Laser surface hardening is also called laser transformation hardening or laser hardening. It is a technique to obtain hard and wear resistant surface layer with a typical thickness of 0.5 to 1.5 mm [19]. A laser is as a heat source, scans and heats the surface, the rest of the component acts as a heat sink resulting in a high cooling rate. Laser hardening is a promising process for ferrous family to produce a hardened layer on the surface as shown in Figure 2-4.

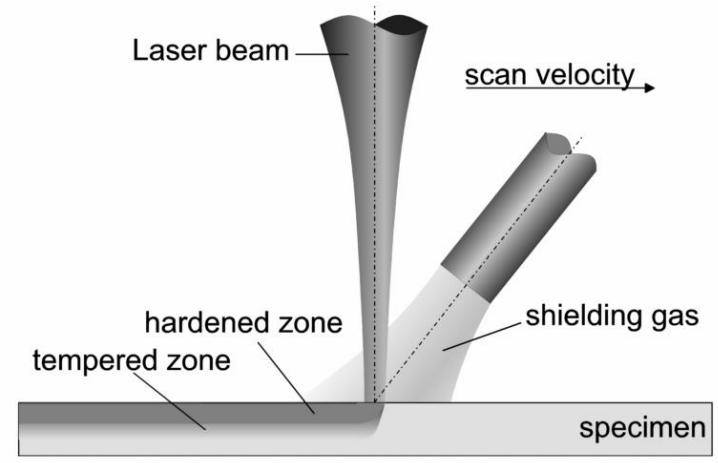

Figure 2-4 Principle of laser hardening Process [8].

2.3.1 Process description

The surface of the material is heated rapidly above the Ac_3 temperature, then the structure is transformed from the initial ferritic / pearlitic structure (α + Fe3C) to an austenitic where the carbon is dissolved. Hardening takes place when the material is subsequently cooled down at a high cooling rate that there is not enough time available for the reverse transformation and the carbon does not excrete but remains in the crystal structure. Instead of the ferritic or pearlite, very hard and compact martensite structure is obtained [20][21][22].

The formation of martensite is a multiply factors process, Figure 2-5 shows the detail phase transitions during the laser surface hardening.

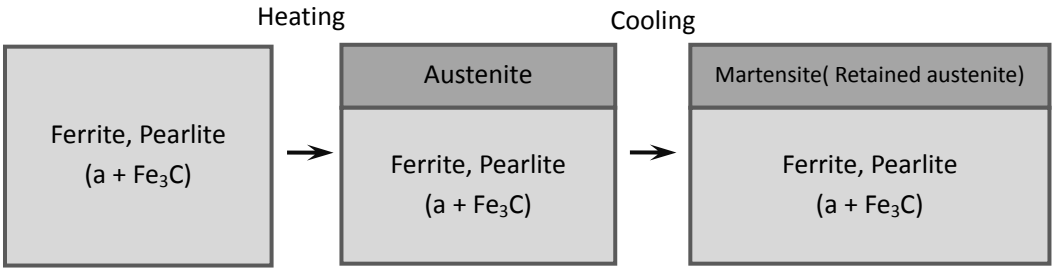

Figure 2-5 Process and material component during laser hardening process.

There are some important criteria which affect the process strongly [23] [24][25]:

1. Surface temperature of the hardened zone should reach austenization temperature. Only if the surface temperature reaches the austenization temperature level Ac_3, both the pearlite and ferrite will transform to austenite.
2. Between the heating and cooling cycle, surface of the substrate should be maintained above the austenization temperature long enough for carbon diffusion to form homogeneous austenite and get a uniform hardness in hardened zone.
3. The heated surface of the workpiece should not reach the melting temperature.
4. The heating and cooling rate should be high enough. At the heating phase, a high temperature gradient is required to heat a sufficient thick surface layer in a short time and to prevent heating the bulk material. For cooling phase, martensite is a non equilibrium phase; the cooling rate should be fast enough to avoid the formation of pearlite and ferrite.
5. The transformation temperatures and the process are affected by the microstructure, *e.g.* the presence and the distribution of alloying elements in the material.

In conventional hardening the product is heated by flame, in a furnace or electron beam. Compared with these ways, the advantages of laser heat treatment can be categorized as following [26][27]:

1. Due to limited energy input, only the surface is heated, the bulk is still cool; self-quenching is established during the process.
   - Laser heat treatment is a saving energy process and the heat affected region of the component is limited.
   - Minimal thermal distortion of the work piece after the treatment.
   - No milling, grinding or cleaning is needed for the final workpiece.
2. Without the need of quenching, laser hardening could be the last process in a production line and the hardening process is clean for environment [28].
3. Laser hardening is a flexible process.
   - The energy of the laser can be well controlled by software or hardware.
   - With different optical system, *e.g.* focusing lenses, different degrees of defocus and scanning system, the dimension and shape of the laser beam can be easily changed.
   - With the assist of smart movement system, laser hardening can be adapted to complex shape workpiece.
4. Laser hardening is also a high productivity process.
   - Laser hardening is a rapid process, because of the fast heating and cooling phase.
   - It is suitable to incorporate a laser source in an automation production line.

Figure 2-6 shows the comparison in the process chain between internal laser hardening and external induction hardening in the production of a metal forming tool [29], the left column shows the time consuming and costly in conventional way, the right column demonstrates the target laser process.

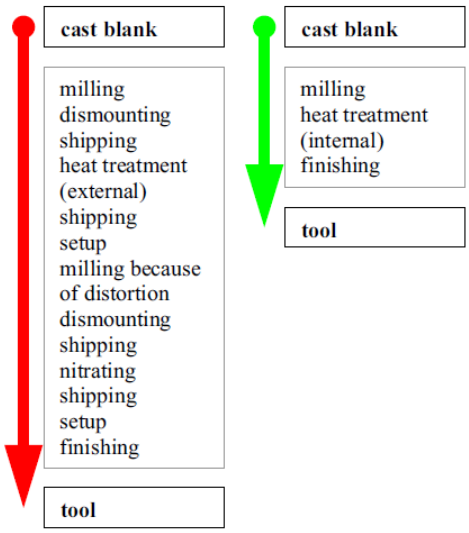

Figure 2-6 Comparison of the process chain when laser hardening and induction hardening are used.

2.3.2 Process development

In early work laser hardening process is related with CO_2 and Nd:YAG lasers. C.H.Chen applied a continuous 10 kW CO_2 laser to harden nodular and gray cast iron for enhanced hardness and erosion resistance [30]. Henrikki Pantsar studied the oxide layer during the process; it makes the oxide film increases the absorptivity especially distinct in CO_2 laser [31].

Study has shown a possibility of applying low power CW CO_2 laser (100W) laser to improve the microhardness of the steel surface [32]. With the development of diode laser, more and more laser hardening is carried out with a diode laser source. At 1997 Chen W, Roychoudhuri CS and Banas CM got a 0.1 mm thickness hardened zone using a 15 W fiber delivered HPDL on 400 series stainless-steel surface [2]. Klocke et al successfully hardened 42CrMo4 steel to hardness over 700HV with a depth of approximately 0.5mm using a 650W HPDL [3]. Until now, up to 10kW diode laser has been applied in industrial surface treatment.

2.3.2.1 Parameters and microstructure analysis

As the temperature range for laser hardening is very narrow (should be above the Ac_3 temperature and below the melting point), and the process is very fast, laser hardening is an unstable process, it is quite difficult to get a high quality and repeatable hardened zone. Laser hardening process involves different parameters, such as the initial condition and thermo-physical properties of the base material, the laser beam properties i.e. power, shape and energy distribution, scanning speed. All these parameters highly influenced the performance of the treatment. At the early stage of the laser hardening development, the parameters investigations were studied by most researches to obtain a hardened zone.

Pashby studied the depth of laser hardened zone under different power and scan speed combinations [33], the result shows that both 080M40 and 817M40 (British standard) can be surface hardened using a high power diode laser. The affected depths (up to 0.5 mm) and maximum hardness achieved varied with power and speed, as well as with steel type. I.RF. Lusquinos used a pyrometer and closed loop control for AISI 1045 flat sheets HPDL hardening [34], confirmed the hardened depth is proportional to the power divided by the inverse square root of the laser spot size times speed, as shown in Figure 2-7.

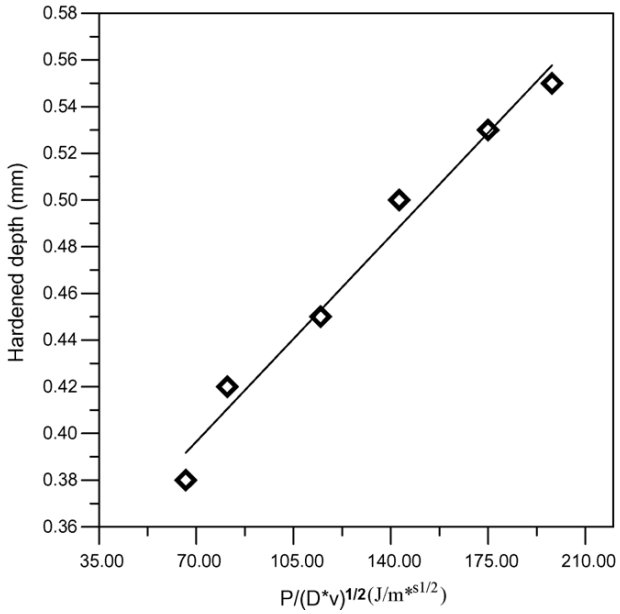

Figure 2-7 Evolution of the hardened dept with the parameter $P/(V*D)^{1/2}$ [34].

Different kinds of laser beam shapes are also investigated. Shakeel Safdar investigated the influence of circular, rectangular and triangular beam geometries for laser hardening [35]. Relationships between temperature and time, hardness and depth, microstructures of hardened zones were given for different laser shapes. Figure

2-8 gives an example of difference of the obtained hardened zones, (a) obtained by circular laser beam and (b) obtained by rectangular laser beam.

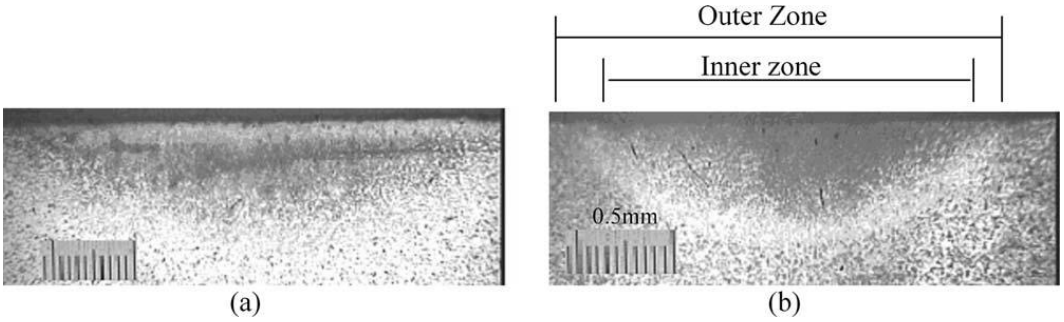

Figure 2-8 hardened zones obtained by different laser beam shapes [35].

Based on the results, the beam geometry strongly influences the temperature distribution during the process; a relative low heating rate is beneficial for the laser transformation hardening process, if the cooling rate is fast enough. This result agrees well with the basic transformation hardening theory established in the [36]. An experimental and numerical study [37]of non-uniform energy distribution during the hardening process strongly recommended a uniform power distribution for the laser spot, whereas the shape of the beam plays less important role in the same process. The relationships between geometry of the hardened track/hardened depth and laser beam distributions were investigated [38] as shown in Figure 2-9.

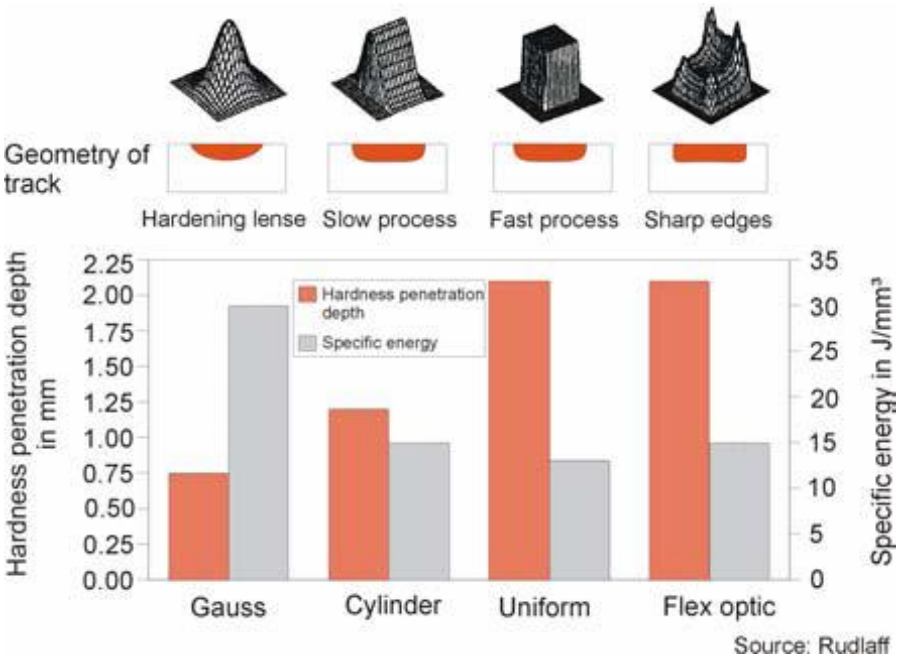

Figure 2-9 Hardened shape and depth obtained by different laser beam distributions.

In metallurgical point of view, the correlation between the surface temperature and cooling rate on the resulting hardness was explained by K. Subramanian [39], which confirmed a cooling rate were about 5000℃ /s, and a 2-fold increase in wear resistance for the laser-hardened AISI 5135steel. The retained austenite was studied in [40] for carbon and low-alloyed steels, indicating the cooling rate is high only at high temperatures. But when the temperature decreases, the cooling phase could be even lower than typical rates for conventional quenching. This leads to bainite transformation and, as result, increased retained austenite content. Hardened zones also were analyzed in terms of microhardness, dislocation density, and grain size by K. Obergfell [41], different pro-processes of the base materials affect the microhardness distribution. When the base material was tempered at 300℃ before hardening, the constant microhardness was observed near the top surface. On the contrary, microhardness started to decrease from the top surface if tempered by 600℃, but both tempering conditions shown a transition zone where the values decrease. Other than different kinds of steels, cast irons are the other group materials which are suitable for laser hardening process. The surface layer hardening to martensite takes place mainly by transformation of the perlitic region of the gray iron, the ferrite zones become totally or partially martensite due to the graphite solution [42]. Martensite or/and ledeburite eutectic, including certain retained austenite were also observed in the hardened zone of the gray cast iron [43].

2.3.2.2 Modeling and simulation

Finite Element Methods (FEM) is applied to study the influence of the process parameters on the thermal cycles and hardening results. Some researchers involve modeling the temperature distribution during the process in order to predict the microstructure, hardening depth, hardness and the residual stresses of the hardened zone. Rahul Patwa and Shin successfully set a 3D kinetic temperature distributions model in the cylindrical workpiece to predict the near surface structure and hardness [44]. In order to verify the simulation results, an experiment was carried out; it achieved a case depth of 0.54mm with uniform hardness of 63 RC in the AISI 5150 steels with 500W diode laser power. Skvarenina et al also successfully predicted and experimentally achieved 2.5 mm hardening depth with a uniform hardness of 57 HRC on a 1536 steel cylinder of 60 mm diameter with 2.9 mm/s scanning speed and 1220W diode laser power [45]. It indicated that with complex geometric feature, both of the hardness and depth decrease, in case of 2 mm radius, a depth of 1.5 mm and hardness of 55 HRC hardened zone is achieved. A transient 3D thermal and kinetic model is gotten by Neil S. Bailey et al [46]. Tobar established a combined methodology for building a laser transformation hardening with good predicting capabilities, the model allows detailed study and optimization on the selected parameters range [47].

2.3.2.3 Sensor and process control

With the increased requirement of industrial applications, control and optimizing laser hardening process are widely studied. The main reasons of control can be summarized as

- Heat accumulates during the hardening process; in this case, the initial condition is changing.
- Absorptivity of the surface for laser beam energy increases as the temperature increases [48], also the dust or oil which is on the surface influences the absorptivity.
- The geometry of the component is a most common disturbance of the laser hardening process.

In these cases using a constant laser beam power and constant scanning speed will lead to a non-uniform hardened surface. From the efficiency point of view, industry production should be high efficiency and minimize the time and money cost. Offline measurement and control result a lot of time and money loss, because correcting errors or doing the whole process again with a new workpiece would be required. Other than that, a control system should be inexpensive and less complicated. Therefore real time online measurement and control was developed for by many researchers [49][50][51]. The temperature at the spot could be used as control signal during the process; the temperature signal could be obtain by measuring the emitted inferred energy from the high temperature surface with a pyrometer or sensor. Based on the real time temperature obtained, the laser power and /or scanning speed can be controlled as expected, and then the surface temperature could be maintained on the required level.

A pyrometer controlled laser hardening system for 4140 steel and class 40 gray cast iron was investigated in [52], the surface temperature of the spot was monitored and the output power was controlled to maintain a constant temperature on the surface. The hardness and depth could be controlled in some degree by the input power and scanning speed. By the pyrometer temperature measurement, the hardness in the range of 50-65 RC and depth between 0.7 to 1.5 mm could be produced. It also indicates that laser surface transformation hardening not only increases the wear resistance, but under certain conditions the fatigue strength is also increased due to the compressive tresses induced on the surface of the component. A low cost CCD camera based sensor system was used by Steffen Bonss et al. [53], the camera had a larger field of view than the laser spot size, contains over 400.000 single infrared sensitive measuring points, but the price was only about 20% of the standard infrared camera system. Zhiyue Xu used an infrared sensing system to monitoring Nd:YAG laser hardening [54], the infrared monitor was integrated into the Nd:YAG laser beam delivery optics and off-axis to get the infrared emission signal. The system collected

the infrared emission signal associated with laser hardening process to monitor the hardness and depth of the hardened zone. The results show a linear relationship between the monitor output DC level voltage and hardness up to the maximum hardness possible and also between the monitor output DC level voltage and depth as shown in Figure 2-10.

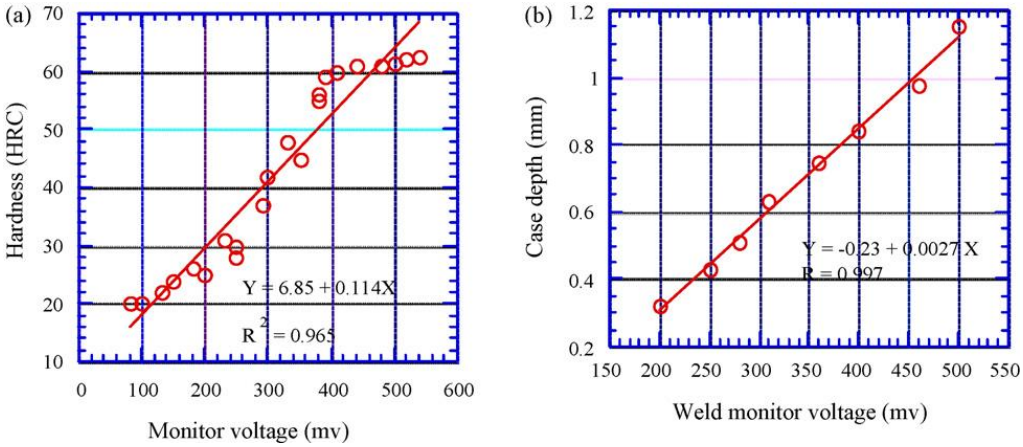

Figure 2-10 Plots of (a) hardness and (b) depth vs. monitor DC voltage level for gray cast iron [54].

Dietmar Hömberg and Wolf Weiss have developed PID control strategies for laser hardening the non uniform geometrical workpiece [55], it induced an idea that the best solution is not controlling the temperature on the top surface, but controlling the temperature close to the lower boundary of the hardened zone on a constant temperature (Ac_3), and then computing the optimal temperature in the laser spot. The computed temperature is the control signal for the real process to obtain a uniform hardened layer. Figure 2-11 gives an example of the control strategies for a variable thickness workpiece.

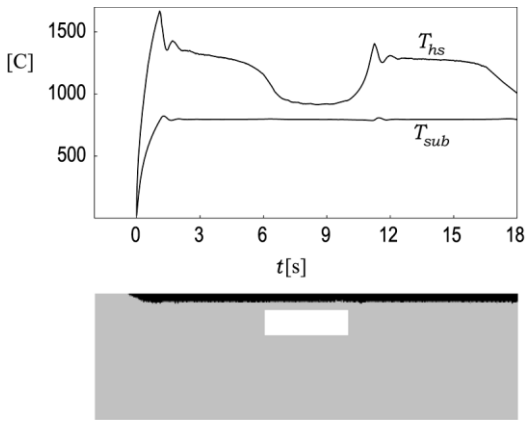

Figure 2-11 A hardened zone obtained by PID controlling of subsurface temperature.

2.3.3 Industry applications

Because of the low distortion, localized hardening position and other advantages in the laser hardening process compared with the conventional ways, laser hardening process has been widely used in industry. The automotive industry is one of those industries which benefit a lot from laser hardening for mass and precise production, exhaust valves, valve guides and gears could be laser hardening to enhance ware resistance [56]. One example for complex shape and local hardening application is shown in Figure 2-12. Torsion springs could be hardened over 170 °and depth 0.2-0.4 mm by two diode lasers, the rest of the component was not affected by the process as shown in the cross section [17]. A cast iron of grade SCh25 or VCh40 made valve is hardened by a continuous CO_2 laser with a power up to1.2 KW. The mean hardening depth is 0.2 mm, whereas the micro hardness in the hardened zone was 600 – 800 HV, as showed in figure 2-13 [57].

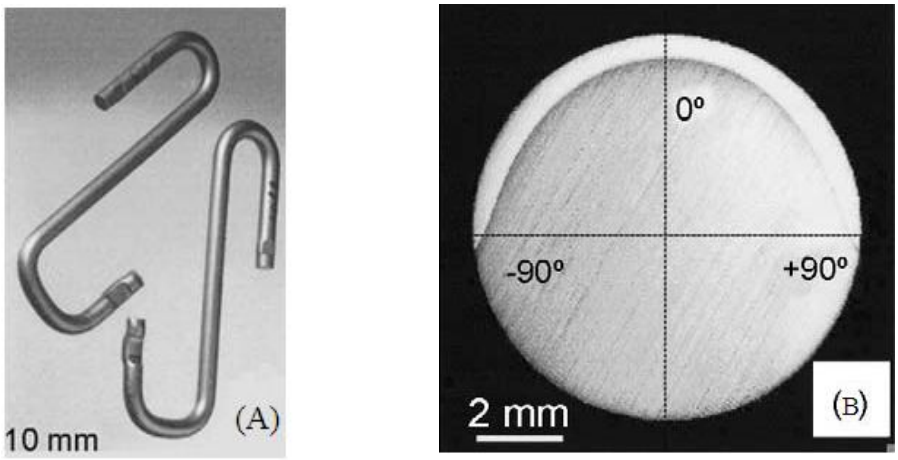

Figure 2-12 Hardening of torsion springs and the hardened zone.

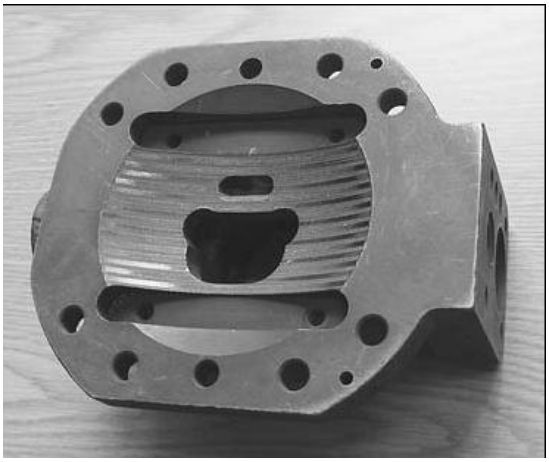

Figure 2-13 A hardened surface of regulating valve body.

2.4 Existing drawback and solutions for laser hardening

The localized laser hardening has been widely applied in nowadays industry; one limitation for the laser hardening application is the large surface hardening.

2.4.1 Main drawback of laser hardening – Back tempering

As the laser beam has a limited spot dimension, when the area to be hardened is larger than the laser spot, multiple passes have to be applied, the later track reheats the previous track slightly, due to the less severe thermal cycles undergone by the overlapped area, the existing martensite is transformed into tempered martensite, which characters as lower hardness, this is the well known back tempering problem as shown in Figure 2-14 [58].

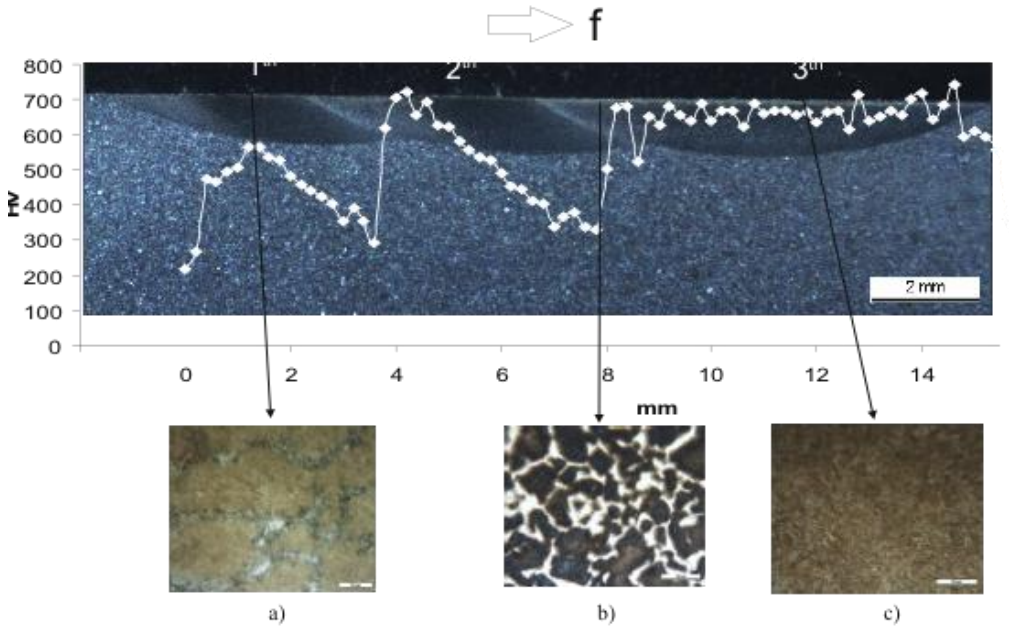

Figure2-14 Microstructure changes in laser hardened steel.

As a consequence a local reduction in hardness is observed [59]. Overlapping process was also applied to cast iron used for marine diesel piston ring [60], it confirmed a hardness drop from 800-950 to 470 $HV_{0.1}$ in the overlapped zone. The result of overlapping is non-uniform on hardness and depth, as illustrated in Figure 2-15 [61]. Many works have been performed in order to understand the influence of the overlapping and the effects of different overlapping conditions.

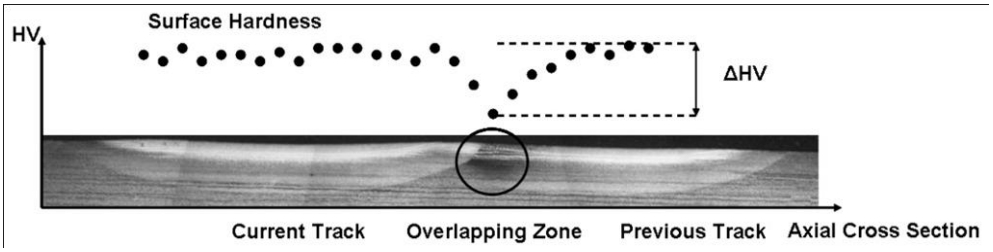

Figure 2-15 Back tempering effect in the overlapping technique.

The overlapping process happens not only in the large planar surface, but also in the cylindrical surface, such as steel shafts, camshafts, cylinder liners, pistons, piston rings. When a large scale surface is hardened, the cylindrical workpiece will be rotated by a lathe; in the meantime, a laser beam scans the surface parallel to the rotation axis. In this way, a continues helicoidal track is obtained [62], and the

overlapping still exists between the adjacent tracks. The overlapping happens also when a narrow annular surface is hardened, in this kind of application, the initial part and the finishing part are overlapped, and back tempering occurs in this zone.

A. Fortunato presents a polynomial expression tempering model to predict the hardness reduction in multiple laser paths for hypo eutectoid steel and the software is able to simulate other laser hardening processes [63]. Ritesh S. Lakhkar, Yung C. Shin developed a three-dimensional transient temperature model and a kinetic hardening–tempering mode to predict the case depth [64], hardness for AISI 4140 steel and determine the optimum operating conditions in which the hardenen depth gets maximize (at least obtain 2 mm) and reduces back tempering. The optimized process was carried out by changing the extent of overlapping of the tracks, the major portion of the back tempered track was in the range of 480–571HV. The difference in the case depths of the two adjacent tracks was approximately 0.2 mm. Based on the single track hardening, the overlapping was studied on grey cast iron surface by a temperature measuring and control system [65], decreased hardness 400HV was observed in the overlapped zone for grey cast iron. The soften behaviors of different materials (C45, 9Cr2Mo and W18Cr4V steel) were also investigated by authors [66], the softening width of C45 steel was the broadest and that of W18Cr4V steel was the narrowest as shown in Figure 2-16. The authors also pointed out, by tempering the laser hardened samples, a uniform hardness distribution will be obtained in the cross section (see Figure 2-17).

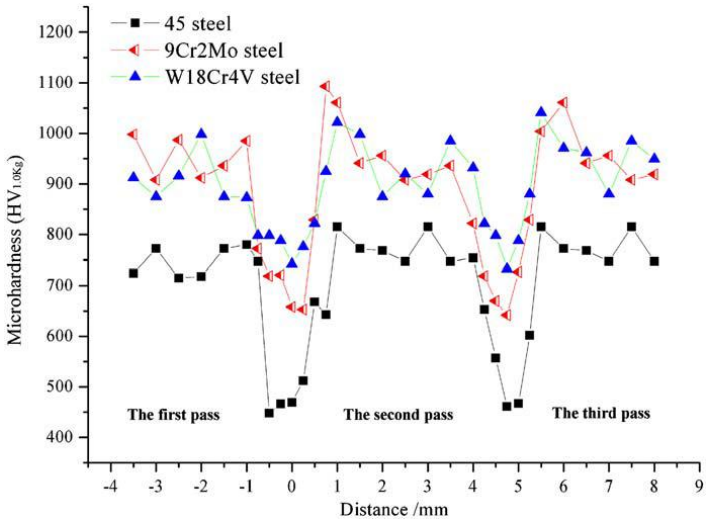

Figure 2-16 Hardness distributions of different materials by laser-overlapping hardening.

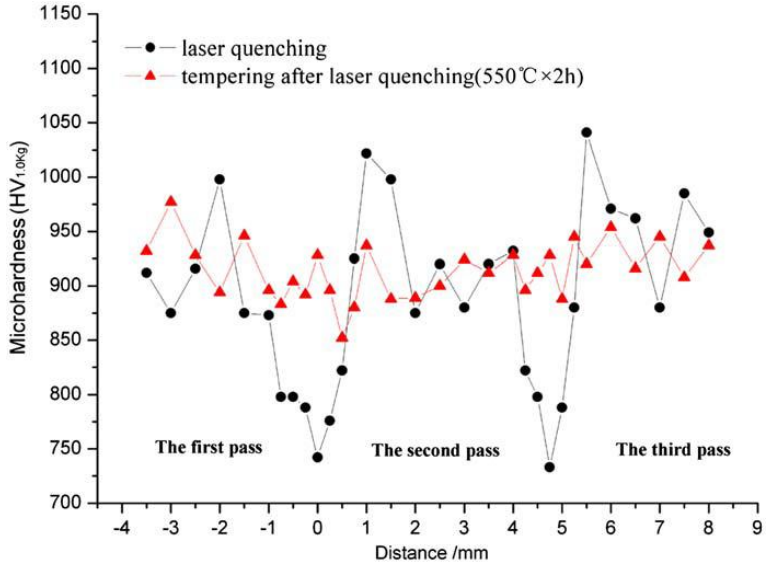

Figure 2-17 Hardness distributions after laser-overlapping hardening and tempering.

Guy Claus focused on the hardening of large areas on flat surfaces and other geometrical workpiece [67], by testing different degrees of the overlapping, a high overlapping degree gave the best results in terms of hardness variations as shown in Figure 2-18, but hardness in the non overlapped zones also decreased compared with the 0% overlapping process.

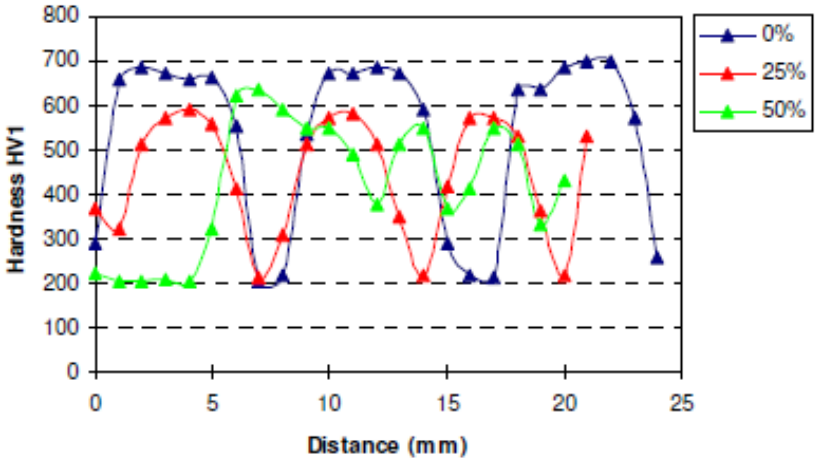

Figure 2-18 Hardness distributions with different overlapping degrees.

Overlapping quote, focus height and beam velocity were studied to optimize the hardening process for cylindrical surface [68], the works indicated the hardness decrease in overlapped zone was mainly related to the thermal cycle, it should not depend on the overlapping. It is more likely to accumulate heat inside the specimen

when a cylindrical workpiece was rotated by a lathe and irradiated by laser [69], Figure 2-19 shows that the hardening depth, width and overlap length gradually increase as the number of hardening tracks increases.

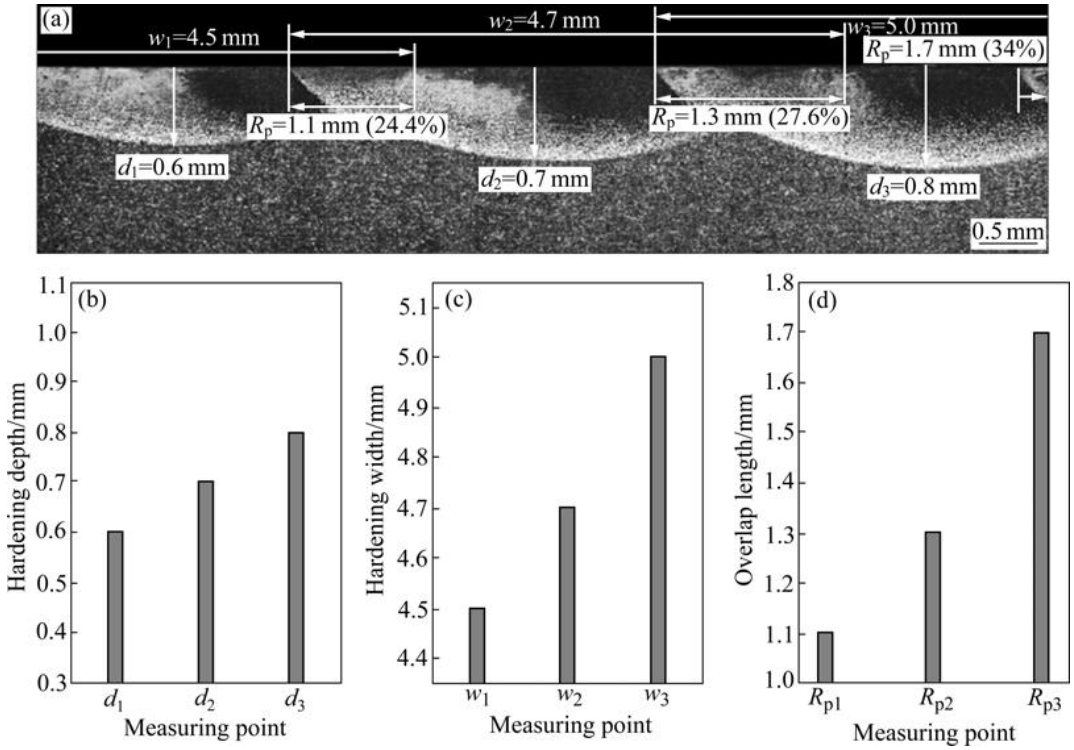

(a) Cross section image; (b-d) Measured values of each hardened track

Figure 2-19 Effect of heat deposition on hardening depth, width and overlap length.

2.4.2 Solutions to overlapping on planar surface

Literally the solution to the back-tempering consists substantially in avoiding the overlapping making use of very large spots. The spot can be enlarged with a traditional solution by a scanner head, which allows large, shaped spot to be obtained moving the laser beam with high frequency and programmed paths in x and y directions. Laser hardening making use of scanner head permits to cover larger area, even though the industrial experience limits the spot no larger than 100 mm, since the laser power has to be correspondently increased. Thanks to the recent events of high power fiber laser, this limit can be exceeded, and it is time to apply the laser hardening to the large surface in industry. Once the process operability range was investigated and auxiliary equipments, such as pyrometer or thermocameras to keep

the control of the surface temperature, have been optimised for the active fiber laser sources. Figure 1.5 gives an example of the scanner head hardening.

M. Seifert, S. Bonß, B. Brenner, E. Beyer [70] used a 4 kW HPDL with scanning optics to investigate the influence of different scanning functions on the hardening results. Different laser power density distributions were obtained by different scanning functions, and the structures in the cross sections shows that the geometrical features of the hardened zone are influenced by the scanning function (see Figure 2-20 (a) (b), (a) sine function, (b) triangle function).

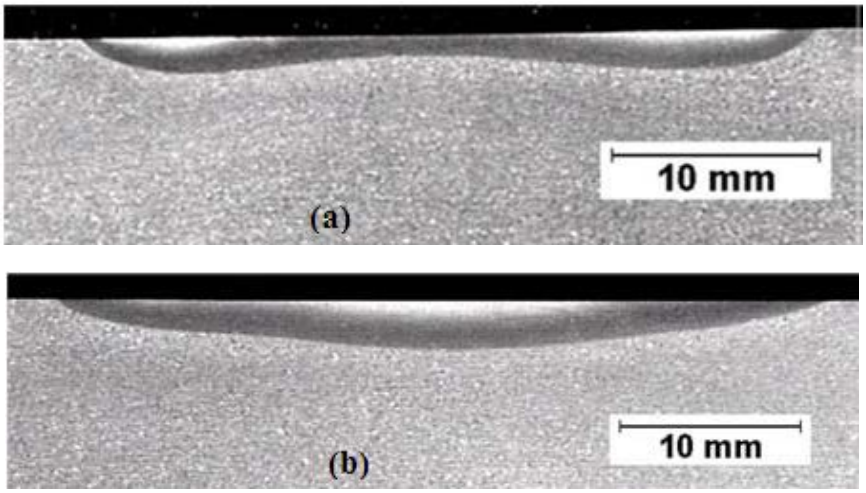

Figure 2-20 hardened zones with scanning laser head technique.

In Figure 2-21, a 27 mm wide hardened track was obtained with homogenous hardness distribution across the hardening zone.

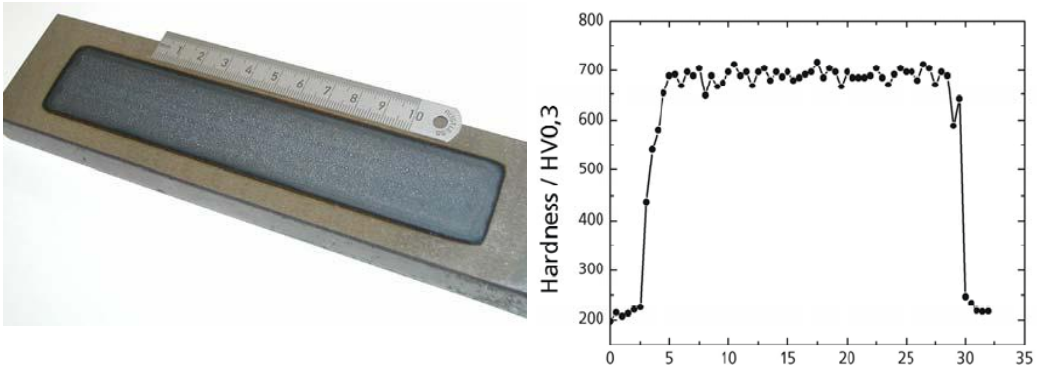

(a) Top surface (b) hardness distribution

Figure 2-21 Top surface microview and hardness distribution in carbon steel treated with a diode laser source and scanning optics.

S. Bonss [71] applied two separate 6 kW high power diode lasers for simultaneous laser hardening, and use beam splitter optics. Under these conditions on high alloyed steel a 100 mm wide track is possible to generate. Figure 2-22 also shows a designed laser beam for the hardening process, the hardened width is 10 – 42 mm.

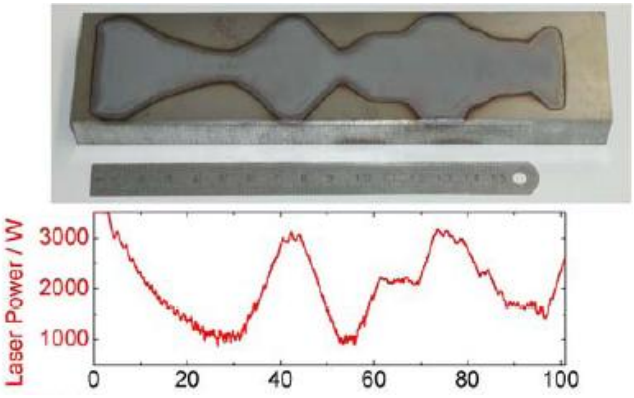

Figure 2-22 Heat treatment of tool steel with scanning optics and variable track width.

The scanning head technique is supported by the high laser power; for HPDL a main problem to scan the laser beam is to find a suitable scanning mirror with high reflectivity for the combination of two different wavelengths (808 and 940 nm) [66].

The other solution for the overlapping phenomenon is laser melting. With this technique the melting temperature is reached, so a part of the material adjacent to the surface melts, through the rapid solidification, very fine microstructures with improved hardness and wear resistance are yielded [72].

On grey and nodular irons surfaces, fine grained and very hard ledeburite microstructures were created in the melted surface layer and greater depth of the austenite transformation in the material was achieved [73][74]. Tulloch melted the gray cast camshafts for combustion engines applications [75], V. Lopez investigated the laser melting process with different ductile cast irons [76]. The melting process eliminated the porosity on the surface, but transverse cracks appeared on the surface with this treatment, the research also pointed out that the treatment process was strongly affected by the attributes of the materials, only the ductile iron with a perlitic matrix produced a layer of uniform hardness. H13 steel, which usually has bad thermal conductivity and diffusivity, was also investigated [77]. C. Li et al [78] developed an FEM based mathematical model to predicted that an ideal hardness and residual stress distribution can be obtained by choosing 30% overlapping ratio by melting process, but hardness still dropped in the overlapped zone. Experiments [79] also showed that the greatest residual stress at the surface is obtained when there is no overlap of the melted tracks.

2.4.3 Solutions to overlapping on cylindrical surface

Another solution to back tempering, in the case of cylindrical workpiece proposed by the authors, is to rotate the workpiece at high speed instead of low speed in traditional, and then increase the dimensions of the laser spot in a fictitious way. E. Capello and L. Giorleo [60] got an apparent spot (AS) by rotating a cylinder of 15mm diameter at 2100 rpm; a 1200 W diode laser was used to harden the surface of the cylinder. Uniform hardened zones without overlapping were achieved in AISI 1040 steel under different explosion time; the hardness is stable around 600HV and without drop. The effects of the process parameters (rotation speed, laser power and diameter of the workpiece) on the dimensions and hardness values of the hardened zones were pointed out [80]. Guy Claus and M. Seifert use two 6 kW high power diode laser [81], four different diameters 30, 40, 50, 60 mm. cylinders made of 42CrMo4V. Internal holes with diameters 10 mm and 20mm in 20 mm are hardened at 6000 rpm and different scan speeds. Hardness around 65HRC was achieved and its hardening depth between 0.3-0.8 mm depends on the different processes. Their research also indicates that the holes are more sensitive to the process. G.Tani used Finite Difference Method to develop a laser hardening simulator [82] [83], the simulator could choose the correct process parameters for operating time to treat the cylindrical workpiece by high rotation speed. The result of the simulator matches the real experiment results, that a hollow martensitic stainless steel AISI 420 cylinder of 72 mm diameter, a thickness of 2 mm could be hardened at 2 kW laser and 900 rpm.

Steffen Bonss [84] integrated the laser hardening system for cylindrical workpiece into production line to meet the industrial requirements. The valve cones were hardened within the turning machines, only 1.5 s was needed for the process.

However this technique still has to be addressed while lack of existing knowledge and deeper investigation is needed.

2.5 Conclusions

The review of the state of the art showed that laser hardening is a promising process for heat treatment, especially suitable for the workpieces need local hardening and/or with complex geometry. Nowadays, High Power Diode Laser (HPDL) is considered as a suitable laser source for laser heat treatment due to its beam properties.

But when large areas have to be treated by slightly overlapped multi-pass, one well-known drawback is the back tempering in the overlapped zone which induces a hardness decrease. Some studies worked on reducing or eliminating this problem, the

main solutions include scanning the laser beam into a desired shape and laser melting process for the planar surface; for the cylindrical surface, Apparent Spot technique was proposed to cover this drawback.

3 Objectives

This chapter is dedicated to the definition of the main objectives of the thesis work.

Chapter 2 has indicated that the laser hardening is a promising technology in nowadays industry, but the drawback of back tempering limits the laser hardening applications in some industrial areas. With the increase of the industrial requirement, the features and solutions to this drawback are investigated to extend the field of laser hardening applications.

According to this consideration, the main aim of the thesis work is to study the performance of the back tempering phenomenon in large laser hardened surfaces. The back tempering phenomenon on two kinds of surface, *i.e.* planar surfaces and cylindrical surfaces are investigated. Based on the investigation of this drawback, some techniques are proposed to reduce the overlapping and back tempering phenomenon on different surfaces.

With the purpose above, the objectives of this thesis are as follows:

1 Study of the features of the hardened zone obtained by laser hardening process without overlapping.

As the basis of this thesis work, the aims of this objective will be:

- Study the laser hardening performance by single track hardening, establish a relationship between the features of hardened zones, *i.e.* hardness,

geometrical features, and the investigated hardening parameters, *i.e.* scanning speed and hardening temperature.

- Optimize the process parameters to obtain a maximum productivity of the large surfaces hardening process.

2 Study and characterize the back tempering phenomenon in the overlapped zone.

After the investigation of the features of the hardened zone, attention will be focused on the overlapping process and back tempering phenomenon.

- On a planar surface
  (a) Investigate the effects of the overlapping length on planar surfaces to obtain uniform hardened depth.
  (b) Characterize the hardness decrease due to the back tempering phenomenon in the overlapped zones.
- On a cylindrical surface
  (a) Study the laser hardened overlapped zone on annular surfaces, without the laser feed rate.
  (b) Study the overlapped zones on wider cylindrical hardened surfaces.

3 Investigate different techniques to reduce or solve the back tempering phenomenon on large surfaces.

The solutions for the back tempering phenomenon will be proposed based on different kinds of surface.

- Execute laser melting technique on planar surfaces. Hardness features of the new microstructure and the hardness distribution in the overlapped zones during the laser melting process will be studied.
- Apply remote laser hardening process. Analyze the parameters used in the remote scanner head laser hardening process to obtain a large laser spot for large surfaces hardening.
- Investigate Apparent Spot (AS) technique to treat annular and cylindrical workpiece.

4 Base material, experimental setup, measurement procedure

In this chapter the experimental setup of the laser hardening process is introduced, including the analysis of the investigated base material, the setup of the laser system, and the short description of the measuring equipments and the definition of the measurement procedures.

4.1 Base material analysis

Two types of materials were analyzed in the laser hardening process. For the planar surface, the investigated material wasgrey cast iron, expressly used in mechanical components where the bulk material has to have high toughness and vibration damping properties, while the surface has to have high wear resistance. For the cylindrical workpiece, carbon steel was chosen, as it is one of the most widely used materials for crankshafts, valve cores, couplings and cold headed parts and so on.

4.1.1 Gray cast iron

Gray cast iron castings are readily available in nearly all industrial areas and are used in lots of components such as pistons, guides, and tool beds. Gray cast iron has excellent machining qualities, producing easily disposed of chips and yielding a surface with excellent wear characteristics. The investigated cast iron has a typical microstructure with pearlite matrix and the graphite flakes shown in Figure 4-1. The nominal chemical compositions of the grey cast iron used in the experimentation are listed in Table 4-1.

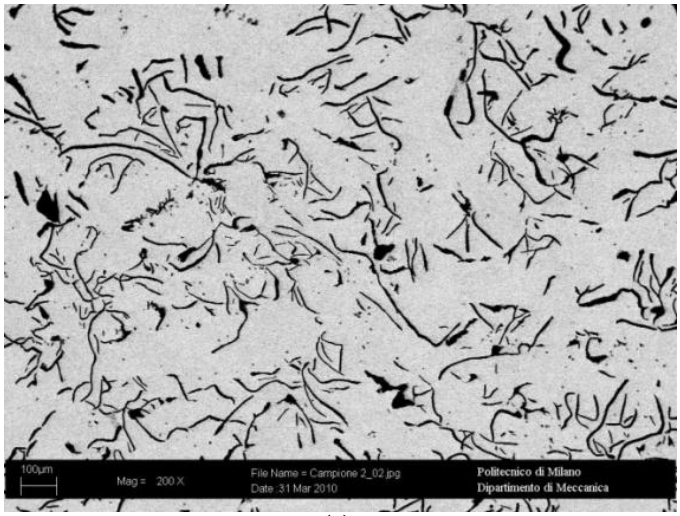

(a)

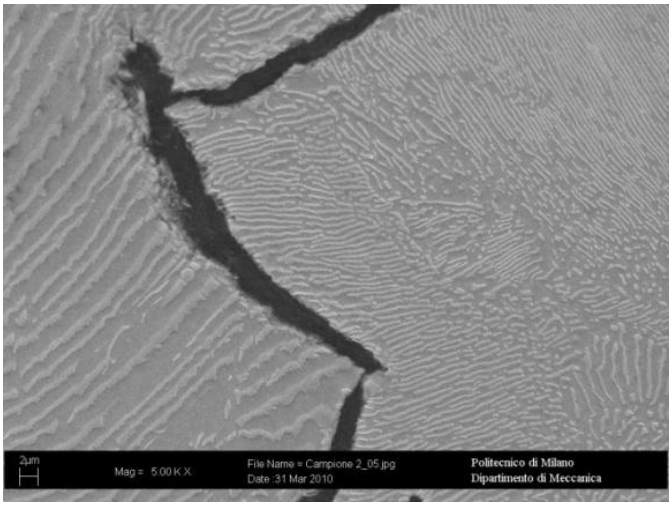

(b)

Figure 4-1 SEM images of microstructure of the cast iron (a) with low and (b) and high magnification.

Table 4-1 Nominal chemical composition (weight %) of the cast iron.

C	Si	Mn	P	S
3 – 3.2	1.5 – 1.8	0.7 – 0.9	< 0.15	< 0.12

In addition to the microstructure and the nominal composition, Vickers hardness tests were taken random positions on the surface to evaluate the original hardness of the basic material. The measured Vickers microhardness values are shown in Table 4-2

Table 4-2 Initial microhardness of the gray cast iron used.

	Microhardness (HV 0.3)								
No.	1	2	3	4	5	6	7	Average	Standard Deviation
HV	244-9	269.4	257.6	239.3	238.5	262.3	237	250	13

Based on the standard Fe-C diagram, the melting temperature of the base material was predicted using the carbon content, determined in the chemical composition analysis, as shown in Figure 4-2. This temperature was then confirmed to be around 1150-1200 ℃ by temperature measurements made with a pyrometer (details of the experiment will be explained in chapter 5).

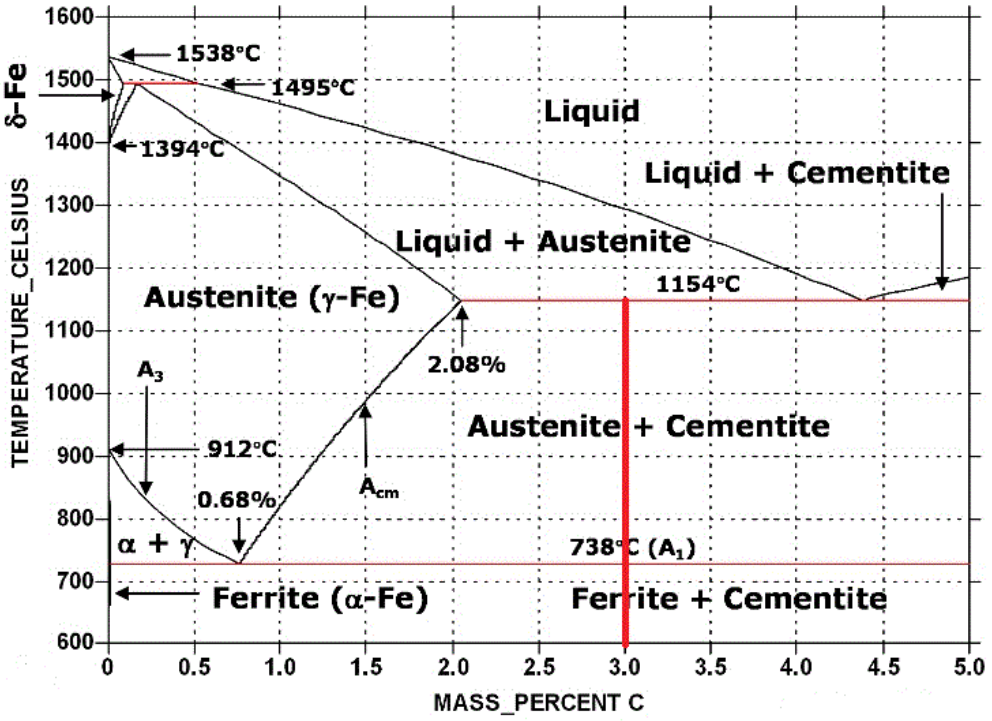

Figure 4-2 Fe-C% diagram.

The melting temperature of the base material was predicted by evaluating the chemical composition, and then was confirmed to be around 1150-1200 ℃ by temperature measurements made with a pyrometer (details of the experiment will be explained in chapter 5).

4.1.2 Carbon steel

Medium carbon steel, AISI 1040, was selected as working material for the cylindrical workpiece, with the microstructure shown in Figure 4-3, and the nominal chemical composition and microhardness of the used steel are reported in Table 4-3. The melting point was predicted and measured in the same way as cast iron, which was then found to be in the range of 1500-1550 ℃.

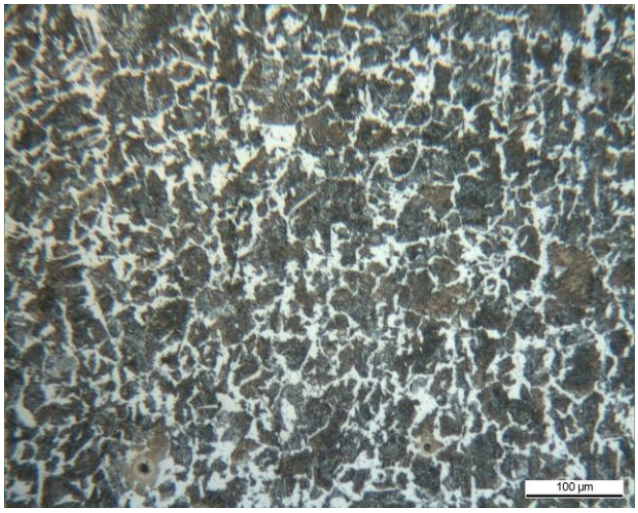

Figure 4-3 Microstructure of AISI 1040 the carbon steel.

Table 4-3 Nominal chemical composition (weight %) of the carbon steel.

C	Fe	Mn	P	S
0.37-0.44	Bal.	0.6-0.9	< 0.04	< 0.05

Table 4-4 Initial microhardness of the AISI 1040 carbon steel.

Microhardness (HV 0.5)												
No.	1	2	3	4	5	6	7	8	9	10	Average	Standard Deviation
HV	221	234	246	257	209	226	238	243	258	235	237	15

4.2 Laser hardening systems

Two different strategies, involving two different types of laser equipment, are investigated. Firstly, the heat treatment of large areas was obtained by slightly overlapping several single passes that are laser hardened by a proximity head focusing a direct diode laser beam (Figure 4-4(a)). This configuration is named in the following "proximity laser hardening". Successively, a short experimentation is also performed making use of a scanning laser head, operating with an active fiber laser, which allows obtaining large spot area by the fast oscillation of the laser beam in two directions. This configuration, named in the following "remote laser hardening", is depicted in Figure 4-4(b).

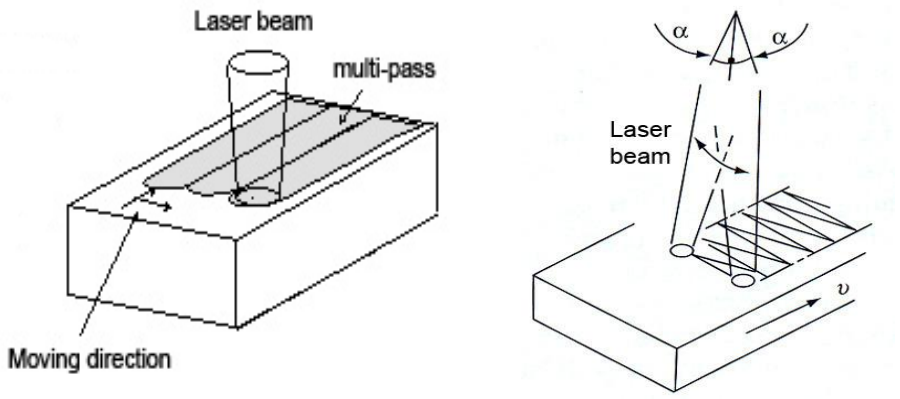

(a) Proximity laser hardening (b) Remote laser hardening

Figure 4-4 Scheme of laser hardening systems.

4.2.1 Proximity laser hardening equipment

The proximity laser hardening system is composed by a diode laser, an anthropomorphic ABB robot, a pyrometer and a control system. The scheme and practical setup of the hardening system is shown in Figure 4-5. Tset is the reference temperature value, T(t) is the real time measured temperature, based on these two values, P(t) – the laser power is controlled in real time.

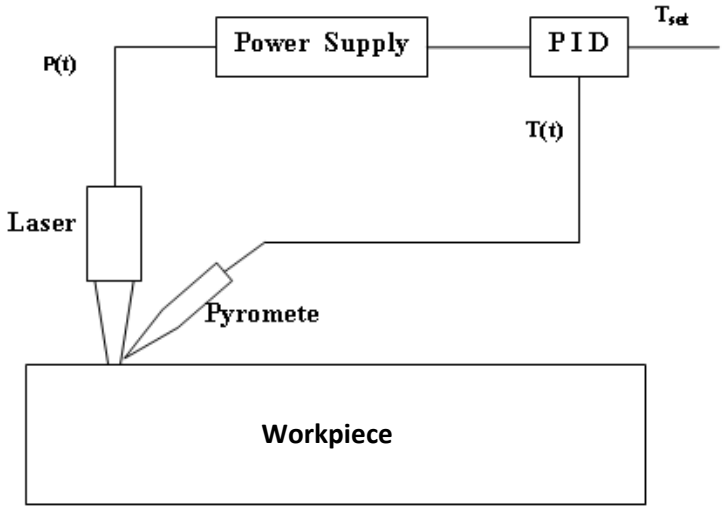

(a) Scheme of the proximity laser system.

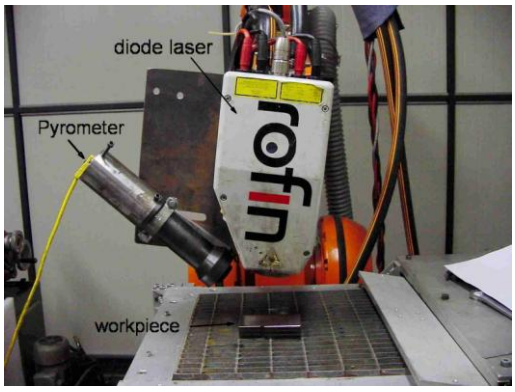

(b) Practical setup for planar surface.

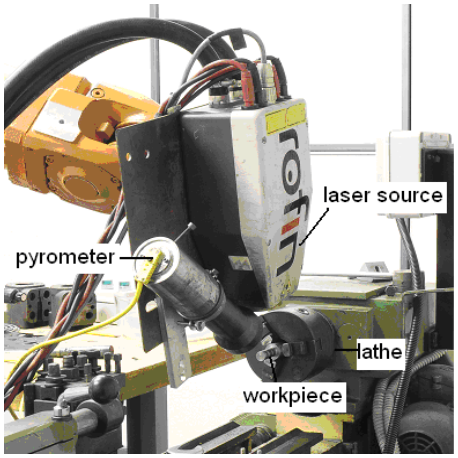

(c) Practical setup for cylindrical surface.

Figure 4-5 Scheme and practical setup of the hardening system.

Diode lasers have many inherent properties which make them particularly suitable for heat treatment applications. Some of their main characteristics are as follows:

– Wavelength

The wavelength of the radiation emitted from most practical diode is between 800 and 940 nm. Due to its shorter wavelength, diode laser radiation has a considerably higher degree of absorption into metallic surfaces compared with CO_2 or Nd:YAG laser. This means coating is not necessary for the hardening process.

– Beam profile

The beam profile of diode laser is generally top-hat in the slow axis direction and Gaussian in the fast axis direction with a rectangular shaped spot due to the nature of the beam formation process. Figure 4-6 shows the laser beam profile of the diode laser used in the experimentation.

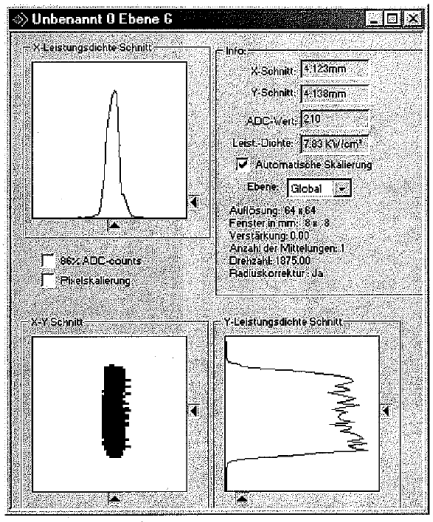

Figure 4-6 Diode laser beam profile of SITEC.

In addition, diode laser is also known for the high wall plug efficiency, compact size, and high temporal stability.

At SITEC, a 1250 W continuous wave Rofin DL022 diode laser (λ=808 nm and 940 nm) is used for laser hardening. The laser is fixed on a 6- axis ABB robot. The laser spot has a rectangular form with dimensions of 2 mm x 6 mm. In order to achieve the maximum power density on the hardening area, the laser was focused on the material surface. During the process, the laser scanning direction is parallel to the slow axis of the spot as shown in Figure 4-7 (a). For the cylindrical surface, the 2 mm axis of the laser beam was parallel to axis of the workpiece. The directions of the laser beam are shown in Figure 4-7(b). No shield gas was applied.

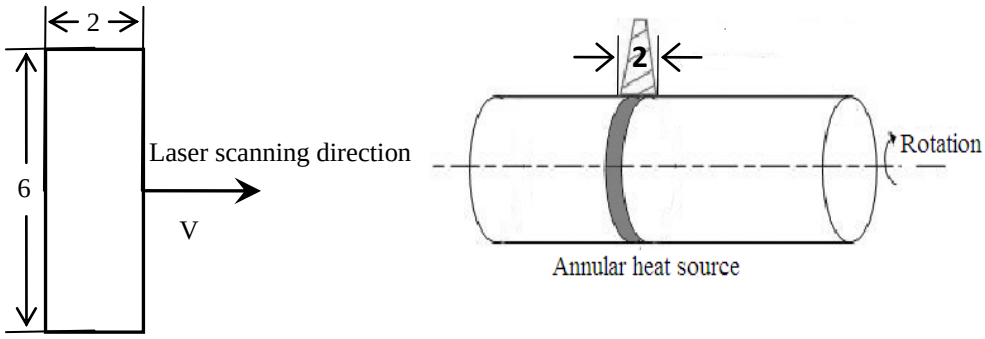

(a) on planar surface (b) on cylindrical surface

Figure 4-7 Geometry features of the laser beam on the workpieces.

Some typical features of the laser hardening process that require further attention can be listed as such:

- Laser hardening is a very fast process, the heating and cooling rates in the order of 1000 K/s are common;
- The operating window is quite narrow from austenite temperature AC_3 to melting point;
- The coefficient of absorption of a metallic surface has a stepwise increase when the temperature reaches the melting point and can vary significantly in presence of superficial discontinuities, such as roughness difference, dirt and oil traces, different colour and optical properties.

Therefore to monitor and control the hardening temperature is essential to keep the depth of the treated area constant. For this purpose, In SITEC the power supply of the laser is connected to a measurement and close-loop control system composed of a pyrometer and a PID regulator.

- Pyrometer

The SITEC handmade pyrometer is composed by a germanium sensor, several filters and a focus lens. The germanium sensor has a very large pass band from 800 to1800 nm, and is sensible in the near infrared zone, where the optical power of the surface at high temperature is at maximum. A set of filters are used for cutting off the reflection of the diode laser beam and avoiding the attenuation of the air. The focus lens is used to focus the emitted optical energy on the germanium sensor. The scheme and practical parts of the pyrometer are reported in Figure 4-8

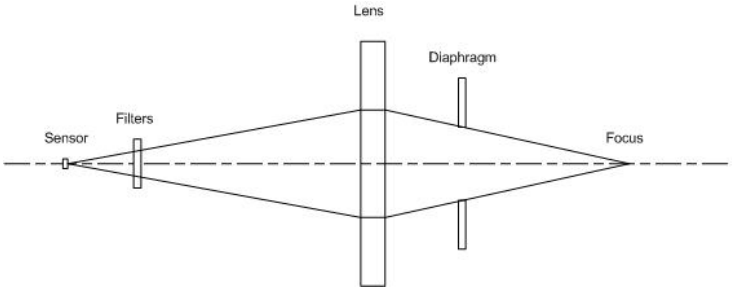

(a) Scheme of the pyrometer

(b) Practical pyrometer

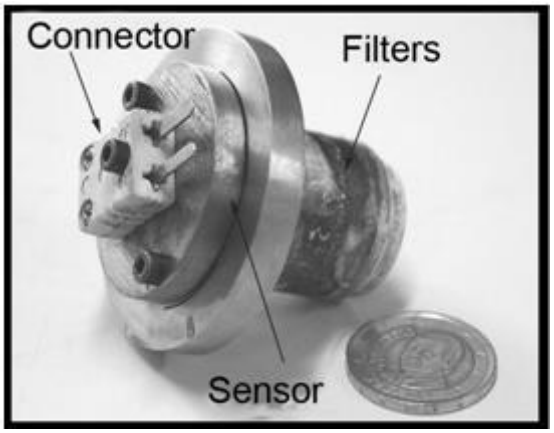

(c) Practical parts of the pyrometer

Figure 4-8 scheme and practical parts of the pyrometer.

- Control system

The control system is composed by LabView software and a data acquisition board provided by National Instruments (NI-DAQ) for signal acquisition. An amplification circuit is adopted to amplify the electrical signal generated by the pyrometer to several voltages which can be measured by the DAQ. During the process, the pyrometer measures the thermal radiation from the workpiece surface and then transforms the measured emission to temperature values. This temperature values is then compared to a reference value. Then the PID regulator produces a signal used by

the laser source to control the power. The surface temperature is kept at the reference temperature by varying the laser power.

The most important features of the pyrometer are reported in Table 4-5, where t_r is the rise time of the pyrometer considering the delay of both the amplifying and the measuring circuit.

Table 4-5 Important features of the pyrometer.

t_r [ms]	Measurement spot Diameter [mm]	Accuracy [℃]	Measuring range [℃]
0.3	2	± 20	700 - 1500

With this measuring and control system, it is possible to control and get a stable temperature on the workpiece surface, as shown in the example of Figure 4-9.

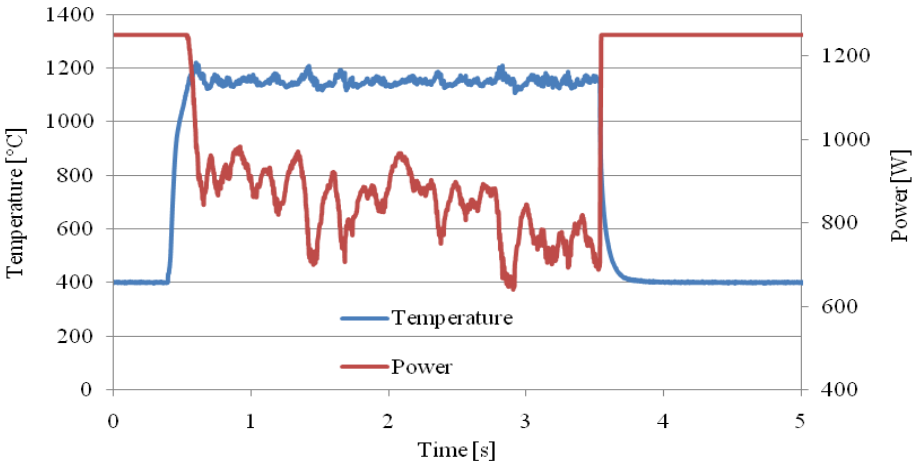

Figure 4-9 Real time measurements of temperature and controlled laser power.

With the measurement and control system, different combinations of temperature on the surface and laser scanning speed were tested to optimize the hardening process.

4.2.2 Remote laser hardening equipments

As discussed above, the remote laser hardening is based on high power laser; the scanning laser head system is composed by an IPG 5kW fiber laser and a galvanometric scanner heard produced by Gruppo El.En. The scanner and the laser system are shown in Figure 4-10.

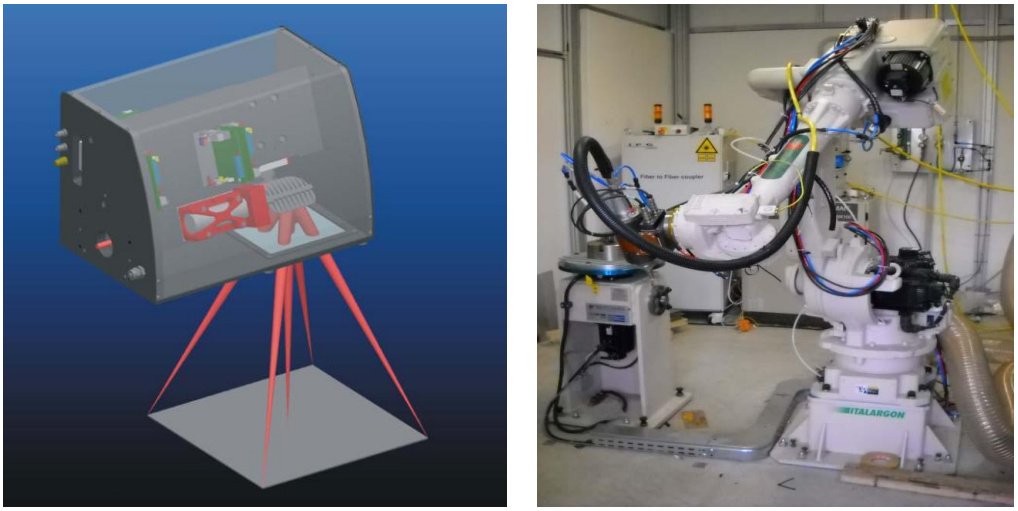

(a) Galvanometric scanner (b) Laser system

Figure 4-10 Remote laser hardening system.

The scanner head is composed by a collimating lens, focus lenses, two galvanometers and digital control system. The parameters of the scanner head are listed in Table 4-5. Table 4-6 gives the characteristics of the fiber laser.

Table 4-5 Parameters of the scanner head.

Collimating length	Focusing length to gavanometers	Focusing length of the system	Working distance
60 [mm]	135 [mm]	300 [mm]	214.2 [mm]

Table 4-6 Characteristics of the fiber laser.

1. Optical characteristics							
N	Characteristics	Test conditions	Symbol	Min.	Typ.	Max.	Unit
1	Operation Mode			CW / Modulated			
2	Polarization			Random			
3	Nominal Output Power		P_{nom}	5000			W
4	Output Power Tuning Range			10		105	%
5	Emission Wavelength	Output power: 5000 W	λ	1070		1080	nm
6	Emission Linewidth	Output power: 5000 W	Δλ		3	6	nm
7	Switching ON/OFF Time	Output power: 5000 W			50	100	μs
8	Output Power Modulation Rate	Output power: 5000 W				5	kHz
9	Output Power Instability	Output power: 5000 W Time interval: 8 hrs (T=Constant)			±1	±2	%
10	Red Guide Laser Power				0.5	1	mW

2. Optical output							
N	Characteristics	Test conditions	Symbol	Min.	Typ.	Max.	Unit
1	Feeding Fiber connector			HLC-8, QBH-compatible			
2	Beam Parameter Product (1/e2)	Feeding Fiber core diameter 50 μm length 15 m	BPP		2	2.5	mm* mrad
3	Feeding Fiber Core Diameter			50			μm
4	Feeding Fiber Length		L	15			m
5	Feeding Fiber Bending Radius		R	100			mm

4.3 Measurement and analysis procedure

After the experiments the treated samples were analyzed for geometric features, hardness values and wear behavior of the hardened zone. Sections of the heat treated tracks were prepared under some common metallographic procedures. The samples were cut along the cross sections using an abrasive disc while water cooling was used to avoid microstructure damage. Abrasive papers with different grit meshes were used in the initial fine grinding; the finest abrasive paper is 2500. Water cooling and lubricate were used throughout the grinding process. Three kinds of nylon cloth

wheel, 6μm, 3μm and 1μm were used in sequence for final polishing, ethanol was applied for lubricant. 2% Nital reagent (2% nitric acid and 98% ethanol) was applied for 5-10 seconds to etch the samples.

4.3.1 Geometrical features of the treated samples

In single pass laser hardening the cross section of the hardened zone was observed with the optical microscope and the SEM. The geometric features of the treated area, width (W_H) and depth (D_H) were measured by means of standard image analysis with the standard image analysis software.

In laser hardening process the measured geometric features of the hardened zone are shown in Figure 4-11.

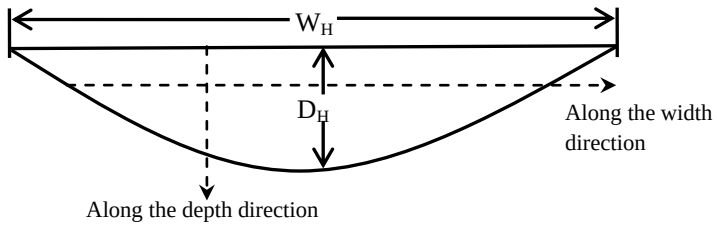

Figure 4-11 Geometrical features of the laser hardened zone.

In laser melting process two kinds of treated zones are observed, i.e. the melted zone in the upper part of the surface and the heat treated zone in the lower part. The two kinds of the treated zones are shown in Figure 4-12. The geometrical features of the treated zone are the same as the hardening process; the dimension of the melted zone is measured in terms of width (W_M) and depth (D_M).

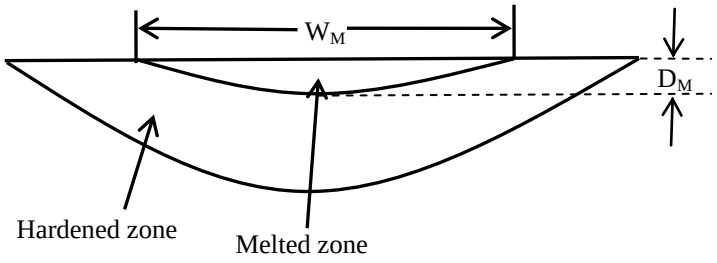

Figure 4-12 Geometrical features of the laser melted zone.

In multi-pass laser hardening two geometrical attributes, overlapping length (OL) and overlapping depth (OD), allows the overlapping zone to be characterized, as shown in Figure 4-13. In preliminary design of the experimentation, the approximate OL was

calculated considering the width of the hardened zone equals to the width of laser spot.

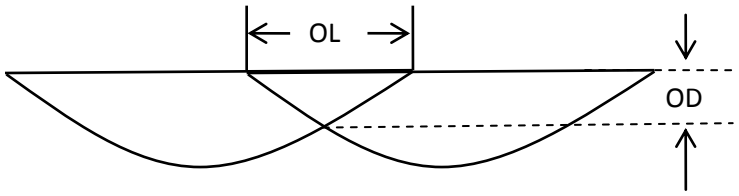

Figure 4-13 Overlapping length (OL) and overlapping depth (OD) in the multi-pass process.

4.3.2 Hardness measurements

Hardness measurements are used to obtain information on the mechanical properties of the hardened layers and base material, Vickers hardness tests were applied. The measurements were performed with a load of 300 g applied for 15 seconds. Micro hardness tests in the hardened zone were executed in longitudinal direction at certain distance, *e.g.* 0.15 mm, from the top surface and along the depth direction at a centre of the treated area as shown in Figure 4-14 (a). In the overlapping process, the hardness tests were executed also in the overlapped zone (see Figure 4-14 (b)).

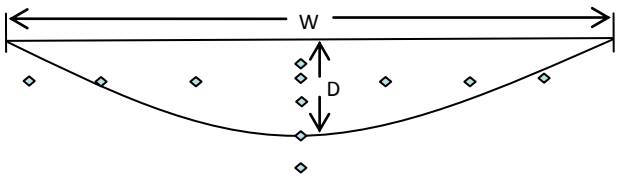

(a) Hardness measurement in the hardened zone

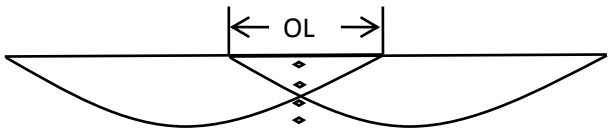

(b) Hardness measurement in the overlapping area

Figure 4-14 Vickers hardness test procedure.

5 Proximity laser hardening on planar workpiece

With the measurement and control diode laser system, both single track hardening and multi-pass hardening were carried out on the cast iron surface. In the single track process, different combinations of scanning speed and constant temperature on the surface were investigated; geometrical features and microhardness of the hardened zone were analyzed. Based on the single track hardening, multi-pass hardening was executed with different overlapping length.

5.1 Base material melting point analysis

The hardening temperature and the scanning speed are parameters that influence the process mostly. Higher temperature on the surface induces deeper hardened zone, and when the temperature is set, the limitation of the scanning speed is determined by the laser power.

To ensure the transformation of pearlite to austenite is completed, high temperature above Ac_3 and below the melting point on the surface should be achieved, and the melting point of cast iron is lower, so the operating window of the hardening process,

so the melting point has to be ascertained for the maximum hardening temperature level. By the Fe-C% diagram, the melting point of cast iron is between 1100-1200 ℃; three levels of temperature in this range and two levels of scanning speed were chosen to investigate the melting point of the basic material. The parameters of experimental setting up are in Table 5-1.

Table 5-1 Experimental parameters for melting point test.

No.	temperature (℃)	Scanning speed (mm/s)
1	1200	10
2	1100	10
3	1100	4
4	1150	4

The experimental results showed that from 1150 ℃ with the lower scanning speed 4mm/s, the surface starts to melt as shown in Figure 5-1, there was a distortion on the top surface because of the melting (a) and the structure on the top surface is shown in (b), in the centre of the top surface, compared with the hardened zone, the graphite flakes were not present, but dissolved in the melted surface. The experimental tests confirmed the melting point of the basic material from the Fe-C% diagram; the melting point of the base material is 1150 ℃ – 1200 ℃. With the measurement and control system, it is possible to control the temperature on surface below the melting point. 1100 ℃ was chosen as the maximum temperature for the subsequent experiments.

(a) Deformed top surface by melt

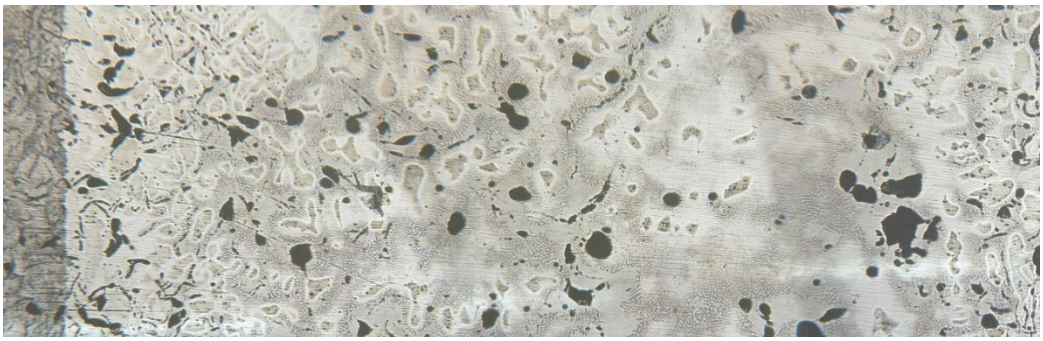

(b) Melted top surface

Figure 5-1 Cross section and top surface of the melted sample (1150 ℃-4 mm/s).

5.2 Proximity single track laser hardening

5.2.1 Experimental parameters for proximity single track laser hardening

Two experimental campaigns of single track laser hardening were designed to investigate the parameters of the process. Independent single passes were executed to understand the effects of different levels of scanning speed and temperature on the hardened zone. The temperature and scanning speed levels are listed in Table 5-2.

Table 5-2 Process parameters used in single pass hardening campaign.

Temperature on the surface [℃]	1100, 1000
Scanning speed [mm/s]	10, 7, 4

For each process condition the temperature values and the controlled laser power were recorded in real time as shown in Figure 5-2.

Speed [mm/s]	Temperature [℃] 1100	1000
4	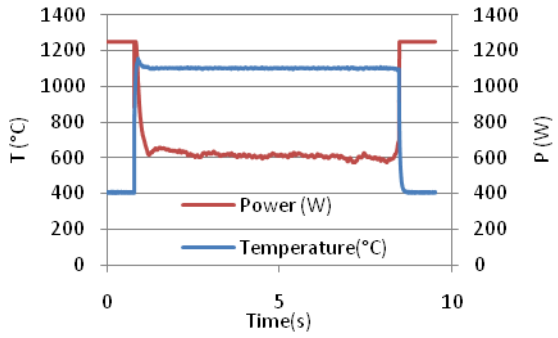	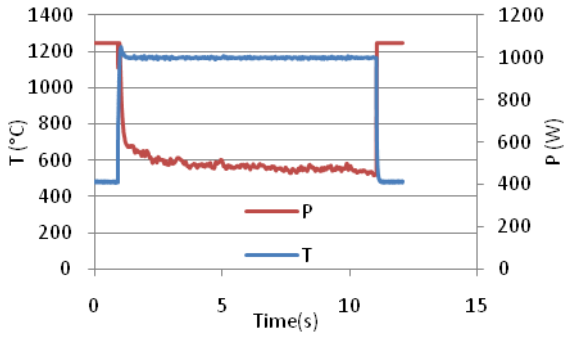
7	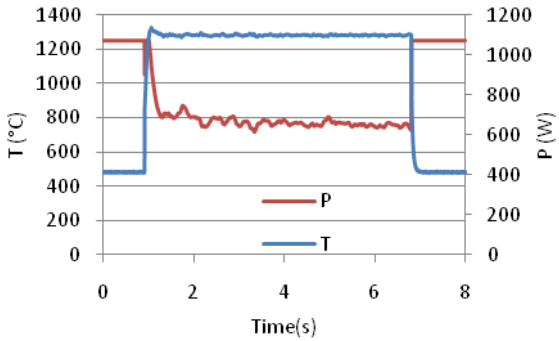	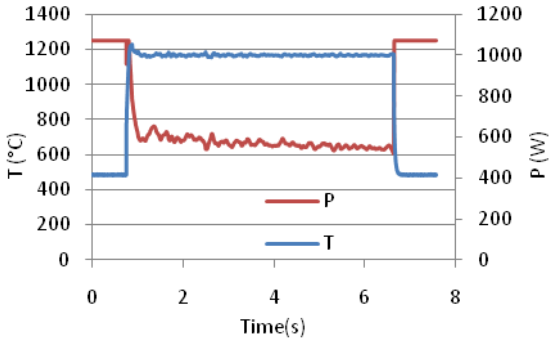

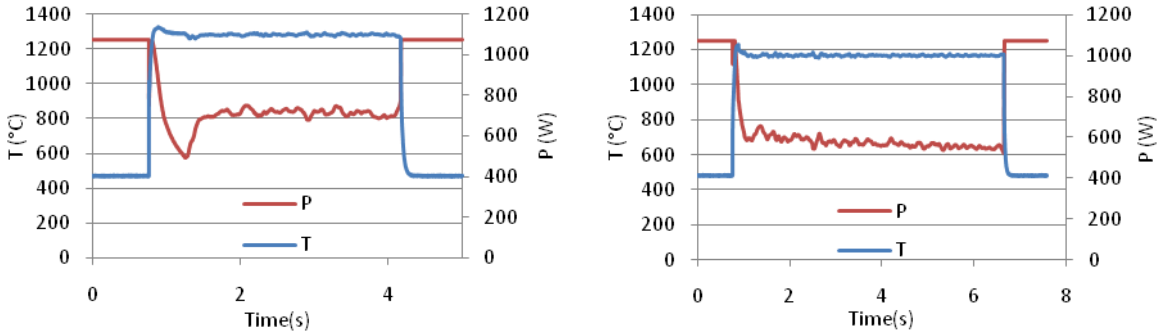

Figure 5-2 Real time measured temperature and controlled laser power for single track.

Five intervals were taken to evaluate the average power for every process. During every interval, one average power was calculated by averaging the power measurements in the stable phase. The five average powers for every process are shown in Figure 5-3.

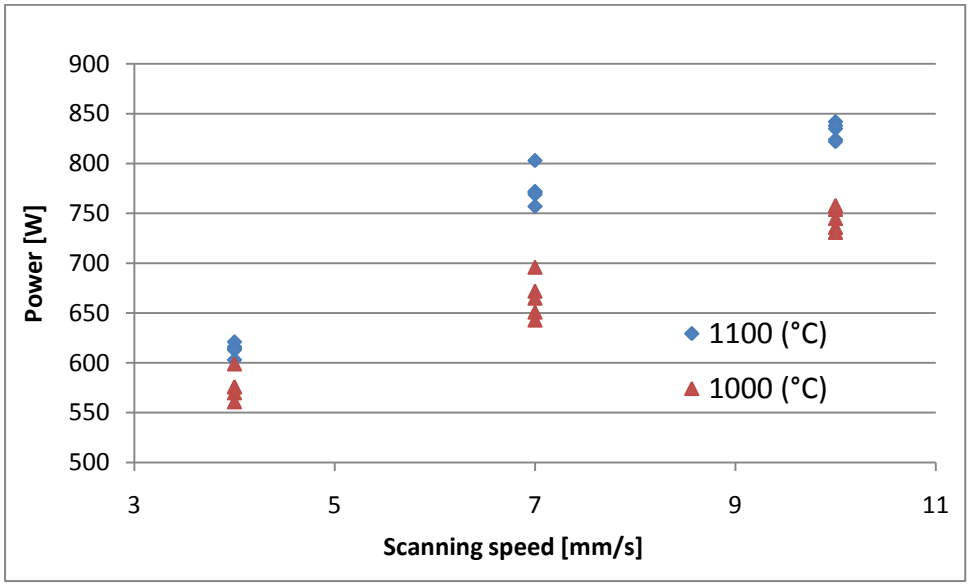

Figure 5-3 Laser power related with scanning speed and temperature.

5.2.2 *Microhardness feature for proximity single track hardening*

Figure 5-4 (a)-(d) shows the microstructure and microhardness analysis along the depth of the hardened zone. The analysis of results shows that during the laser hardening process, a homogeneous microstructure is obtained in the hardened zone regardless of the depth.

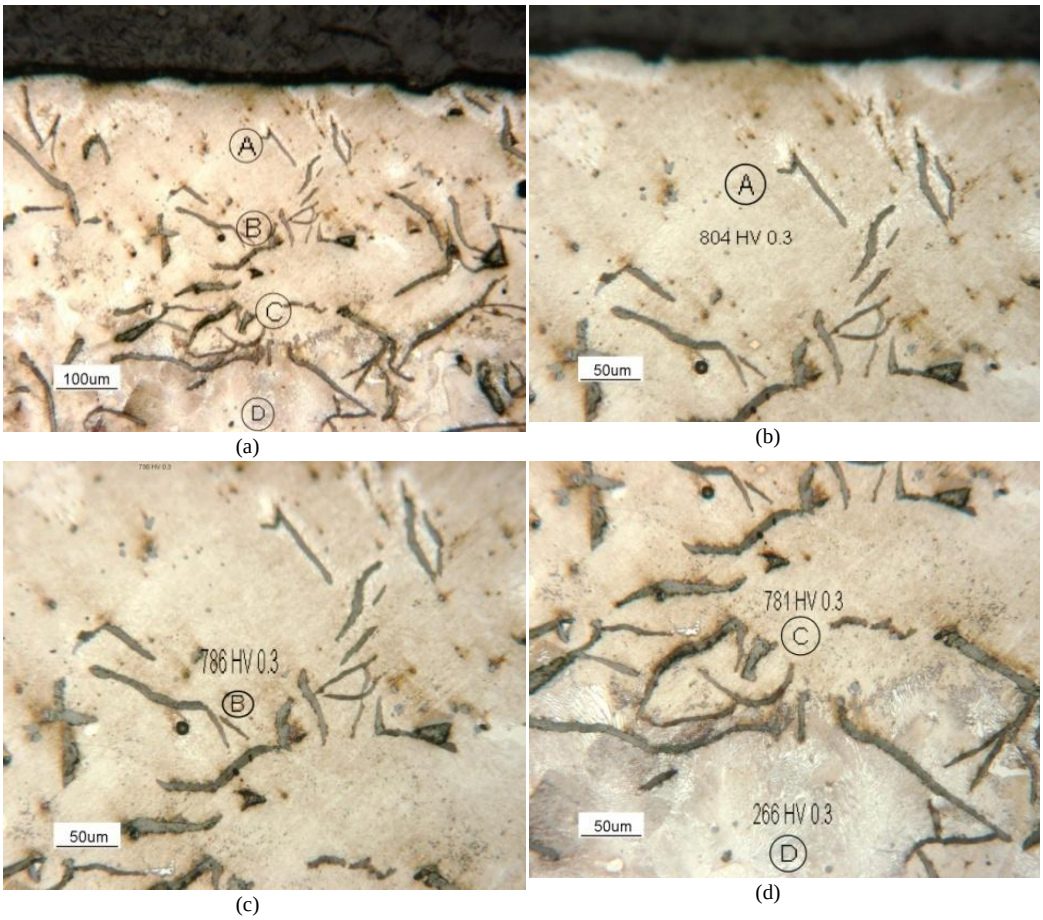

Figure 5-4 Microstructures of the hardened zone by single track hardening.

For every hardened sample, the hardness tests were carried out along the width and depth direction of the hardened zone, the hardness profiles are reported in Figure 5-5 and 5-6. Hardness profiles indicate that the hardness is related neither to the temperature nor to the scanning speed. A uniform hardness distribution is obtained in each hardened zone. The hardness range was 700-800$HV_{0.3}$.

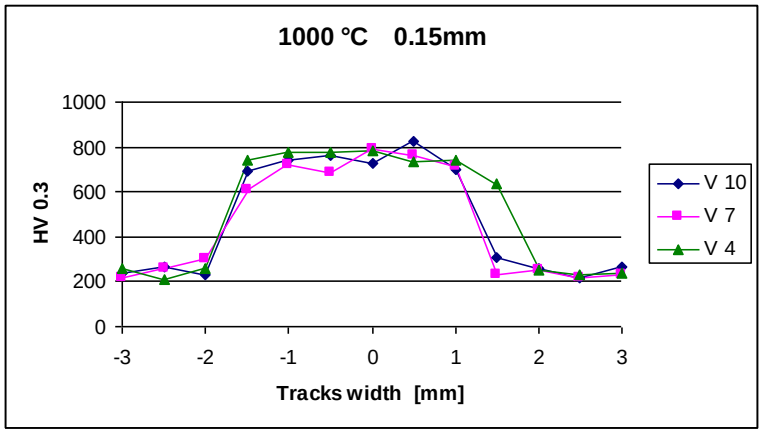

(a)

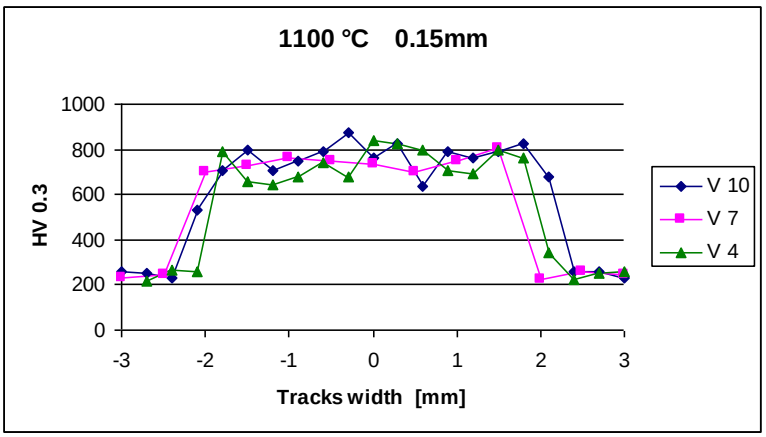

(b)

Figure 5-5 Hardness profile along the track width of the single track hardening.

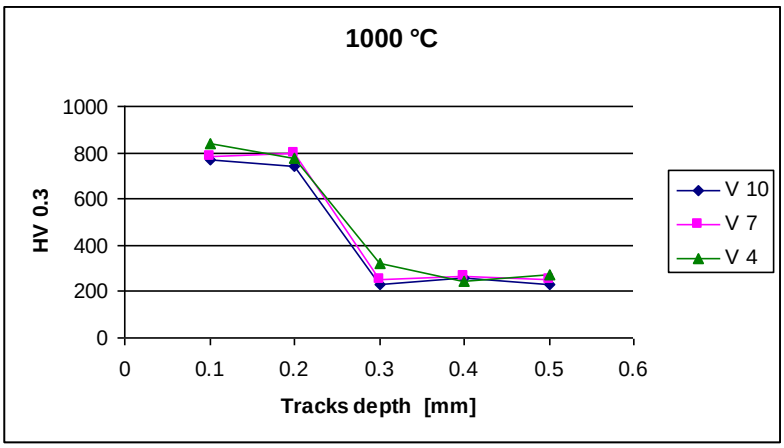

(a)

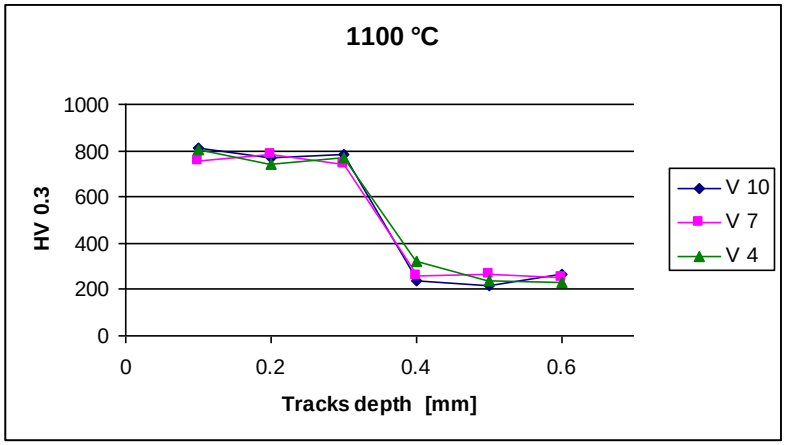

(b)

Figure 5-6 Hardness profile along the track depth of the single track hardening.

The results of the single track hardening show that by the measurement and control system, when the temperature reaches Ac_3, each combination of different levels of temperature and scanning speed produces a homogeneous hardened zone and uniform hardness distribution. This is also confirmed by the SEM as shown in Figure 5-7. Microstructures were analyzed along the depth of the hardened zone, the pearlite on the top and in the middle of the hardened zone have been completely transformed; on the other hand, some pearlite and partially transformed materials were observed at the boundary of hardened zone and base material. The depth of the hardened zone is strongly influenced by the investigated parameters. Considering the high productivity, high temperature and high scanning speed were chosen as the parameters for multi-pass investigation.

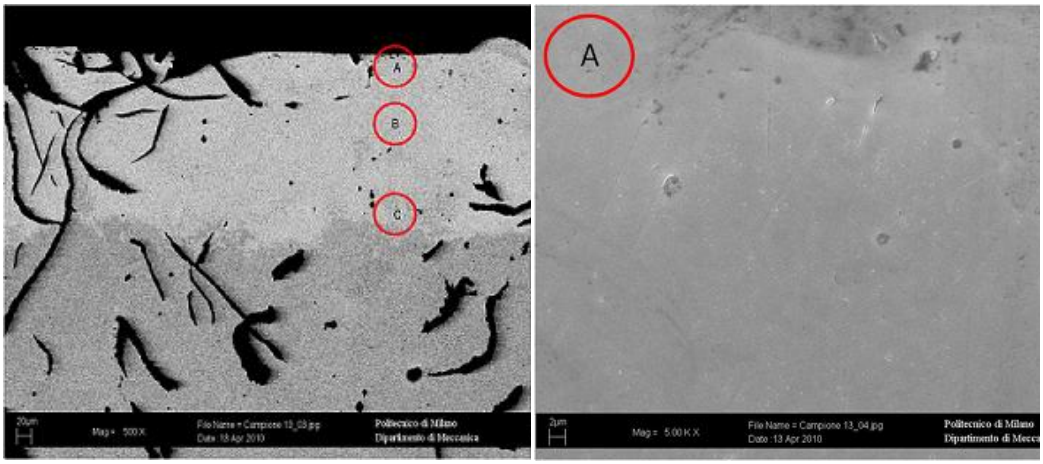

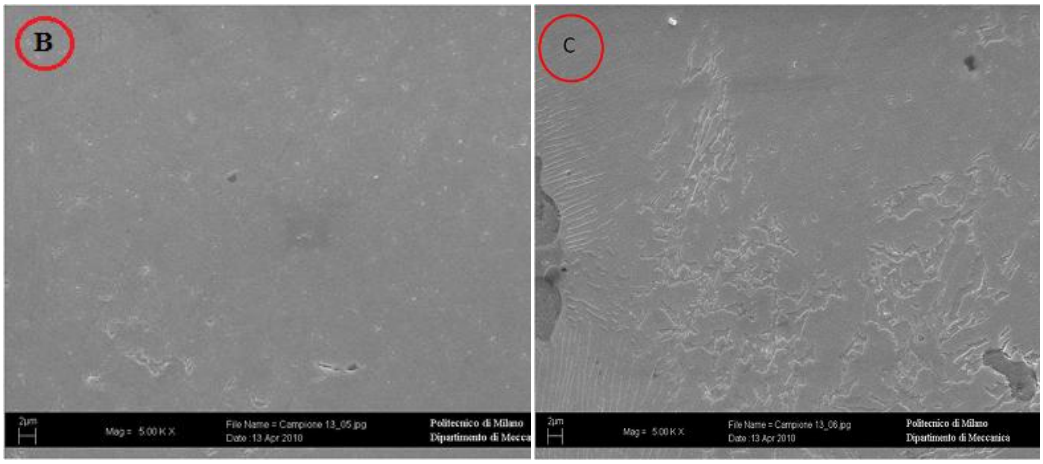

Figure 5-7 SEM analysis of the hardened zone.

5.2.3 Selection of the best condition

The microhardness tests confirmed the high hardness was obtained in the hardened zone; the geometrical features were investigated to obtain an optimized process and ensure a required hardened depth.

Figure 5-8 shows the typical geometric dimensions of the laser hardened zones. In Figure 5-9, the experimental results are reported in terms of width and depth as a function of scanning speed and surface temperature.

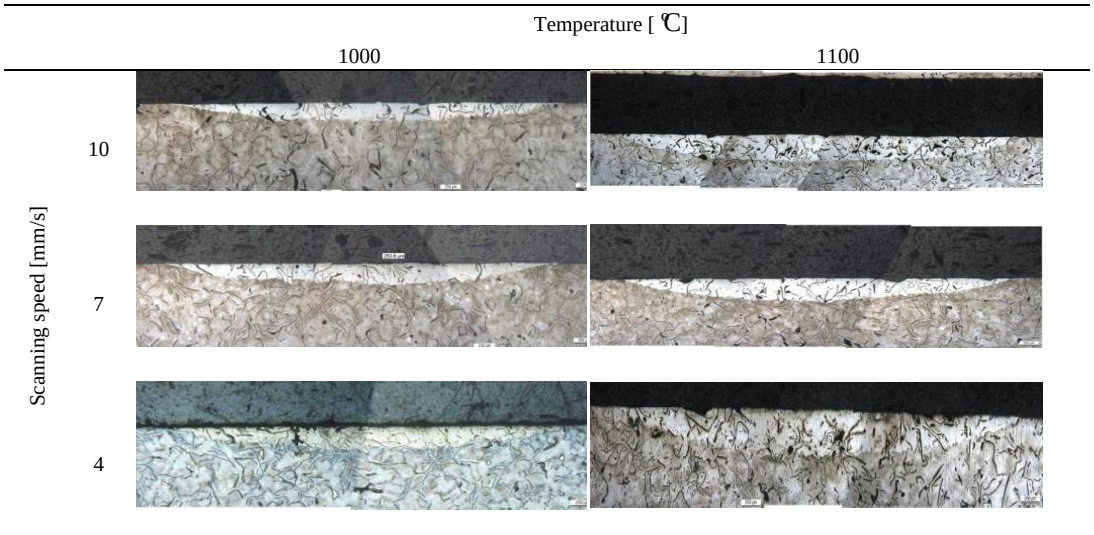

Figure 5-8 Hardened zone obtained by different parameters.

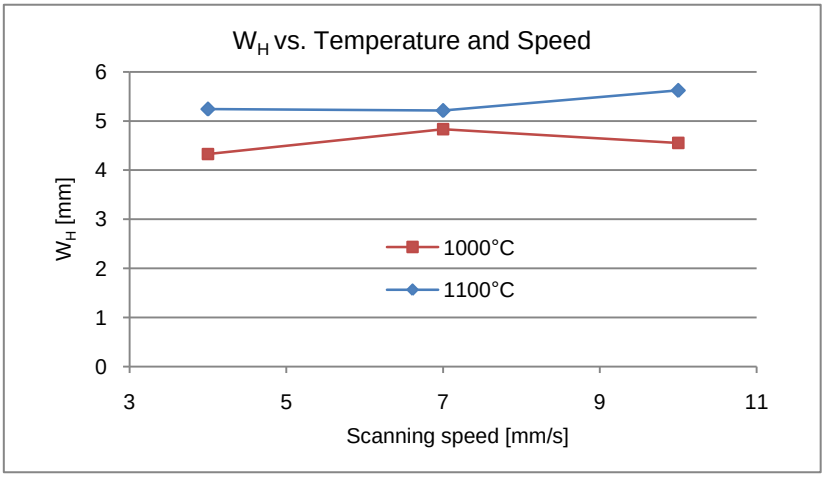

(a) Hardened width vs. temperature and scanning speed

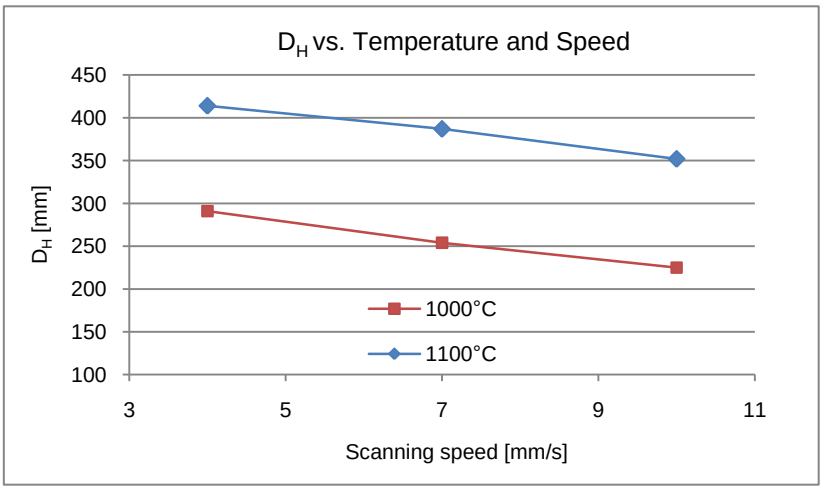

(b) Hardening depth vs. temperature and scanning speed

Figure 5-9 Geometric dimensions of laser hardened zone.

The width of the hardened zone is mainly determined by the dimension of the laser spot, on the contrary the treated area depth is affected by both parameters: temperature and speed.

In terms of the temperature values, it can be interpreted that higher temperature on the surface means more energy input, which induces a deeper hardened zone. When the temperature on the surface is constant, faster scanning speed needs higher laser power and induces a faster thermal cycle that produces a thinner hardened zone. The maximum hardening depth can reach 0.41 mm by keeping the temperature at 1100 ℃, and scanning the workpiece at the lowest speed 4 mm/s.

With higher temperature on the top surface, deeper hardened zone was obtained, considering the productivity, higher temperature 1100 ℃ and higher scanning speed 15 mm/s were chosen as the parameters for the multi-pass laser hardening.

5.3 Proximity multi-pass laser hardening

To treat a large area, multi-pass technique is adopted. Since the overlapping process induces two main drawbacks: non uniform surface hardness and non uniform hardening depth, the parameters should be adopted carefully to minimize these drawbacks.

5.3.1 Experimental parameters for proximity multi-pass laser hardening

Based on the results of single pass hardening, process parameters for overlapping process were set and overlapping experiments were carried out. From the results of the previous experiment, temperature and scanning speed parameters were set as 1100 ℃ and 15 mm/s to get a productive system. Four levels of overlapping lengths were adopted: 0.75 mm, 1 mm, 1.25 mm, 1.5 mm.

5.3.2 Microhardness and geometrical features for proximity multi-pass hardening

A large surface was treated by the overlapping process with different overlapping length, as shown in Figure 5-10. The top surface was covered by the hardened zones; and the overlapped zones exist between the two adjacent hardened zones. The microstructure shows the reheated material in the previous track, it is tempered martensite with lower hardness.

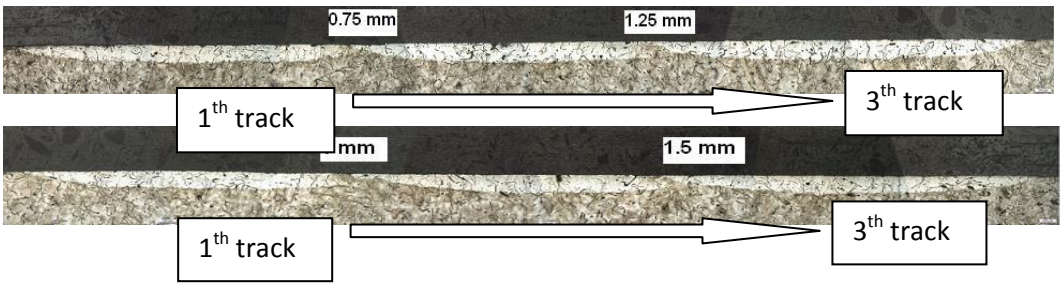

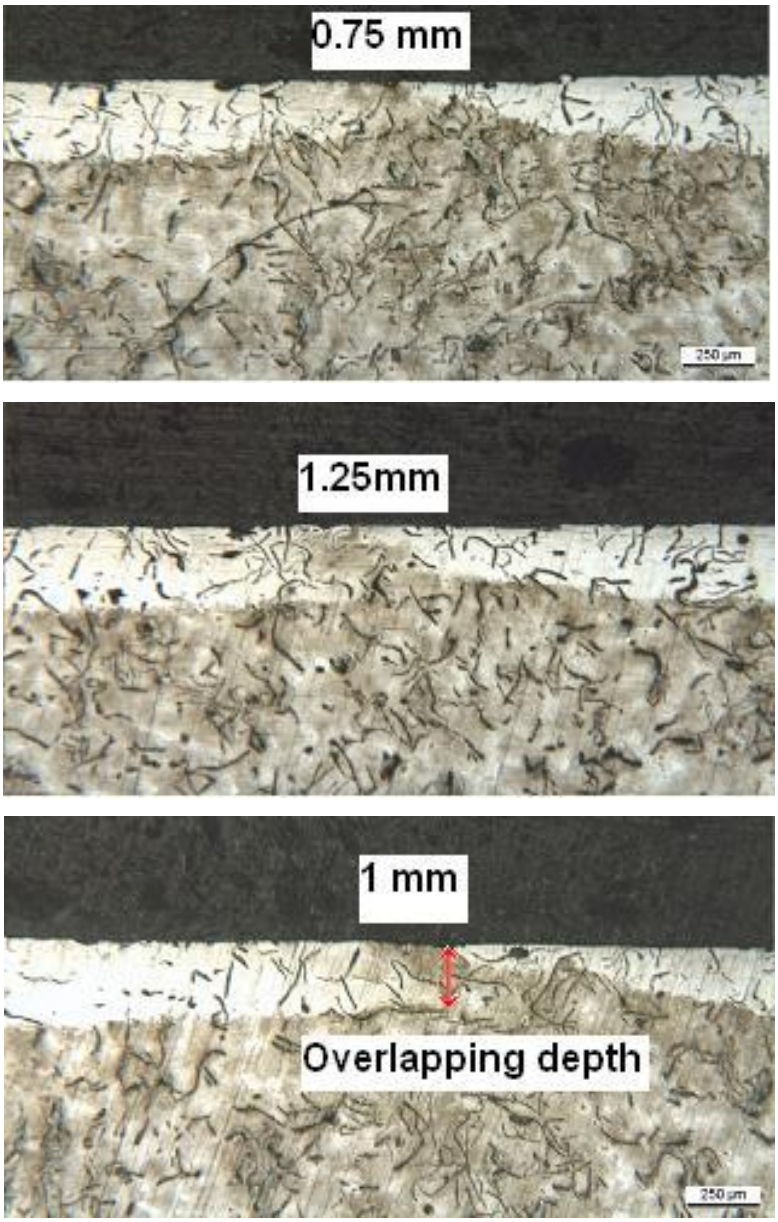
0.75 mm
1.25mm
1 mm
Overlapping depth

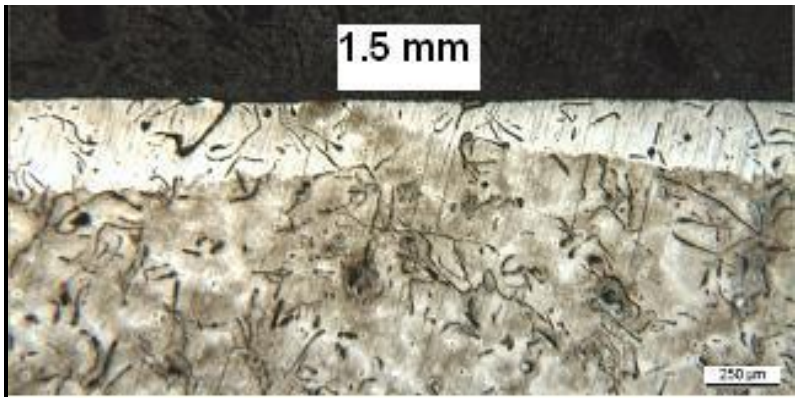

Figure 5-10 Microstructures of hardened zone with different overlapping lengths.

The measured temperature and controlled laser power were recorded in real time and listed in Figure 5-11, the measurements show that by means of the control system, the power of the laser decreased because of the accumulated heat in the bulk, constant temperature was obtained for each track, in the meantime.

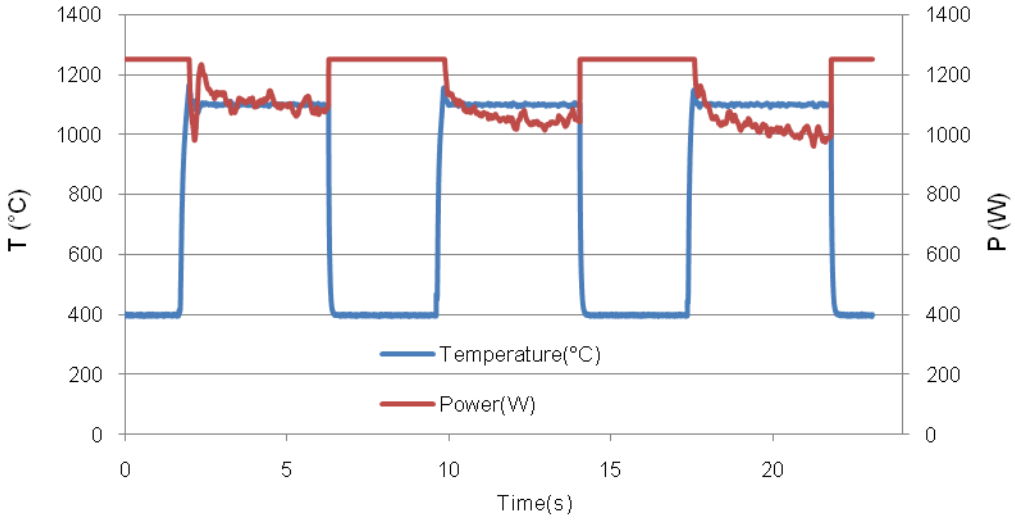

Figure 5-11 Real time temperature and laser power for multi-pass hardening.

One disadvantage exists in the overlapping process is the non uniform depth of the hardened zone; it is influenced by the overlapping depth. With different overlapping lengths, different overlapping depths were achieved. For every overlapping depth, five measurements were carried out; the results are reported in Figure 5-12. Only a thin layer is obtained with a small overlapping length equal to 0.75mm. An increased depth was obtained by adopting larger overlapping length.

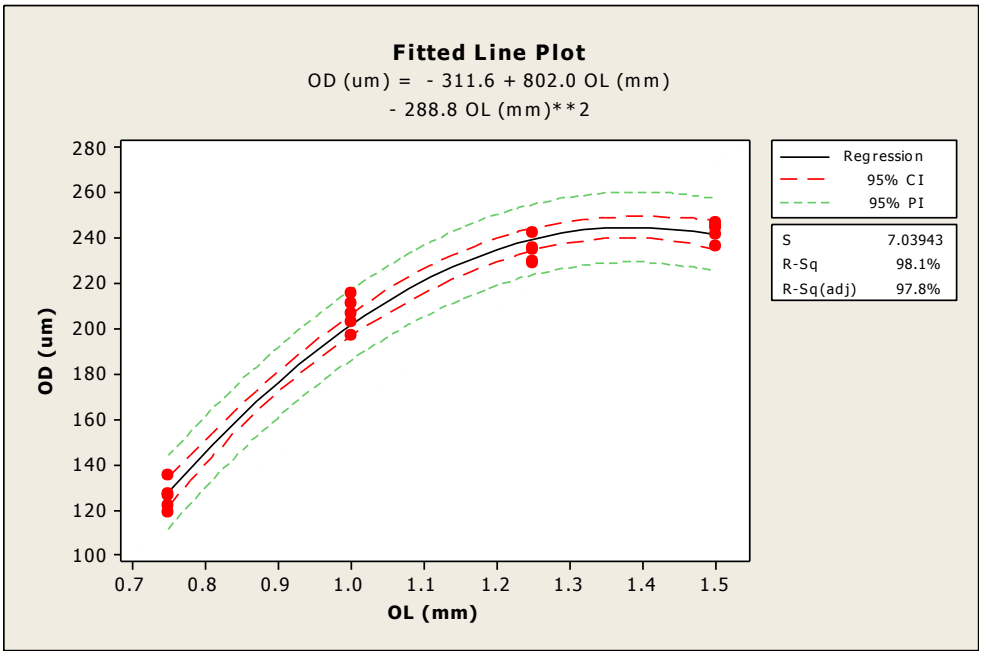

Figure 5-12 Overlapping depths (OD) in different overlapped zones.

Figure 5-13 shows the hardened top surface by overlapping process, overlapped zones could be recognized on the top surface. Microhardness was tested on the top surface and in the cross section along the width direction, based on the red coordinate axis; in the cross section, the test distance is 0.15 mm from the surface. The distance between each test is 0.3 mm. The microhardness profiles across the transverse direction are reported in Figure 5-14.

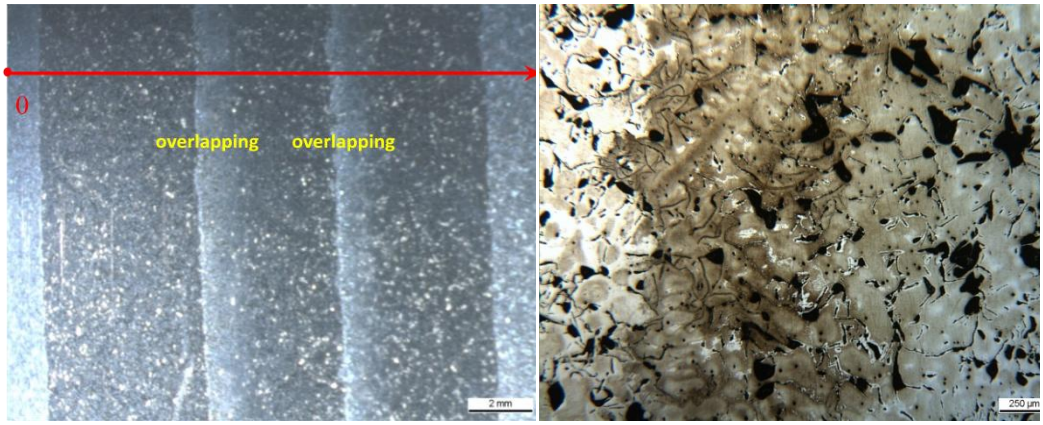

(a) Top surface of the hardened sample by overlapping process

(b) Microstructure of the overlapped zone on the top surface

Figure 5-13 Treated top surface by overlapping process.

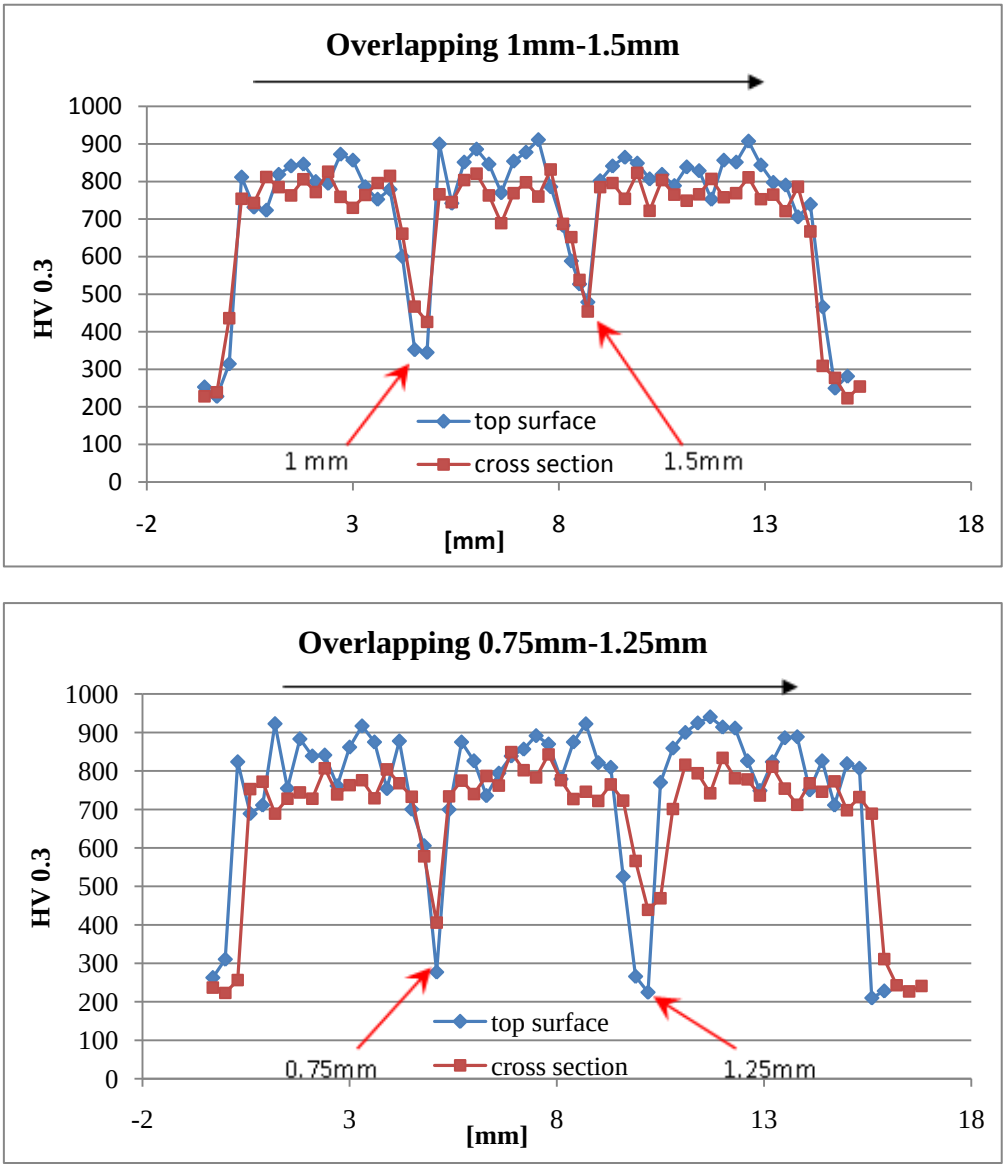

Figure.5-14 Hardness profiles on the surface of overlapped zones.

By comparing the measured hardness on the top surface and in the cross section, the results indicate that, for the hardened zone, the hardness on the surface is higher (in the range of 800HV to 900HV) than it in the cross section (in the range of 700HV to 800HV). On the contrary, the hardness reduction in the overlapped zone was observed both on the top surface and in the cross section, but the hardness decreased severely on the top surface, could be lower than 300HV. To investigate the hardness

distribution in the overlapped zone, the hardness was tested along the depth of the cross section and the hardness profiles are shown in Figure 5-15-

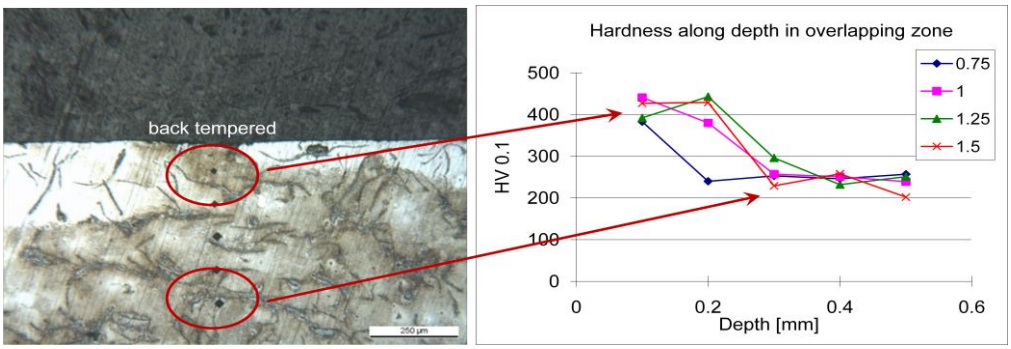

Figure 5-15 Hardness test in the cross section of the overlapped zones.

In the back tempered area the reduction of microhardness values is uniform, the hardness in the overlapped zone is around 400 HV, when the tests were carried out in deeper zone, the hardness decreased to the value of basic material. The hardness tests in the overlapping also indicate the overlapping depths in different overlapping width process, for small overlapping length process, *i.e.* 0.75 mm, only 0.1 mm overlapped zone with 400HV was obtained, and then the hardness drops to the base material value. With wider overlapping length (1 mm-1.5mm), overlapping depth more than 0.2 mm was ensured.

High temperature on the top surface ensures a high productivity, under the requirement of certain hardened depth. The hardened tracks obtained by 1100 ℃ were investigated in terms of laser power and geometrical features. The first hardened track during the multi-pass hardening could be considered as a hardened zone treated by single track. Combined with the single track hardening results, the relationship between controlled laser power and scanning speed is shown in Figure 5-16. The other important factor that influences the industrial applications is the depth of the hardened zone, for every hardened zone, five measurements were carried out, and the depth of the hardened zones obtained by different scanning speeds are shown in Figure 5-17. The adjusted coefficient of determination R^2_{adj} is 98.5%. The normal probability plot of the residuals shown in Figure 5-18 also indicates that data are distributed normally.

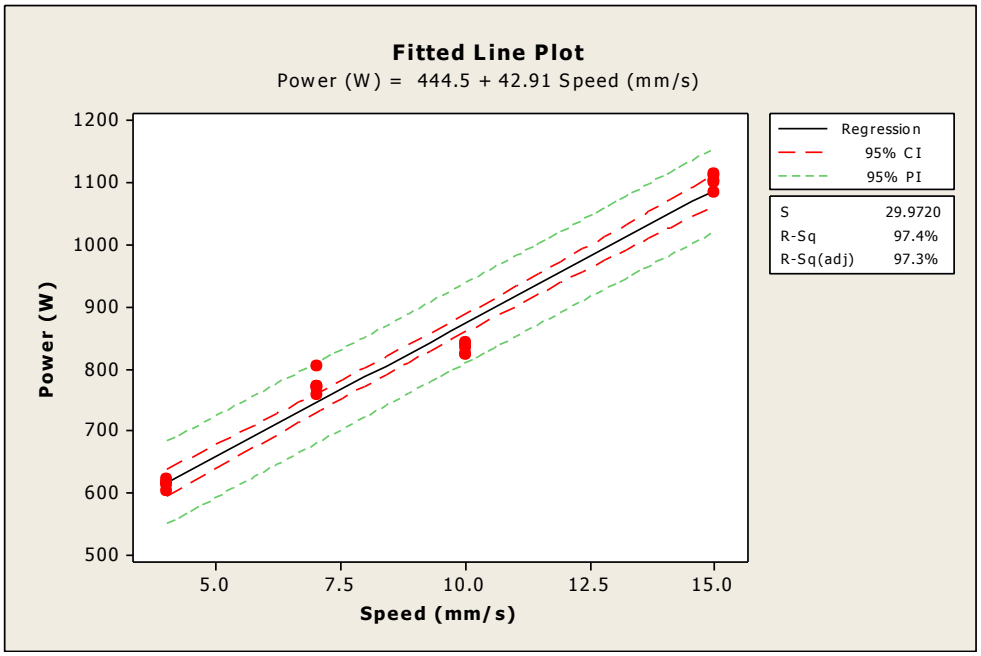

Figure 5-16 Relationship between controlled laser power and scanning speed.

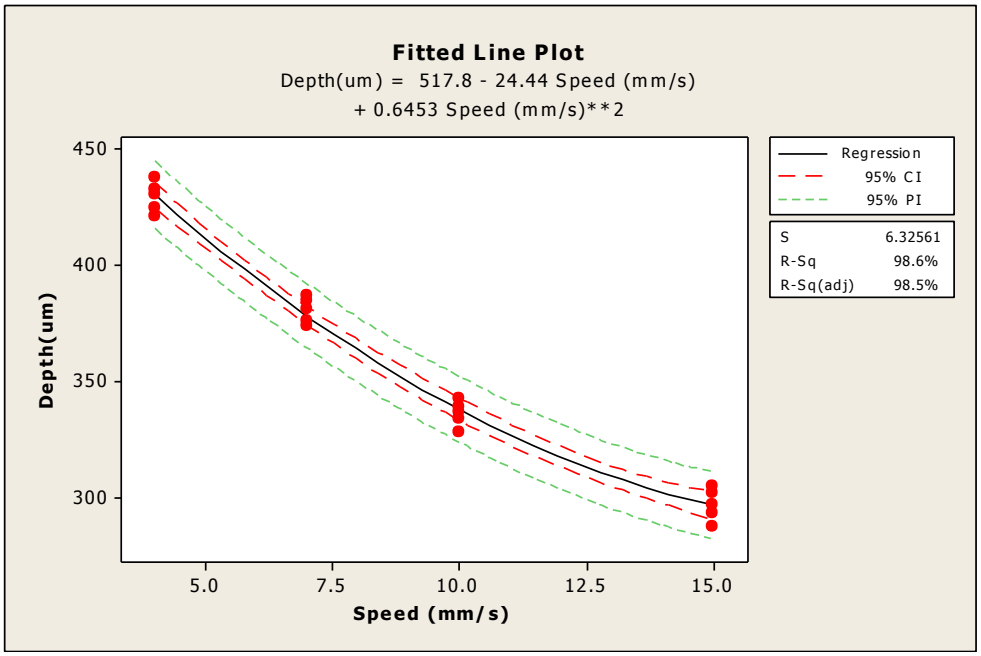

Figure 5-17. Relationship between depth of the hardened zone and scanning speed.

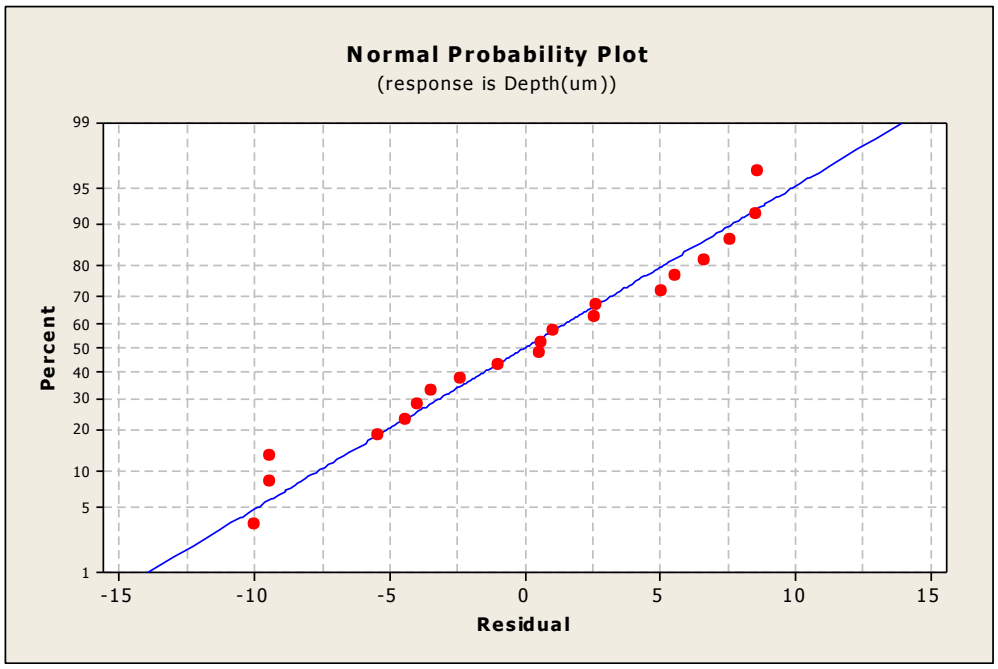

Figure 5-18 Normal probability plot of the residuals for hardened depth.

Considering the combination of uniformity of hardening depth and uniformity of hardness, the parameters for overlapping process can be optimized. Larger overlapping length ensures a uniform hardening depth, but for a given surface, it also means more hardening tracks, and induces more overlapped zones with hardness reduction. In case of diode laser hardening with a rectangular laser spot and uniform energy distribution, the depth of the hardened zone is more uniform than that obtained by other kinds of laser with a Gaussian distribution. In diode laser hardening, when overlapping length reaches a certain point, the depth in overlapped zone does not increase significantly, and a uniform hardened zone in depth can be obtained. When the overlapping length exceeds this point, it induces more overlapped zones and hardness reduction. For this experimental campaign, the critical point is 1.25mm. A valid range for overlapping length is from 1 mm to 1.25 mm, which corresponds to the 16.7-20.8% of the nominal hardening track width. The following experiments for wear test selected the overlapping length within this window.

5.4 Conclusions

A uniform hardened zone can be obtained in single pass laser hardening of gray cast iron with a high power diode laser. Within the operable window, two levels of high temperature (1000 ℃ and 1100 ℃) were chosen and different scanning speeds were carried out to study the effects of the parameters on the hardened zone, in terms of geometrical features and hardness distribution. Considering of the high productivity,

a higher speed 15mm/s was used to investigate the back-tempering phenomenon in the overlapping area.

The main conclusions of this experimental study are:

1. Uniform hardness was obtained in the laser hardened zone, whose hardness values range from 700 to 800 $HV_{0.3}$ in the cross section, regardless to the temperature and scan speed. The hardness on the top surface was higher than it in the cross section (800 – 900 $HV_{0.3}$).
2. Geometrical features of the hardened zone were determined by both temperature and scanning speed.
   - The width of the hardened zone was mainly determined by the dimension of the laser spot.
   - The depth of the hardened zone is affected by both parameters. High temperature and low scanning speed induce more heat input, which results deeper hardened depth.
   - In the industrial applications, the hardening temperature on the surface is set before the hardening process; in this case, considering the temperature as a constant, under a certain requirement of hardened depth, the scanning speed and minimum laser power are decided.
3. In the overlapping area the micro-hardness values show an abrupt decrease, due to the re-heating of the previous obtained martensite which is temped. The loss of hardness value is uniform in depth; the hardness in the overlapped zone is 400HV. Different overlapping lengths do not affect the range of hardness decrease.
4. Large overlapping length ensures a uniform overlapped depth. In this experimental study, the overlapping length from 1 mm to 1.5 mm ensures 0.2 mm overlapping depth.

6 Laser surface melting

As discussed in the previous chapters, back tempering phenomenon is the main drawback of the laser hardening applications on large surfaces. In this chapter, one solution to the back tempering problem – laser surface melting technique is proposed for planar surfaces. When the surface of the base material is heated above the melting point, a fine grained microstructure with high hardness is obtained in the melted zone, with appropriate melting process, a uniform thickness of the melted surface could be ensured in spite of the overlapping process. Other than the uniform thickness, greater depth of hardened zone is achieved. Experimental campaigns for laser melting process were designed with a standard diode laser for single track and multi-pass. Different melting conditions were studied and a large surface was treated by laser melting, no hardness decrease was observed in the overlapped zones

6.1 Single track laser melting process

The single track laser melting experiments were carried out to understand the effects of the melting process on the cast iron surface. The features of the melted zone were investigated to look for an optimized condition for the overlapping process.

For single track laser melting process, three levels of temperature above the melting point and two levels of scanning speed were chosen. The investigated parameters are

listed in Table 6-1, the real time measurements and the microstructures of the melted zones are shown in Table 6-2 and 6-3.

Table 6-1 Process parameters used in single pass melting campaign.

Temperature on the surface (T) [℃]	1300, 1400, 1500
Scanning speed (V) [mm/s]	3, 5

Table 6-2 Real time measurement for laser melting process.

T [℃]	Speed [mm/s]	
	3	5
1300	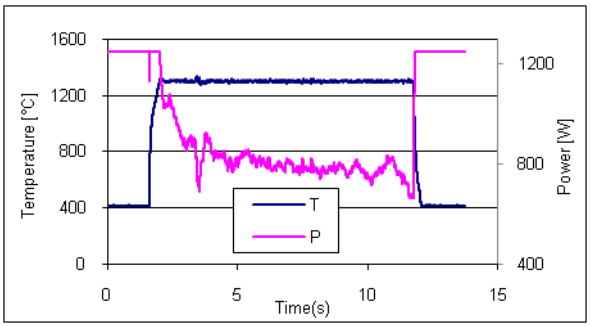	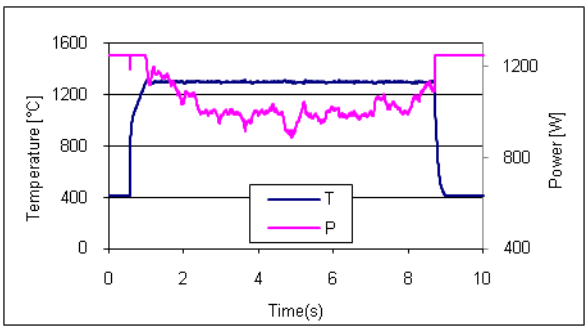
1400	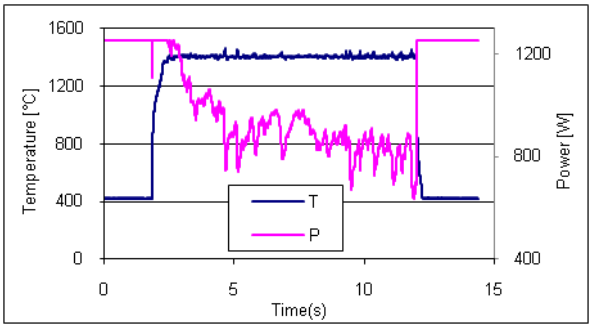	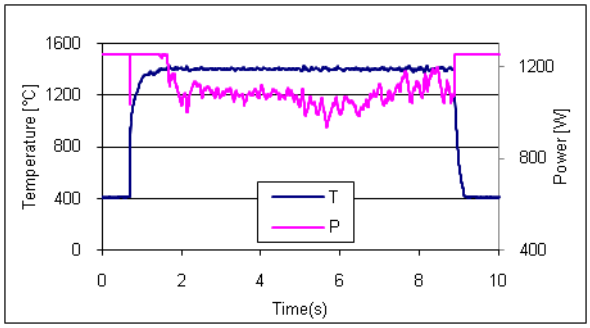
1500	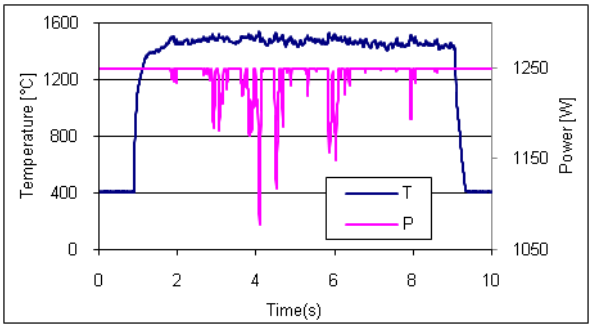	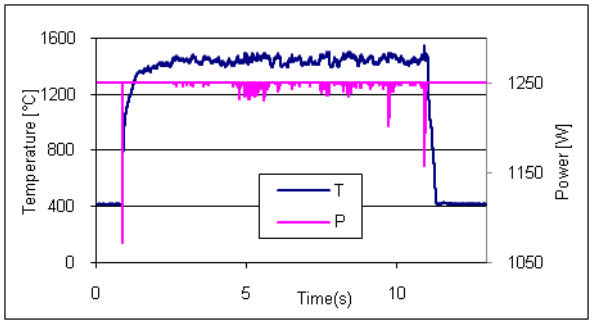

Table 6-3 Melted-hardened zones obtained in the melting process.

V[mm/s]	T[℃]	Melted-hardened zones obtained in the melting process
3	1300	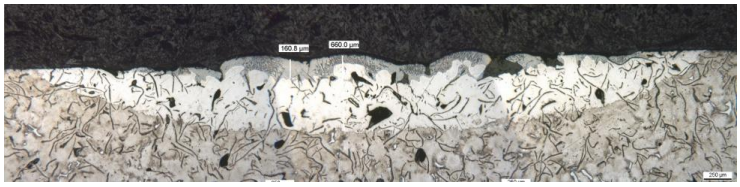
	1400	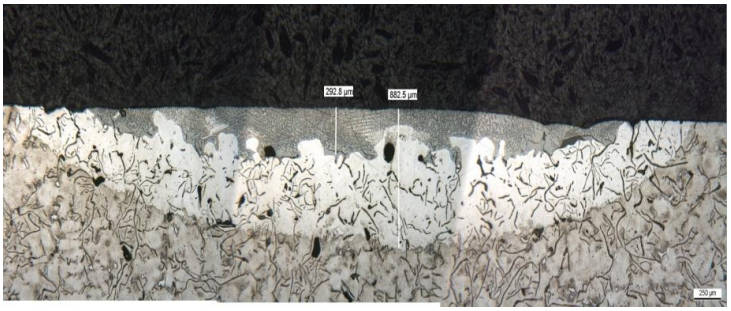
	1500	
5	1300	
	1400	

	1500	

In the single track laser melting process, when the controlled temperature on the top surface is above the melting point, melted layers were obtained in all the experimental conditions regardless to the scanning speed. The modified surface consisted of two different microstructure zones, i.e. a melted zone in the upper part of the surface layer and a hardened zone in lower part. In Figure 6-1(a) and (b) microstructures in the melted zones are shown with different magnification. Compared to the hardening process, the graphite flakes in the base material dissolved in the melted zone, hardened zone was obtained as shown in Figure 6-2.

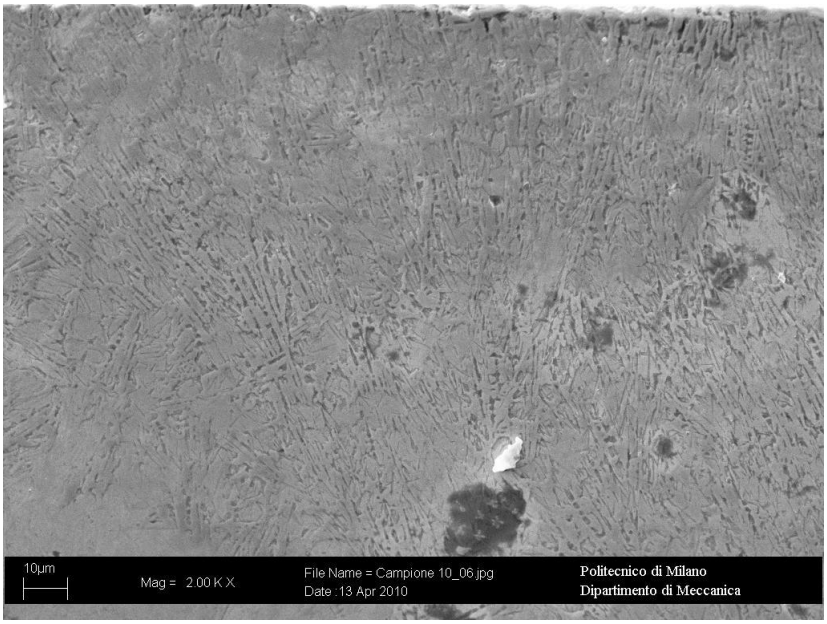

(a) Small magnification

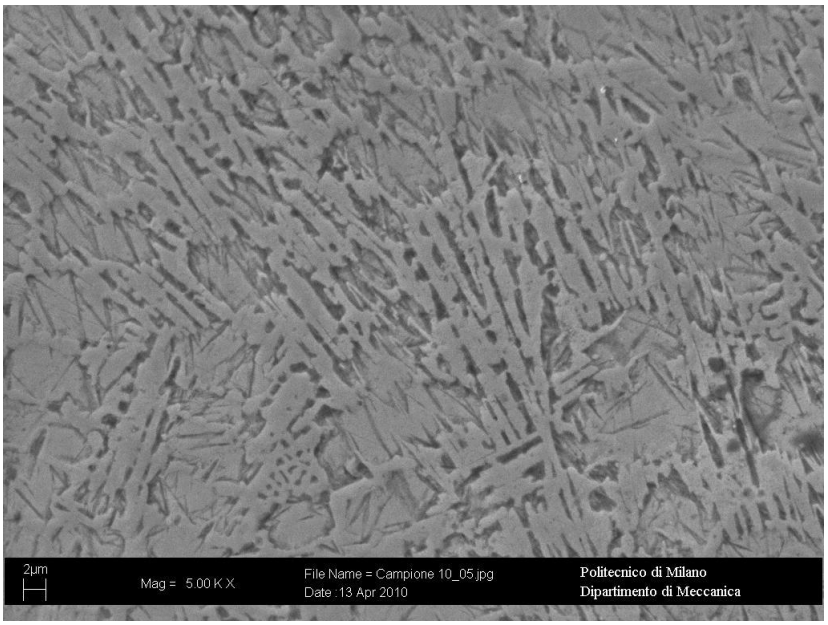

(b) large magnification

Figure 6-1 Microstructures in the melted zone.

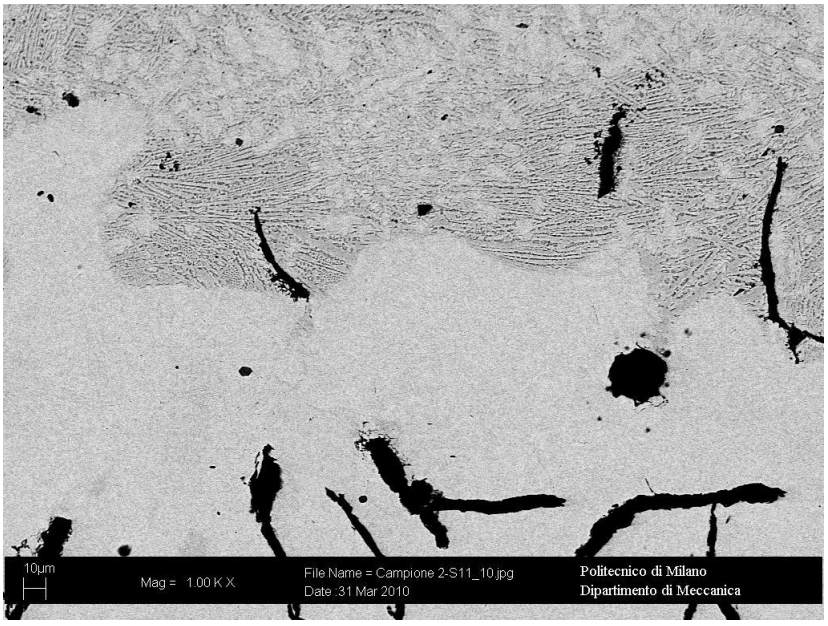

Figure 6-2 The boundary of melted zone and hardened zone.

Although melted zones were obtained in all the process when the temperature is above the melting point, the melted surface is non uniform in the case of low

temperature and high scanning speed. The depth of the melted zone and hardened zone are illustrated in Figure 6-3 (a) and (b).

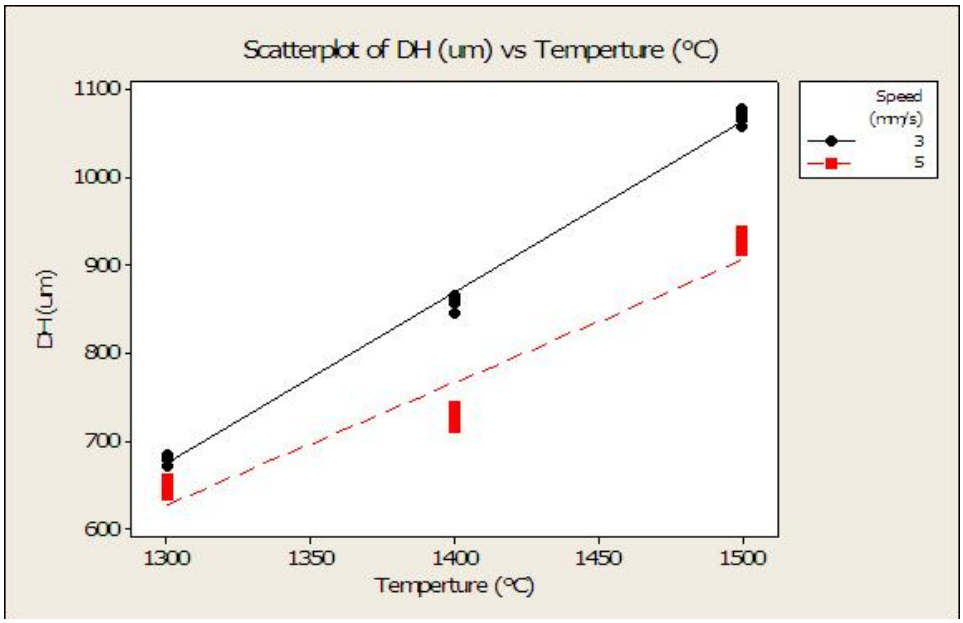

(a) Hardened zone

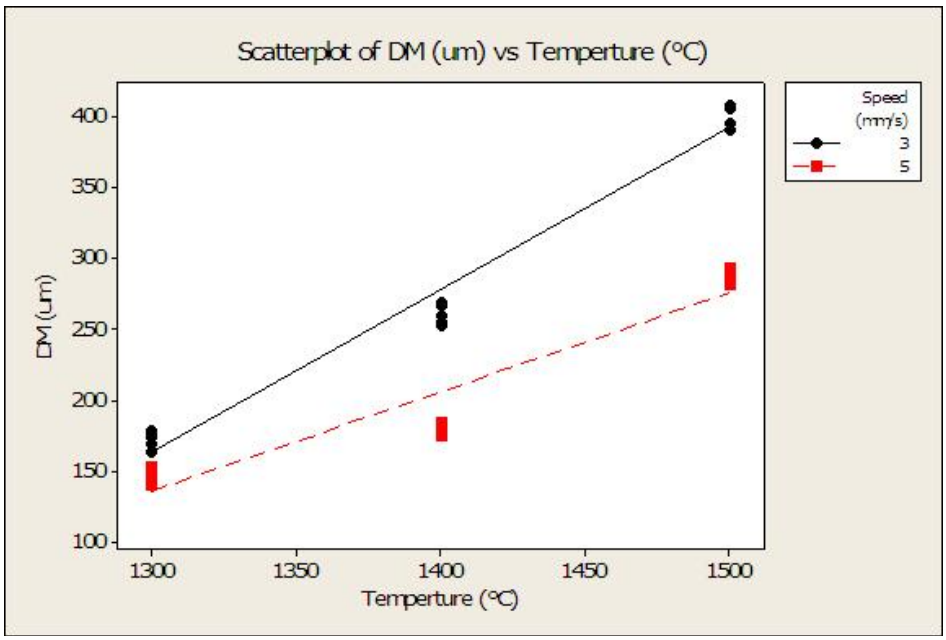

(b) Melted zone

Figure 6-3 Depth of the hardened and melted zone in laser melting process.

Bothe of the structures and the depths of the melted-hardened zones indicate that only a slight melted layer is on the top surface, when the temperature is a hundred above the melting temperature or the specimen was scanned with a high speed. In order to get a large and uniform melted zone which is not affected by the overlapping process, a combination of high temperature and low scanning speed makes the most sense.

The microhardness was tested in the cross section of the sample (1500 ℃ – 3 mm/s), the hardness profiles along the width and depth are given in Figure 6-4(a) and (b). The hardness tests along the width were carried out under the top surface 0.15 mm. The hardness profiles indicate that in the high temperature and low scanning speed process, a uniform hardness distribution is achieved in the melted zone. The microhardness in the melted zone is higher than that of hardened zone, 800-900 HV 0.3.

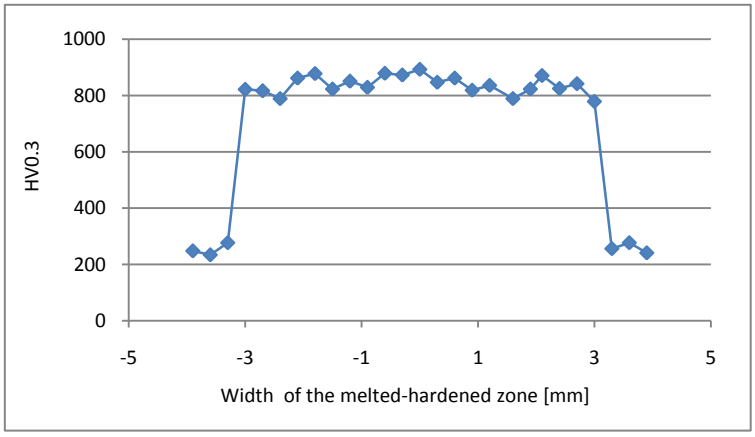

(a) Hardness distribution along the width

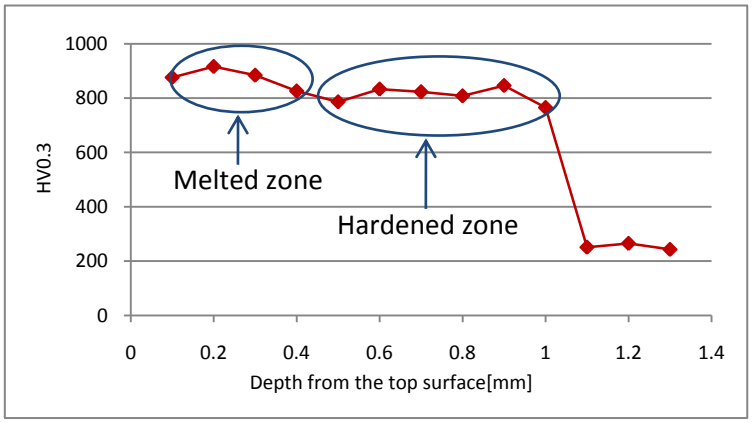

(b) Hardness distribution along the depth

Figure 6-4 Hardness profiles in the cross section of melted-hardened zone.

6.2 Multi-pass laser melting process

As discussed in chapter 6-2, a new microstructure with high hardness was observed in the melted zone, the results of single track hardening show that high temperature and low scanning speed ensure a deeper and uniform melted layer on the top surface. To obtain a uniform melted zone on a wide surface, low scanning speed (3mm/s) and temperature range from 1300 ℃ to 1500 ℃ were adopted during the multi-pass process. Lower temperatures were also adopted in the overlapping process to study the trend of the reduction of the back tempering effect due to the melted layer. Compared with hardening process, the width of the hardened zone is larger, more than 6 mm, thus smaller overlapping length was chosen in the overlapping length window. The parameters used in the overlapping laser melting process are listed in Table 6-4.

Table 6-4 Experimental parameters for overlapping laser melting process.

Temperature (℃)	Scanning speed (mm/s)	overlapping length (mm)
1300		
1400	3	1
1500		

After the experiments, the results were evaluated in terms of the uniformity of the melted surface depth, as the microhardness distribution along the width of the treated surface.

6.2.1 Multi-pass laser melting process by 1300℃ and 1400℃

When low temperature controlled at 1300 ℃ was on the top surface, the melted surfaces were obtained only in the center of every treated track; no melted layer was obtained in the overlapped zones. In the hardened zone, the martensite was reheated and back tempering occured as in the multi-pass hardening process, the structures of the melted and hardened zones are shown in Figure 6-5. Under the top surface 0.15 mm the hardness tests were carried out, the hardness profile (see Figure 6-6) in the cross section confirmed the hardness decreased in the overlapped zone.

(a) Cross section

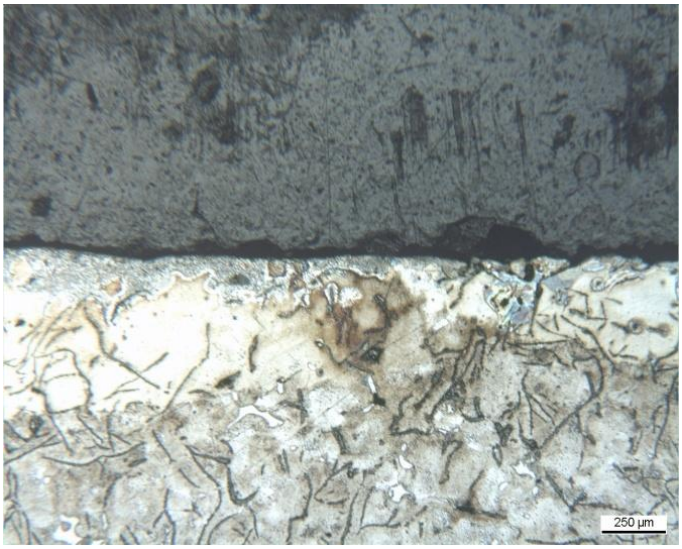

(b) Overlapped zone between 1st and 2nd tracks.

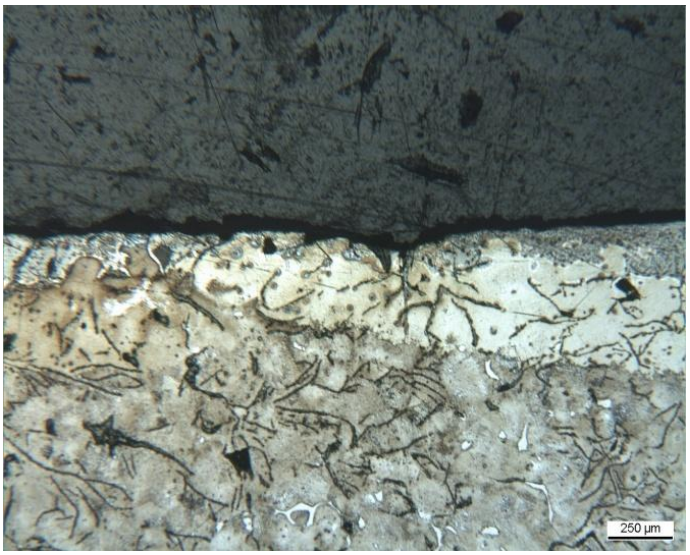

(c) Overlapped zone between 2th and 3th track

Figure 6-5 Structures of the overlapping melted zone – 1300 ℃, 3mm/s.

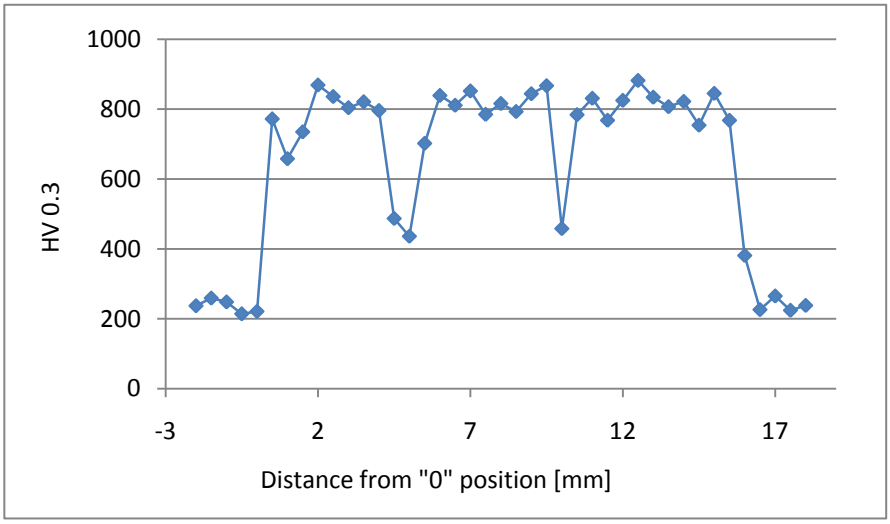

Figure 6-6 Hardness profile in the cross section of the overlapping melted zone – 1300 ℃.

The microstructures and hardness tests confirm that with lower temperature, only slight melted layers were obtained in the center of the treated tracks, these melted layers could not cover the overlapped zones when multi-track was applied.

Higher temperature 1400 ℃ was induced to enlarge the melted zone; the results are shown in Figure 6-7.

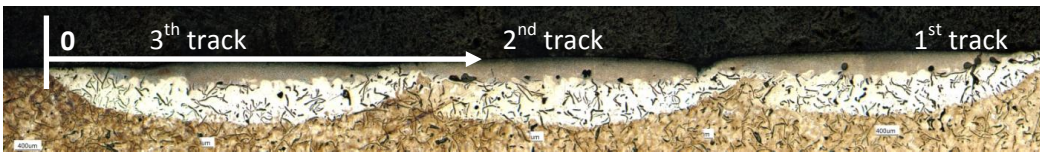

(a) Cross section

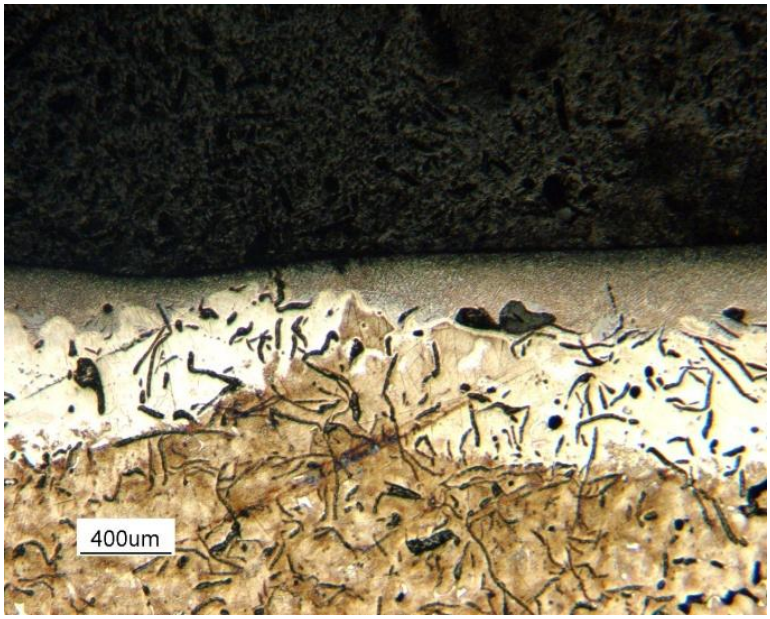

(b) Overlapped zone between the 2nd track and 3th track

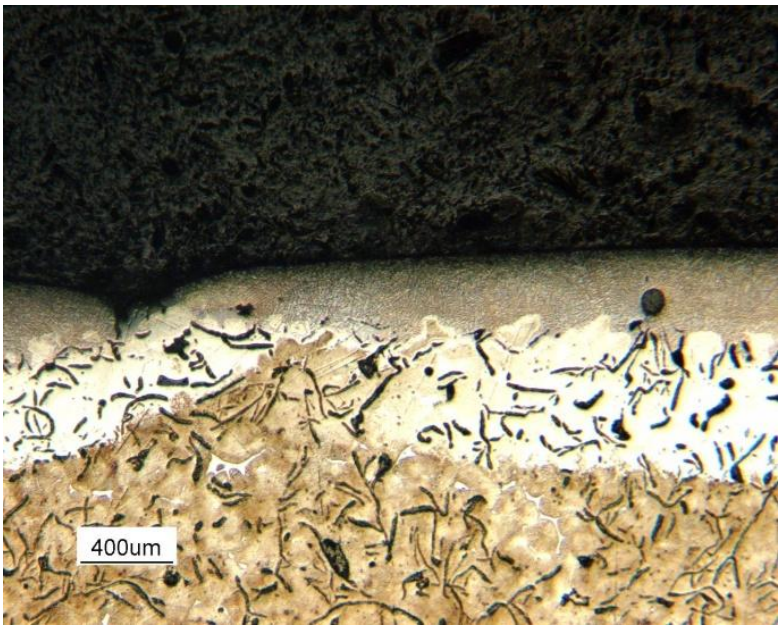

(c) Overlapped zone between the 1st track and 2nd track

Figure 6-7 Structures of the overlapping melted zone – 1400 ℃, 3mm/s.

With a higher temperature, a melted layer was obtained on the top surface; the shape of the melted zone is similar to the hardened zone, which has a maximum depth in the center, and decreases gradually to the edge of the melted zone. According to the

microstructures of the cross section, above the overlapped zones, melted surfaces were observed. Although melted surfaces up to 300 μm were achieved in the center of the melted zone, the melted layer is still superficial in the overlapped zones, as shown in Figure 6-7 (b) and (c), the minimum depth of the melted layer above the overlapping is less than 100 μm. The hardness test (Figure 6-8) along the width direction also indentified the hardness decrease in the overlapped zone which is covered by a superficial melted layer (Figure 6-7(b)). The hardness tests were carried out under the top surface 0.15 mm.

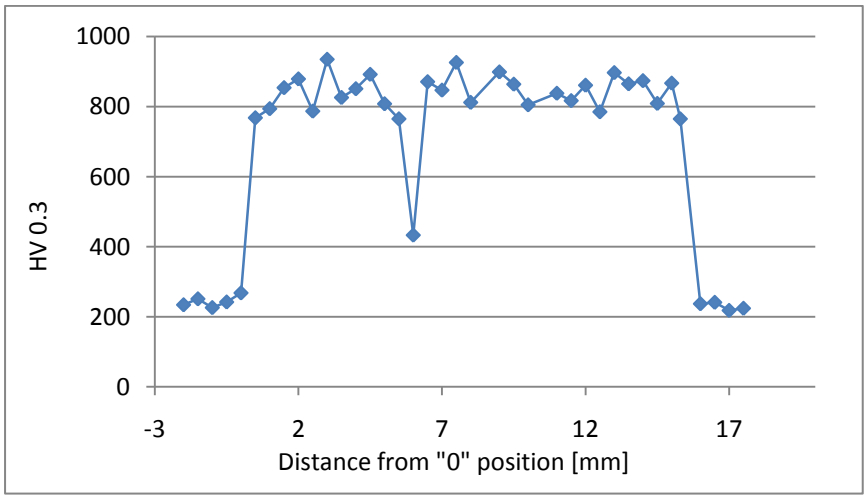

Figure 6-8 Hardness profile in the cross section of the overlapping melted zone – 1400 ℃.

Although hardness still decrease in the overlapped zone due to the superficial melted layer, the hardness tests show an improved behavior over its obtained by 1300 ℃, the areas with hardness decreased due to the fact that back tempering was reduced.

6.2.2 Multi-pass laser melting process by 1500 ℃

The overlapping melting processes with 1300 ℃ and 1400 ℃ have proved the melted layer could improve the hardness behavior in the overlapped zone by increasing the temperature. With higher temperature (1500 ℃ was adopted to treat a large surface); a uniform melted layer was obtained on the larger surface, as shown in Figure 6-9.

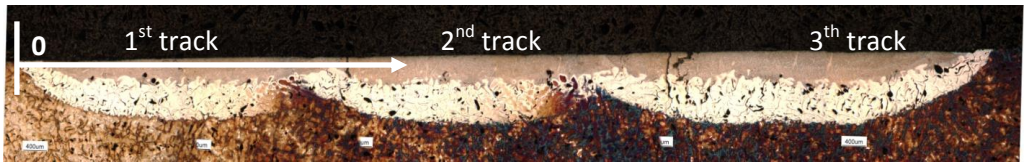

(a) Cross section

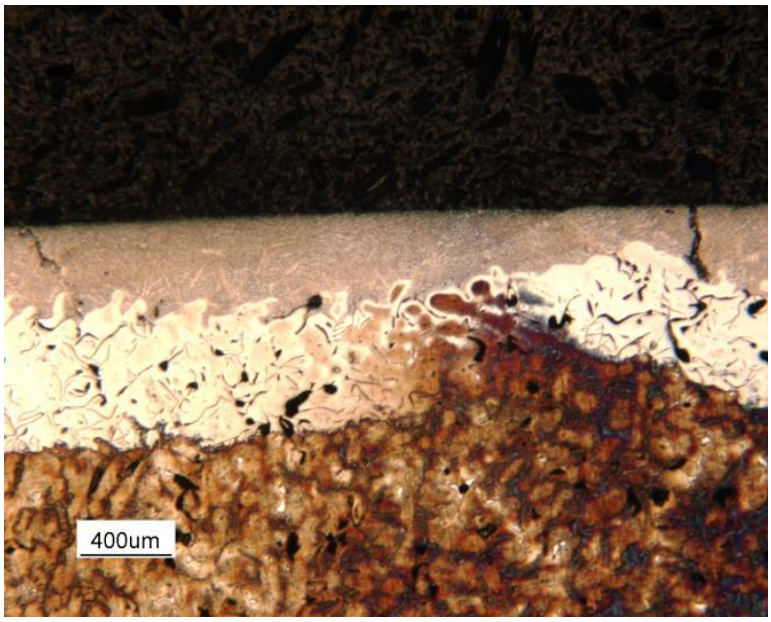

(b) Overlapped zone between the 1st track and 2nd track

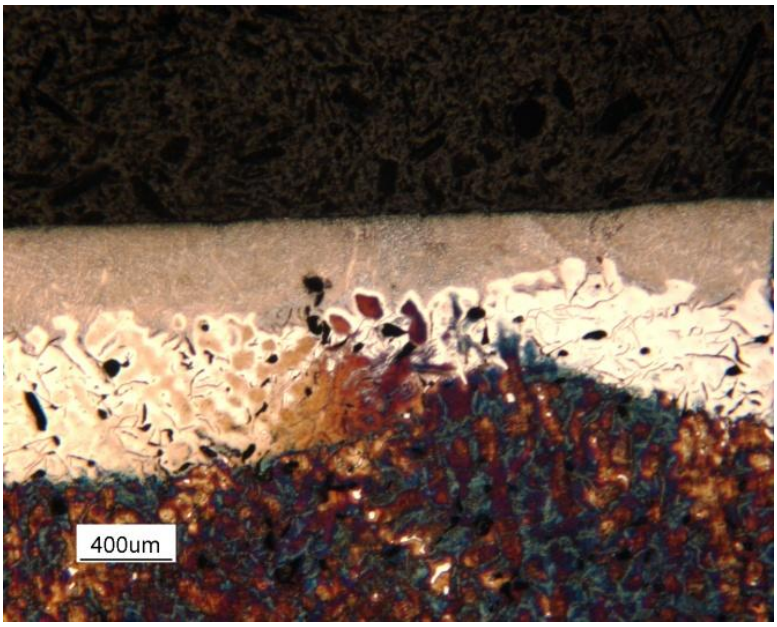

(c) Overlapped zone between the 2nd track and 3th track

Figure 6-9 Structures of the overlapping melted zones – 1500 ℃, 3mm/s.

Figure 6-9 shows that even if the back tempering phenomenon still esists in the hardened material inside overlapped zones, a uniform melted layer was obtained for all the treated surface, including the overlapped zone. The minimum scale of melted

surface in the overlapped zone can achieve 200 μm. Microhardness measurements were carried out along the width direction as the arrow shown in Figure 6-9 (a) at different distances (0.1 mm, 0.2 mm and 0.4 mm) from the top surface and also along the depth direction at different distances (3 mm, 5 mm, 8 mm, 10 mm and 13 mm) from the "0" position.

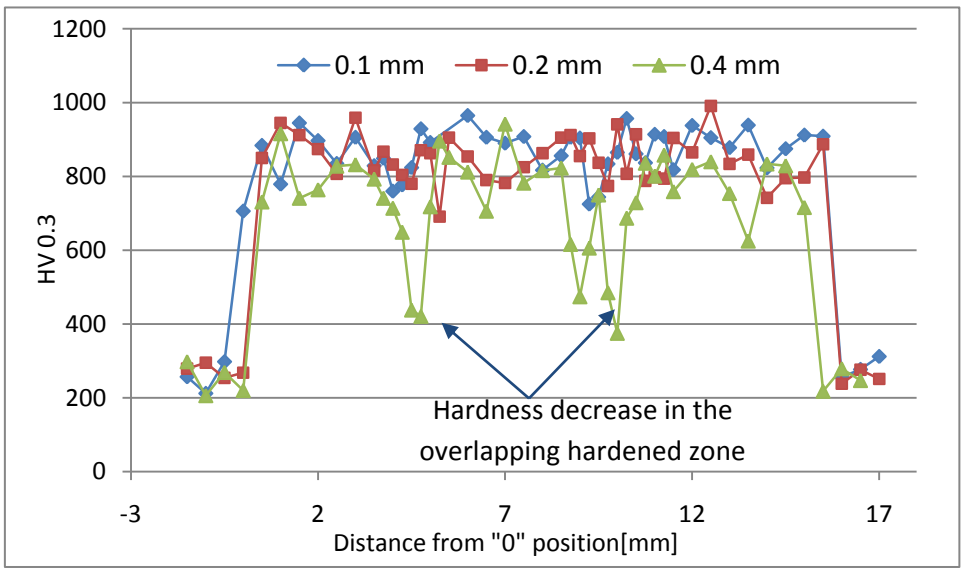

(a) Hardness profiles along the width direction

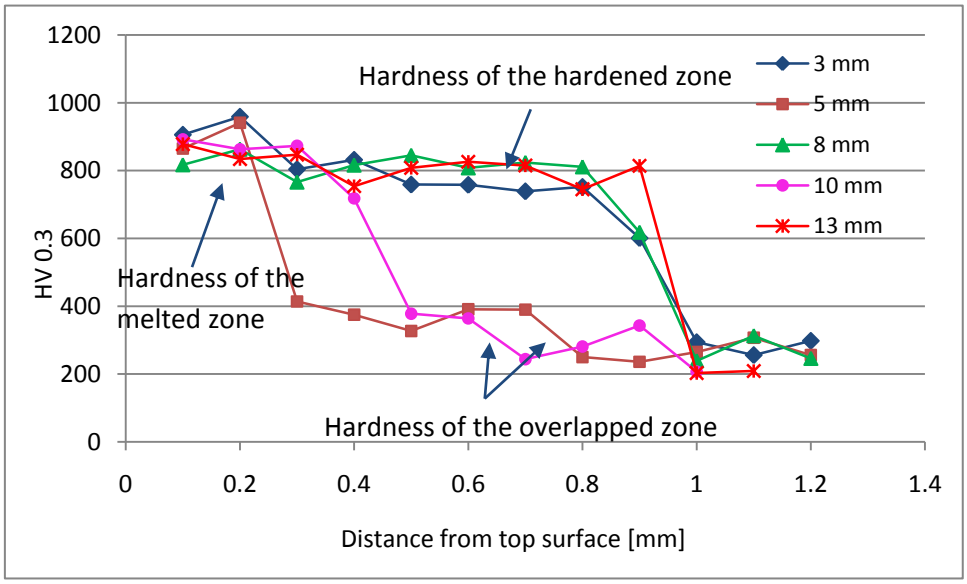

(b) Hardness profiles along the depth direction

Figure 6-10 Hardness distribution in the treated zones obtained by multi-pass laser melting.

The hardness tests in the cross section show that a treated surface with a uniform hardness distribution was obtained in the cross section by laser melting process, the depth of the treated surface reached 0.2 mm, and the microhardness was between 800 – 900$HV_{0.3}$. As the depth increased, hardened zones were obtained, the martensite in the hardened zones were affected by the back tempering decrease of hardness in overlapping zones was found under the surface 0.4 mm in the microhardness. The hardness profiles along the depth also confirm the back tempering phenomenon in the overlapped zone for the hardened materials.

A single specimen was executed with the high temperature and low scanning speed, a melt layer was covered on the surface of the specimen as shown in Figure 6-11.

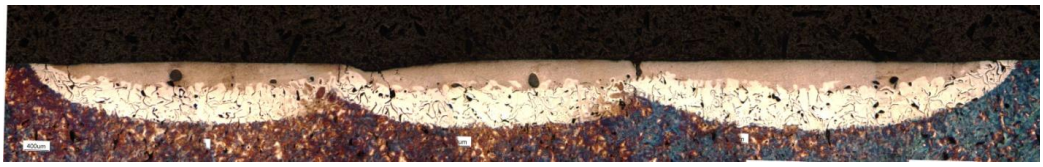

Figure 6-11 Single specimen performed with the optimized multi-pass laser melting process.

The multi-pass experimental campaigns have proved that, a large melted surface which can cover the overlapped zone could be obtained by increasing the temperature on the surface, and the uniform melted layer could improve the hardness behavior in the overlapped zones.

6.3 Conclusions

The laser melting process is a very promising surface treatment method for larger workpieces which cannot get a homogeneous hardened zone by traditional laser hardening. A fine grained microstructure with uniform microhardness and depth is obtained in the melted zone.

1. In single track laser melting process of gray cast iron, when the temperature on the surface is above the melting point, melted zones can be obtained by different combination of temperature on the surface and scanning speed.
    - When the temperature is above the melting point, the base melts and the graphite flakes dissolve into the melted material, due to the fast cooling, new microstructure with high hardness presents on the top surface.
    - The dimension of the melted zone is strongly affected by the process parameters, high temperature and low scanning speed should be adopted to obtain a uniform melted layer. In other words, high energy input is required during the melting process.

- The hardness of the melted zone was 800 – 900$HV_{0.3}$, which is higher than the hardened zone (700 – 800$HV_{0.3}$).

2. The microstructures and hardness profiles in the cross section of the multi-pass laser melted zones confirm that high energy should be used to get a large uniform melted surface.
   - Under low temperature condition, only the center of the treated zone was melted, the melted layer cannot cover the overlapping zone, hardness decrease still occurs at 0.15 mm under the top surface.
   - By high temperature on the surface, a melted layer was achieved on the whole surface of the treated zone, a surface without hardness drop was ensured; the depth of the uniform surface is 0.2 mm.
3. Although laser surface melting is one solution for back tempering problem, there are several drawbacks of the melting process.
   - The pores in the melted zone. They are induced mainly by the graphite dissolution and volume increase.
   - The thermal crack. It is a common drawback when a rapid solidification is achieved.
   - Post machining is necessary for applications.

7 Remote laser hardening

As the development of laser power, new techniques are proposed to overcome the back tempering phenomenon in the large surface treatment. With a high power laser, it becomes possible to defocus the laser beam to obtain a large laser beam, whose energy is still high enough for the laser hardening process.

Except defocusing the laser beam to enlarge the laser beam, shaping laser beam into a desired and large treated area becomes a new trend for the laser hardening process. With some high frequency scanning optics, the laser beam could be scanned into different shapes to meet the requirement for large surface; it is named remote laser hardening.

7.1 Experimental parameters for remote laser hardening

Along with the laser power and scanning speed, some new parameters were considered and under investigation (shown in Figure 7-1).

1. Laser spot Diameter (LD): Fiber laser is featured high beam quality, bringing new future of laser cutting and welding. But in the application of laser hardening, the laser usually works out of the focus to get a big laser spot with lower power

density. For a given laser power output, different laser spots determine the power density, and eventually, the scanning speed.

2. Scanning shape: other than shaping the laser beam straight into a line, other shapes were tested in the end of the experiment, *e.g.* round, ellipse.
3. Scanning Stroke (SS): It is the distance between the starting and finishing point of the laser beam during scanning the laser head. For the ellipse scanning shape, the scanning stroke includes scanning width (SW) and scanning length (SL).
4. Scanner head Frequency: It affects the time cost for shaping the laser spot into a line. In case of round and ellipse scanning locus, it is calculated from scanner head speed (m/min).

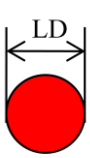

(a) Laser spot diameter

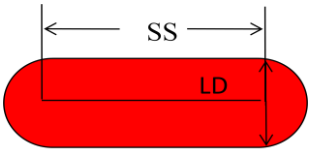

(b) Line shaped laser beam

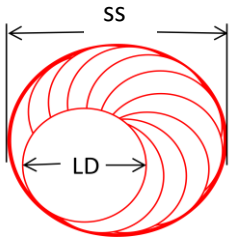

(c) Round shaped laser beam

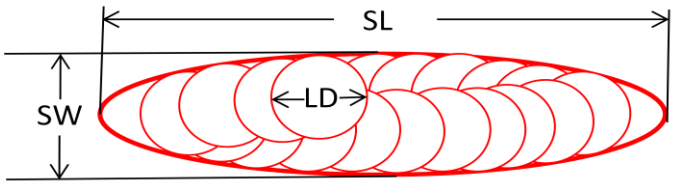

(d) Ellipse shaped laser beam

Figure 7-1 Sketch of fiber laser spot diameter and scan stroke.

No power measurement equipment was applied in the process. The initial condition of the remote laser hardening was chosen on the basis of the proximity laser hardening which was executed by diode laser. In the case of the laser spot size at 2 mm, and the scanner stroke at 6 mm, the shaped laser beam has the same dimension as the diode laser spot. 1250 W and 15 mm/s were chosen to simulate the proximity laser hardening. The initial parameters of the remote laser hardening are listed in Table 7-1; the power density is the same as the proximity laser hardening.

Table 7-1 Initial parameters of the remote laser hardening.

Hardening type	Laser	Power	Scanning speed	Power density
Proximity laser hardening	Diode laser	1250 W	15 mm/s	104 W/mm^2
Remote laser hardening	Fiber laser	1250 W	15 mm/s	104 W/mm^2

The surface was melted under the same condition as the diode laser hardening, and the surface is shown in Figure 7-2. Parameters were regulated based on this initial condition; Table 7-2 lists all the combinations of experimental parameters in the following experiments.

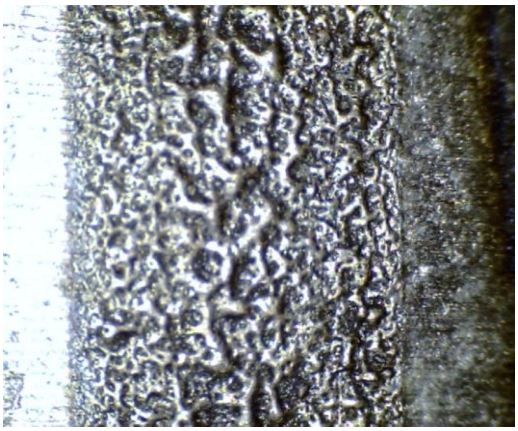

Figure 7-2 Treated surface of the remote laser hardening- initial parameters.

Table 7-2 Different experimental condition for fiber laser hardening.

Sample No.	Power	Speed	Spot size	Scanner stroke	Frequency	Scanning shape	Result
	(W)	(mm/min)	(mm)	(mm)	(Hz)		
1	1250	900	2	6	400	Line	Melt
2	1000	900	2	6	400	Line	Melt
3	3000	3000	2	6	400	Line	Melt
4	1000	1000	2	6	400	Line	Melt slightly
5	3000	5000	2	6	400	Line	Melt
6	1500	2500	2	6	400	Line	Hardening only in the center
7	1500	2000	2	6	400	Line	Hardening only in the center
8	2500	2000	2	11	400	Line	Melt
9	2500	3000	2	11	400	Line	Melt
10	1000	1000	5	-	400	-	Good
11	1200	1000	5	2	400	Line	Good
12	1200	1000	5	8	400	Line	No hardening
13	3600	1000	5	8	400	Line	Good
14	1200	330	5	8	400	Line	OK
15	5000	1000	5	32	400	Line	Not uniform
16	3000	1000	5	8	400	Line	OK

17	3000	1000	5	8	400	Line	Good
18	2000	1000	5	6	400	Line	No hardening
19	2000	1000	5	6	400	Line	No hardening
20	2000	1000	3	8	50	Line	Melt
21	2000	2000	3	8	50	Line	Melt
22	1000	2000	2	8	50	Line	Melt
23	2000	1000	5	8	50	Line	Melt in center
24	2000	1000	5	8	50	Line	Melt in center
25	2000	1000	5	8	200	Line	No hardening
26	2000	1000	5	8	400	Line	No hardening
27	2000	600	5	8	200	Line	OK
28	2000	500	5	8	200	Line	OK
29	2000	400	5	8	200	Line	Good
30	2000	1000	5	2	200	Line	No hardening
31	2000	1000	5	-	200	Line	Melt slightly
32	2000	1200	5	-	200	Line	Melt
33	2000	1000	5	2	200 m/min	Round	Melt
34	2000	1000	5	3	200 m/min	Round	Good
35	2000	1000	5	3	200m/min	Round	Good
36	2000	1000	5	6	200m/min	Round	No hardening
37	2000	1000	5	6x2	200m/min	Ellipse	No hardening
38	2000	1000	5	12x2	200m/min	Ellipse	No hardening
39	2000	1000	5	9x2	200m/min	Ellipse	No hardening

The remote scanner head laser hardening was carried out for every condition. The results show that the hardening with a scanner head is a complex process, which is affected by all the parameters. Different defects on the treated surface, *i.e.* all the treat surface is melt, the surface is melt in the center, rather hardened, were observed during the processes.

7.1.1 Influence of the laser spot diameter (LD)

With a small LD (2 mm and 3 mm), the power density of the laser beam is high; this could induce the surface melting. Under a small LD (2 mm), Figure 7-3 shows the melted surfaces of samples. Sample 1 was obtained by the same power and scanning speed as the diode laser (1250W, 900mm/min). This melted surface can be explained by Gaussian power distribution of fiber laser. When the laser beam was less

defocused; a small laser spot was formed, so the power density is quite high in the laser spot, it induces a melt surface

To reduce the melting phenomenon, sample 4 was treated with a decreased power (1000 W) and increased scanning speed (1000 mm/s), no hardened layer was obtained at the edges of the track, but the center of the surface was still melted. This means the temperature distribution in non homogenous in the shaped laser beam.

	Power	Scanning speed	LD	SS	Frequency
Sample 1	1250W	900 mm/min	2 mm	6 mm	400
Sample 4	1000W	1000 mm/min	2 mm	6 mm	400

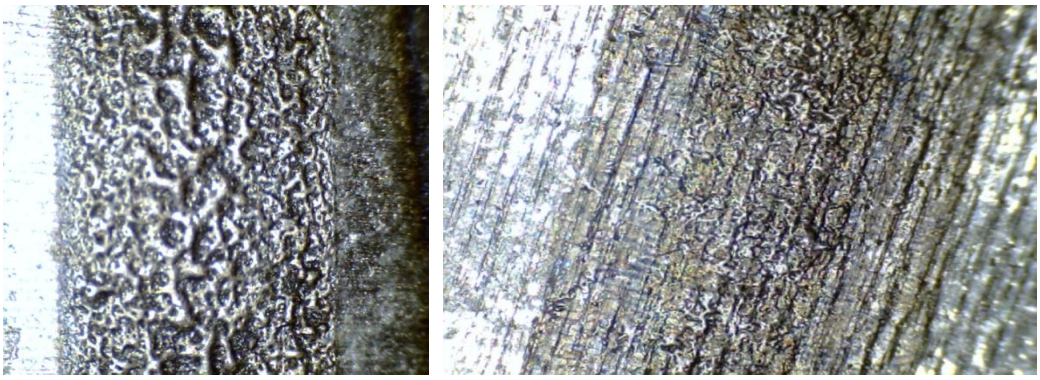

(a) Sample 1 (b) Sample 4

Figure 7-3 Melted surface obtained by the small LD.

7.1.2 Influence of the scanner head frequency

Three kinds of frequency 400 Hz, 200 Hz and 50 Hz were applied in the experiments. Figure 7-4 shows three samples which are hardened under same conditions except the frequency. (a) sample 24: 50 Hz, melting happened in the center of the surface; (b) sample 25: 200 Hz, no hardened zone; (c) sample 26: 400 Hz no hardened zone even worse than sample 25. The common treated condition is as following:

Power	Scanning speed	LD	SS	Frequency
1000W	2000 mm/min	5 mm	8 mm	50

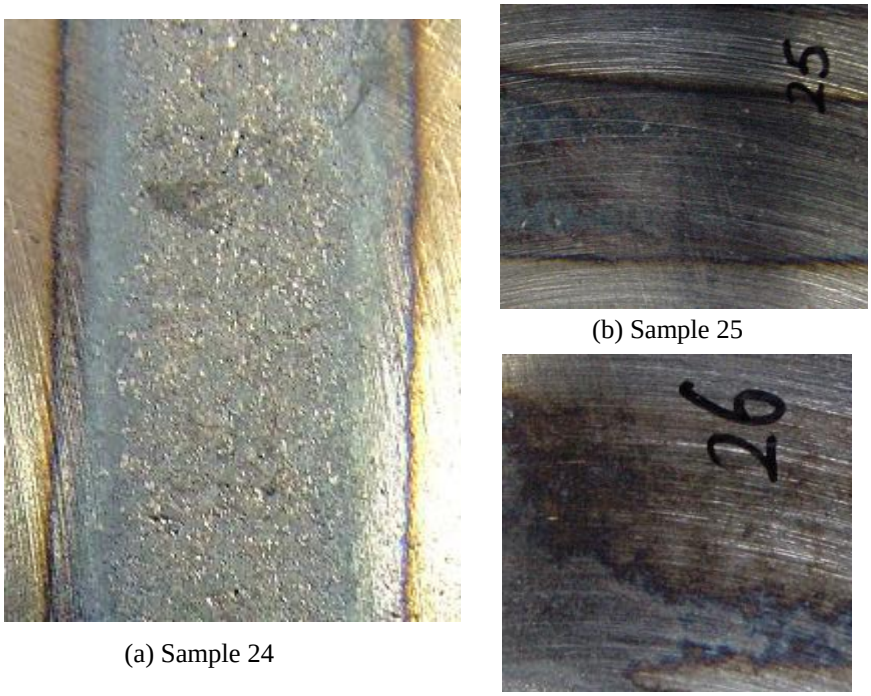

(a) Sample 24

(b) Sample 25

(c) Sample 26

Figure 7-4 Comparison of treated surfaces by different frequency.

Low scanning frequency is the other reason for the melted surface lower speed of the laser beam along the cross section induces longer heating time. Figure 7-5 (sample 22) shows a treated surface by the combination of small LD and low scanner head frequency, the treated condition is as following:

	Power	Scanning speed	LD	SS	Frequency
Sample 22	1000W	2000 mm/min	2 mm	8 mm	50

Compared with sample 4 and sample 24, sample 22 has the most serious melting phenomenon. On the contrary, under a high scanner head frequency, a hardened zone was achieved by increasing the power and decreasing the scanning speed, as shown in Figure 7-6 (sample 27).

	Power	Scanning speed	LD	SS	Frequency
Sample 27	2000W	600 mm/min	5 mm	8 mm	200

Figure 7-5 Melted surface obtained by small LD and low scanner head frequency.

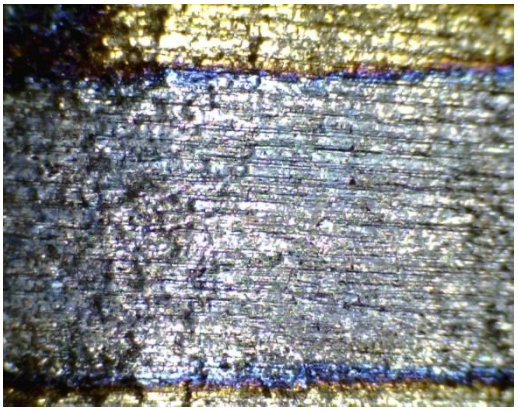

Figure 7-6 Hardened surface obtained by large LD and high scanner head frequency.

Insufficient energy input resulted in the non-hardened surface (Figure 7-7); it could be caused by low laser power, high scanning speed, large scanning stroke and high scanner head frequency.

Sample 18	Power	Scanning speed	LD	SS	Frequency
	2000W	1000 mm/min	5 mm	6 mm	400

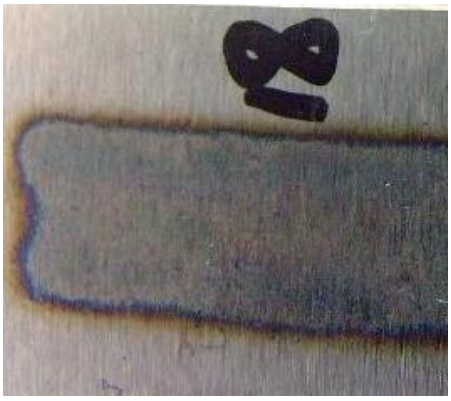

Figure 7-7 Non-hardened surface by the scanner head laser.

7.2 Hardness analysis for remote laser hardening

After the results evaluated by eyes at the first sight, hardness tests were executed on the surface of selected samples. The selected samples for hardness test are highlighted

in Table 7-1. The microstructure in cross section was investigated in Sample 13 to understand the depth of the hardening zone.

The microhardness tests were carried out for the samples which were highlighted in Table 7-1. The tests were carried out on the top surface, the tested positions are shown in every picture of the treated sample with a red line.

1. Sample 10

Sample No.	Power (W)	Speed (mm/min)	Spot diameter (mm)	Scanner stroke (mm)
10	1000	1000	5	-

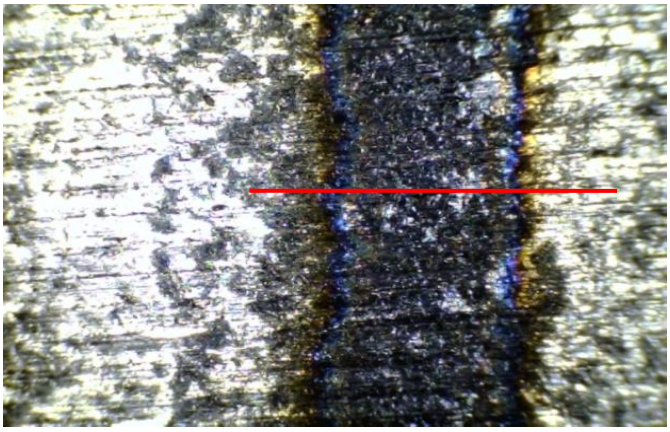

(a)

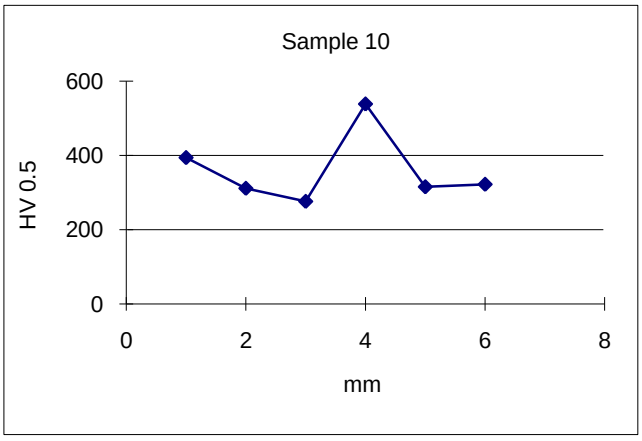

(b)

Figure 7-8 Structure and hardness test on the surface of fiber laser hardening sample 10.

2. Sample 11

Sample No.	Power (W)	Speed (mm/min)	Spot diameter (mm)	Scanner stroke (mm)
11	1200	1000	5	2

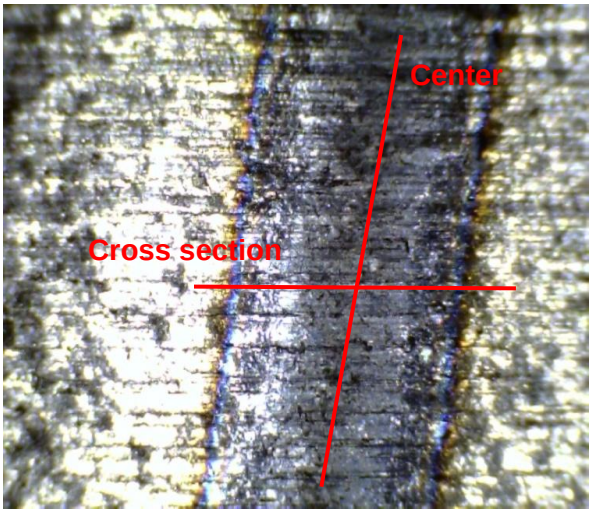

(a)

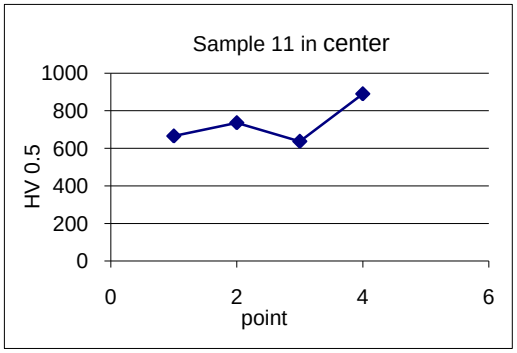

(b)

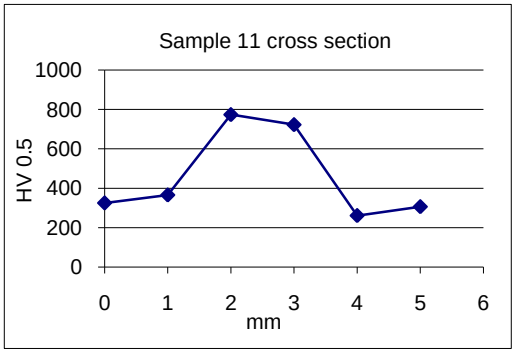

(c)

Figure 7-9 Structure and hardness test on the surface of fiber laser hardening sample 11.

3. Sample 13

Sample No.	Power (W)	Speed (mm/min)	Spot diameter (mm)	Scanner stroke (mm)
13	3600	1000	5	8

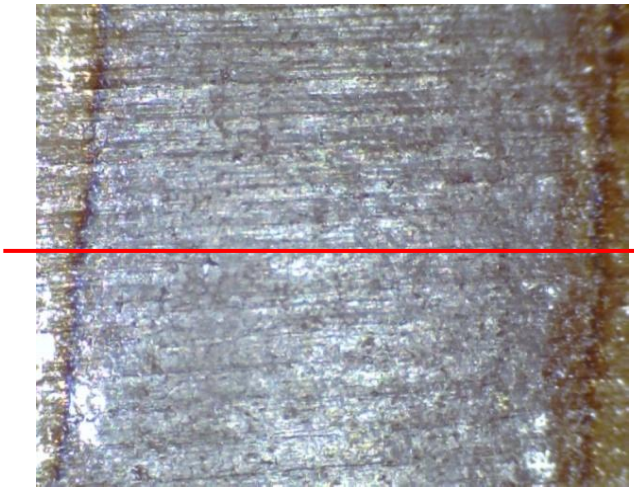

(a)

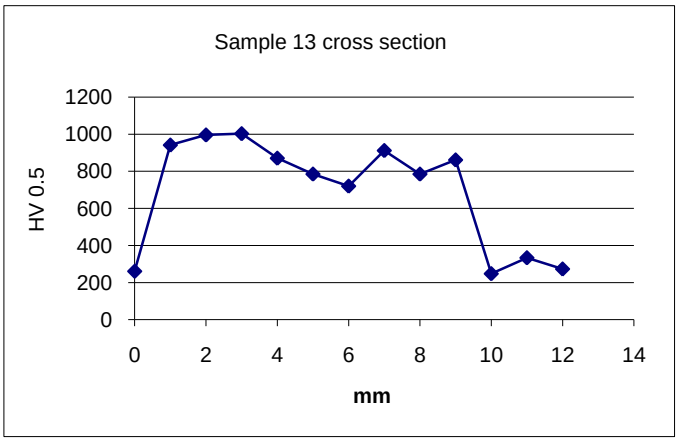

(b)

Figure 7-10 Structure and hardness test on the surface of fiber laser hardening sample 13.

The hardness test along the cross section shows that a hardened layer with hardness higher than 800 HV and width 8 mm was obtained. In order to get more detail about the hardened zone, the microstructure of the cross section was investigated (Figure 7-12).

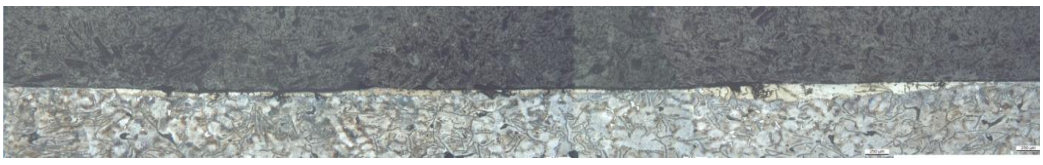

(a)

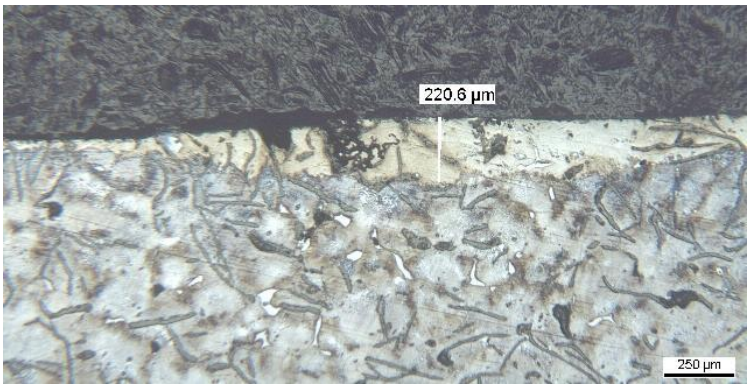

(b)

Figure 7-11 Microstructure in the cross section of fiber laser hardening sample 13.

In the cross section, a hardened layer was obtained by the remote scanner head laser hardening, as confirmed in the hardness test on the top surface, the microstructures of the cross section show that the depth of the hardened layer is quite shallow and non-uniform. The maximum depth of the hardening zone is 220.6 µm, the depth of other position is 10 -20 µm.

4. Sample 14

Sample No.	Power (W)	Speed (mm/min)	Spot diameter (mm)	Scanner stroke (mm)
14	1200	330	5	8

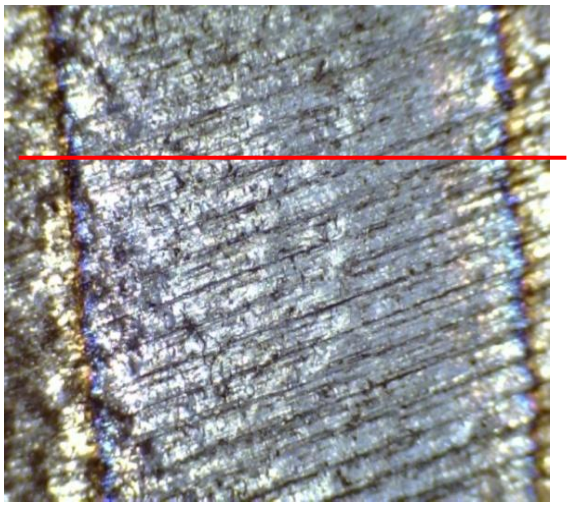

(a)

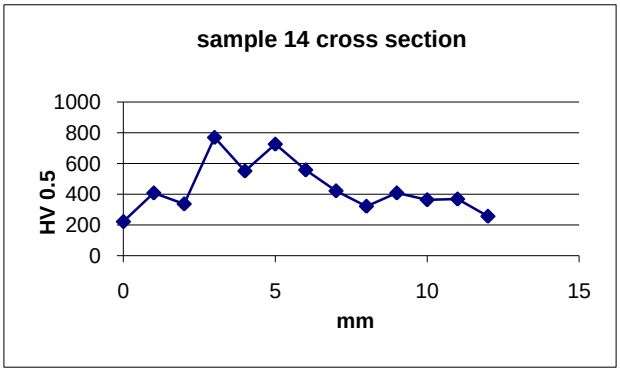

(b)

Figure 7-12 Structure and hardness test on the surface of fiber laser hardening sample 14.

5. Sample 15

Sample No.	Power (W)	Speed (mm/min)	Spot diameter (mm)	Scanner stroke (mm)
15	5000	1000	5	32

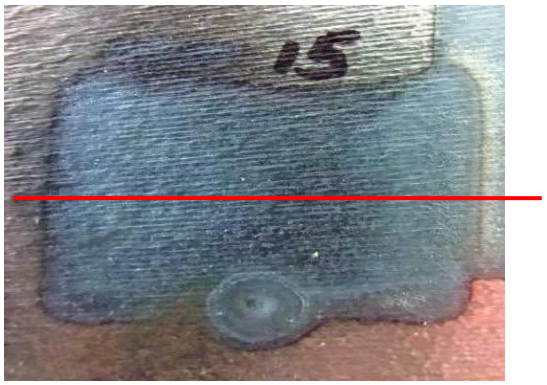

(a)

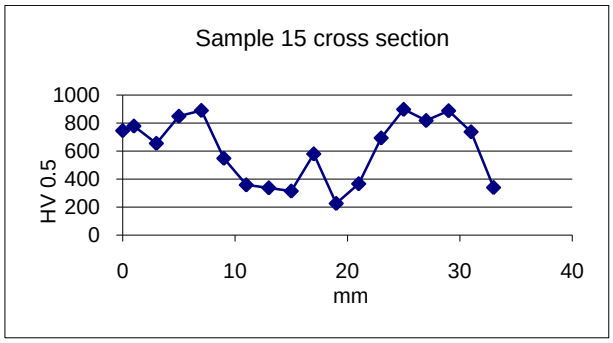

(b)

Figure 7-13 Structure and hardness test on the surface of fiber laser hardening sample 15.

6. Sample 18

Sample No.	Power (W)	Speed (mm/min)	Spot diameter (mm)	Scanner stroke (mm)
18	2000	1000	5	6

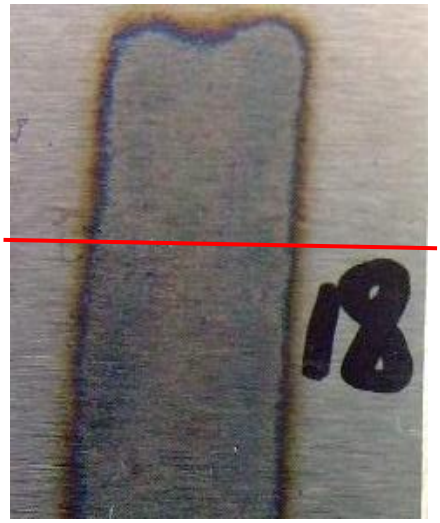

(a)

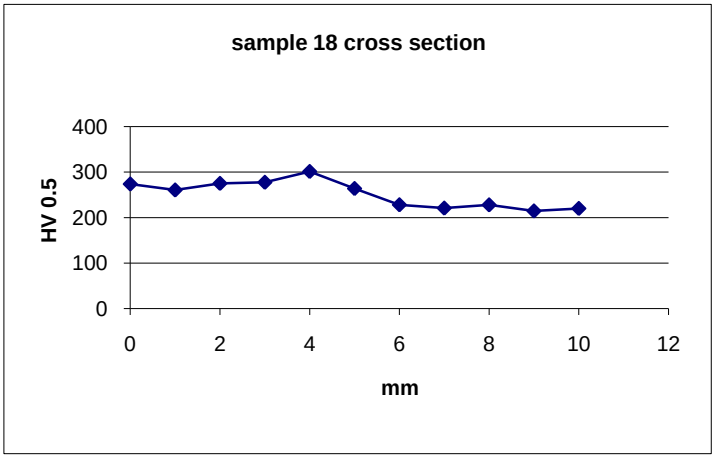

(b)

Figure 7-14 Structure and hardness test on the surface of fiber laser hardening sample 18.

7. Sample 34

Sample No.	Power (W)	Speed (mm/min)	Spot diameter (mm)	Scanner stroke (mm)
34	2000	1000	5	3

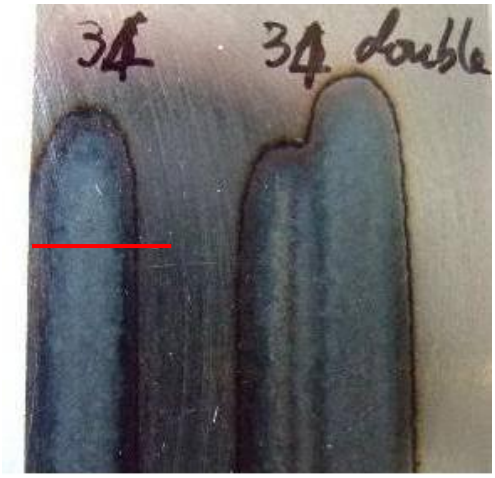

(a)

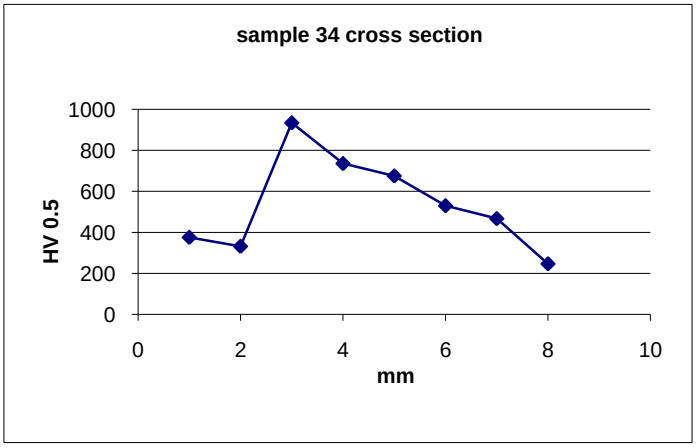

(b)

Figure 7-15 Structure and hardness test on the surface of fiber laser hardening sample 34.

The hardness tests for the hardened samples uncovered a common problem that most samples were hardened only in the center of the tracks. This is because of the Gaussian power distribution and heat accumulation in the hardened track. With a Gaussian power distribution, the power is centralized, if the laser beam gets defocused, the power in the periphery of the laser beam decreases, so that no hardened zone was obtained in the edge of the treat track.

7.3 Conclusions

With the high power fiber laser and a scanner head, it is possible to shape the laser beam into large dimension to treat a large surface. Except of the laser power and

scanning speed, some new parameters, *i.e.* laser spot diameter (LD), scanning stroke (SS) and scanner head frequency, were investigated. Through the experimental campaigns, the following results and conclusions were given:

1. The hardening process is strongly influenced by the energy distribution in the laser beam. The energy in the fiber laser has a Gaussian distribution, a small defocus length which means high power density could induce melted surface. Large laser beam with lower power density is necessary for a good hardening process.
2. The scanner head frequency is another essential factor for a successful hardening. Ceteris paribus, the lower scanner head frequency induces longer heating time for every treated point where melt surface is obtained, whereas higher frequency means repeated fast heating and cooling phases for a certain cross section, induces slow temperature increase.
3. An 8 mm width of hardened layer was obtained on the top surface. But the microstructure in the cross section indicated that the minimum depth of the hardened zone is only 10-20 μm, which is the result of the low absobtivity of metal for the fiber laser beam.
4. The hardness in the cross section shows a non-uniform distribution, the center of the hardened track obtained high hardness, and then the hardness decreased in the radius till the edges. This could be explained by the Gaussian energy distribution, when a large defocus length is applied, the power density decreases fast on the periphery of the laser beam, and therefore no hardened zone is obtained on the edge of hardened track.

According to the above results, it can be concluded that to obtain a hardened surface with a scanner head, lower power density in the laser spot (compared to laser welding or cutting process) and high scanner head frequency are required. Then based on the required hardened width, scanning stroke is determined with appropriate laser power and scanning speed.

8 Apparent Spot technique

As discussed in the previous chapters, back tempering happens not only on planar surfaces, but also on cylindrical surfaces. In this chapter, the back tempering phenomenon will be studied on cylindrical surfaces, and a new technique – Apparent Spot (AS) will be proposed to eliminate this drawback for cylindrical workpiece.

8.1 Back tempering on the cylindrical surface

Circular laser hardening is a particular treatment used in case of cylindrical workpieces. During the circular laser hardening, the workpiece is rotated by a lathe, in the mean time, laser beam treats the surface, and an annular hardening zone is obtained during the rotation.

There are two kinds of applications of this circular hardening technique: single annular track hardening and cylindrical surface hardening. The single annular track is used when the treatment of a narrow surface is required, *e.g.* for the treatment of bearing housing of a shaft, valve cone. In this case, only one revolution of the workpiece is executed and one annular hardened track is obtained. The cylindrical surface hardening is applied when a wider surface of the cylindrical workpiece is to be treated. In this application, a feed rate parallel to the rotation axis of the workpiece is given to the laser; this eventually results in a continuous helicoidal hardened track,

as shown in Figure 8-1. For the hardened cylindrical workpiece, the drawback of back tempering happens on both single annular workpiece and wider cylindrical surface.

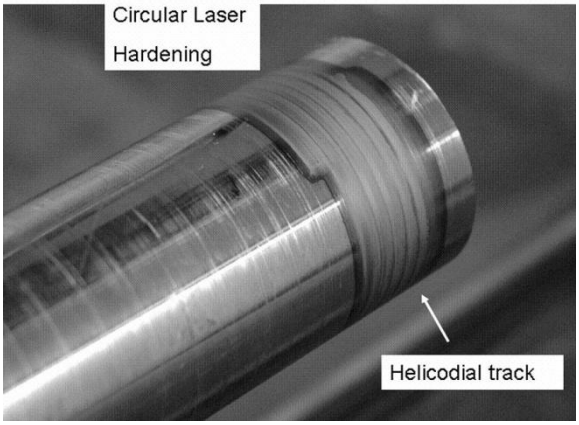

Figure 8-1 wider hardened surface obtained by helicodial track.

8.1.1 Overlapping phenomenon on single annular surface

When only one revolution is executed to the cylindrical workpiece, the laser beam does not move, during the laser hardening, the initial and final points of the workpiece are overlapped and treated twice as shown in Figure 8.2, and the back tempering happens in the initial/finishing part.

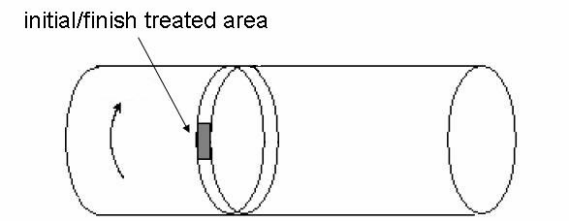

Figure 8-2 Scheme of single annular track laser hardening.

A shaft (Ø 15mm) was used to investigate the single annular hardening, the shaft was rotated at 45 rpm, and 1200 ℃ was chosen as the temperature on the top surface. Figure 8-3 gives the microstructure and microhardness of hardened surface.

(a) Microstructure of the single annular hardened surface

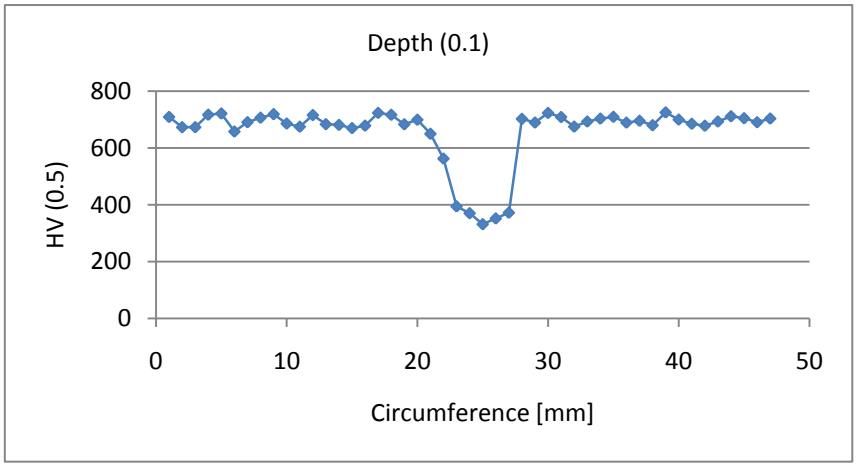

(b) Microhardness of the single annular hardened surface

Figure 8-3 Single annular hardened surface for cylindrical workpiece.

By single annular hardening process, the treated surface got a uniform hardness 700 $HV_{0.5}$, except of the initial and finishing parts. The hardness decreased less than 400 $HV_{0.5}$ in the overlapped zone.

8.1.2 Overlapping phenomenon on wider cylindrical surface

As discussed above, if a wider cylindrical surface to be treated, the laser scans the workpiece along the rotation axis. In this case, the overlapping phenomenon happen between the helicodial tracks, as shown in Figure 8-4.

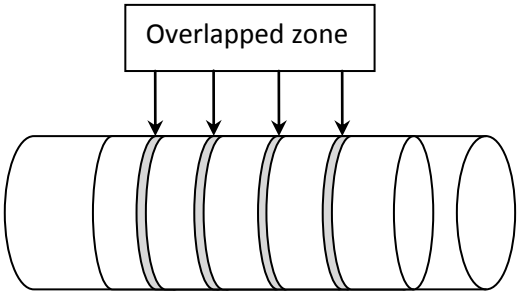

Figure 8-4 Scheme of wider cylindrical surface laser hardening.

The back tempering drawback of overlapping tracks process has the same theory as it happens on a planar surface – the current track reheats the previous one. When the back tempering happens in the overlapped zone, the microstructure and the hardness distribution in the overlapped zone of a cylindrical workpiece are shown in Figure 8-5. A shaft with 15 mm diameter was used, and the temperature on the surface was kept at 1200 ℃.

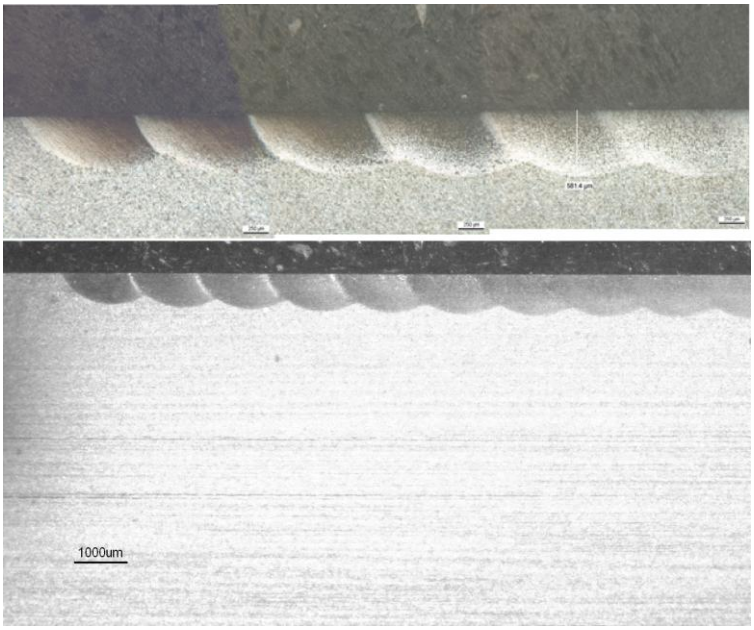

(a) Structures in the overlapped tracks with different magnifications

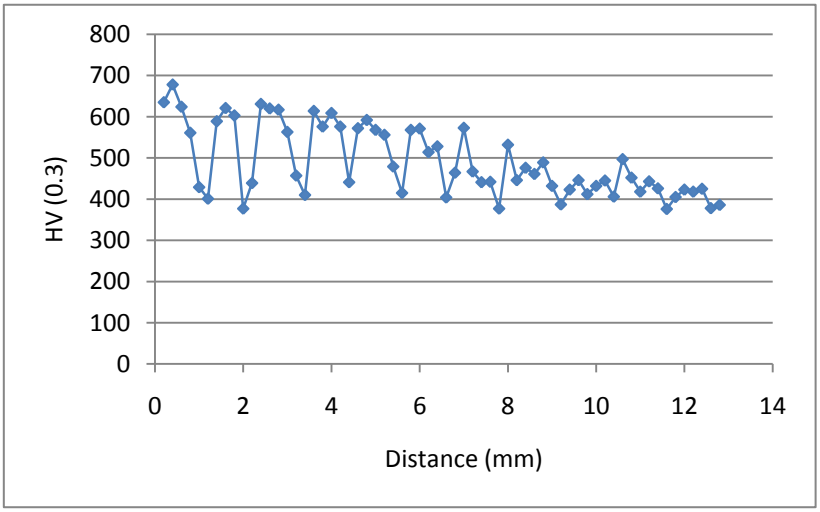

(b) Hardness distribution in the overlapped zones

Figure 8-5 Overlapping track applied in cylindrical workpiece.

The hardness tests in the cross section shows that, back tempering happened in the overlapped zone between two hardened tracks, the hardness dropped from 600 $HV_{0.3}$ to 400 $HV_{0.3}$, the hardened depth was 0.5 mm. As the hardened tracks increased, no obvious overlapped zone was observed, and the hardness decreased to 400 $HV_{0.3}$ in the hardened zones. The microstructures of the 1st, 6th, 11th and 16th overlapped zones are shown in Figure 8-6 (a) – (d) respectively.

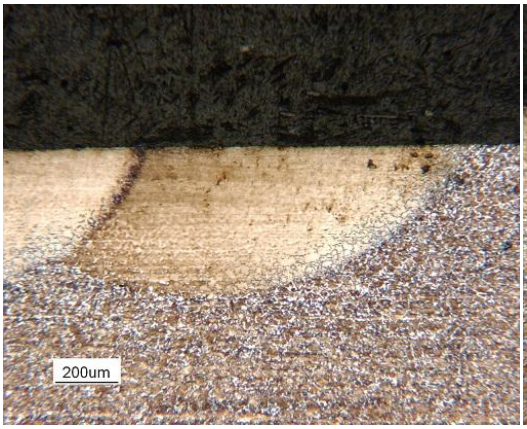

(a) the 1st overlapped zone

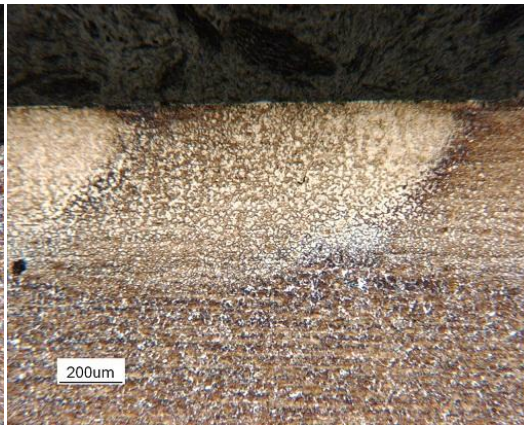

(b) the 6th overlapped zone

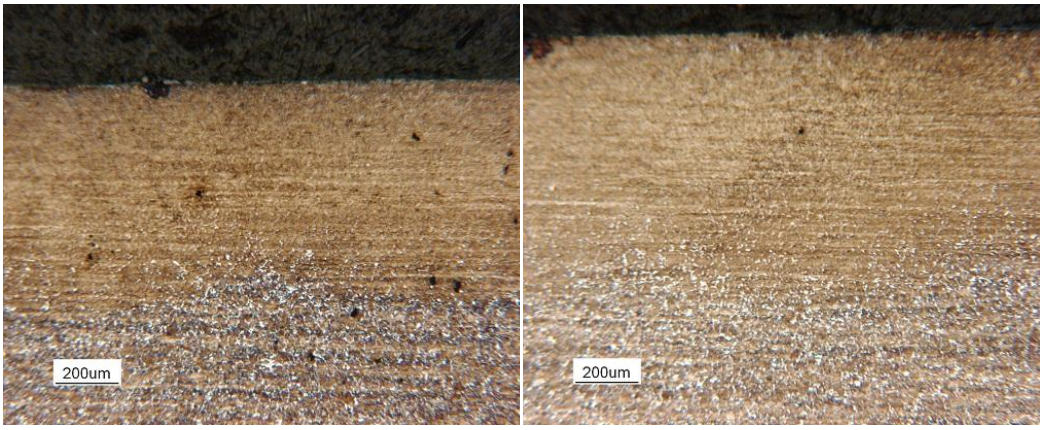

(c) the 11th overlapped zone (d) the 16th overlapped zone

Figure 8-6 Overlapped zones in the cylindrical workpiece.

The microstructures of different overlapped zones explained the hardness decrease along the axis direction in the cross section of the hardened sample. While the treatment was carried out, continuous laser beam radiated the workpiece, so the heat has been accumulated in the workpiece. Only the first several tracks were hardened when the bulk material was still cold. With the heat accumulation, the cooling phase was not enough for the last tracks, the austenite transformed or partly transformed into pearlite and ferrite, no hardened material was obtained.

The structures of the overlapped zone also show a non-uniform depth of the hardened surface, which is the same drawback on the planar surfaces.

8.2 Parameters investigation of Apparent Spot technique

In order to solve the back tempering phenomenon, a new technique was proposed for the surface hardening of cylindrical workpieces. This technique uses a high speed rotation instead of a low speed rotation during the circular hardening process. Due to this high speed rotation an apparent circular spot can be obtained as Figure 8-7, so this new technique is also called Apparent Spot (AS) technique. It increases the dimensions of the laser spot in a fictitious way, and the laser power distributes uniformly along this virtual circular laser spot. This circular spot has the same circumference as the workpiece, in this case, the laser beam treats the annular circumference at the same time, and a uniform hardening zone without overlapping and back tempering is obtained. If a wider surface has to be treated, a feed along the longitudinal direction can be imparted to the laser beam. Thanks to the AS technique, both the back tempering effect and the non-uniform hardness depth are solved.

Figure 8-7 Apparent Spot technique applied in cylindrical surface.

Due to the complexity of the AS technique the proper selection of processing parameters has to be carefully. Parameters involved in AS are the laser spot dimension, laser power, rotating speed, heating time and diameter of the workpiece. The parameters' choosing is based on some important considerations:

1. Power density. It is a combination of the laser spot dimension and laser power. High power density assures a fast heating phase, which avoids heating the bulk materials as in the self-quenching process. In order to achieve the maximum power density, the working distance is set equal to the focus one.
2. Heating time (t_H). With the control system, the heating time is controlled by the pre-set temperature on the surface. Once the measured temperature reaches the setting point, the laser power will be shut off automatically while the real time temperature is recorded by the system (see Figure 8-8).

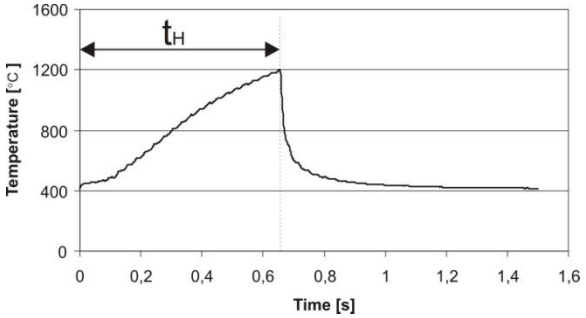

Figure 8-8 real time temperature and heating time during AS hardening.

3. Rotation speed. The thermal condition of every point on the circular surface consists in a heating phase and a cooling phase when one revolution is executed. With a high rotation speed, heating phases and cooling phases are repeated; whereas the heat accumulates and the temperature on the top

surface is reaching the setting point. The rotation speed affects the treatment mode and temperature increasing rate of the workpiece. Figure 8-9 show two simulated temperatures during the hardening process under different rotation speeds. Since the heating time is controlled against temperature, the rotation speed affects the heating time. A high revolution speed allows that the small spot becomes a ring-shaped heat source and induce a uniform temperature filed to the workpiece.

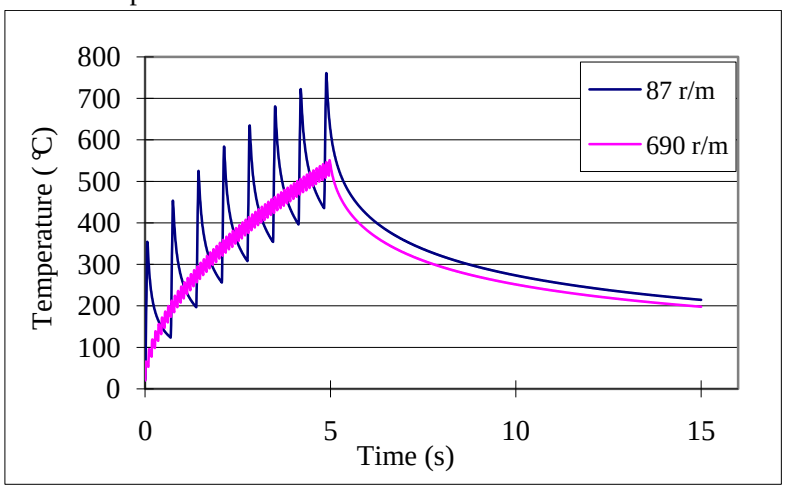

Figure 8-9 Influence of different rotation speed.

4. Diameter of the workpiece. It affects the dimension of the Apparent Spot, under a fixed laser power; it means that the power density of the Apparent Spot is affected by the diameter of the workpiece.

8.3 Experimental campaigns for annular surface by AS technique

As mentioned above, annular hardened surface is required by industrial applications, *e.g.* bearing housing of a shaft, and Apparent Spot technique is s solution of the overlapping phenomenon when a low rotation speed is applied during the hardening process. A set of experimental campaigns were investigated the effects of different parameters.

8.3.1 Experimental parameters for annular track hardening

Experimental campaigns are designed in order to understand the effects of different process parameters on single annular track laser hardening executed by the AS technique. The parameters are listed in Table 8-1.

Table 8-1 Process parameters used in the annular surface AS experimental campaign.

Process parameters	Levels
Power *P*	1250, 1000 [W]
Rotational speed *n*	2100, 1150 [rpm]
Temperature	1200 [℃]
Input energy *E*	28.6, 35.7, 52.2, 65.2 [J]
Workpiece diameters *Φ*	5,10,15,20,25 [mm]

The input energy E is the energy for every revolution, and is calculated by:

$$E = \frac{P}{n/60}$$

For each condition, four replicas were executed.

8.3.2 Experimental results of annular track AS hardening

Both the geometrical features and the hardness were investigated for the treated samples. Figure 8-10 gives some samples of the hardened zones, (a)-(f) are treated under same condition: 1250 W, 2100 rpm, but with different diameters of the workpiece, (f) shows a non treated surface.

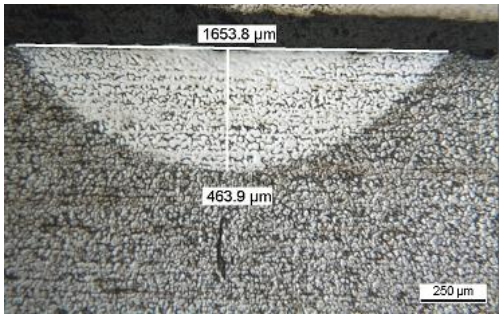

(a) 5 mm

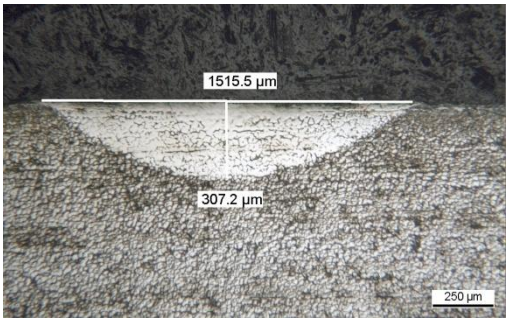

(b) 10 mm

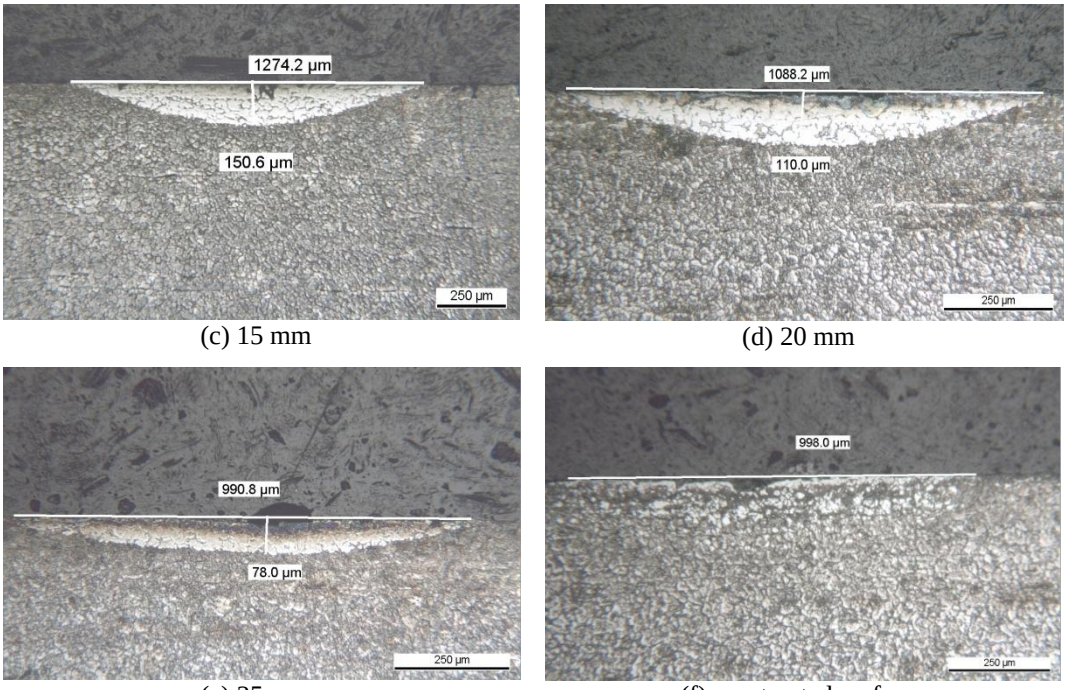

(c) 15 mm (d) 20 mm

(e) 25 mm (f) non treated surface

Figure 8-10 hardened zone obtained by single track AS technique.

Based on the measurements of the width and depth of hardened zones, Figures 8-11 and 8-12 report the geometrical features of the hardened zones, in terms of height and width as a function of the workpiece diameters.

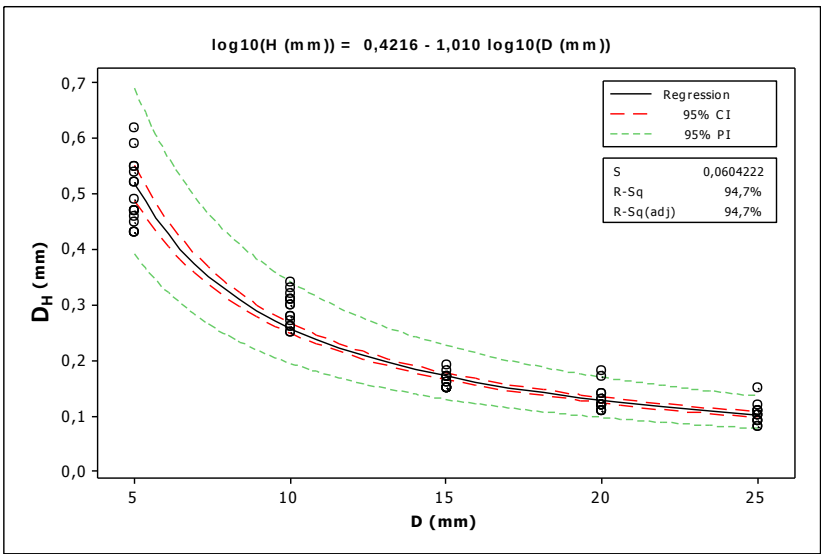

Figure 8-11 Height of the hardened zone vs. workpiece diameter (AS).

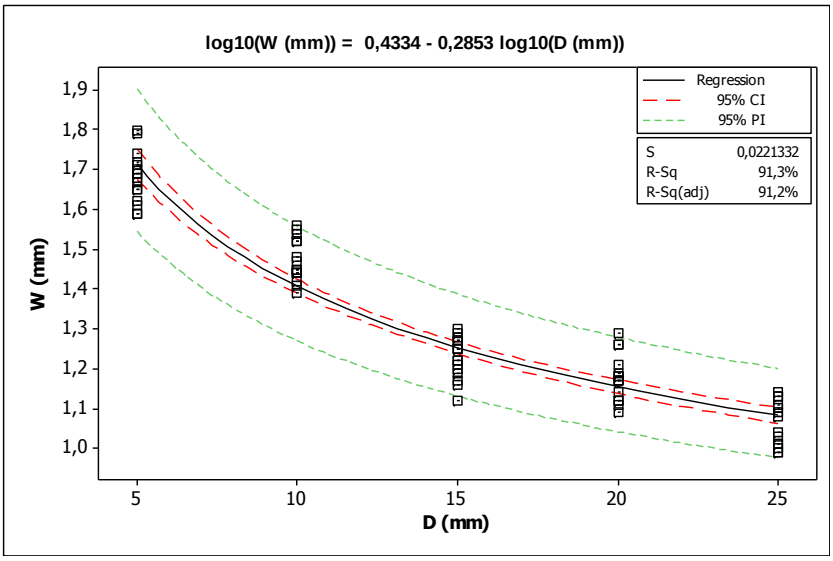

Figure 8-12 Width of the hardened zone vs. workpiece diameter (AS).

The regression analysis confirms that the geometrical attributes, *i.e.* W and H, are not affected by the energy input, but by the workpiece diameter. Both of them indeed decrease when the workpiece diameter increases.

The microhardness tests were carried out in the cross section of the samples. The tests show two different behaviors depending on the workpiece diameters (see Figure 8-13).

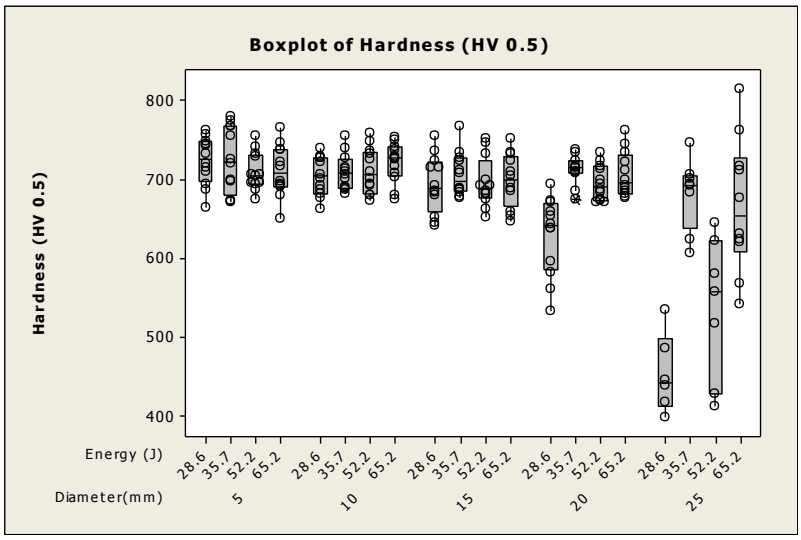

Figure 8-13 Microhardness vs. input energy and workpiece diameter (AS).

For the workpieces whose diameter is smaller than 15 mm, hardened layers were obtained. In this diameter range, neither the input energy nor the diameter affect the microhardness values (average value: 709±22 HV), as the ANOVA analysis confirms. On the contrary in the case of larger workpiece diameters, *i.e.* 20 and 25 mm, the input energy affects the laser hardening results. Particular in the case of 20 mm diameter, the single track hardened zones are obtained only by higher energy inputs. When it comes to the largest diameter, *i.e.* 25 mm, surface is not completely laser hardened even in the case of the highest input energy. This is probably due to the long heating time that characterizes the largest diameter, especially in the case of the lowest energy input. As shown in figure 8-14, when the workpiece diameter increases, the time that is needed to reach the fully austenization strongly increases, that the bulk material is not able to rapidly cool down the treated surface layer.

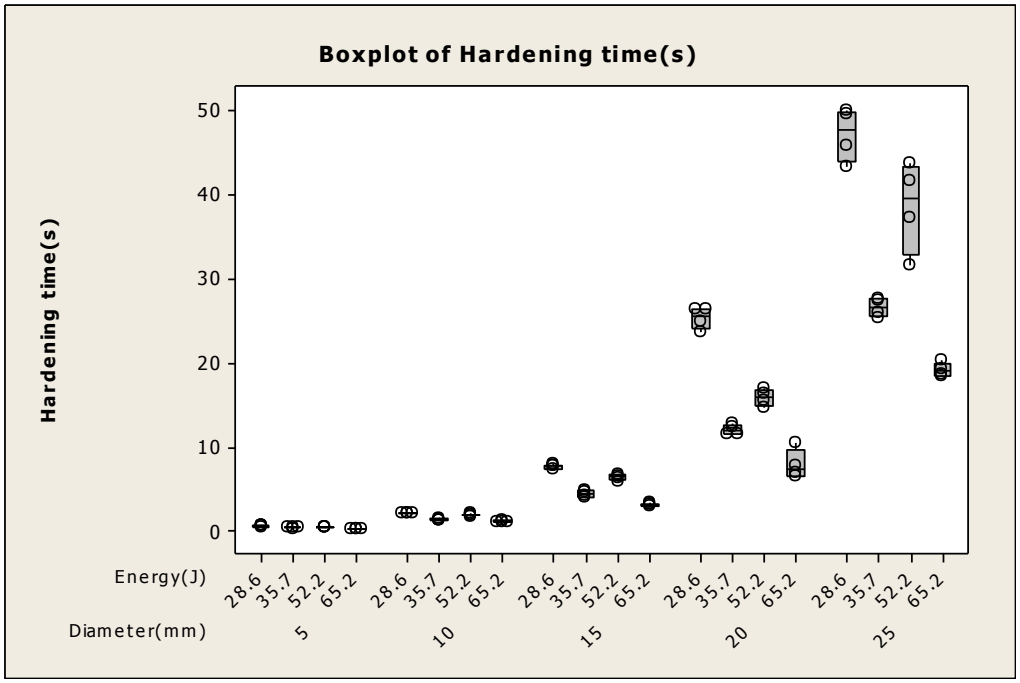

Figure 8-14 Heating time vs. input energy and workpiece diameter (AS).

The experiments pointed out the effects of the process parameters on the dimensions and hardness values of the single track in case of a circular laser hardening executed by AS technique. The results show that workpiece diameter is the major factor of the hardened surface, while the input energy is less effective. In particular, with a fixed laser power the AS technique has a limitation of the workpiece diameters, which makes it inapplicable to the large workpiece diameters. This can be explained by considering that when the diameter increases the heating time increases to the point that the consequent rapid self-quenching is not further guaranteed.

8.4 Preliminary experiments of overlapping AS hardening

To obtain a wider hardened surface two steps are included in the AS technique. For the first step, the workpiece was treated by an annular track AS hardening, considered as preheat step, during this step, the maximum power was applied without regulation. When the temperature on the surface reaches the setting point as the trigger of the second step, then the laser begins to move along the direction of the rotation axis. During the second step, the power of the laser is regulated to keep the temperature at a constant level.

Based on the annular surface AS hardening, to reduce the heat accumulation in the substrate material, high power density was applied. A shaft with 20 mm diameter was chosen, as the maximum diameter that could be treated by AS technique with a 1250 W diode laser. Other than the parameters investigated in the single track annular AS hardening experiments, the feed rate of the laser beam is also in consider. Two feed rates (1 mm/s and 2 mm/s) were executed to hardening the shaft. The details of the hardening condition are listed in Table 8-2. The treated surface is shown in Figure 8-15.

Table 8-2 Process parameters used in the cylindrical surface AS experimental campaign.

Process parameters	Levels
Power *P*	1250 [W], automatic controlled
Rotational speed *n*	1150 [rpm]
Temperature	1200 [℃]
Rotation speed	1150 [rpm]
Input energy *E*	65.2 [J]
Workpiece diameters *Φ*	20 [mm]
Feed rate	1,2 [mm/s]

Figure 8-15 A wider cylindrical hardened surface obtained by AS technique.

By different feed rates of the laser beam, laser power was regulated and the real time laser power and temperature are reported in Figure 8-16. In the first phase, because of the power in maximum the temperature increased fast until the temperature reached the setting point (1200 ℃) and then the laser beam started to move. For the first seconds of the second step, the temperature on the surface drops due to the cold bulk material, so maximum power was applied automatically. Because of the heat accumulation in the cylindrical workpiece, the temperature reached the setting point and power started to decrease to keep a constant temperature (see Figure 8-15 (a)). On the contrary, when a fast feed rate is given, the maximum power will not be enough to keep the temperature on the set valve as shown in Figure 8-15 (b).

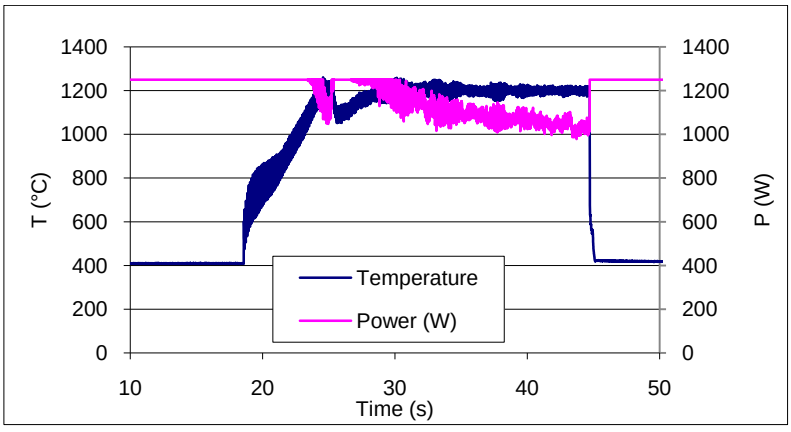

(a) feed rate – 1 mm/s

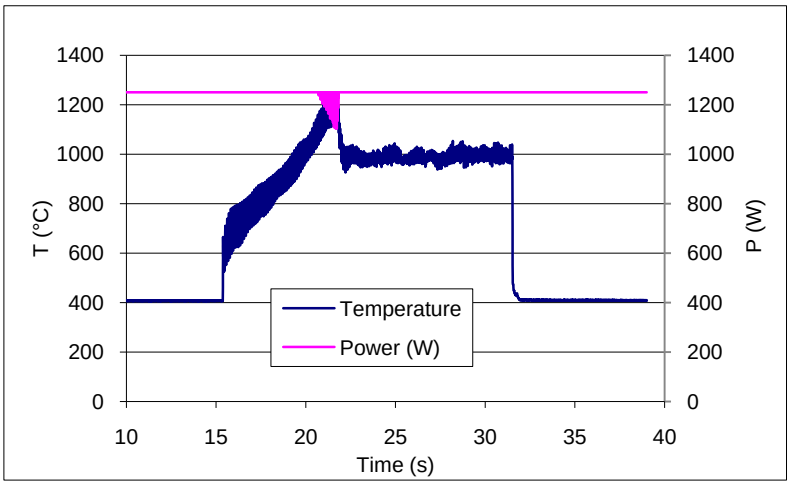

(b) feed rate – 2 mm/s

Figure 8-16 Real time and power record in overlapping AS hardening.

The hardness tests in the cross section were carried out under the surface 75 μm, the profiles are given in Figure 8-17.

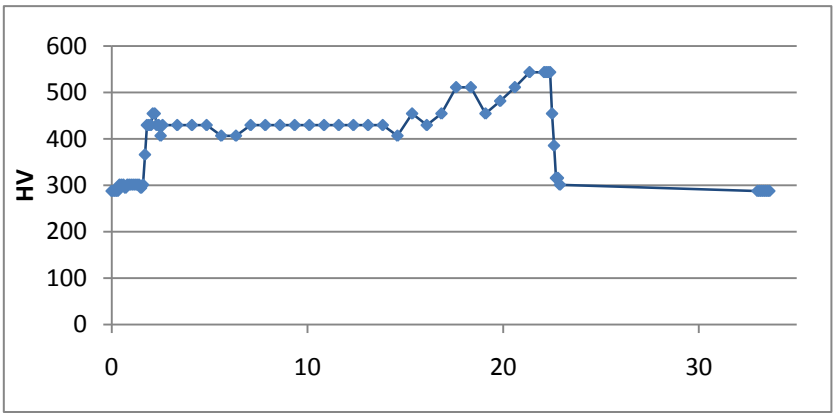

(a) feed rate – 1 mm/s

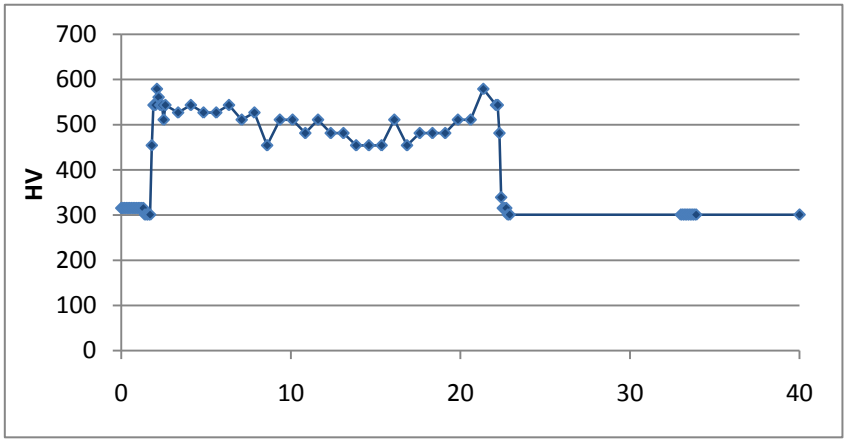

(b) feed rate – 2 mm/s

Figure 8-17 Hardness profiles of the hardened samples by overlapping AS technique.

The records of the real time power and temperature of the heated shaft reveal that by automatic controlling the laser power, the cylindrical surface AS hardening takes place. It can be noted from the hardness profiles that, the hardness of the treated layer is not uniform and lower than the single annular track hardening. This can be ascribed mainly to the temperature increase in the bulk of the shaft as discussed above. To avoid or reduce the heat accumulation, high feed rate should be carried out, and as a result, high laser power should be guaranteed.

8.5 Conclusions

In this chapter, the laser hardening process was applied to cylindrical workpiece. Different hardening methods were discussed, due to back tempering drawback happened in the cylindrical workpiece, a new technique – AS hardening was proposed.

The main results are listed as following:

1. During the laser hardening process for a cylindrical workpiece, if a low rotation speed is imparted to the workpiece, overlapping has to be applied for both single annular treated surface and wider treat surface.
   - A single annular hardened surface could be obtained by rotating the workpiece only one revolution. The overlapping happens in the initial and finishing parts of the hardened surface, other positions of the hardened zone have a uniform hardness.
   - In the overlapping process of the low rotation speed hardening, the overlapping was applied for every rotation; in this case, the back tempering happens in the

entire hardened surface. As the overlapping tracks increases, the hardness decreases along the axis direction; this is due to the heat accumulation in the workpiece.

2. The Apparent Spot technique is proposed to solve the overlapping and back tempering phenomenon in the cylindrical workpiece. This technique is the combination of high rotation speed and high laser power.
   - For the single track AS hardening, annular hardened zones are obtained in the case of the small diameter workpiece.
   - The geometrical features of the hardened zone were related only to the diameter of the workpiece, the power density and rotation speed have no effect on the geometrical features. Both the width and height of the hardened zone decrease as the diameter of the workpiece enlarged.
   - The hardness tests of the AS hardened zone are decided by the diameter and input energy. For small diameter (less than 15 mm), the hardness is effected neither by diameter nor input energy, a uniform hardness 709 ± 22 HV is obtained. For bigger diameter (20 mm) the hardened layer is obtained only by the high input energy. For the shaft with 25 mm diameter, no uniform hardness was obtained even by the high input energy.
3. With the automatic power control, AS technique is applied to treat the wider surface. The hardness of the treated surface is lower than it in the single track AS hardening process. This is mainly due to the discussed heat accumulation in the shaft.

Finally, this AS technique has still to be addressed since a lack of knowledge exists and deeper investigation is needed.

9 Conclusions

In this chapter the main conclusions of the thesis work are reported and discussed.

Laser hardening has been developing fast and widely applied in industrial fields due to its unique advantages such as self-quenching, small deformation and flexible controlled. The limited dimension of the laser beam makes the laser hardening be suitable for the complex geometrical workpiece and localized hardening; on the other hand, treatment on a large surface becomes its limitation currently.

The purpose of this research work was to study and reduce the overlapping and back tempering phenomenon in the case of a large surface treated by laser. In this thesis work both planar surface and cylindrical surface are investigated under the overlapping condition, and then some solutions are proposed to reduce or eliminate this back tempering drawback.

Different results are obtained by this thesis work.

For planar surface:

1. The effects of laser hardening parameters on the hardened surface were studied. Thanks to the control system, where the temperature was controlled in the feasibility window, hardened surface can be obtained by different combinations of laser power and scanning speed. The hardness drops in the overlapped zone when a large surface is treated.

2. One solution to the back tempering phenomenon is laser melting. When the surface of the workpiece is melted and solidified rapidly, a new refined structure with high hardness is formed on the top surface, this new structure is not affected by the back tempering in the overlapped zone, and a uniform treated surface could be obtained by overlapping laser melting process. To get a uniform melted surface on the top surface, high temperature must be guaranteed.
3. Scanning laser head to shape the laser spot into a large dimension is a way to avoid the overlapping process. Under the investigation of scanning a fiber laser beam, the most important two facts are the dimension of the laser beam and scanning frequency. An 8 mm width of hardened layer was obtained on the top surface. But due to the low absobtivity of metal for the fiber laser beam, the minimum depth of the hardened zone is only 10-20 μm.

For the cylindrical surface:

1. The back tempering phenomenon happens in both single annular track hardening and wider surface hardening, if the cylindrical workpiece is under a low speed rotation during the hardening process. When a single annular track is required, the overlapping exists in the initial and finishing parts. For a large cylindrical surface, the overlapping happens between the nerghbor tracks as it in the planar surface.
2. Apparent Spot hardening is a new technique to solve the overlapping phenomenon for the cylindrical workpiece. The mechanism of this technique is to rotate the workpiece at a high speed, and a virtual circular laser spot is obtained around the circumference of the workpiece.
3. When the AS technique is applied to treat a single annular track, the hardened results are depend on the diameter and input energy. When the diameter of the workpiece is too large, the input energy cannot get a fast heating phase. Consequently, the rapid self-quenching is no longer ensured and lower hardness is obtained in the hardened zone.
4. The heat accumulation in the cylindrical workpiece is an important factor which has to be considered during the hardening process for a cylindrical workpiece. To treat a lager surface by AS technique, high power and high feed rate must be applied to reduce the heat accumulation in the bulk material.

List of Figures

List of Tables

References

1 John C. Ion, (2005), Laser processing of engineering materials pp.15-16

2 C. Emmelmann, C. Tuchel (2001), Latest production innovations in of laser technologies-shown with diode pumped solid state lasers. High productive joining processes, Proc. 7th International Aachen Welding Conference (ASTK 01)

3 L. Migliore, Laser material processing. Laser Kinetics, Inc., Mountain View, California. Theory of laser operation, pp.1-30.

4 Beyer, (2006), Fiber laser welding. Industrial laser solution 21 (7).

5 L. Li, R. Dewhurst (1999), Chewing gum removal by lasers. UK Patent Application, GB9926638.9, Tidy Britain Group.

6 L. Li, (2000), The advances and characteristics of high power diode laser materials processing, Opt. Lasers Eng. 34, pp.231-253.

7 P. Molian, (1989) Surface modification technologies-An engineers guide TS Sudarshan (NewYork: Marcel Dekker), pp.421

8 J.M.F. Vollertsen, K. Partes., (2005), State of the art of laser hardening and cladding, Proceeding of The Third International WLT Conference.

9 J.C. Ion, (2002), Laser transformation hardening, Surface Engineering 18, pp.14-31,

10 R.A. Seban, (1965), J. Heat Transfer, pp.173

11 W.W. Duley, (1986) Laser material interactions of relevance to metal surface treatment, Proceedings of NATO Advanced Study Institute on Laser Surface Treatment of Metals, Martinus Nijhoff Publishers, Dordrecht, pp. 3.

12 T.J. Wieting, J.T. Schriempf, J. Appl. (1976) Phys. 47 4009

13 G. Stern, (1990) Proceedings of the Third European Conference on Laser Treatment of Materials, pp. 25

14 J. Grum, T. Kek, (2004), The influence of different conditions of laser-beam interaction in laser surface hardening of steels, Thin Solid Films 453 -454, pp. 94-99

15 Wolfgang Schulz, Reinhart Poprawe, (2000) Manufacturing with Novel High-Power Diode Lasers, IEEE Journal of Selected Topics In Quantum Electronics 6

16 F. Dausinger, J. Shen, (1993), ISIJ Int. 33, pp.925.

17 Friedrich Bachmann, (2003), Industrial applications of high power diode lasers in materials processing, Applied Surface Science 208-209, pp.125-136

18 Henrikki Pantsar, Veli Kujanpaa, (2004), Diode laser beam absorption in laser transformation hardening, Journal of Laser Applications 16, pp.147-153

19 E. Kennedy, G. Byrne, D.N. Collins, (2004), A review of the use of high power diode lasers in surface hardening, Journal of Materials Processing Technology 155–156, pp.1855–1860

20 R. Komanduri, Z.B. Hou, (2001), Thermal analysis of the laser surface transformation hardening process, International Journal of Heat and Mass Transfer 44, pp.2845-2862

21 R. Komanduri, Z.B. Hou, (2004), Thermal analysis of laser surface transformation hardening – optimization of process parameters, International Journal of Machine Tools & Manufacture 44, pp.991–1008

22 Stephen Skvarenina, Yung C. Shin, (2006), Predictive modeling and experimental results for laser hardening of AISI 1536 steel with complex geometric features by a high power diode laser, Surface & Coatings Technology 201, pp.2256–2269

23 A. Weisheital, B.L. Mordike, (1991) Laser surface modification of materials, Processing IMT Conf., Birmingham,

24 F. Lusquinos, J.C. Conde, S. Bonss, A. Riveiro, F. Quintero, R. Comesana, J.Pou, (2007), Theoretical and experimental analysis of high power diode laser (HPDL) hardening of AISI 1045 steel, Applied Surface Science 254, pp.948–954

25 L.J.YANG, S.JANA, S.C.TAM, (1990) Laser Transformation Hardening of Tool-Steel Specimens, Journal of Materials Processing Technology 21, pp.119-130

26 J. Grum, (2007), Comparison of different techniques of laser surface hardening, Journal of Achievements in Materials and Manufacturing Engineering 24, pp.17-25

27 S.A.Fedosov, (1999), Laser Beam Hardening of Carbon and Low Alloyed Steels: Discussion Of Increased Quantity Of Retained Austenite, Journal of materials Science 34, pp.4259-4264

28 Jae-Ho LEE, Jeong-Hwan JANG, Byeong-Don JOO, Young-Myung SON, Young-Hoon MOON, (2009), Laser surface hardening of AISI H13 tool steel, Trans. Nonferrous Met. Soc. China 19, pp.917-920

29 J. Hannweber, S. Bonss, B. Brenner, E. Beyer, (2004) Integrated laser system for heat treatment with high power diode laser. ICALEO 2004 congress proceedings

30 C.H.Chen, C.J.altstetter, J.M. Rigsbee, (1984) Laser Processing of Cast Iron for Enhanced Erosion Resistancee, Metallurgical Transactions A, volume 15A

31 Henrikki Pantsar, Veli Kujanp, (2006), Effect of oxide layer growth on diode laser beam transformation hardening of steels, Surface & Coatings Technology 200, pp.2627– 2633

32 R.A.Ganeev, (2002), Low Power Hardening of Steel, Journal of Materials Processing Technology 121, pp.414-419

33 I.R. Pashby, S. Barnes, B.G. Bryden, (2003), Surface hardening of steel using a high power diode laser, Journal of Materials Processing Technology 139, pp.585–588

34 F. Lusquinos , J.C. Conde, S. Bonss, A. Riveiro, F. Quintero, R. Comesana, J. Pou, (2007), Theoretical and experimental analysis of high power diode laser (HPDL) hardening of AISI 1045 steel, Applied Surface Science 254, pp.948–954

35 Shakeel Safdar, Lin Li, M. A. Sheikh, Zhu Liu, (2006) An Analysis of the Effect of Laser Beam Geometry on Laser Transformation Hardening, Journal of Manufacturing Science and Engineering 128, pp.659-667

36 H. J. Hegge, J. T. M. De Hosson, (1987), The Relationship between Hardness and Laser Treatment of Hpyo-Eutectoid Steels, Scr. Metall, 21, pp.1737–1742.

37 L. M. Galantucci, L. Tricario, (1999), An Experimental and Numerical Study on the Influence of Not Uniform Beam Energy Distribution in Laser Steel Hardening, Annals of the CIRP Vol. 48/1/1999, pp.155-158

38 P. Hoffmann, R. Dierken, (2003) Temperature Controlled Hardening of Single Part Tools for Automotive Industry With High Power Diode Laser Systems, Proceedings of the Second International WLT-Conference on Lasers in Manufacturing

39 J. Senthil Selvan, K. Subramanian, A.K. Nath, (1999), Effect of laser surface hardening on En18 (AISI 5135) steel, Journal of Materials Processing Technology 91, pp.29-36

40 S. A. FEDOSOV, (1999), Laser Beam Hardening of Carbon and Low Alloyed Steels: Discussion of Increased Quantity of Retained Austenite, Journal of Materials Science 34 pp.4259 - 4264

41 K. Obergfell, V. Schulze ,O.Vohringer, (2003), Classification of microstructural changes in laser hardened steel, Materials Science and Engineering A355, pp.348-356

42 J.Ruiz, V.Lòpez, B.J.Fernandez, (1996), Effect of surface laser treatment on the microstructure and wear hehaviour of grey iron, Material & Design 17, pp.267-273

43 X. Liu, G. Yu, J.Guo, Q.Shang, Z.Zhang, Y. Gu, (2007), Analysis of Laser Surface Hardened Layers of Automobile Engine Cylinder Liner, Journal of iron and steel research, international 14(1), pp.42-46

44 Rahul Patwa, Yung C. Shin, (2007), Predictive modeling of laser hardening of AISI5150H steels, International Journal of Machine Tools & Manufacture 47, pp.307–320

45 Stephen Skvarenina, Yung C. Shin, (2006), Predictive modeling and experimental results for laser hardening of AISI 1536 steel with complex geometric features by a high power diode laser, Surface & Coatings Technology 201, pp.2256–2269

46 Neil S. Bailey, Wenda Tan, Yung C. Shin, (2009), Predictive modeling and experimental results for residual stresses in laser hardening of AISI 4140 steel by a high power diode laser, Surface & Coatings Technology 203, pp.2003–2012

47 M.J.Tobar, C. Álvarez, J.M. Amado, A. Ramil, E. Saavedra, A. Yáñez. (2006), Laser Transformation Hardening of a Tool Steel: Simulation-based parameter optimization and experimental results, surface & coatings technology 200, pp.6362-6367

48 H.Pantsar and V.Kujanpaa, (2004), Diode laser beam absorption in laser transformation hardening of low alloy steel, Journal of Laser Applications 16, pp.147-153.

49 E.Hensel, (2003) Close-loop Hardening of Automotive Components, Proceeding of Advanced automotive laser applications (ALAC2003)

50 E.Capello, M.Castelnuovo, B.Previatli, (2006), Optimization of production rate in diode laser hardening, ICALEO 2006 Congress Proceedings.

51 E.Capello, M.Castelnuovo, (2005), Real time control of diode laser hardening in view of near net-shape manufacturing, Proceeding of the 58th annual assembly and international conference of international institute of welding.

52 C.M.Cook, J.M.Haake, (2000), Monitoring and controlling the temperature in a high power direct diode laser surface hardening application, 20th ASM Heat Treating Society Conference Proceedings, pp.183-191

53 Steffen Bonss, Marko Seifert, Jan Hannweber, Udo Karsunke, Eckhardt Beyer, (2005), Low Cost Camera Based Sensor System for Advanced Laser Heat Treatment Processes, ICALEO 2005 Congress Proceedings, pp.851-855

54 Zhiyue Xu, Keng H. Leong, Claude B. Reed, (2008), Nondestructive evaluation and real-time monitoring of laser surface hardening, Journal of Materials Processing Technology 206, pp.120–125

55 Dietmar Hömberg, Wolf Weiss, (2006), PID Control of Laser Surface Hardening of Steel, IEEE Transactions on Control Systems Technology 14, pp.896-904

56 K. Bewilogua, G. Brauer, A. Dietz,J.Gabler, G. Goch, B. Karpuschewski, B.Szyszka, (2009), Surface Technology for Automotive Engineering, CIRP Annals - Manufacturing Technology, CIRP-436,

57 V. S. Maiorov, S. V. Maiorov, (2009), Solid laser hardening of iron parts, Metal Science and Heat Treatment Vol. 51, pp.106-108

58 Edoardo Capello, Barbara Previtali, (2008), Optimization of production rate in diode laser hardening, Journal of Laser Applications 20

59 Ritesh L.J.Yang, S.Jana and S.C.Tam, (1990), The Effects of Overlapping Runs in The Laser Transformation Hardening of Tool-Steel Specimens, Journal of Materials Processing Technology 23, pp.133-147

60 J.H Hwang, Y.S Lee, D.Y Kim, J.G Youn, (2002), Laser Surface Hardening of Gray Cast Iron Used for Piston Ring, Journal of Materials Engineering and Performance, Volume 11(3) June, pp.294-300

61 E. Capello, L. Giorleo, (2008), Apparent Spot in Circular Laser Hardening, conference proceeding AMST 2008, pp 405-416

62 A.N. Savonof, (1997), Basic directions of effective use of laser equipment for heat treatment of alloys, Metal Science and Heat Treatment 39, pp. 275

63 G. Tani, L. Orazi, A. Fortunato, (2008), Prediction of hypo eutectoid steel softening due to tempering phenomena in laser surface hardening, CIRP Annals - Manufacturing Technology 57, pp.209–212

64 Ritesh S. Lakhkar, Yung C. Shin, (2008), Matthew John M. Krane, Predictive modeling of multi-track laser hardening of AISI 4140 steel, Materials Science and Engineering A 480, pp.209–217

65 A. Liu, B. Previtalia, (2010), Laser surface treatment of grey cast iron by high power diode laser, conference proceeding LANE 2010, pp.439-488

66 C. Yao, B.Xu, J.Huang, P.Zhang, Y.Wu, (2010), Study on the softening in overlapping zone by laser-overlapping scanning surface hardening for carbon and alloyed steel, Optics and Lasers in Engineering 48, pp.20–26

67 Guy Claus, Transformation hardening with high power diode laser systems using single and multiple tracks, ICALEO 2004 Conference Proceedings

68 E. Capello, B. Previtali, (2005), Effect of overlapping quote, focus height and beam velocity in the optimization of line laser hardening, 7th AITEM Conference

69 J.D. Kim, M.H.n Lee, S.J. Lee, W.J. Kang, (2000), Laser transformation hardening on rod-shaped carbon steel by Gaussian beam, Transactions of Nonferrous Metals Society of China 19, pp.941-945

70 M. Seifert, S. Bonß, B. Brenner, E. Beyer, (2004), High power laser beam scanning in multi-kilowatt range, ICALEO 2004 Conference Proceedings

71 S. Bonss, J. Hannweber, M. Seifert, F. Tietz, S. Kühn, U. Karsunke, B. Brenner, E. Beyer, (2007), Novel machine system for simultaneous heat treatment with dynamic beam shaping, ICALEO 2007 Congress Proceedings, pp.1081-1086

72 B.L. Mordike, (1995), Surface treatment with high power lasers, Laser in Engineering 4, pp. 187-200

73 Janez Grum, Roman Sturm, (1997), Laser surface melt-hardening of gray and nodular irons, Applied Surface Science 109/110, pp. 128-132

74 Janez Grum, Roman Sturm, (1998), Influence of laser surface melt-hardening conditions on residual stresses in thin plates, Surface and Coatings Technology 100-101, pp. 455-458

75 M.H.Tulloch, (1992), Laser melting of camshafts saves wear, Photonics Spectra, pp.20

76 V. Lopez, J. M. Bello, J. Ruiz and B. J. Fernandez, (1994), Surface laser treatment of ductile irons, Journal of Materials Science 29, pp. 4216-4224

77 K.A Chiang, Y.C. Chen, (2005), Laser surface hardening of H13 steel in the melt case, Materials Letters 59, pp. 1919– 1923

78 C. Li, Y. Wang, Z. Zhang, B. Han, T. Han, (2010), Influence of overlapping ratio on hardness and residual stress distributions in multi-track laser surface melting roller steel, Optics and Lasers in Engineering 48, pp. 1224–1230

79 J. Grum, R. Sturm, (2005), Influence of laser beam guiding and overlapping on residual stress in melting process, Surface Engineering 2, pp.27-34

80 L.Giorleo, A.Liu, B.Previtali, (2010), Apparent spot in circular laser hardening: effect of process parameters, conference ESAFORM 2010, pp. 1119 – 1122

81 Guy Claus, M. Seifert, (2007), High speed rotation hardening of steel shafts and holes with high power diode laser, ICALEO 2007 Congress Proceedings, pp.266-270

82 A.Fortunato, L.Orazi, G.Campana, A.Ascari, G.Cuccolini, G.Tani, (2009), Laser hardening of large cylindrical martensitic stainless steel surface, Proceedings of the Fifth International WLT-Conference LIM 2009

83 G. Tani, A. Fortunato, A. Ascari, G. Campana, (2010), Laser surface hardening of martensitic stainless steel hollow parts, CIRP Annals-Manufacturing Technology 59, pp.207–210

84 S.Bonss, J.Hannweber, U.Karsunke, S.Kuehn, M.Seifert, E.Beyer, G.N.Drollinger, (2008), Integrated laser beam hardening in turing machines for process chain reduction, ICALEO 2008 Congress Proceedings, Poster Presentation Gallery, pp.94-99